DIGITAL METHODS IN DYNAMIC RESPONSE ANALYSES OF TURBO-ALTERNATOR UNITS

A Thesis submitted

to

The Victoria University of Manchester

for

The Degree of Doctor of Philosophy

by

TARAK NATH SAHA

May 1966

ProQuest LLC.
789 East Eisenhower Parkway
P.O. Box 1346
Ann Arbor, MI 48106 – 1346

PREFACE

The author graduated in Electrical Engineering from the Jadavpur University, Calcutta, India, with a First Class degree in 1959. Having completed his graduate apprenticeship with the Calcutta Electric Supply Corporation, he worked in industry, both in India and in the United Kingdom. He joined the Manchester College of Science and Technology in October 1962 and obtained the degree of M.Sc. Tech. in December 1963. Since then he has been engaged in research work, the major part of which is the content of the present thesis.

SUMMARY

The predetermination of the performance of synchronous generators, for the wide range of conditions under which they operate in power supply systems, assumes a major importance in present-day power-system engineering practice. For all but the simplest cases, a formal long-hand analysis is usually an intractable task, and some form of computing aid is required for accurate and reliable studies.

The present thesis has been devoted to an investigation of digital techniques of analysis with particular reference to the transient conditions that frequently give rise to the main operational limitations. A comprehensive mathematical model for a complete turbo-alternator unit, including the voltage regulator and governing system, is presented in a form in which its equations are amenable to solution by automatic calculator. In this way, a more detailed and accurate representation than hitherto appears to have been available has been developed and in which particular emphasis has been placed upon the representation of the complex distribution of eddy currents in the solid rotor of round rotor machines. The validity of the different models investigated has been checked by comparing the results of extensive computer analysis with those obtained from instrumented site tests on a 30 MW set at Goldington Power Station, and a 120 MW set at Belvedere Power

Station. Having in this way confirmed the accuracy with which practical operating and disturbance conditions may be represented, the digital methods developed have been applied to detailed appraisals of rotor over-voltages in a.c. excited generators, short periods of asynchronous running, and controlled synchronising and spontaneous resynchronising conditions. Finally, the methods have been applied to long-range predictions in experimental analyses of the detailed performance of large power generating units of capacity upto 660 MW.

CONTENTS

LIST OF PRINCIPAL SYMBOLS

GENERATOR

i_a, i_b, i_c	Phase currents
Ψ_a, Ψ_b, Ψ_c	Phase flux-linkages
l_{aa}, l_{bb}, l_{cc}	Self-inductances of stator windings
l_{ab}, l_{bc}, l_{ca}	Mutual-inductances between stator windings
$l_{afd}, l_{bfd}, l_{cfd}$	Stator-to-field mutual inductances
$l_{akd}, l_{bkd}, l_{ckd}$	Stator-to-d-axis damper winding mutual inductances
$l_{akq}, l_{bkq}, l_{ckq}$	Stator-to-q-axis damper winding mutual inductances
R_a, R_b, R_c	Phase Resistances
L_o	Stator zero-phase-sequency inductance
ψ_{fd}	Field flux-linkage
ψ_{kd}, Ψ_{kq}	Damper winding flux-linkages
$l_{ffd}, R_{fd}(r_{fd})$	Field self-inductance and resistance respectively
l_{kkd}, l_{kkq}	Damper winding self inductances
$R_{kd}, R_{kq}(r_{kd}, r_{kq})$	Damper winding resistances
l_{fkd}	Field-to-d-axis damper winding mutual inductance
i_{kq}, i_{kd}	Damper winding currents
v_a, v_b, v_c	Stator phase resistances
v_{fd}, i_{fd}	Field voltage and current respectively
θ $(p\theta = \omega_o + p\delta)$	Angle between d-axis and axis of phase 'a' measured in the direction of rotation, rad
ψ_d, ψ_q	Axis flux-linkages
ψ_o	Flux-linkage in the zero-phase-sequency

l_{fd}, l_{kd}, l_d	Direct-axis field, damper and stator inductances.
l_{kq}, l_q	Quadrature-axis damper and stator leakage inductances.
v_d, v_q	Axis voltages
i_d, i_q	Axis currents
i_o	Zero-phase-sequence component of stator current
X_d, X_q	Synchronous reactances in the d- and q-axes respectively
L_d, L_q	$\frac{X_d}{\omega_o}$, $\frac{X_q}{\omega_o}$ respectively
ω_o, f_o	Rated frequency, rad/sec. and c/s respectively
ω, f $(\omega = \omega_o + p\delta)$	Instantaneous machine frequency, rad/sec and c/s respectively.
τ'_{do}, τ'_d	D-axis transient open- and short-circuit time-constants respectively, sec.
τ''_{do}, τ''_d	D-axis subtransient open- and short-circuit time-constants respectively, sec.
τ''_{qo}, τ''_q	Q-axis open- and short-circuit time-constants respectively, sec.
τ_{kd}, τ_{kq}	D- and q-axis damper leakage time-constants respectively, sec.
X_f, X_a	Field and armature leakage reactances respectively in per-unit.
X_{1d}, X_{1q}	Leakage reactances in the d- and q-axis damper windings respectively, in per-unit
X'_d	Direct-axis transient reactance in per-unit
X''_d, X''_q	Sub-transient reactances in the d- and q-axes respectively, in per-unit.
ψ_{at}	Total air gap flux
v_m	Terminal voltage, $\sqrt{v_d^2 + v_q^2}$
T_e	Air-gap torque
G	Rotor-stator direct-axis transfer-constant $\frac{X_{ad}}{R_{fd}}$

G_{kd}, G_{kq}	Transfer-constants associated with the d- and q-axis damper windings respectively
$\tau'_{kdo}, \tau''_{kqo}$	$\frac{X_{ad} + X_{kd}}{\omega R_{kd}}$, $\frac{X_{aq} + X_{kq}}{\omega R_{kq}}$ respectively
P_i	Power input
P_e	Electrical terminal power
K_d	Frictional loss coefficient
P_l	Sum of rotor and stator copper losses
H	Inertia constant kw-sec/kVA
M	$\frac{H}{\pi f}$
δ	Rotor-angle, rad
P_a	Electrical terminal reactive power

AUTOMATIC EXCITATION CONTROL SYSTEM (of Goldington Test Set)

V_d	Reference input
K_o	Gain constant of comparator
K_1, K_2	Gain constants of magnetic amplifiers 1 and 2 respectively
K_e	Gain constant of exciter, including rectifiers
K_3, K_4	Gain constants of derivative stabilising loops
τ_3, τ_5	Time-constants of derivative stabilising loops
τ_1, τ_2	Time-constants of magnetic amplifiers 1 and 2 respectively, sec.
τ_e	Exciter time-constant, sec.
τ_4, τ_6	Time-constants of derivative stabilising loops, sec.
v	Error signal
v_1, v_2	Voltage outputs of magnetic amplifiers 1 and 2 respectively

v_{s1}, v_{s2}	Stabilising signals derived from output of magnetic amplifier 2 and exciter respectively
C_1, C_2	Bias constants of magnetic amplifiers 1 and 2 respectively
C_e	Bias constant of exciter
$v_1 min, v_1 max$	Saturating limits of magnetic amplifier 1
$v_2 min, v_2 max$	Saturating limits of magnetic amplifier 2

PRIME-MOVER AND GOVERNOR

u	Sleeve movement
u_o	Governor constant determined by speeder-gear setting
G_1	Constant of governor
u_1	Governor valve position
G_2	Gain constant of governor valve and relay system
τ_7, τ_8	Time-constant of governor valve
G_3	Transfer constant of stop valve
P_s	Steam power admitted to turbine
T_i	Torque input to rotor
τ_q	Turbine delay, sec.

TRANSMISSION CIRCUIT

V_b	132 kv bus-bar voltage
X_t, R_t	Total reactance and resistance respectively between generator terminals and bus-bar
$\Delta v_d, \Delta v_q$	Voltages between generator terminals and bus-bar in d- and q-axes respectively

p is the derivative operator $\frac{d}{dt}$, time in seconds.

N.B. The numerical values used in the thesis are in Reciprocal Per-Unit System unless otherwise stated.

CHAPTER 1

INTRODUCTION

(1.1) PROBLEMS OF MODERN POWER SYSTEM OPERATION

With the rapid changes in the present-day power system development, the analysis of power systems and synchronous machines has assumed a major importance in recent years. The continued trend towards larger individual generating units due to economic reasons and the transport of bulk power over long distance transmission line at extra high voltage due to the geographical separation of load areas from the generating stations, has resulted in complication of system operation. Depending on the severity of the disturbance, rotating plant may, at times, be projected into regions from which it may not spontaneously recover thereby causing a disruption or deterioration in supply. Automatic controlling devices are, therefore, being increasingly used in order to assist the system or the connected machines to ride through a disturbance or respond spontaneously to varying system operating conditions. The desirability of increasing the efficiency of a system has resulted in the tendency of operating the system and the generators within a narrow margin of the stability limit.

While recognising the various improvements that have been achieved from the modern trend in power system planning,

design and efficient operation, it is accepted that, in recent years, a number of specific problems having increasing influence on the system performance have emerged.

(a) The special features of the modern design of a synchronous generator are:

(i) Increasing generator rating
(ii) Lower inertia
(iii) Lower short-circuit ratio
(iv) High reactance

(b) In case of an interconnected network with increasing transmission system voltage, the technical problems confronting the operation of the system are:

(i) Insulation co-ordination
(ii) Protection of interconnected network
(iii) Voltage stability and regulation for a long distance transmission line
(iv) Reactive power compensation
(v) Recovery of normal operation after a system disturbance, particularly when single circuit lines are used.

All these factors, therefore, emphasise the importance of an analytical technique for the reliable pre-determination of the steady state, and transient performance of synchronous systems and machines.

(1.2) MATHEMATICAL REPRESENTATION APPROPRIATE TO DIFFERENT STUDIES

When assessing the transient response of an integrated system it seems rewarding to recognise a division of interest between studies of interconnected network system, on the one hand, and those concerned more with the response of individual

generators on the other. In the former, the complete system analyses, it is usual to carry out checks of the steady state and transient stability limits when designing new systems or reinforcing the existing ones. The essential requirement in these is that of adequately representing an integrated system of generators, transmission and distribution circuits and loads. It is also necessary to postulate from a very wide range of possibilities the combination of conditions for which the analyses are to be carried out, since it may not be possible, it may neither be necessary to design a system to cater for all possible conditions of operations.

Much of the success of such analyses which are invariably of a large scale nature, rests on reducing the system representation to the simplest form whilst, at the same time, preserving its essential physical properties. Sometimes a gradation of the simplification of system representation may be necessary depending on the location of the point of disturbance.

In relating the system reduction to the specific requirements of a study it should also be consistent with the tolerance to be allowed on problem data, the grouping of generators within a power station for representation as a single equivalent generating unit and the probability of the conditions adopted for analysis occurring in practice in the postulating combination. The real nature of these analyses

is in many cases less concerned with the solution of the system equations and more with the trend of these solutions for a range of different conditions of interconnections.

It therefore frequently follows that, in large scale system stability analyses, the emphasis is usually much less on the accuracy with which the system is represented and more on giving consideration to as wide a range of system conditions as possible. Specific conditions may, however, sometime perforce a satisfactory representation of a part of the integrated network. Analyses of voltage sensitive loads may be considered as an example.

Coming to the specific analyses of individual generating units a much more comprehensive mathematical formulation of generator electrodynamics becomes necessary. Such requirements are usually necessary for assessing the performance of a generator when new design features are incorporated and for developing new controlling techniques relating their applications to the synchronous machine. The development of new components such as excitation system, automatic voltage regulator or governing mechanisms are more conditioned by the characteristics of individual generating units to which such components are attached than by the integrated system. Here again, the degree of representation of the different parts of the complete unit should be compatible as an insufficient representation of one part might well invalidate

or influence the correct contribution of others that themselves are adequately represented. The relationship among the representation of the various elements of the complete unit is then an essential consideration in the detailed analyses of the transient performance of a generating unit.

(1.3) THE IMPORTANCE OF FULL SCALE TESTS

The results obtained from the purely theoretical study have been accepted, in the past, as adequate. With the continued trend towards operating a system or a generator within the narrow stability margin a doubt is cast as to the maintenance of the well-established analytical technique based on approximate methods. Within the last decade or so an increasing emphasis has been given to the experimental verification of the validity of the purely mathematical analysis. The interest for such a searching study has arisen from two main reasons:

(a)[17] It is not only that the experimental results check the accuracy of the computations and give confidence in the theory, but, more important, an experimental program provides pointers to the way in which the theory needs to be developed. The formulation of the theory is more likely to introduce errors than the computation.

(b) Once the confidence on the validity of the

theoretical work is gained by experimental verification and thus adding refinement to the theory, the degree of extrapolation required to predict adequately the behaviours of a larger machine or a system of new design may be reliably minimised.

In the United Kingdom several full-scale tests have been carried out with various sizes of generating units and different degree of network interconnection.[27-29] While in several instances the purpose of the tests was to investigate the dynamic performance of a generator connected to a large system and subjected to disturbances of varying severity, the assessment of the contribution of fast acting voltage regulators and other controlling devices has formed the main purpose of several other tests.

(1.4) PURPOSE OF THE PRESENT INVESTIGATION

In the present investigation a mathematical model of a synchronous machine in terms of the dqo reference frame was developed including the quantities that are usually neglected in conventional machine analyses. In further developing the analytical technique to establish a general model, it was required to collect together the equations of typical excitation systems and, as far as possible, the equations of a steam turbine and its associated governing system.

An important part of the complete investigation has been

the verification of the mathematical representations by comparing the results obtained from computer analyses with those obtained from tests carried out in Goldington and Belvedere power stations. To incorporate improvements into the mathematical model it was required to develop a method by which the effects of magnetic saturation are represented throughout a complete transient study. An essential part of the present research has been devoted to formulate improved methods for representing the complicated distribution of eddy-currents in solid rotor under transient conditions.

The model was also put to the test of experimental analyses of pole-slipping conditions in order to assess the peak induced rotor voltages in an a.c. excited generator under conditions of operation in which, owing to the voltage regulator action, the mmf balance between the stator and the rotor is lost, thereby giving rise to a rapid variation in rotor flux-linkage and an attended high induced voltage to which the rectifiers are subjected.

A flexible digital computer program was developed so that, apart from studying the various aspects of a single machine system, it can be extended to study a system where more than one machine is present.

CHAPTER II

(2) MATHEMATICAL MODEL OF A TURBO-ALTERNATOR UNIT

(2.1) THE SYNCHRONOUS GENERATOR

The layout of the windings of a 2-pole 3-phase synchronous generator is shown in Fig.1. The field and the armature windings are represented by f,a,b and c respectively. The axis of the field winding lies along the magnetic axis of the rotor. The rotor body of a turbo-alternator is usually forged from solid iron and so, under any transient operating conditions, eddy-currents are induced in the rotor due to variation of flux linking with it. The eddy-current paths are not easily definable and initially they are represented by two short-circuited coils, k_d and k_q, one of which lies along the magnetic axis of the rotor and the other is electrically at quadrature to it. The direction of rotation of the rotor is taken to be anti-clockwise.

(2.1.1) THE BASIC EQUATIONS

Based on the above arrangement, the following basic equations may be written in generalised M.K.S. units[1]. For power frequency operation, any capacitive effect is small compared with resistances and reactances and is neglected.

(a) Instantaneous voltage equations

(i) Stator:

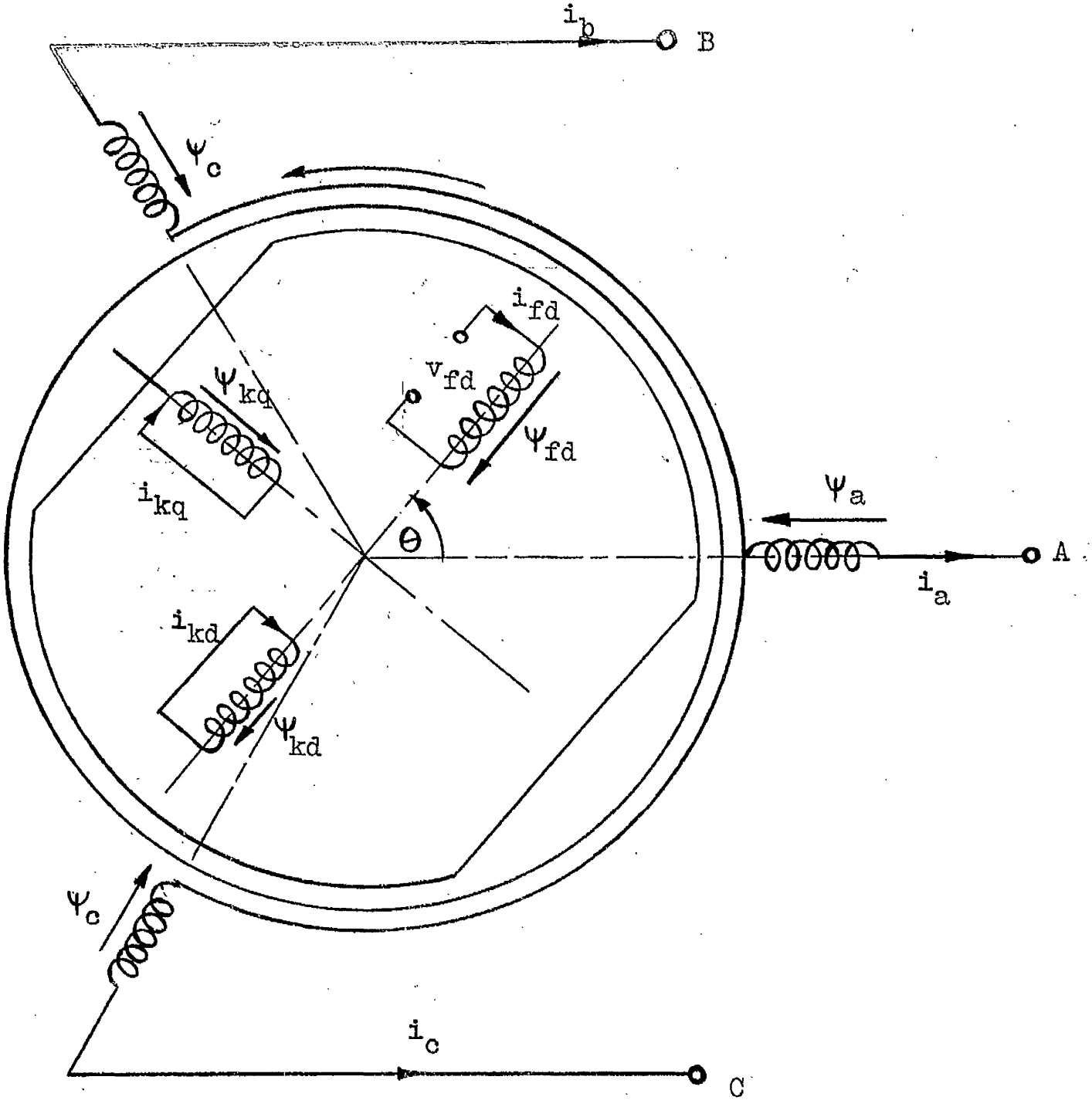

FIG. 1 SCHEMATIC LAYOUT OF THE WINDING OF A SYNCHRONOUS MACHINE

$$v_a = p\psi_a - R_a i_a$$
$$v_b = p\psi_b - R_b i_b \qquad (2.1)$$
$$v_c = p\psi_c - R_c i_c$$

(ii) Rotor

$$v_{fd} = p\psi_{fd} + R_{fd} i_{fd}$$
$$0 = p\psi_{kd} + R_{kd} i_{kd} \qquad (2.2)$$
$$0 = p\psi_{kq} + R_{kq} i_{kq}$$

(b) Instantaneous flux-linkage equations

(i) Stator:

$$\psi_a = -l_{aa} i_a + i_{ab} i_b + l_{ac} i_c + l_{afd} i_{fd} + l_{akd} i_{kd} + L_{akq} i_{kq}$$
$$\psi_b = +l_{ba} i_a - l_{bb} i_b + l_{bc} i_c + l_{bfd} i_{fd} + l_{bkd} i_{kd} + l_{bkq} i_{kq} \qquad (2.3)$$
$$\psi_c = +l_{ca} i_c + l_{cb} i_b - l_{cc} i_c + l_{cfd} i_{fd} + l_{ckd} i_{kd} + l_{ckq} i_{kq}$$

(ii) Rotor:

$$\psi_{fd} = -l_{fad} i_a - l_{fbd} i_b - l_{fcd} i_c + l_{ffd} i_{fd} + l_{fkd} i_{kd} + l_{fkq} i_{kq}$$
$$\psi_{kd} = -l_{kad} i_a - l_{kbd} i_b - l_{kcd} i_c + l_{kfd} i_{fd} + l_{kkd} i_{kd} + l_{kdq} i_{kq} \qquad (2.4)$$
$$\psi_{kq} = -l_{kaq} i_a - l_{kbq} i_b - l_{kcq} i_c + l_{kfq} i_{fd} + l_{kqd} i_{kd} + l_{kkq} i_{kq}$$

(c) Electrical power output at the terminal

$$P_e = v_a . i_a + v_b . i_b + v_c . i_c \qquad (2.5)$$

(d) Electro-dynamic equation of motion

$$P_i = Mp^2\delta + P_e + P_l - p\theta \qquad (2.6)$$

(2.1.2) THE BASIC ASSUMPTIONS

The equations (2.1) to (2.4) cannot be solved since the instantaneous values of the inductance coefficients given above are not yet known. It is, therefore, necessary to

define the instantaneous values of these coefficients so that the equations become amenable to solution. To do so the following assumptions are necessary.

(i) So far as the mutual effects with the rotor are concerned the stator windings are sinusoidally distributed along the air-gap.

(ii) The reluctance of the air gap varies sinusoidally round the rotor periphery.

(iii) Harmonics are neglected.

(iv) Hysteresis is neglected.

From the constructional point of view, every attempt is made to satisfy the first two assumptions and any imperfections which may create harmonics are negligibly small. The importance of hysteresis will be discussed later, but for the present purpose it is neglected, otherwise the equations become complicated because of the difficulty of mathematical representation of the hysteresis loop.

On the basis of these assumptions, the inductance coefficients can be expressed in the following way.[4] For an instantaneous angle θ between the field-winding axis and the axis of the phase 'a' as shown in Fig. 1,

The stator self inductances

$$\begin{aligned} l_{aa} &= L_{aao} + L_{aa2}\cos 2\theta \\ l_{bb} &= L_{aao} + L_{aa2}\cos 2(\theta - 120^{o}) \\ l_{cc} &= L_{aao} + L_{aa2}\cos 2(\theta - 240^{o}) \end{aligned} \qquad (2.7)$$

The stator mutual inductances

$$\begin{aligned} l_{ab} &= l_{ba} = L_{abo} + L_{aa2}\cos 2(\theta + 30^{o}) \\ l_{bc} &= l_{cb} = L_{abo} + L_{aa2}\cos 2(\theta - 90^{o}) \\ l_{ca} &= l_{ac} = L_{abo} + L_{aa2}\cos 2(\theta + 150^{o}) \end{aligned} \qquad (2.8)$$

The rotor self-inductances

$$\begin{aligned} l_{ffd} &= L_{ffd} \\ l_{kkd} &= L_{kkd} \\ l_{kkq} &= L_{kkq} \end{aligned} \qquad (2.9)$$

The rotor mutual inductances

$$\begin{aligned} l_{fkd} &= l_{kfd} = L_{fkd} \\ l_{kfq} &= l_{fkq} = l_{kqd} = l_{kdq} = 0 \end{aligned} \qquad (2.10)$$

The stator to rotor mutual inductances

$$\begin{aligned} l_{afd} &= l_{fad} = L_{afd}\cos\theta \\ l_{akd} &= l_{kad} = L_{akd}\cos\theta \\ l_{akq} &= l_{kaq} = -L_{akq}\sin\theta \\ l_{bfd} &= l_{fbd} = L_{afd}\cos(\theta - 120^{o}) \\ l_{bkd} &= l_{kbd} = L_{akd}\cos(\theta - 120^{o}) \\ l_{bkq} &= l_{kbd} = -L_{akq}\sin(\theta - 120^{o}) \\ l_{cfd} &= l_{fcd} = L_{afd}\cos(\theta - 240^{o}) \\ l_{ckd} &= l_{kcd} = L_{akd}\cos(\theta - 240^{o}) \\ l_{ckq} &= l_{kcq} = -L_{akq}\sin(\theta - 240^{o}) \end{aligned} \qquad (2.11)$$

Substituting these inductances into equations (2.3) and (2.4) a new flux linkage relationship is obtained as shown in matrix form in Fig.2.

Ψ_a	$-L_{aao} - L_{aa2}\cos 2\theta$	$L_{abc} + L_{aa2}2(\theta+30^o)$	$L_{abo} + L_{aa2}\cos 2(\theta+150^o)$	$L_{afd}\cos\theta$	$L_{akd}\cos\theta$	$-L_{kaq}\sin\theta$	i_a
Ψ_b	$L_{abo} + L_{aa2}\cos 2(\theta+30^o)$	$-L_{aa2} - L_{aa2}\cos 2(\theta-120^o)$	$L_{abo} + L_{aa2}\cos 2(\theta-90^o)$	$L_{bfd}\cos(\theta-120^o)$	$L_{bkd}\cos(\theta-120^o)$	$-L_{kbq}\sin(\theta-120^o)$	i_b
Ψ_c	$L_{abo} + L_{aa2}\cos 2(\theta+150^o)$	$L_{abo} + L_{aa2}\cos 2(\theta-90^o)$	$-L_{aao} - L_{aa2}\cos(\theta-240^o)$	$L_{cfd}\cos(\theta-240^o)$	$L_{ckd}\cos(\theta-240^o)$	$-L_{kcq}\sin(\theta-240^o)$	i_c
Ψ_{fd}	$-L_{fdd}\cos\theta$	$-L_{fbd}\cos(\theta-120^o)$	$-L_{fcd}\cos(\theta-240^o)$	L_{ffd}	L_{fkd}		i_{fd}
Ψ_{kd}	$-L_{kad}\cos\theta$	$-L_{kbd}\cos(\theta-120^o)$	$-L_{kcd}\cos(\theta-240^o)$	L_{kfd}	L_{kkd}		i_{kd}
Ψ_{kq}	$L_{kaq}\sin\theta$	$L_{kbq}\sin(\theta-120^o)$	$L_{kcq}\sin(\theta-240^o)$			L_{kkq}	i_{kq}

FIG.2 FLUX LINKAGE RELATIONSHIP IN abc SYSTEM

(2.2) MATHEMATICAL MODEL IN d-q-O REFERENCE FRAME

The flux-linkage relations that are given in Fig.2 are complicated for solution because the instantaneous value of the inductance coefficients depends on the position of the rotor axis at every instant, and some simplification of the equations is desirable. Mathematically, there are different ways of transforming the same equations into different frames of reference. In fact Kron[2] has broadly classified the various reference-frames into which electrodynamic equations of machine analysis can be transformed. The choice of any of these frames depends on the type of problem under investigation as all of them are not equally suitable for a particular problem. As Kron[3] asserts, in electrodynamics, for each type of phenomena there exists a most simple and practical form. In power system analyses the dqo frame of reference is most widely used. Blondel[4], later Doherty and Nickle[5] and subsequently Park[6] used this transformation which leads to what is commonly known as "Two Reaction Theory". In this frame of representation both the rotor and the stator windings are regarded as being rigidly connected to the rotor or the field structure. The transformation resolves the time-varying inductances into two fixed components along two axes - one along the polar axis of the rotor, called the direct axis, and the other along the interpolar axis, called the quadrature axis. The

physical significance of Park's transformation is that the 3-phase a.c. machine is replaced by an equivalent 2-phase generator with brushes on the direct and quadrature axes.

(2.2.1) PARK'S TRANSFORMATION

The process of transformation of the 3-phase variables to dqo frame of reference is achieved in the following way.

Writing $[P]$ for Park's transformation matrix

$$\frac{2}{3}\begin{bmatrix} \cos(\theta) & \cos(\theta-120^{o}) & \cos(\theta-240^{o}) \\ -\sin(\theta) & -\sin(\theta-120^{o}) & -\sin(\theta-240^{o}) \\ \frac{1}{2} & \frac{1}{2} & \frac{1}{2} \end{bmatrix} \qquad (2.12)$$

and $[P]^{-1}$ for the matrix for inverse transformation which is

$$\begin{bmatrix} \cos\theta & -\sin(\theta) & 1 \\ \cos(\theta-120^{o}) & -\sin(\theta-120^{o}) & 1 \\ \cos(\theta-240^{o}) & -\sin(\theta-240^{o}) & 1 \end{bmatrix} \qquad (2.13)$$

the relations between the 3-phase and dqo variables are given in the following way:

$$[dqo] = [P][abc] \qquad (2.14)$$

and

$$[abc] = [P]^{-1}[dqo] \qquad (2.15)$$

where $[abc]$ and $[dqo]$ designate the variables of the 3-phase machine and those of the quasi-nonholononic reference frame respectively.

A more detailed description of the process of Park's transformation is given in Appendix A, including the different

stages that are involved in the transformation. It may be concluded from what is described in Appendix A that the analysis of a 3-phase machine for balanced and symmetrical operation is carried out by taking only phase 'a' into consideration. The effect of other two phases is eliminated during the process of transformation. Validity of such analyses is maintained due to the fact that for symmetrical operation, whether under steady-state or transient operation, the effects in all the phases are identical except 120^{o} phase-differences. This has been verified during full-scale site-tests.[7]

Applying the transformation to the phase variables of a 3-phase machine the following expressions for flux linkages and voltages are obtained in the dqo frame of reference.

Flux-linkage equations

$$\begin{aligned}
\psi_d &= L_{afd}i_{fd} + L_{akd}i_{kd} - L_d i_d \\
\psi_q &= L_{akq}i_{kq} - L_q i_q \\
\psi_o &= - L_o i_o \\
\psi_{fd} &= L_{ffd}i_{fd} + L_{fkd}i_{kd} - \tfrac{3}{2}L_{afd}i_d \\
\psi_{kd} &= L_{fkd}i_{fd} + L_{kkd}i_{kd} - \tfrac{3}{2}L_{akd}i_{kd} \\
\psi_{kq} &= L_{kkq}i_{kq} - \tfrac{3}{2}L_{akq}i_{kq}
\end{aligned} \qquad (2.16)$$

Voltage equations

$$\begin{aligned} v_d &= p\psi_d - R_d i_d - \psi_q p\theta \\ v_q &= p\psi_q - R_q i_q + \psi_d p\theta \\ v_o &= p\psi_o - R_o i_o \\ v_{fd} &= p\psi_{fd} + R_{fd} i_{fd} \\ 0 &= p\psi_{kd} + R_{kd} i_{kd} \\ 0 &= p\psi_{kq} + R_{kq} i_{kq} \end{aligned} \qquad (2.17)$$

where

$$\begin{aligned} L_d &= L_{aao} + L_{abo} + \tfrac{3}{2}L_{aa2} \\ L_q &= L_{aao} + L_{abo} - \tfrac{3}{2}L_{aa2} \\ L_o &= L_{aao} + 2L_{abo} \end{aligned} \qquad (2.18)$$

(2.2.2) EQUATIONS IN PER-UNIT SYSTEM

Among the various per-unit systems which provide a procedure for nondimensionalizing the different variables of a machine, the reciprocal system is found most attractive in case of a machine having damper windings.[8] Application of this per-unit system makes the mutual inductances among the different windings along each axis assume a fixed value. The method of developing the reciprocal per-unit system is illustrated in Appendix B following the approach suggested by White & Woodson[9] and in reference (21)

The generator equations when converted into reciprocal per-unit system are:

Direct axis:

$$\begin{aligned} \psi_d &= L_{ad}i_{fd} + L_{ad}i_{kd} - L_d i_d \\ \psi_{fd} &= L_{ffd}i_{fd} + L_{ad}i_{kd} - L_{ad}i_d \\ \psi_{kd} &= L_{ad}i_{fd} + L_{kkd}i_{kd} - L_{ad}i_d \end{aligned} \tag{2.19}$$

$$\begin{aligned} v_d &= p\psi_d - R_d i_d - \psi_q p\theta \\ v_{fd} &= p\psi_{fd} + R_{fd}i_{fd} \\ 0 &= p\psi_{kd} + R_{kd}i_{kd} \end{aligned} \tag{2.20}$$

Quadrature axis:

$$\begin{aligned} \psi_q &= L_{aq}i_{kq} - L_q i_q \\ \psi_{kq} &= L_{kkq}i_{kq} - L_{aq}i_q \end{aligned} \tag{2.21}$$

$$\begin{aligned} v_q &= p\psi_q - R_q i_q + \psi_d p\theta \\ 0 &= p\psi_{kq} + R_{kq}i_{kq} \end{aligned} \tag{2.22}$$

The above equations describe the electrodynamics of a 3-phase synchronous generator under symmetrical and balanced conditions except for the fact that the axis currents, i_d and i_q, depend on the external machine connections. Otherwise, with two equivalent short-circuited coils to represent eddy-current phenomena, equations (2.19) to (2.22) represent the complete process of electro-mechanical energy conversion in a synchronous machine. In conventional synchronous generator analyses with network analyser or analogue computer many assumptions are made to simplify the above equations.[10] Some of the usual ones are:

(a) The stator voltages induced by rate of change of

flux-linkage (i.e. $p\psi_d$ and $p\psi_q$) are assumed negligible.

(b) The speed-change during a transient is assumed to be negligible (i.e. $\Delta p\theta = 0$).

(c) Subtransient effects are neglected and thus the eddy-current phenomena are ignored and, instead, the torque due to eddy current and mechanical friction is represented by a single torque which is proportional to the instantaneous departure of the rotor speed from fundamental frequency.

(d) Saturation is neglected.

(e) Transient and subtransient saliency are neglected.

The quantitative effect of making some of the above mentioned assumptions are discussed later.

To complete the mathematical model the other equations that are required are:

Output power

$$P_e = v_d i_d + v_q i_q \qquad (2.23)$$

Terminal voltage

$$v_m = \left\{v_d^2 + v_q^2\right\}^{\frac{1}{2}} \qquad (2.24)$$

Dynamic equation of motion

$$P_i = Mp^2\delta + P_e + P_1 + k_d p\theta \qquad (2.25)$$

(N.B.) The equations relating to the output currents of the machine have been omitted at this stage as they depend on the nature of the external connection and, as such, no general expression can be written down at this stage.

(2.3) THE TRANSMISSION SYSTEM EQUATIONS

A turbo-alternator is usually connected to system busbar through a unit transformer and a short length of cable or transmission line. The busbar and the system to which the machine is connected may be considered, for a specific problem of analysing a single machine system, to be a voltage source of constant amplitude and frequency and remain unaffected during any transient that may arise in the machine. The magnetising current and the phase-shift caused by it in the unit transformer is negligibly small. Lumped series inductance and resistance are used to represent the transformer and the transmission circuit and capacitances of any kind are neglected for power frequency operation. The effect of transformer tap position may be taken into consideration by knowing the turns ratio of each tap position.

By using Park's transformation the transmission system equations may then be resolved into the generator direct and quadrature axes and the following relations are obtained.

$$\begin{aligned} \Delta v_d &= \frac{X_t}{\omega_o} p i_d + R_t i_d - \frac{\omega}{\omega_o} X_t i_q \\ \Delta v_q &= \frac{X_t}{\omega_o} p i_q + R_t i_q + \frac{\omega}{\omega_o} X_t i_d \end{aligned} \qquad (2.26)$$

where

$$\begin{aligned} \Delta v_d &= v_d - v_b \sin \delta \\ \Delta v_q &= v_q - v_b \cos \delta \end{aligned} \qquad (2.27)$$

(2.4) AUTOMATIC VOLTAGE REGULATOR AND EXCITATION SYSTEM

The effective contribution of a fast-acting automatic voltage regulator towards accurate control of terminal voltage and increasing the dynamic stability limit of synchronous machines is well established[11]. The action of a controlled excitation system in generating positive damping during transients in an alternator has been experimentally verified in previous analytical studies[12]. Proposals[13] have been made in recent years for the development of additional subsidiary feedback signals from various strategic sources in the machine so that the action of such regulating systems momentarily over-rides or supplements the main terminal voltage signals in order to stabilise the operation of the generators when their conditions deviate from those of normal power generation.

A part of the author's M.Sc. work[14,30] was concerned with the investigation of the possible ways of optimising the operation of a modern voltage regulator when connected to a particular machine. A searching study was also made to find out the possible contribution that can be derived from subsidiary feedback signals depending on various functions of rotor-angle.

A typical excitation system including an automatic voltage regulator is shown in the form of a block diagram in Fig.3. The main forward loop consists of an error-sensing element, the output of which drives two stages of magnetic

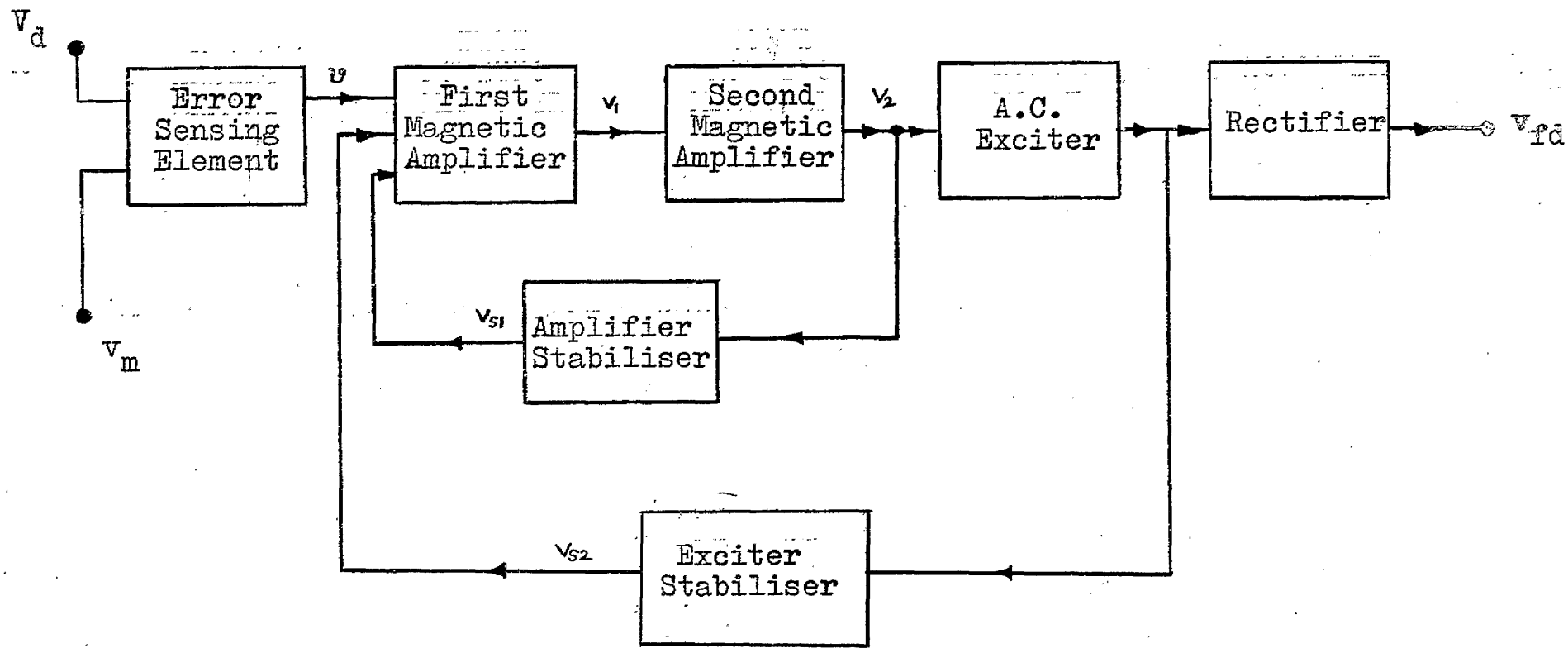

FIG. 3 BLOCK DIAGRAM OF A VOLTAGE REGULATING SYSTEM

amplifiers. The output of the second amplifier controls the field of the main exciter. The saturation limits of the magnetic amplifiers and the main exciter are considered by linear approximation as shown in Fig.4. Among the various possible derivations of stabilizing loops, two of them are shown in the block diagram of Fig.3.

The response characteristics of the automatic voltage regulator and the exciter are based on the following assumptions.

(a) The transfer characteristics of the control and main exciters may be represented by straight line segments.

(b) The parameters of the regulator remain constant throughout any transient.

(c) The characteristics of the rectifier in an a.c. excitation system may be represented by constraining the rotor current to have one polarity only.

(d) Operation of the var limiter is assumed to be absent.

The equations are then:

Comparator:

$$v = k_o(V_d - \vartheta_m) \tag{2.28}$$

Magnetic amplifier (1):

$$v_1 = \frac{k_1}{1 + {}_1p}(v - v_{s1} - v_{s2}) + C_1 \tag{2.29}$$

$$\text{for } v_1 \text{min} \leq v_1 \leq v_1 \text{max}$$

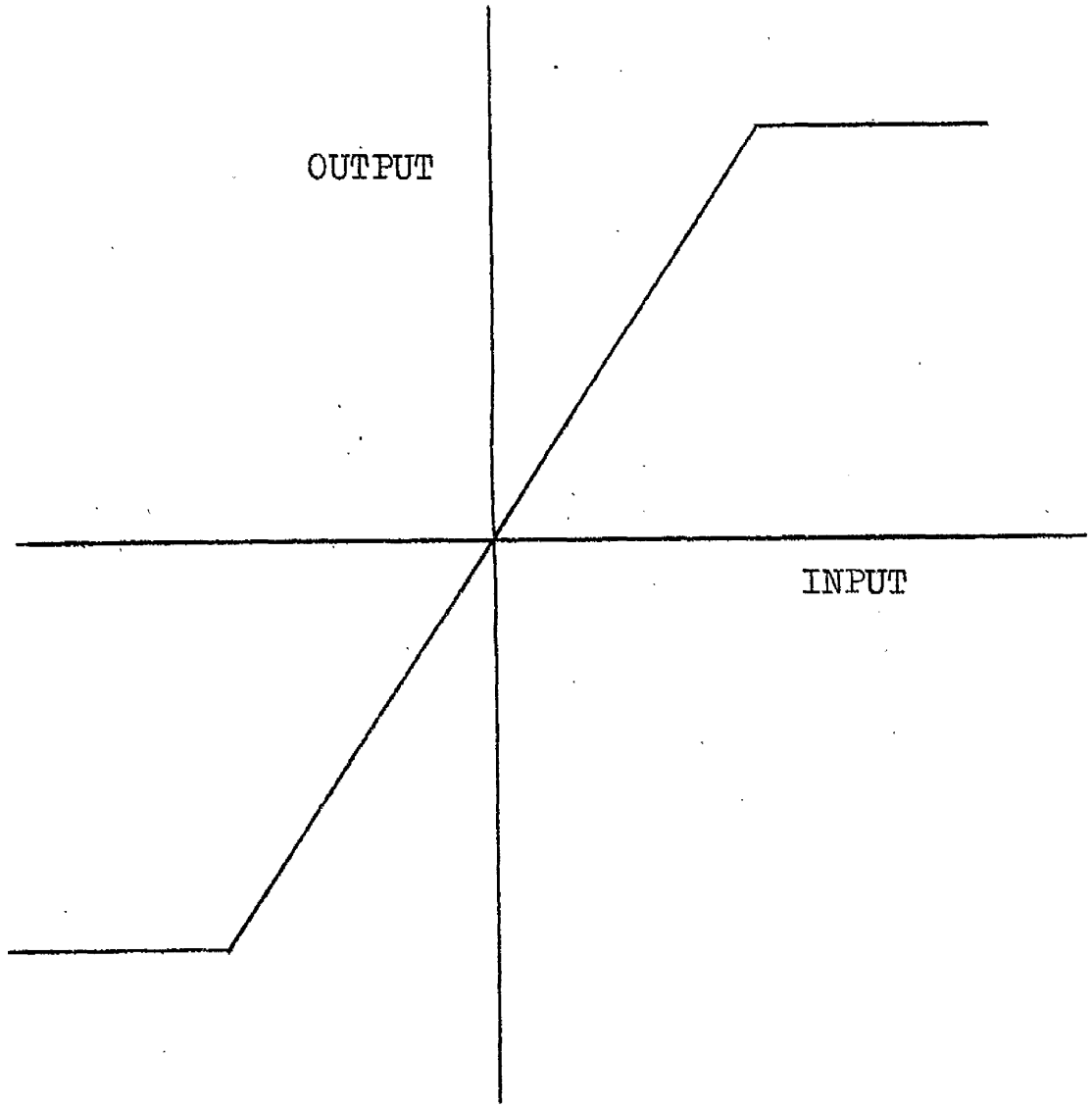

FIG. 4 REPRESENTATION OF EXCITER AND MAGNETIC AMPLIFIER SATURATION

Magnetic amplifier (2):

$$v_2 = \frac{k_2 v_1}{1 + \tau_2 p} + C_2 \qquad (2.30)$$

$$\text{for } v_2 min \leq v_2 \leq v_2 max$$

The main exciter:

$$v_{fd} = \frac{k_e v_2}{1 + \tau_e p} + C_e \qquad (2.31)$$

Stabilising signal from magnetic amplifier (2):

$$v_{s1} = \frac{k_3 \tau_3 p v_2}{1 + \tau_4 p} \qquad (2.32)$$

Stabilising signal from the main exciter:

$$v_{s2} = \frac{k_4 \tau_5 p v_{fd}}{1 + \tau_6 p} \qquad (2.33)$$

(2.5) PRIME MOVER AND GOVERNOR

The governor, considered here, is a standard oil-servo type. The power admitted to the turbine through the stop-valve and pilot valves is controlled in accordance with the main shaftspeed which operates the centrifugal governor. A simplified representation of the physical system is shown in Fig.5 and are based on assumptions, the most significant of which are:

(a) The delays in the prime-mover, governor valve and pilot valve are represented by single time-constants.

(b) The delays in the centrifugal governor and relay mechanism are neglected.

(c) Boiler control are assumed to be inoperative

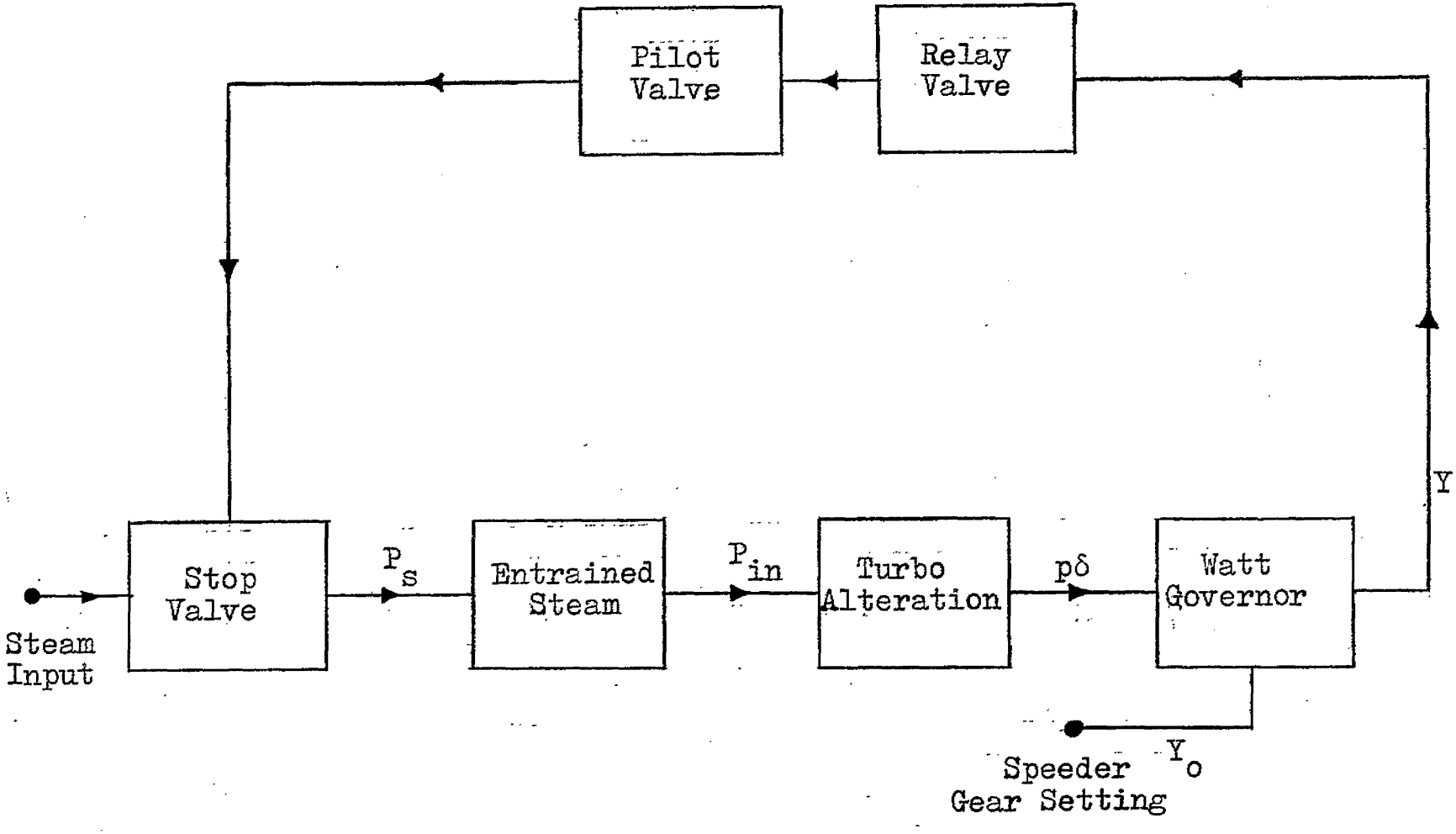

FIG.5 BLOCK DIAGRAM OF GOVERNING SYSTEM

during the transient period and so the power input to the stop-valve is constant.

(d) The governor sleeve movement responds instantly to changes in the generator shaft speed.

Then sleeve movement of the centrifugal governor:

$$u = U_o - G_1 p\delta \qquad (2.34)$$

for $0 \leq u \leq 1$

in which U_o is determined by the speeder-gear setting.

The governor valve position:

$$u_1 = \frac{G_2 u}{(1 + \tau_7 p)(1 + \tau_8 p)} + u_k \qquad (2.35)$$

for $0 \leq u_1 \leq 1$

The position of the stop-valve is taken to exert a linear control on the power admitted to the prime-mover, and so the steam power at the stop valve is

$$P_s = G_3 u_1 \qquad (2.36)$$

Finally power input to the turbine:

$$P_i = \frac{P_s}{1 + \tau_9 p} \qquad (2.37)$$

CHAPTER III

SOLUTION OF THE EQUATIONS OF THE TURBO-ALTERNATOR MODEL

(3.1) GENERAL

The equations of the turbo-alternator model including excitation and governing systems as developed in Chapter II are inherently nonlinear involving multi-order differential equations having variable coefficients. The inclusion of the nonlinearities arising from magnetic circuit saturation in the generator and in the excitation control system, increases the difficulty in achieving a solution. A simplified linear form of analysis may be preserved where the studies may be confined to small perturbations of the system variables about a nominal operating point, if the parameters appropriate to this point are known. Small oscillation studies of this form have been used, in the past, in specific investigationsof the performance of excitation control systems[15]. It is, however, invariably necessary to follow this by large-disturbance studies to indicate the additional effects caused by limiting some of the system variables due to saturation and other constraints such as governor valve limits. A linearised form of solution is of limited value and often doubtful in the investigation of transient phenomena such as operation of a machine following a disturbance in the stator circuit, load rejection and

asynchronous running, for these give rise to conditions that depart substantially from those on which small oscillation studies are based. A realistic appraisal of the different modes of generator operations requires a detailed inclusion of all the nonlinearities.

At the same time, it is apparent that there is merit in a general mathematical formulation of the machine equations so that they are amenable to use for different kinds of studies including those in which it is required to represent more than one machine. The method of digital solution given here stems from the proposal for flexibility and generality in the analytical approach, it also provides the essential bases for small oscillation or large disturbance analysis or multi-machine assessments alike, without the need for rearrangement of the basic method of solution.

In the present investigation, the solution is confined to the study of a single synchronous generator, but the extension of the method to analyse a system having two or more machines is described later.

(3.2) SOLUTION OF THE DIFFERENTIAL EQUATIONS

The following differential equations are obtained when equations (2.19) to (2.21) are rearranged.

Direct axis:

$$\psi_d = L_{ad} \frac{(1 + \tau_{kd}p)}{1 + (\tau_{do}' + \tau_{kdo}')p + \tau_{do}'\tau_{do}''p^2} \cdot \frac{v_{fd}}{r_{fd}} - \frac{1 + (\tau_d' + \tau_{d1})p + \tau_d'\tau_d''p^2}{1 + (\tau_{do}' + \tau_{kdo}')p + \tau_{do}'\tau_{do}''p^2} \cdot L_d i_d \quad (3.1)$$

$$\psi_{fd} = L_{ffd} \frac{(1 + \tau_{do}''p)}{1 + (\tau_{do}' + \tau_{kdo}')p + \tau_{do}'\tau_{do}''p^2} \cdot \frac{v_{fd}}{r_{fd}} - \frac{(1 + \tau_{kd}p)}{1 + (\tau_{do}' + \tau_{kdo}')p + \tau_{do}'\tau_{do}''p^2} \cdot L_{ad} i_d \quad (3.2)$$

$$i_{fd} = \frac{(1 + \tau_{kdo}'p)}{1 + (\tau_{do}' + \tau_{kdo}')p + \tau_{do}'\tau_{do}''p^2} \cdot \frac{v_{fd}}{r_{fd}} + \frac{(1 + \tau_{kd}p)}{1 + (\tau_{do}' + \tau_{kdo}')p + \tau_{do}'\tau_{do}''p^2} \cdot \frac{L_{ad}(pi_d)}{r_{fd}} \quad (3.3)$$

$$i_{kd} = \frac{L_{ad}}{r_{kd}} \cdot \frac{p(i_d - i_{fd})}{(1 + \tau_{kdo}'p)} \quad (3.4)$$

Quadrature axis:

$$\psi_q = - \frac{1 + \tau_q''p}{1 + \tau_{kqo}''p} L_q i_q \quad (3.5)$$

$$i_{kq} = L_{aq} \cdot \frac{1}{(1 + \tau_{kqo}''p)} \cdot \frac{pi_q}{r_{kq}} \quad (3.6)$$

where the time constants as defined in the list of symbols are calculated from the following expressions:

$$\tau_{do}' = L_{ffd}/r_{fd} \quad (3.7)$$

$$\tau_{do}'' = \frac{1}{r_{kd}} \left\{ l_{kd} + \frac{L_{ad} \cdot l_{fd}}{L_{ad} + l_{fd}} \right\} \quad (3.8)$$

$$\tau_{kdo}' = L_{kkd}/r_{kd} \quad (3.9)$$

$$\tau'_d = \frac{1}{r_{fd}} \left\{ l_{fd} + \frac{L_{ad} \cdot l_d}{L_d} \right\} \qquad (3.10)$$

$$\tau''_d = \frac{1}{r_{kd}} \left\{ \frac{L_{ad} \cdot l_d \cdot l_{fd}}{L_{ad} \cdot l_{fd} + l_d \cdot l_{fd} + l_d \cdot L_{ad}} \right\} \qquad (3.11)$$

$$\tau_{d1} = \frac{1}{r_{kd}} \left\{ l_{kd} + \frac{L_{ad} \cdot l_d}{L_{ad} \cdot l_d} \right\} \qquad (3.12)$$

$$\tau_{kd} = \frac{l_{kd}}{r_{kq}} \qquad (3.12)$$

$$\tau''_{kqo} = \frac{L_{kkq}}{r_{kq}} \qquad (3.14)$$

$$\tau''_q = \frac{1}{r_{kq}} \left\{ l_{kq} + \frac{L_{aq} \cdot l_q}{L_q} \right\} \qquad (3.15)$$

The differential equations given above, as well as those for an automatic voltage regulator, excitation system, turbine and governing system are not directly amenable to solution by step-by-step forward integration methods in a digital computer. To use such methods it is required to derive a sequence containing non-differential terms which define the first order derivative of each of the integrable variables. For such reduction, the introduction of auxiliary variables may be necessary. The solution during an interval is achieved on the basis of the non-differential variables that are calculated from the linear algebraic equations, remaining constant during the step interval, and the differential variables having a constant rate of change as calculated

at the beginning of the interval. At the end of the step, when the final values of the integrable quantities are known, the algebraic equations are then solved to obtain their new values and the process is thus repeated for every step length. The complete rearrangement of the equations and an analysis of the process of solution is given in Appendix C.

(3.3) SOLUTION OF THE ALGEBRAIC EQUATIONS

As mentioned in Section (2.2.2), in Chapter II, the power output, and hence the stator current depends on the way in which the machine is externally connected. To derive an expression for stator current, a simple configuration of system connection as shown in Fig.6 is considered. The synchronous machine with its excitation system and turbine and governing system is connected, through a unit transformer and a short length of transmission line, to a large system which may be considered to remain unaffected by any change in the machine operating conditions. The vector diagram for steady state operation of a loaded machine for such interconnection is shown in Fig.7. The stator currents in the two axes can now be calculated from the following expressions neglecting the effect of flux change in the transmission line.

$$v_q - V_b \cos\delta = R_t i_q + \frac{\omega}{\omega_o} X_t i_d$$

$$V_b \sin\delta - v_d = -R_t i_d + \frac{\omega}{\omega_o} X_t i_q \qquad (3.16)$$

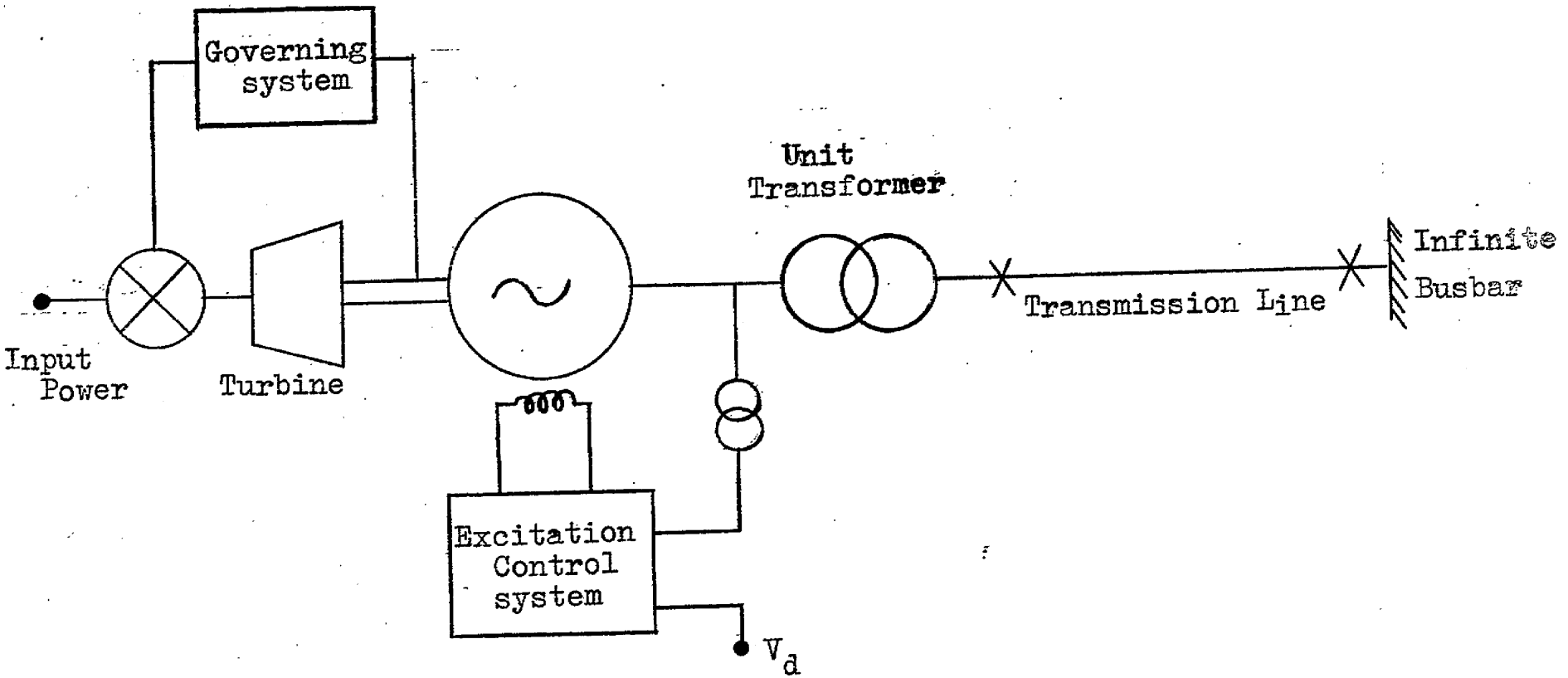

FIG. 6. BLOCK DIAGRAM OF A TURBO-ALTERNATOR UNIT CONNECTED TO AN INFINITE BUSBAR

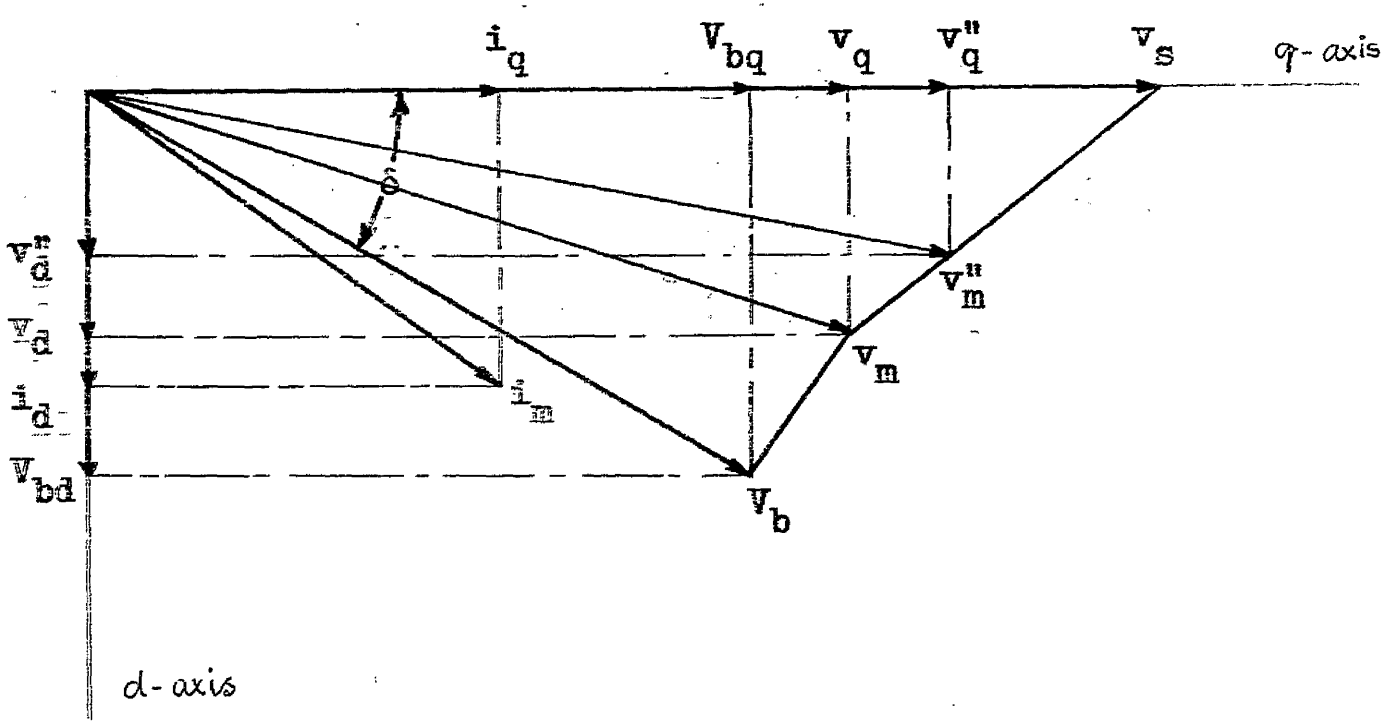

FIG. 7. VECTOR DIAGRAM FOR STEADY STATE OPERATION OF A SYNCHRONOUS MACHINE

These expressions are not, however, applicable during the transient operating conditions of a machine. For example, during a 3-phase short circuit at the machine-terminal when

$$v_q = v_d = V_b = X_t = R_t = 0$$

the stator current cannot be calculated from equation (3.16).

(3.3.1) CONCEPT OF SUBTRANSIENT QUANTITIES

The constant flux linkage theorem due to Doherty[16] states that in any closed electric circuit having no resistance the flux linkages will remain constant immediately after any change in the current, voltage or position of the other circuits to which it is magnetically couplied. In practical cases, where resistance is present, the flux linkages cannot remain constant, but the rate of change depends on the equivalent time constant of the circuit. Similarly, in machine operation the terminal quantities such as voltage, current and power, may be subjected to an abrupt change due to a discontinuity, but some of the internal quantities such as flux linkages follow the change at a much slower rate. For the calculation of rapid transients in synchronous machines it is, therefore, the usual practice to assume that slowly varying quantities remain unchanged during a small interval of time when the interval is small compared with the total time constant of the varying quantities. With an amortisseur winding on each axis, the flux linkage

that will take the longest time to change is that which exists behind the subtransient inductance.

In calculating the terminal variables during transient operations the subtransient voltages calculated from the subtransient flux linkages are considered. When modified, the equation (3.16) will be

$$\begin{aligned} v''_q - V_b \cos\delta &= R_t i_q + \frac{\omega}{\omega_o}(X_t + X''_d) i_d \\ V_b \sin\delta - v''_d &= -R_t i_d + \frac{\omega}{\omega_o}(X_t + X''_q) i_q \end{aligned} \tag{3.17}$$

$$\begin{aligned} \text{where } v''_q &= p\psi_q - R_a i_q + \psi''_d p\theta \\ v''_d &= p\psi_d - R_a i_d - \psi''_q p\theta \end{aligned} \tag{3.18}$$

The derivation of expressions for Ψ''_d and Ψ''_q has been shown in Appendix C.

Considering the example of a 3-phase short circuit, it is now possible to calculate the fault currents from equation (3.17) which gives

$$\begin{aligned} i''_d &= \frac{v''_q}{\frac{\omega}{\omega_o} X''_d} \\ \text{and} \qquad i''_q &= \frac{v''_d}{\frac{\omega}{\omega_o} X''_q} \end{aligned} \tag{3.19}$$

During the rearrangement of the differential equations, an attempt was made to get an expression of a subtransient term whenever possible and thus to maintain the highest accuracy from the step-by-step method of solution.

(3.3.2) THE ALGEBRAIC EQUATIONS

The necessary algebraic equations that are to be solved along with the differential equations are:

$$\psi_d = \psi''_d - L''_d i_d \tag{3.20}$$

$$\psi_{fd} = \psi''_{fd} - L''_{fd} i_d \tag{3.21}$$

$$\psi_q = \psi''_q + L''_q i_q \tag{3.22}$$

$$v_d = p\psi_d - R_a i_d - \psi_q p\theta; \quad v_q = p\psi_q - R_a i_q + \psi_q p\theta \tag{3.23}$$

$$P_e = v_d i_d + v_q i_q \tag{3.24}$$

$$P_\theta = v_q i_d - v_d i_q \tag{3.25}$$

$$v_m = \{v_d^2 + v_q^2\}^{\frac{1}{2}} \tag{3.26}$$

$$p\theta = \omega_o + p\delta \tag{3.27}$$

$$i_{fd} = i''_{fd} - L_d i_d \tag{3.28}$$

$$\psi_m = \{\psi_q^2 + \psi_d^2\}^{\frac{1}{2}} \tag{3.29}$$

$$P_l = \sum i^2 r \tag{3.30}$$

There are several other quantities which require estimation but precise mathematical expressions are not available for them. These are the rates of change of some of the machine variables such as pi_d. They are calculated by straight-line approximation and the method is illustrated in Fig.8. Other methods have been tried by taking into account of the values of the variable for one or two steps preceding the step for which the rate of change is required but for a small step length a single-step approximation has been found to be adequate. The quantities that are calculated in this way for the n th. step are:

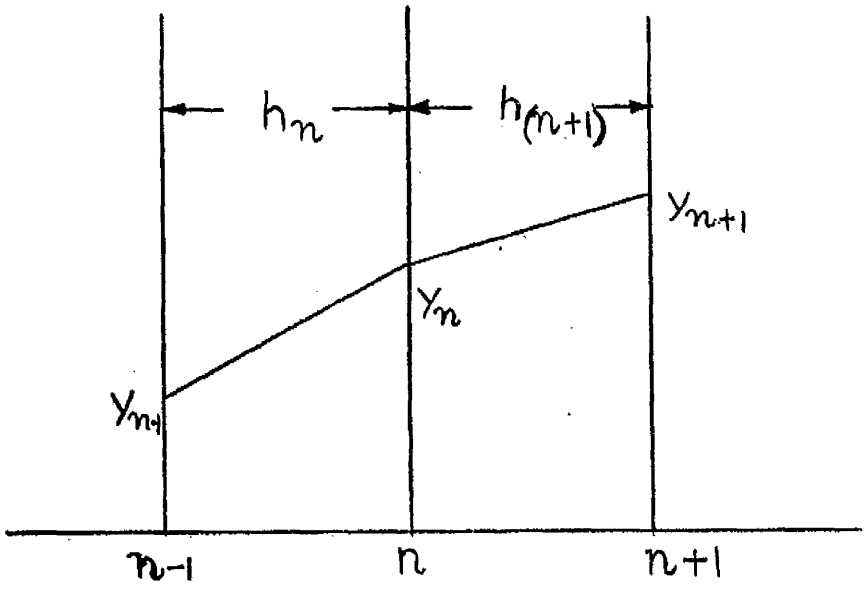

$$pY_{n+1} = \{Y_n - Y_{(n-1)}\}/h_n$$

FIG.8 SOLUTION OF EQUATIONS BY STRAIGHT LINE APPROXIMATION

$$pi_{d(n)} = \{i_{d(n)} - i_{d(n-1)}\}/h \quad (3.31)$$

$$pi_{q(n)} = \{i_{q(n)} - i_{q(n-1)}\}/h \quad (3.32)$$

$$p\psi_{d(n)} = \{\psi_{d(n)} - \psi_{d(n-1)}\}/h \quad (3.33)$$

$$p\psi_{q(n)} = \{\psi_{q(n)} - \psi_{q(n-1)}\}/h \quad (3.34)$$

$$p\psi_{fd(n)} = \{\psi_{fd(n)} - \psi_{fd(n-1)}\}/h \quad (3.35)$$

(3.4) APPLICATION OF DIGITAL COMPUTER FOR SOLUTION OF EQUATIONS

Of all the various computational aids for power-system analyses, the application of digital computers has found the greatest attraction in recent years. The advantages and disadvantages of digital analysis, compared with alternative methods, have been discussed on several occasions[17,18], and the general outcome appears to have been a substantial and apparently increasing preference for the use of digital methods.

In the present investigation a digital computer solution has been chosen because of its all round analytical power in this work and also in a wider pattern of power system research of which the present project is a part. Furthermore, the ease with which a program once developed may, at short notice, be used is in many ways a most significant advantage, particularly in promoting a continuity of work in long term investigational projects.

(3.4.1) INTEGRATION OF THE DIFFERENTIAL EQUATIONS

The integration of the differential equations is achieved by a step-by-step method. Several numerical techniques are available for such forward step solutions, but of these the most widely used and probably the simplest one, is the Runge-Kutta method, or its recent modified version, called the Kutta-Merson method. The use of several other techniques has been proposed [19], emphasising the advantage of longer step-lengths that can be used for different Predictor-Corrector methods for the same accuracy. In the present case, however, the retention of a comparatively small step interval is favoured in order to calculate accurately, the several quantities such as pi_d, $p\Psi_d$ by a straight-line approximation. Using the Kutta-Merson numerical routine, a step length of 5 millisecond has been found satisfactory from a series of studies using different step-lengths.

(3.4.2) VALIDITY OF REARRANGEMENT OF DIFFERENTIAL EQUATIONS

There are several ways in which the rearrangement of the differential equations in Section (3.2) may be carried out. The method chosen and its validity have been checked by taking the following system of equations.

$$f(y) = \frac{x}{1 + (A+B)p}$$

$$f(y) = \frac{x}{(1 + Ap)(1 + Bp)} \qquad (3.36)$$

$$f(y) = \frac{x(1 + Cp)}{(1 + Ap)(1 + Bp)}$$

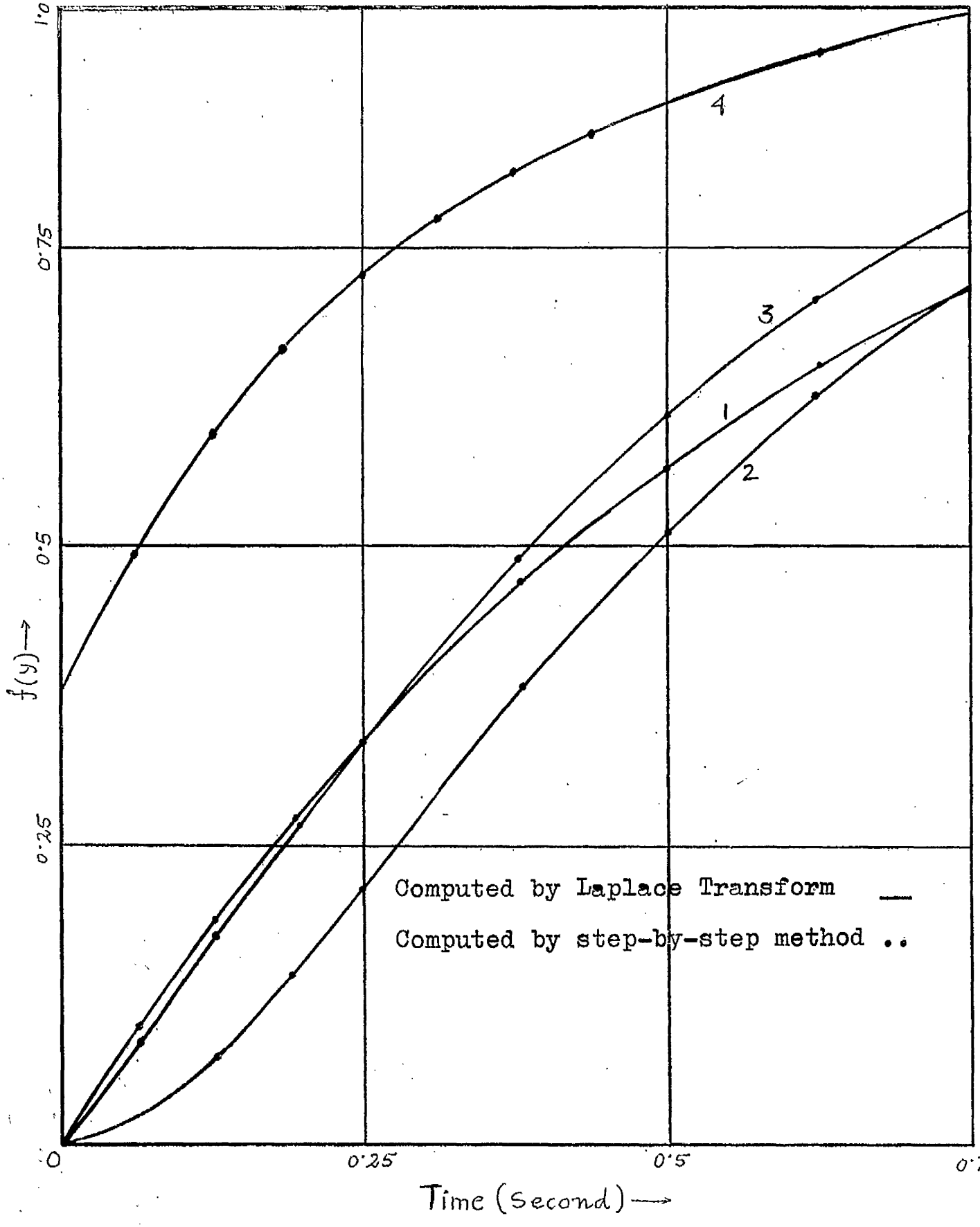

FIG. 9 SOLUTION OF DIFFERENTIAL EQUATIONS BY THE TWO METHODS MENTIONED IN CHAPTER III

and $$f(y) = \frac{x(1 + Cp)(1 + Dp)}{(1 + Ap)(1 + Bp)}$$

These four equations were first solved by applying Laplace Transform and then by the same process of rearrangement as has been adopted in the case of the turbo-alternator model. The result is shown in Fig.9. Assuming that the application of Laplace Transform yields the most exact solution for such differential equations, it is found from Fig.9 that the results obtained by these two methods are almost identical for a step length of 5 millisecond.

(3.4.3) SOLUTION OF THE ALGEBRAIC EQUATIONS

The algebraic equations given in equations (3.20) to (3.35) can be included within the integration routine, or excluded from it, to solve them at the end of each step interval. With a step-length of 5 millisecond, the accuracy gained by including them within the routine is negligibly small. The maximum error that has been found to occur was in the first step interval after a radical discontinuity in the process of solution. This error is eliminated during the subsequent steps without adding any adverse effect to the remainder of the solution since the transient solution is more conditioned by the differential equations than by the algebraic equations. The differential equations are not vulnerable to any sharp change due to the presence of time-constants.

(3.5) COMPARISON OF COMPUTED AND TEST RESULTS

A digital computer program was developed in Extended Mercury Auto-code for the numerical solution of the equations of the turbo-alternator model and to assess the accuracy of the model by comparing the computed results with those obtained from instrumented site tests. The physical system considered for the purpose of comparison is that of the test-arrangement for the site-tests conducted at Goldington Power Station[20,21]. The system connections for the tests are similar to that shown in Fig.6. The automatic voltage regulator, excitation system and prime-mover governing system attached to the test machine are also similar to those shown in block schematic form in Figs. 3 and 5. The rating of the machine and other necessary parameters for the model obtained from the manufacturers and from different test results are given in Tables I-III. Some of the parameters were adjusted following the suggestions made by Shackshaft[20]. The test machine was fitted with a static type a.c. excitation system, and so long as the field current does not attempt to reverse its polarity, the rectifiers do not modify the excitation characteristics, and consequently no extra constraints are necessary to represent the rectifier-characteristics.

(3.5.1) SYMMETRICAL 3-PHASE FAULT AT THE BUSBAR

The symmetrical 3-phase fault is the most severe disturbance condition of all the tests mentioned in Reference

TABLE 1

Parameters	Values supplied	Values computed at 1.0 p.u. terminal voltage
Machine rating	37.5 MVA, 11.8 KV 0.8 p.f.(lag) 3000 R.P.M.	-
X_d	2.00 (unsaturated)	1.816
X_q	-	1.816
X_{ad}	1.86 (unsaturated)	1.676
X_{aq}	1.86 (unsaturated)	1.676
X_{ffd}	2.00 (unsaturated)	1.816
X_a	0.14 (unsaturated)	0.14
X_{Kd}	0.04 (unsaturated)	0.04
X_{Kq}	0.04 (unsaturated)	0.04
X_d'	0.232 (at 1 p.u. voltage)	0.249
X_d''	0.143 (at 1 p.u. voltage)	0.141
X_q''	-	0.169
G	-	1738.3
G_{kd}	-	584.5
G_{kq}	-	584.5
R_{fd}	0.00107	-
R_a	0.002	-
R_{Kd}	0.00318	-
R_{Kq}	0.00318	-

TABLE 1 (continued)

Parameters	Values supplied	Values computed at 1.0 p.u. terminal voltage
τ_{do}'	5.95 sec.	5.403 sec.
τ_{do}''	-	0.169 sec.
τ_{d}'	0.733 sec.(1 p.u. voltage)	0.801 sec.
τ_{d}''	0.029 sec.	0.107 sec.
τ_{kqo}''	-	1.818 sec.
τ_{q}''	-	0.169 sec.
τ_{kdo}'	-	1.718 sec.
τ_{kd}	-	0.04 sec.
H	5.3 kW sec/kVA	-
K_d	-	0.0022
ω_o	100 π rad/sec.	-
M	0.0337	-
X_t	0.1802	
R_t	0.0	

TABLE II

K_o	=	1.0	τ_1	=	0.044 sec.
K_1	=	50.0	τ_2	=	0.10 sec.
K_2	=	11.0	τ_e	=	0.20 sec.
K_e	=	3.05	τ_3	=	0.10 sec.
K_3	=	0.012	τ_4	=	0.10 sec.
K_4	=	0.014	τ_5	=	2.0 sec.
C_1	=	64.2 volts	τ_6	=	2.0 sec.
C_2	=	-129.9 volts	$v_1$min	=	3.5 volts
C_e	=	-15.0 volts	$v_1$max	=	-53.6 volts
			$v_2$min	=	0 volts
			$v_2$max	=	227 volts

TABLE III

G_1	=	1.08×10^{-3}	τ_7	=	0.10 sec.
G_2	=	1.33	τ_8	=	0.188 sec.
u_k	=	-0.267	τ_g	=	0.49 sec.
G_3	=	1.42			

(20). Consequently, this was considered for an appraisal of the validity of the mathematical model. The fault was applied at the terminals of the unit transformer for a duration of 0.38 seconds with the generator initially delivering full load at rated power factor. Subsequently the fault was cleared and the machine restored to normal operation. The computed and test results for several machine variables are shown in Figs. 10,11 and 12, by curve (c) and the steady state values of the same variables before and after the fault is given in Table IV.

(3.5.2) DISCUSSION OF RESULTS

During the fault period the field and stator currents are less than what was obtained during site-test, and consequently the terminal voltage is comparatively high , resulting in a larger stator current as soon as the fault is cleared. The computed field voltage is also higher compared with the test figures. The reasons for these discrepancies are:

(a) Saturation

The self and mutual inductances on both direct and quadrature axes depend on the fluxes in the machine and vary according to the degree of saturation. Use of the unsaturated inductance for the complete range of machine operation is, therefore, unrealistic.

(b) Amortisseur Winding Parameters

It is well known that the resistances and reactances of the eddy current path do not remain constant during

TABLE IV

Test	Symmetrical 3-phase Fault At Transformer Terminals					
	Initial Readings			Final Readings		
	Test	Computed		Test	Computed	
		Variable Inductance	Constant Inductance		Variable Inductance	Constant Inductance
Load (MW)	29.76	30.0	30.0	30.0	30.0	30.0
Load (MVAR)	22.6	22.5	22.5	22.6	22.5	22.5
Field Voltage (volts)	248.0	248.0	230.0	248.0	248.0	230.0
Field Current (amps)	384.8	383.0	367.0	400.0	383.0	359.0
Stator Voltage (kV)	13.05	13.05	13.06	13.05	13.06	13.06
Stator Current (kA)	1.68	1.65	1.65	1.68	1.65	1.65
Rotor Angle (degrees)	36.0	36.4	38.3	not recorded	36.2	38.2

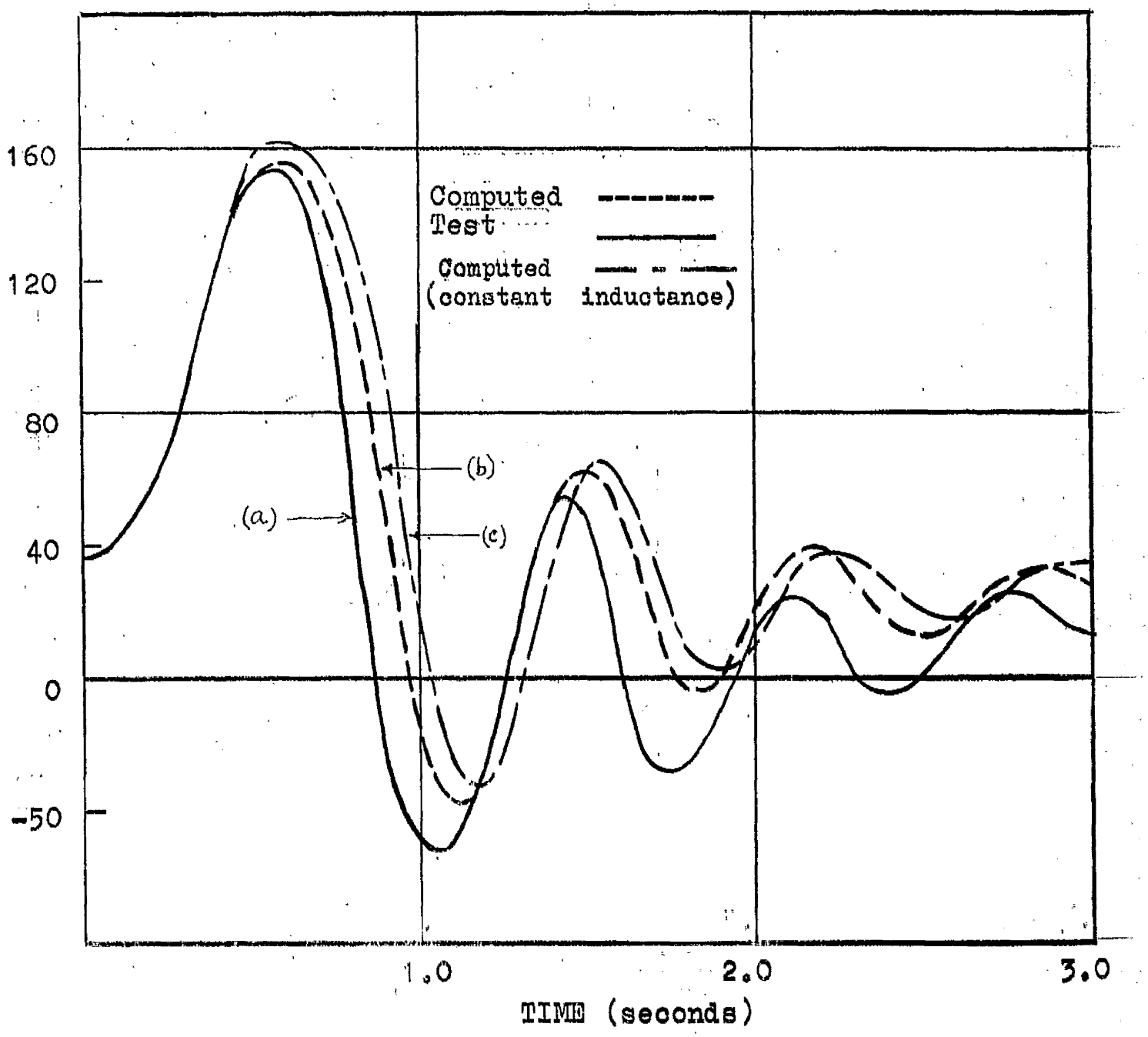

FIG. 10 ROTOR ANGLE TRANSIENT

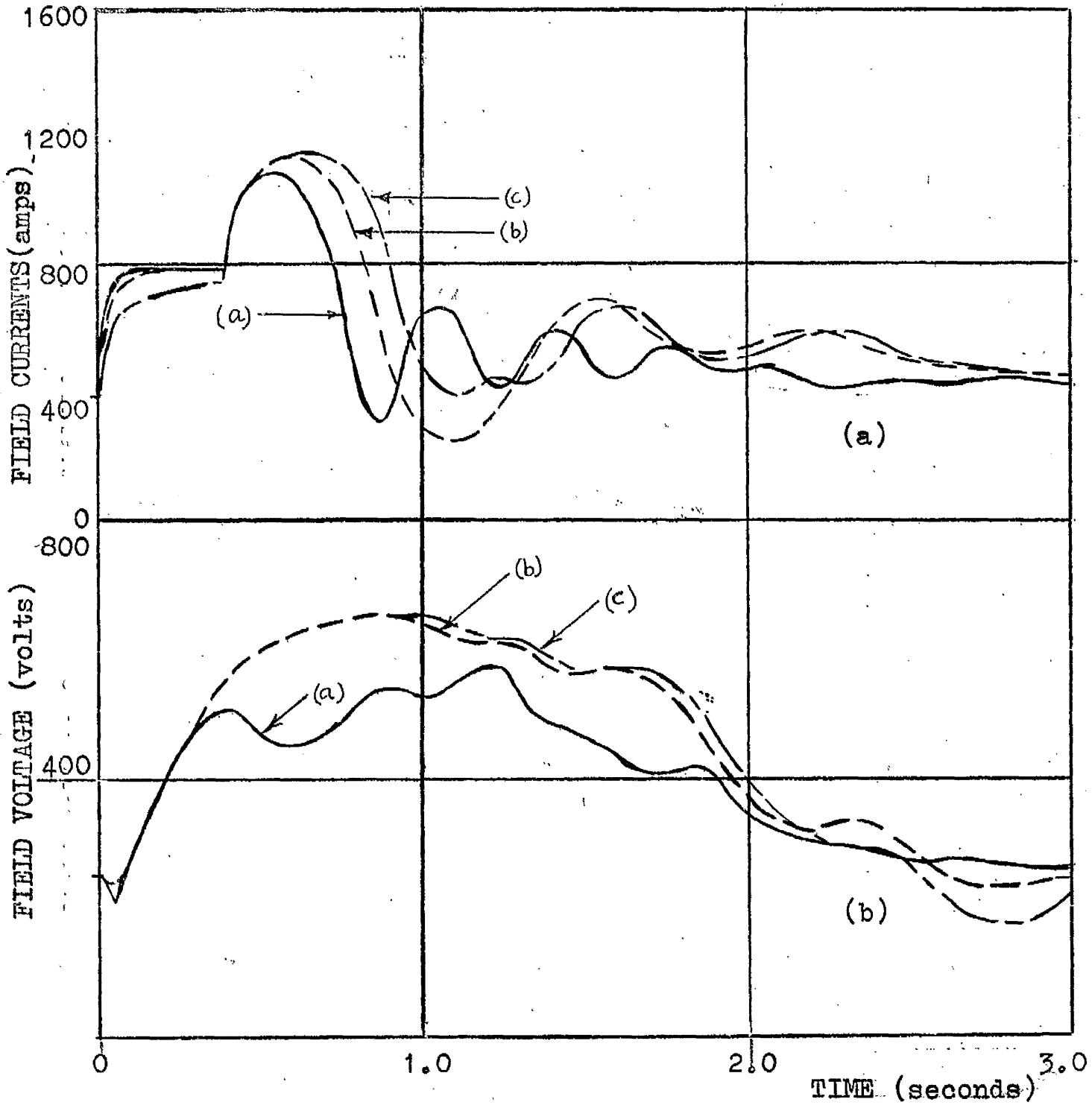

FIG. 11. (a) FIELD CURRENT TRANSIENTS

(b) FIELD VOLTAGE TRANSIENTS

Computed ———
Test ———

Computed — — —
(Const. L)

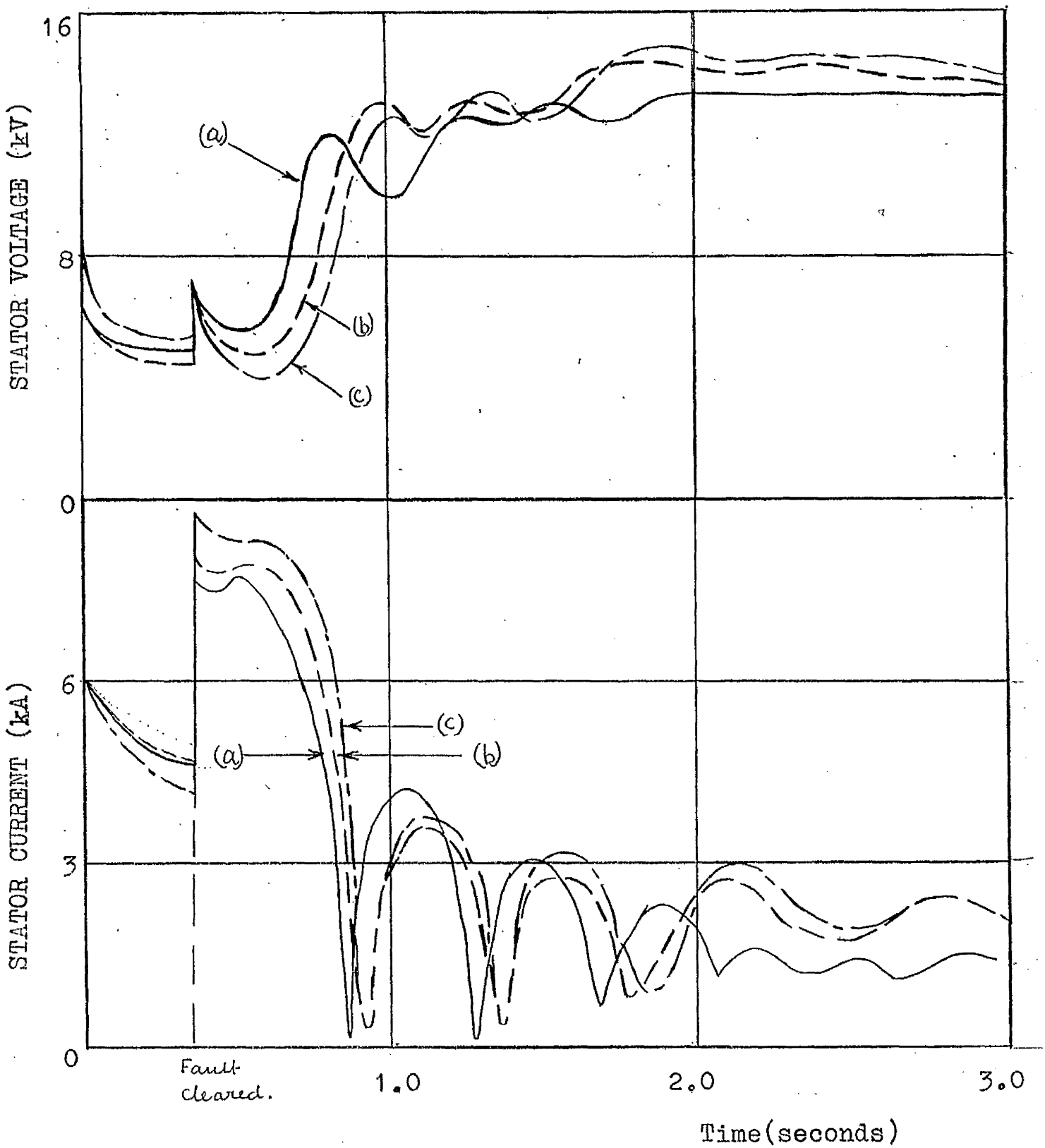

FIG.12 STATOR VOLTAGE AND CURRENT TRANSIENT DURING 3-PHASE FAULT

(a) Test Result _____
(b) Computed with variable inductance- - - -
(c) Computed with constant inductance_ _ _ _

transient operations of a machine. Their computation during asynchronous operation has been considered recently[49] but no information is available for modulating these parameters during machine operations when the flux variation is not sinusoidal.

(c) Exciter Characteristics

The saturation characteristics of the main exciter and magnetic amplifiershave been considered by straight line approximations. In actual cases these, of course, differ from the idealised condition. Moreover, it was not possible to represent the output impedance of the exciter for which, as a result, the field voltage obtained from computation is higher. The gains for the different stages of the excitation system correspond to the open circuit ratios of the input and output quantities.

(d) Saliency

Since no information was available about the saliency of the turbo generator, the quadrature axis synchronous reactance was assumed to be equal to that of the direct axis. It has been confirmed from tests that the turbo generators also have an appreciable saliency, hence such assumption is bound to include errors in the computed results since during leading power factor region, saliency affects substantially the steady state operating conditions of the generator.

CHAPTER IV

VARIABLE PARAMETER MODEL

(4.1) BASIS OF VARYING PARAMETERS

The appreciable discrepancy between the computed results and those obtained from site-tests, as shown in Chapter III, emphasises the necessity of improving the mathematical model so far developed, for obtaining more accurate quantitative information.

This Chapter is devoted to developing a suitable way of including saturation characteristics in machine analyses.

Saturation has been considered in the past in analysing electromagnetic phenomena in ferro-magnetic materials. In previous work[22], the magnetisation curve was approximated by several straight-line segments and, depending on the flux condition within the substance, different values of relative permeability were considered. In machine analyses, however, little effort has been made to consider saturation until recently . The limited progress that has so far been made in this aspect of analysis is due to the relatively limited availability of fast computing aids, because such considerations make it necessary to calculate the transient and sub-transient machine-parameters whenever the flux conditions within the machine change.

(4.1.1) FLUX-PATHS IN SYNCHRONOUS MACHINE

The flux-paths in a synchronous machine, comprise a heterogeneous medium - partly laminated, partly solid iron and partly air. The mutual flux traverses the complete path, the leakage flux, on the other hand, links only the respective windings and their paths are different from that of the mutual flux. In fact, the distribution of leakage flux in a synchronous machine is involved and its precise form is not entirely accounted for at the presen time. It is, however, true to say that leakage flux is usually less than 10% of the mutual flux, and its paths being mainly in air, contributes less significantly to magnetic circuit saturation than does the mutual flux. In this connection, the following assumptions are introduced.

(a) The leakage inductance of each winding is independent of the state of the flux path of that winding and its p.u. value is assumed to remain constant for the entire range of flux variation in the core.

(b) Leakage flux does not contribute to the average saturation of the composite flux-path which is, therefore, determined only by the mutual flux.

(c) Saturation is a function of the total mutual flux in the core calculated from the direct-and quadrature-axis components of flux.

(d) Though the flux in the two axes may be different,

it is assumed that the saturation is effected equally in the two axes.

Following assumption (a), only the mutual inductance changes with saturation, hence

$$\begin{aligned} L_{ad} &= kL_{ado} \\ L_{aq} &= kL_{aqo} \end{aligned} \qquad (4.1)$$

where L_{ado} and L_{aqo} are the unsaturated direct- and quadrature-axis mutual inductances respectively, and

$$k = f(\psi_m)/f(H) \qquad (4.2)$$

where $f(\psi_m)$ and $f(H)$ are the functions of the air gap flux and the magnetising force. From assumption (d)

$$\frac{L_{aq}}{L_{ad}} = \frac{L_{aqo}}{L_{ado}} = \lambda \qquad (4.3)$$

Alternative methods have been suggested for representing saturation. The technique proposed by Boffi and Hass[23], which is suitable for analogue computer solutions, takes only the direct-axis flux condition into account, and assumes that the quadrature-axis magnetic paths remain always unsaturated. Steven[24], on the other hand, has developed a method of formulating an expression for the saturation in the quadrature axis.

(4.2) VARIABLE INDUCTANCE CALCULATION

The total flux in the air-gap is given by

$$\psi_{at} = \left\{\psi_{ad}^2 + \psi_{aq}^2\right\}^{\frac{1}{2}} \qquad (4.4)$$

where ψ_{ad} is the direct-axis air gap flux and is

$$= L_{ad}\left\{i_{fd} + i_{kd} - i_d\right\} \qquad (4.5)$$

and ψ_{aq} is the quadrature-axis air gap flux which is

$$= L_{aq}\left\{i_{kq} - i_q\right\} \qquad (4.6)$$

Hence from equations (4.4), (4.5) and (4.6)

$$\psi_{at} = \left[L_{ad}^2\left\{i_{fd} + i_{kd} - i_d\right\}^2 + L_{aq}^2\left\{i_{kq} - i_q\right\}^2\right]^{\frac{1}{2}} \qquad (4.7)$$

On the basis of assumption (d), equation (4.7) can be written as

$$\psi_{at} = L_{ad}\left[\left\{i_{fd} + i_{kq} - i_d\right\}^2 + \lambda^2\left\{i_{kq} - i_q\right\}^2\right]^{\frac{1}{2}} \qquad (4.8)$$

or
$$\psi_{at} = L_{ad}\left\{H_d^2 + \lambda^2 H_q^2\right\}^{\frac{1}{2}} \qquad (4.9)$$
$$= L_{ad}H_{at}$$

where H_{at} = total equivalent magnetising force

H_d = equivalent magnetising force along the direct axis

$$= L_{ad}\left\{i_{fd} + i_{kd} - i_d\right\}$$

and H_q = equivalent magnetising force along the quadrature axis

$$= L_q\left\{i_{kq} - i_q\right\}$$

Therefore, $L_{ad} = \psi_{at}/H_{at}$ (4.10)

Equation (4.10) suggests that if, at any stage, the magnetising force and the flux produced by it are known, the mutual inductance L_{ad} can be easily calculated. The

relation between ψ_{at} and H_{at} depends on the degree of saturation. The requirement, therefore, is to find a mathematical expression for the physical relation between total air-gap flux and the equivalent total magnetising force in an actual machine, and the expression should be valid for all conditions of machine operation.

From equation (4.7) it is true to say that the magnetising force can be applied for various combinations of the direct- and quadrature-axis currents, but the air-gap flux will be the same for a particular mmf, irrespective of the combination of the different currents involved.

One way of finding the relationship between the air-gap flux and mmf is from the open-circuit characteristic of the machine, since at rated speed

$$v_q = X_{ad} i_{fd} \qquad (4.11)$$

or dividing by ω_o

$$\psi_{at} = L_{ad} i_{fd} \qquad (4.12)$$

because $i_d = i_q = i_{kd} = i_{kq} = 0$.

(4.2.1) EFFECT OF SALIENCY

The open-circuit characteristics, however, do not correspond to the relationship between flux and mmf for a loaded machine having pronounced saliency, for, in this case, the reluctance of the quadrature axis is different from that of the direct axis. For an exact solution of

the problem in the case of a salient-pole machine it is, therefore, necessary to know both H_d and H_q in equation (4.9), in order to be able to calculate L_{ad} and then L_{aq} using assumption (d).

In cylindrical rotor machines, the saliency is comparatively small and, therefore, in order to simplify the method of including saturation, saliency is neglected in so far as the production of air-gap flux is concerned. It is then possible to use the open circuit characteristics to provide a general relationship between flux and mmf for all conditions of machine operation, because equation (4.7) can then be written as

$$\psi_{at} = L_{ad}\left\{(i_{fd} + i_{kd} - i_d)^2 + (i_{kd} - i_q)^2\right\}^{\frac{1}{2}}$$

(4.2.2) VARIABLE INDUCTANCE FROM OPEN CIRCUIT CHARACTERISTICS

Assuming at this stage that a mathematical expression is available for the saturation characteristic, the inductance at any flux condition can be calculated in the following way, provided that the unsaturated value of mutual inductance is known from tests.

Then referring to Fig.13, for a particular air gap flux ψ_s the unsaturated value of flux is ψ_{us}.

$$\left.\begin{aligned} \text{So} \qquad \psi_{us} &= L_{ado}H_{at1} \\ \text{whereas} \qquad \psi_s &= L_{ad}H_{at1} \end{aligned}\right\} \qquad (4.13)$$

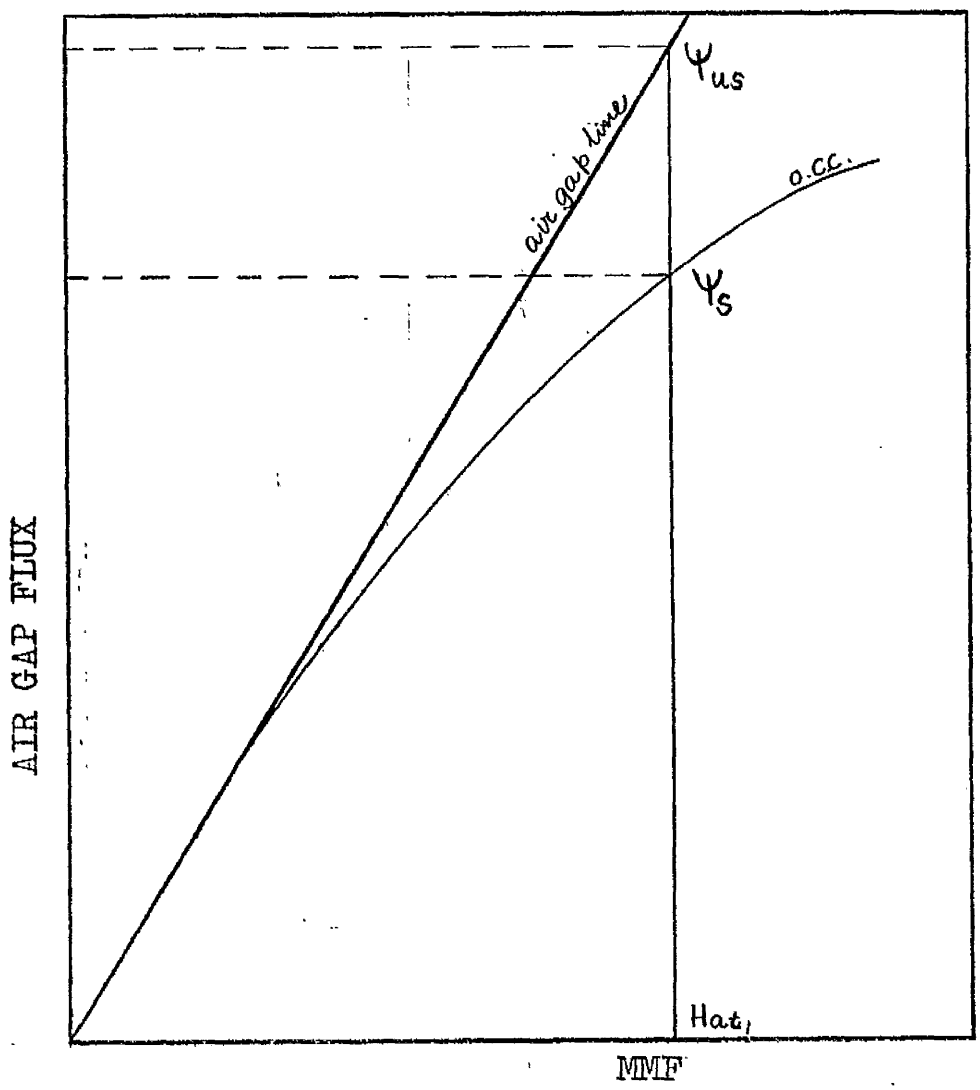

FIG. 13 RELATION BETWEEN AIR GAP FLUX AND MMF

$$\left.\begin{aligned} \text{so} \qquad \frac{\psi_s}{\psi_{us}} &= \frac{L_{ad}}{L_{ado}} \\ \text{or} \qquad L_{ad} &= L_{ado}\,\frac{\psi_s}{\psi_{us}} \end{aligned}\right\} \qquad (4.14)$$

and then $L_{aq} = \lambda L_{ad}$

It is, therefore, required to find out ψ_{us} for a known value of ψ_s, this can be conveniently done by formulating the equations of the air gap line, and the saturation characteristic and expressing, in both cases, the mmf as a function of the open-circuit voltage in the per unit notation.

(4.3) MATHEMATICAL CURVE FITTING FOR OPEN CIRCUIT CHARACTERISTICS

(4.3.1) TSCHEBYCHEFF'S LEAST SQUARE APPROXIMATION

The relation between the mmf and air-gap flux is expressed as a polynomial series of the form

$$y = a_o + a_1 x + a_2 x^2 + a_3 x^3 + \ldots a_n x^n \qquad (3.15)$$

where y = total mmf acting round the circuit

and x = the air-gap flux.

A polynomial of degree n has n+1 coefficients, and n+1 conditions are required to determine the coefficients uniquely. However, a situation may arise where the observations or sample data obtained from some experiment do not conform to any unique solution. In such cases the tendency is to fit a curve $y(x)$ giving a smoothed set of values $y(x_i)$ which are,

in general, different from the observed y_i. Tschebycheff's least square approximation[25] is one of the most suitable methods for such curve-fitting. The least square criterion states that a good estimate for the polynomial is one which minimises the deviations given by

$$\sum_{i=0}^{n}\left[y_i - y(x_i)\right]^2 = f(a_0, a_1, \ldots a_n) \qquad (3.16)$$

(4.3.2) GAUSS-SEIDEL ITERATIVE METHOD

The evaluation of the coefficients $a_0, a_1, \ldots a_n$ can be done by one of several methods. In this particular case of saturation characteristics the "Gauss-Seidel Iterative"[26] method has been found suitable.

The method of iteration lends itself to the solution of n+1 simultaneous equations in n+1 unknowns. The process can be explained in the following way.

Substituting the n+1 pairs of data (x_i, y_i) in equation (3.14) and rearranging, the following equations are obtained.

$$\begin{aligned}
a_o &= y_o - a_1 x_o - a_2 x_o^2 - \ldots\ldots\ldots\ldots - a_n x_o^n \\
a_1 &= y_1 x_1^{-1} - a_o x_1^{-1} - a_2 x_1 - \ldots\ldots\ldots - a_n x_1^{n-1} \\
a_2 &= y_2 x_2^{-2} - a_o x_2^{-2} - a_1 x_2^{-1} - x_2 - \ldots - a_n x_n^{n-2} \qquad (3.17) \\
&\vdots \\
a_n &= y_n x_n^{-n} - a_o x_n^{-n} - a_1 x_n^{-(n-1)} - \ldots\ldots - a_{n-1} x_n^{-1}
\end{aligned}$$

A solution is then sought for the n+1 coefficients. Iteration is initiated by assuming that the values of all the coefficients are zero. Then from the first equation of (3.17) an

approximate value of $a_o = y$ is obtained.

Substituting this value of a_o into the second sequation a value of a_1 is obtained which is now other than zero. After making (n+1) such substitutions a set of approximate values of all the a's are obtained and the least square error can be calculated from equation (3.16). The iteration is then repeated until the least square error is found to be a minimum and the values of the coefficients are retained corresponding to the minimum error only, as is shown in Fig.14.

(4.3.3) ITERATIVE METHOD IN SATURATION CURVE FITTING

In applying the iterative method a polynomial of 8 th. or 10th. order has been found quite sufficient as any increase in the order does not improve the accuracy of the fitted curve. Also the first coefficient a_o can be omitted from the polynomial expression since the saturation characteristics almost always pass through the origin.

The computed curves are compared with the actual magnetisation curves in two cases as shown in Figs. (15) and (16) and Figs. (17) and (18) show the variation of mutual reactance with stator voltage. A flow diagram of the programming of iterative method is shown in Fig.(19).

(4.4) COMPARISON OF COMPUTED AND TEST RESULTS

The turbo-alternator model, now including the effect

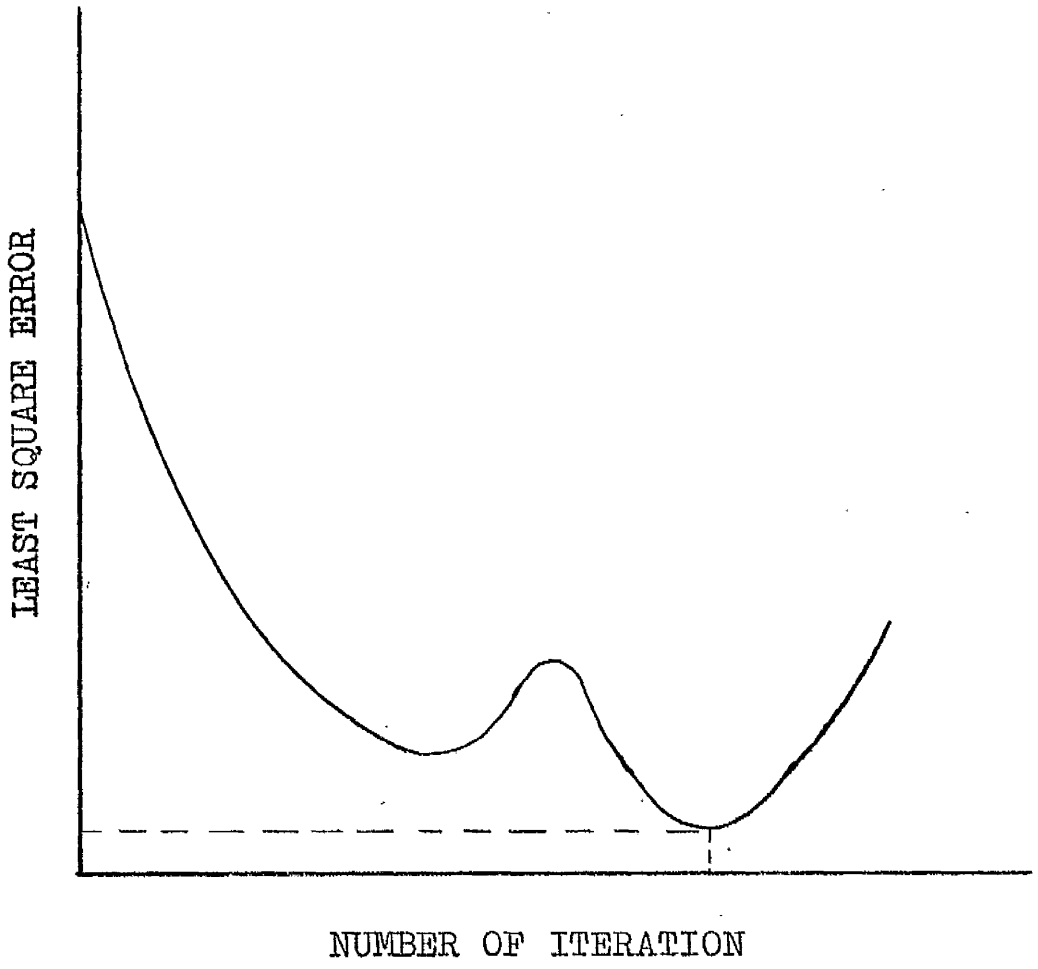

FIG. 14 RELATION BETWEEN NUMBER OF ITERATION AND LEAST SQUARE ERROR

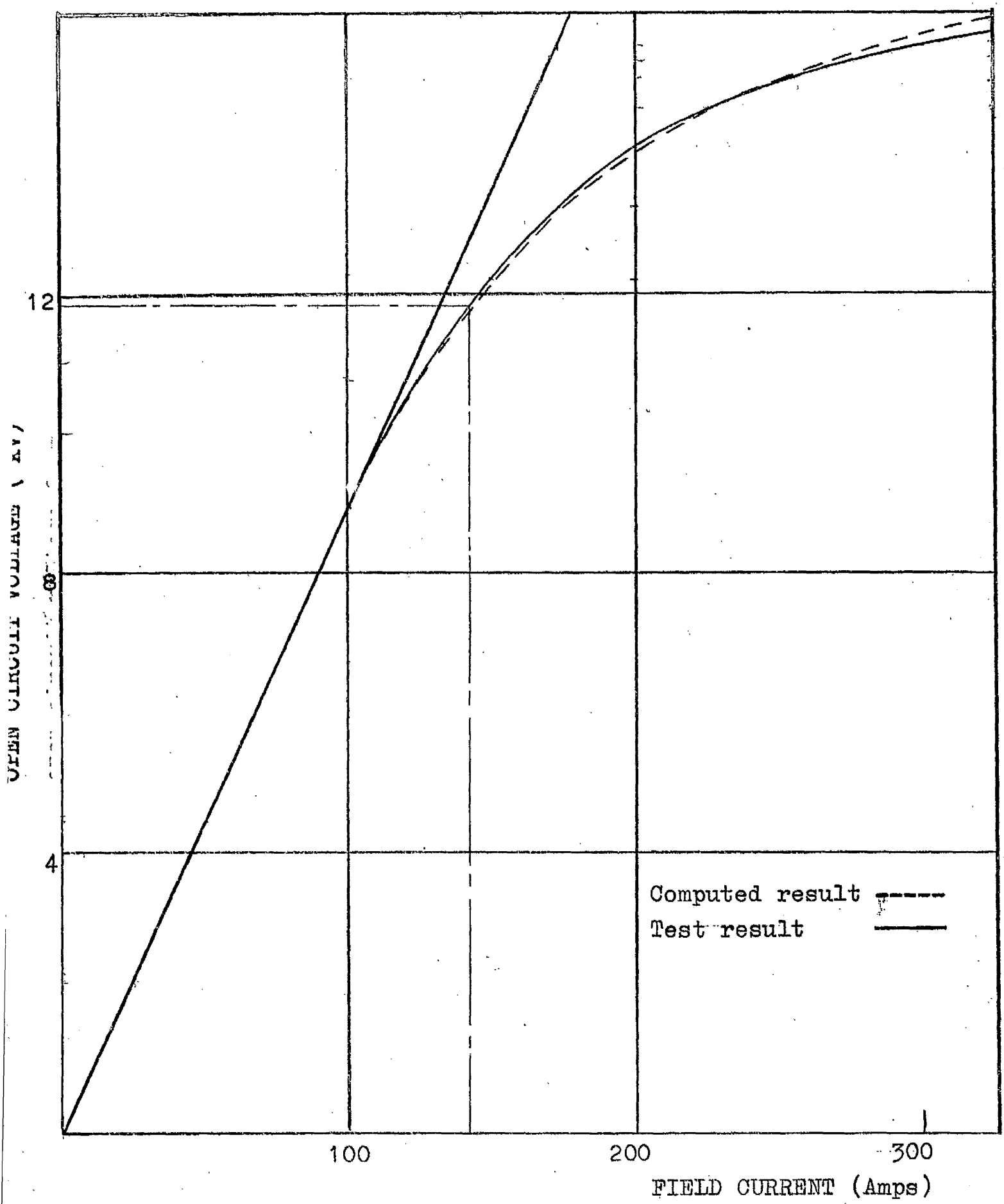

FIG. 15 OPEN CIRCUIT CHARACTERISTICS FOR GOLDINGTON TEST GENERATOR

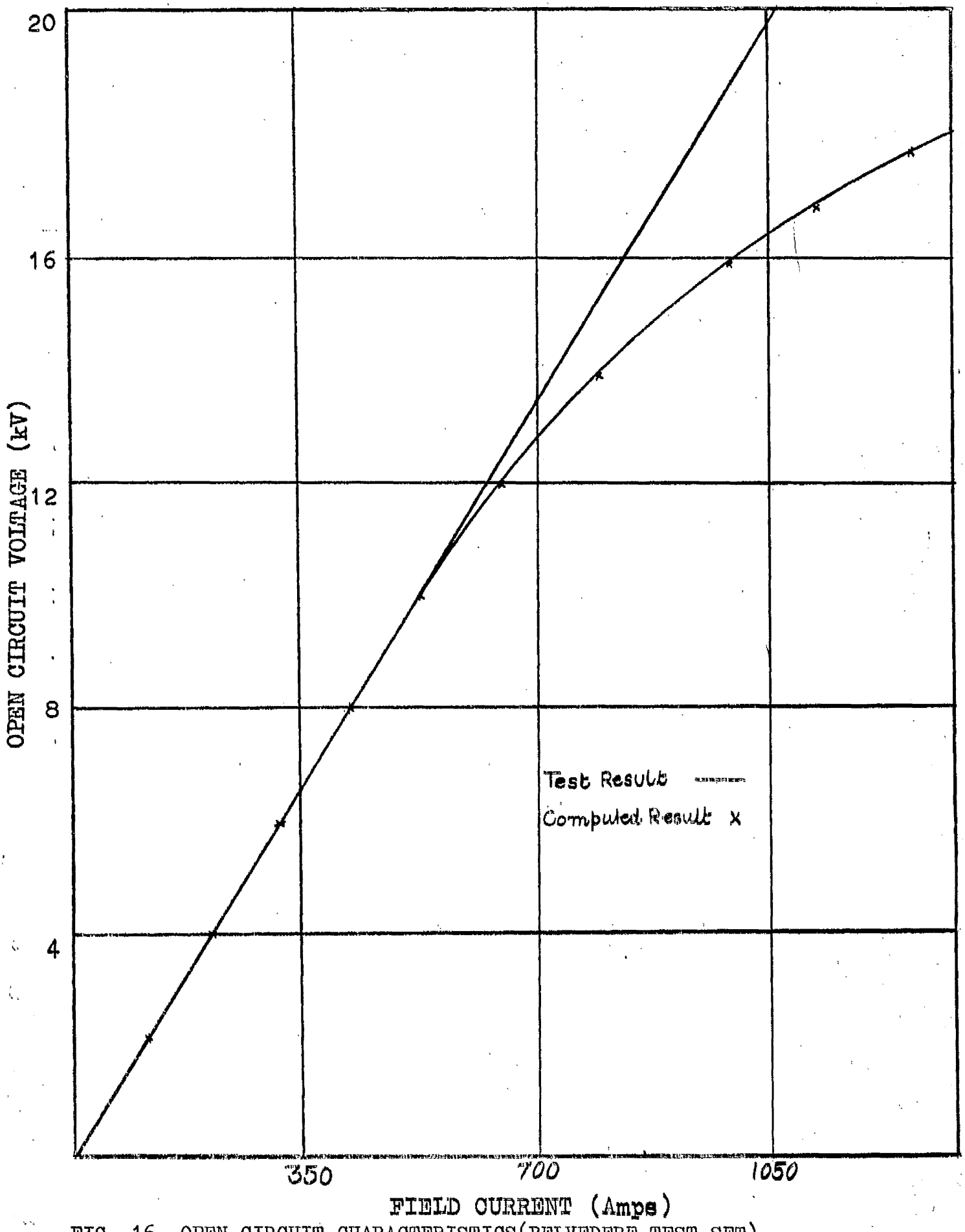

FIG. 16. OPEN CIRCUIT CHARACTERISTICS(BELVEDERE TEST SET)

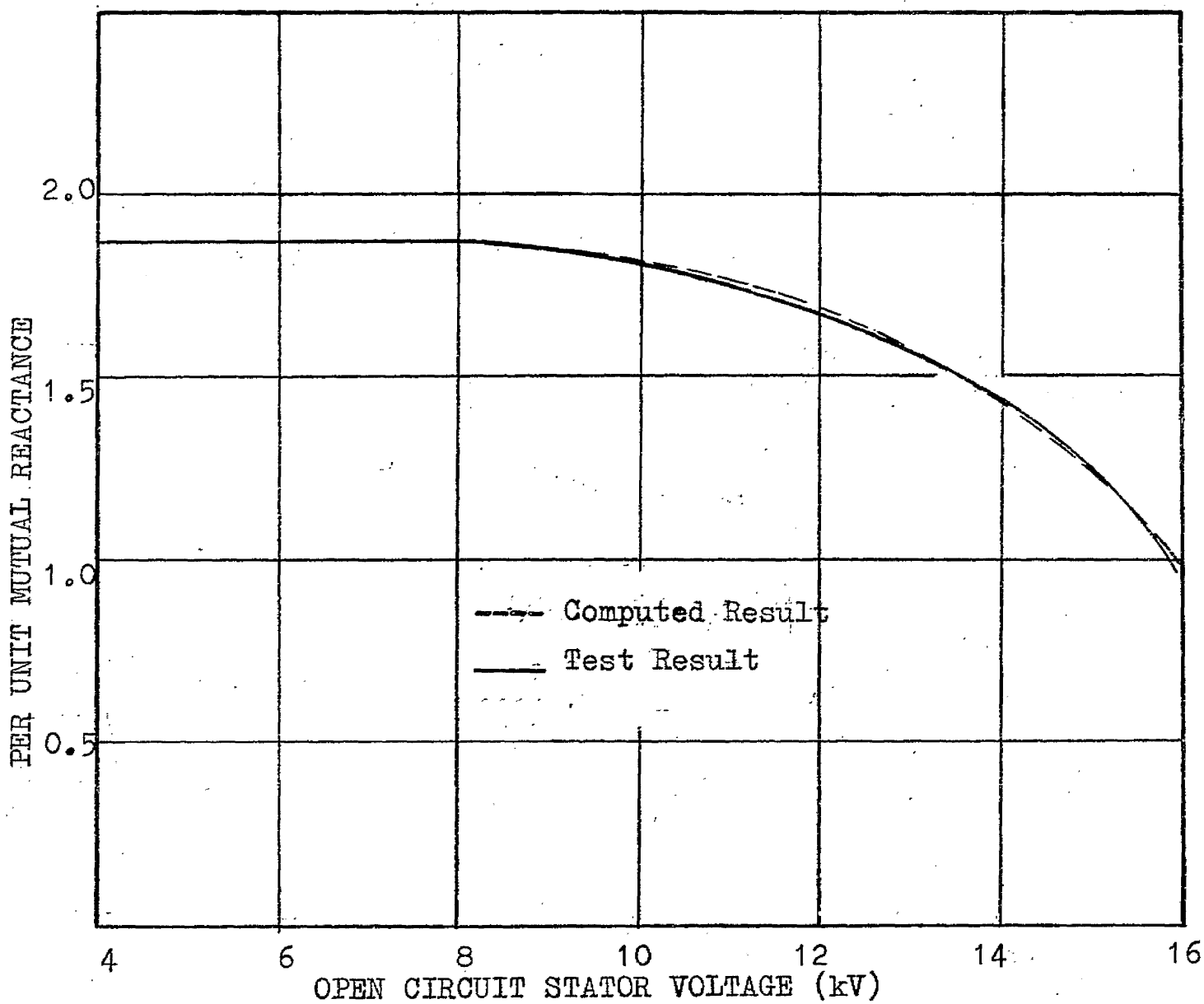

FIG. 17 ---- VARIATION OF MUTUAL REACTANCE WITH STATOR VOLTAGE

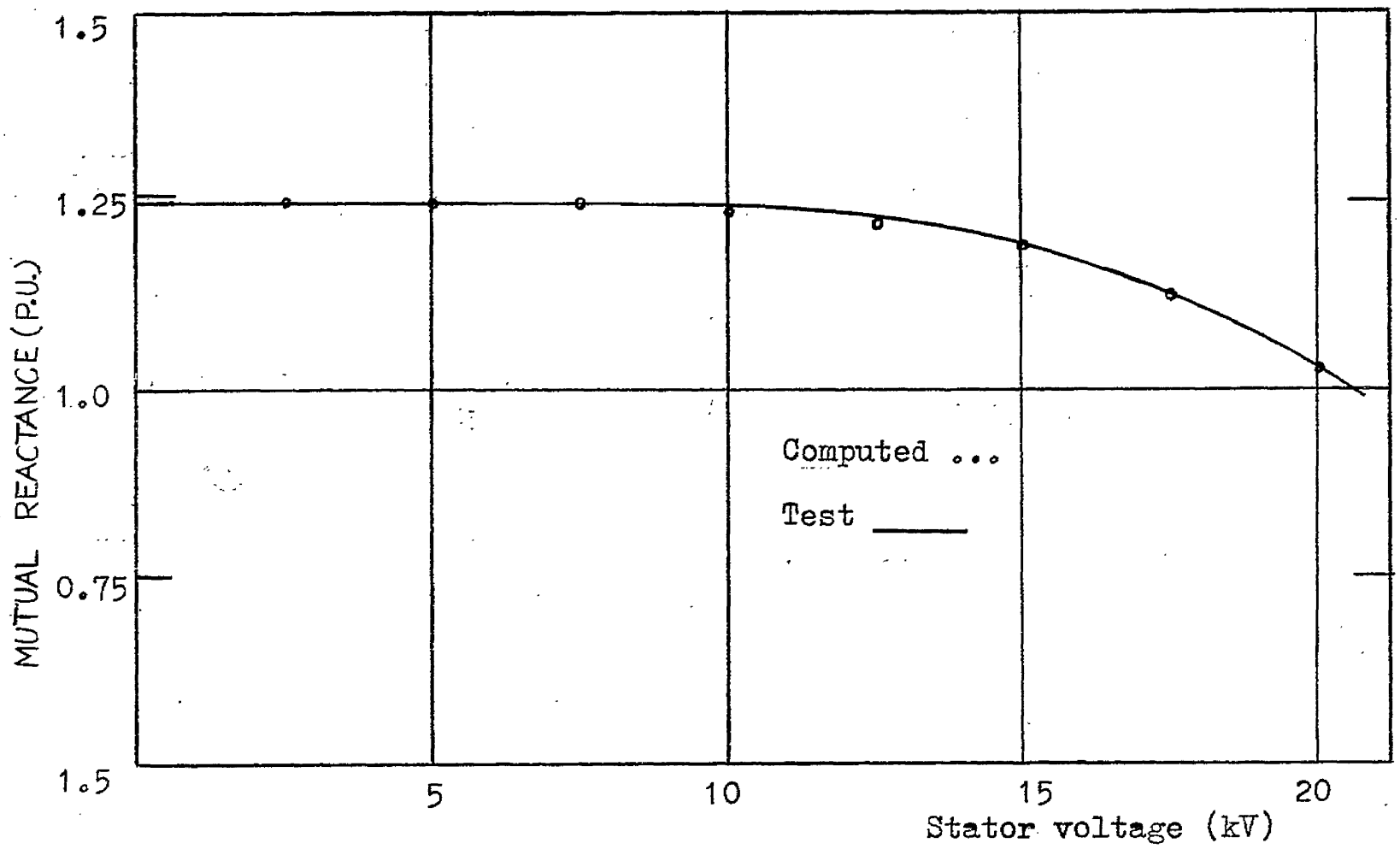

FIG. 18 VARIATION OF MUTUAL INDUCTANCE WITH OPEN CIRCUIT STATOR VOLTAGE FOR BELVEDERE TEST GENERATOR

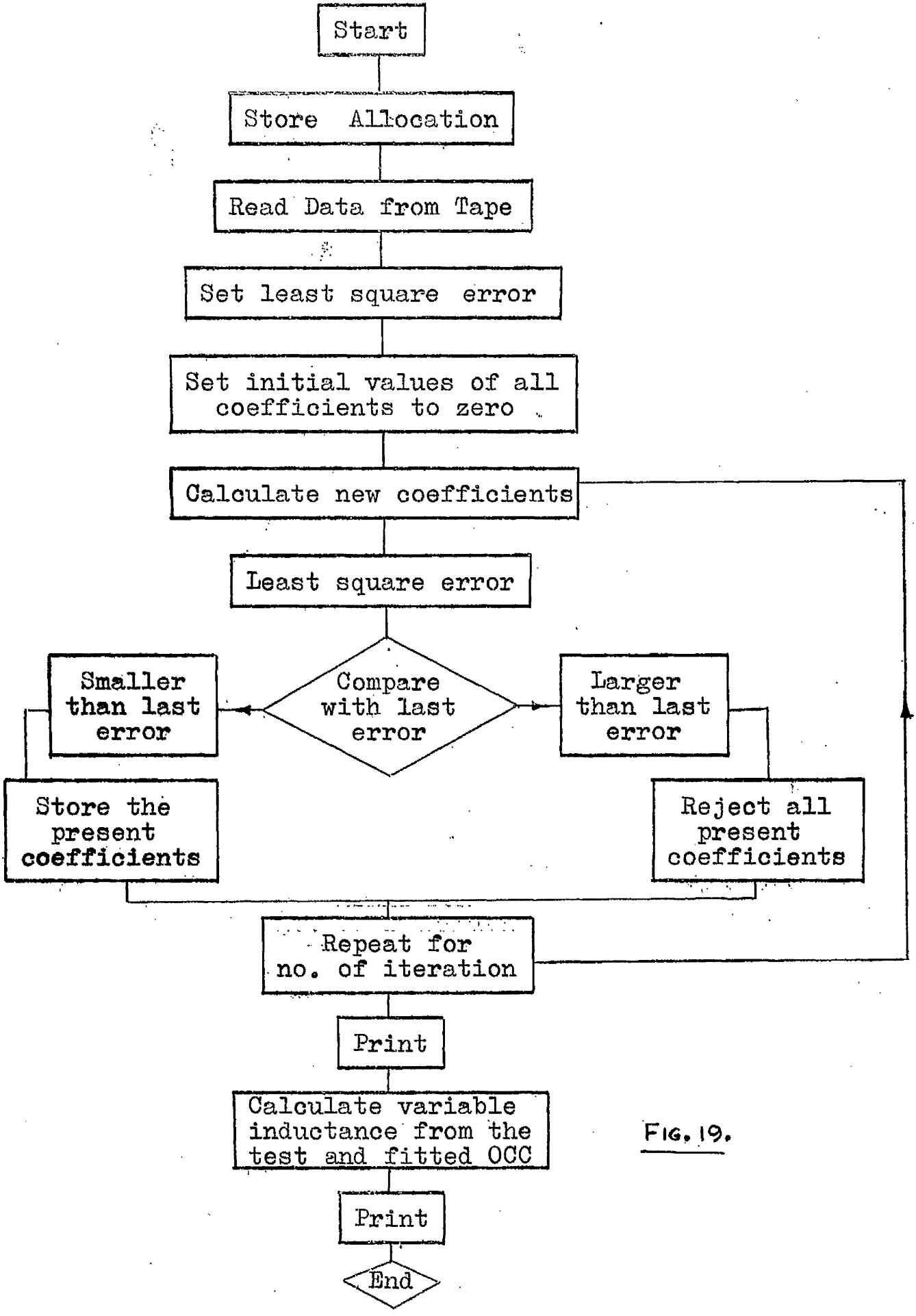
Start
Store Allocation
Read Data from Tape
Set least square error
Set initial values of all coefficients to zero
Calculate new coefficients
Least square error
Compare with last error
Smaller than last error
Larger than last error
Store the present coefficients
Reject all present coefficients
Repeat for no. of iteration
Print
Calculate variable inductance from the test and fitted OCC
Print
End

FIG. 19.

of saturation, was subjected to several tests to ascertain the performance of the variable parameter model. Wherever applicable the parameters used were the same as in Chapter III except those which depend on the saturation characteristics. They are calculated at the beginning of every step interval.

A comparison of the machine parameters supplied by the manufacturers and calculated for 1.0 per unit terminal voltage are shown in Table I .

(4.4.1) LOAD REJECTION TEST

The full-load rejection test was initiated by an imposed constraint corresponding to the opening of the 132 kV circuit breaker in the physical system. The computed and measured values of several machine terminal variables both before and after the disturbance are shown in Table V.

The test and computed results are shown in Figs.(20-21) by curves (a) and (b) respectively. The error of most significance is in the final steady-state stator voltage, which is higher than that computed. This is likely to be due to the voltage regulator having in operation a much lower gain than that specified by the manufacturer. No attempt was made to optimize the operation of the regulator since detailed information on the reduction of gain was not available.

The response of the direct- and quadrature-axis components of stator voltage is shown in Fig.22 which

TABLE V

Test	Full Load Rejection			
	Initial Readings		Final Readings	
	Test	Computed with variable inductance	Test	Computed with variable inductance
Load (MW)	29.80	30.0	0.00	0.0
Load (MVAR)	25.3	25.0	0.70	0.0
Field Voltage (volts)	236.0	252.0	85.0	97.0
Field Current (amps)	386.0	390.0	138.0	147.0
Stator Voltage (kV)	12.10	12.13	12.35	12.16
Stator Current (kA)	-	1.76	-	0.0
Rotor Angle	32.5	39.5	-	-

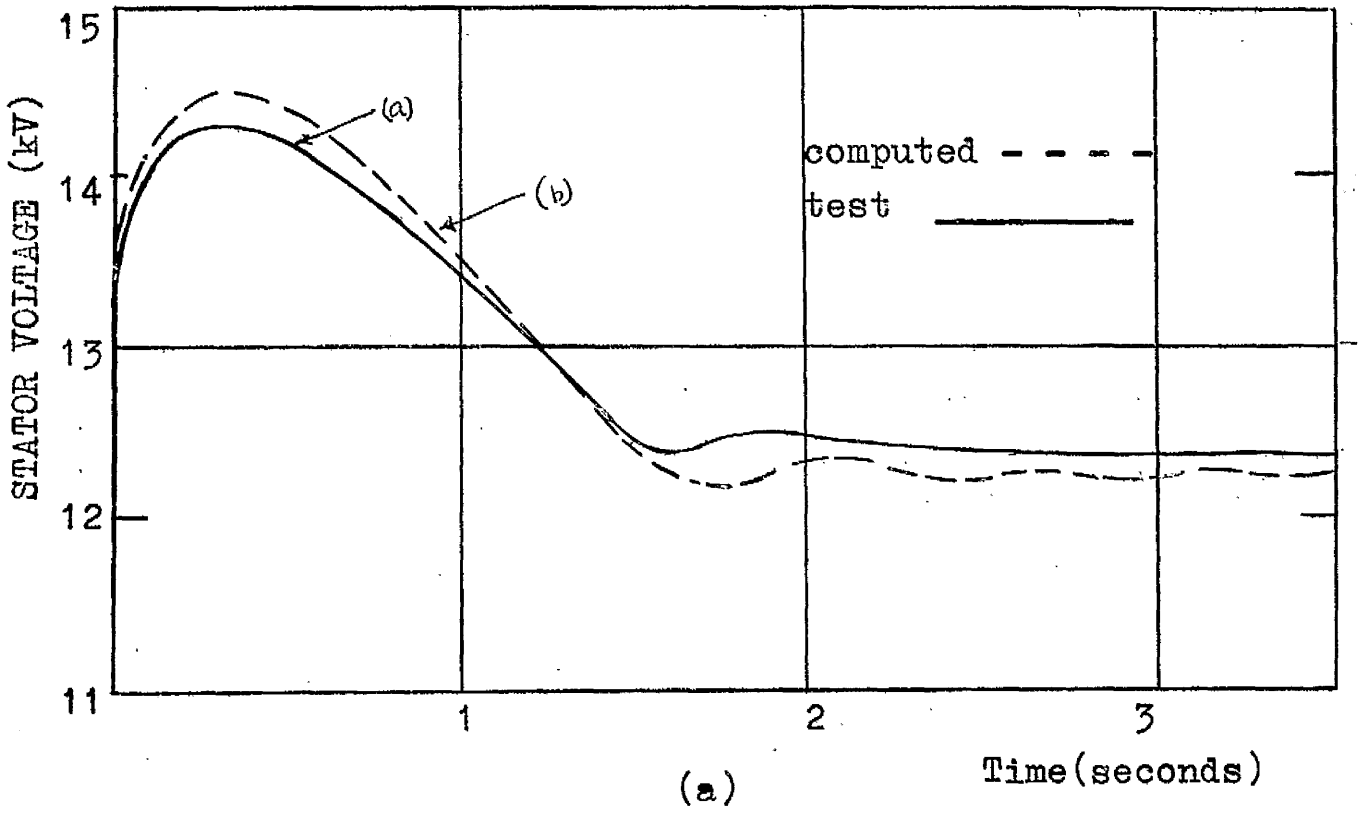

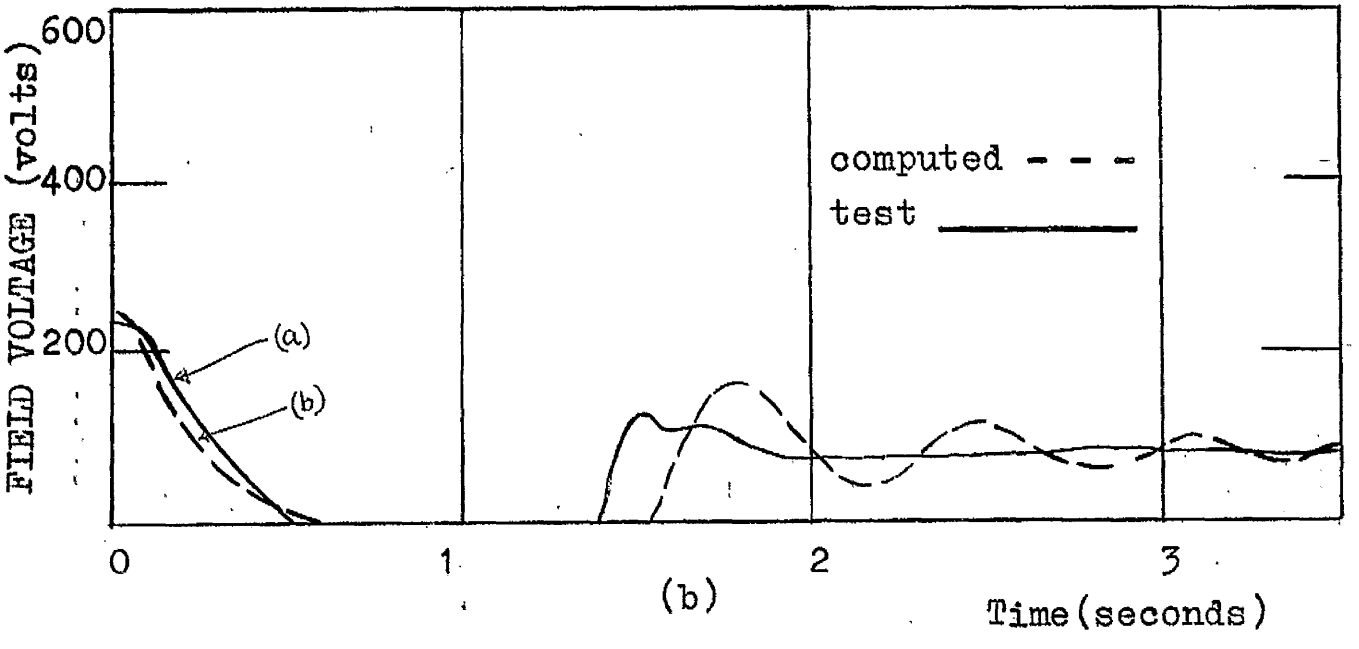

FIG.20 STATOR AND FIELD VOLTAGE RESPONSE DURING FULL LOAD REJECTION TESTS

(a) Stator voltage
(b) Rotor voltage

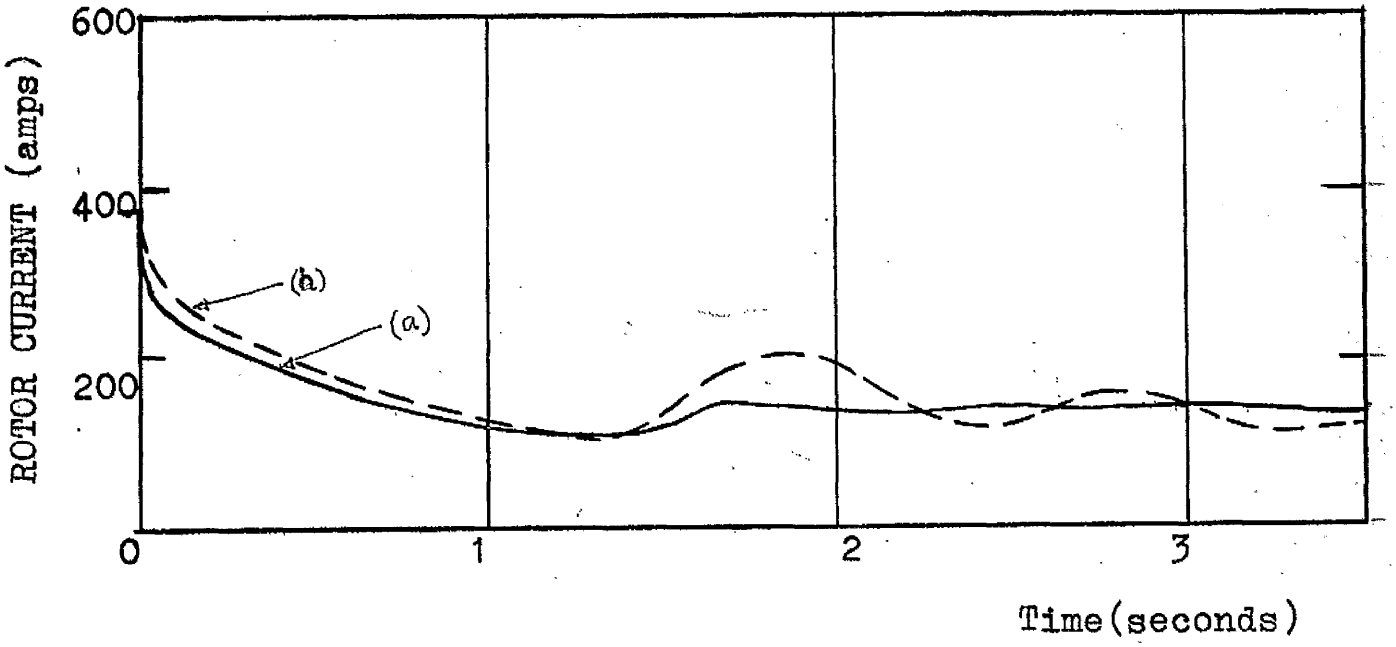

FIG.21 ROTOR CURRENT TRANSIENT DURING FULL-LOAD REJECTION TESTS

Computed - - - -

test ————

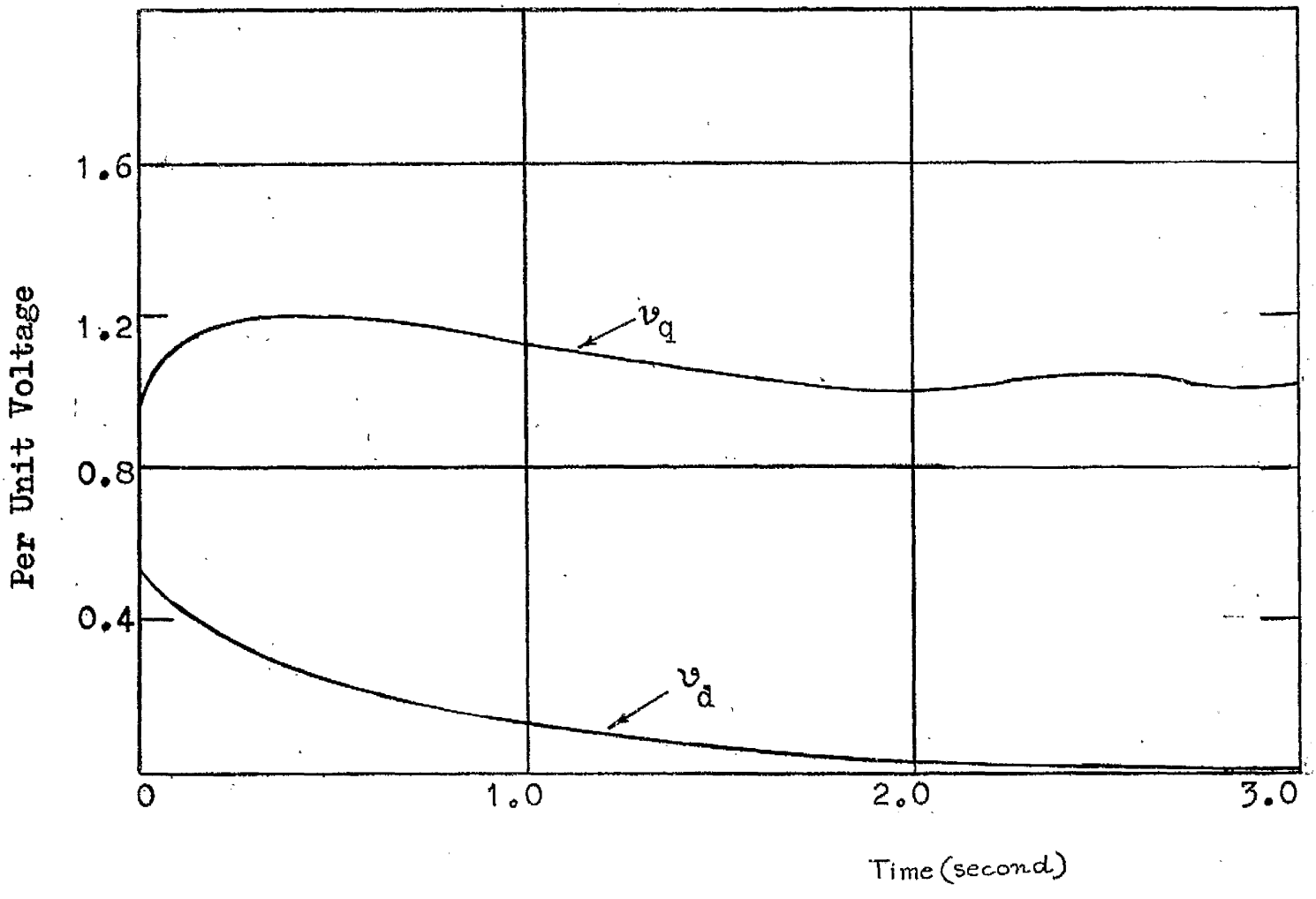

FIG. 22 DIRECT AND QUADRATURE-AXES STATOR VOLTAGE DURING LOAD REJECTION TESTS

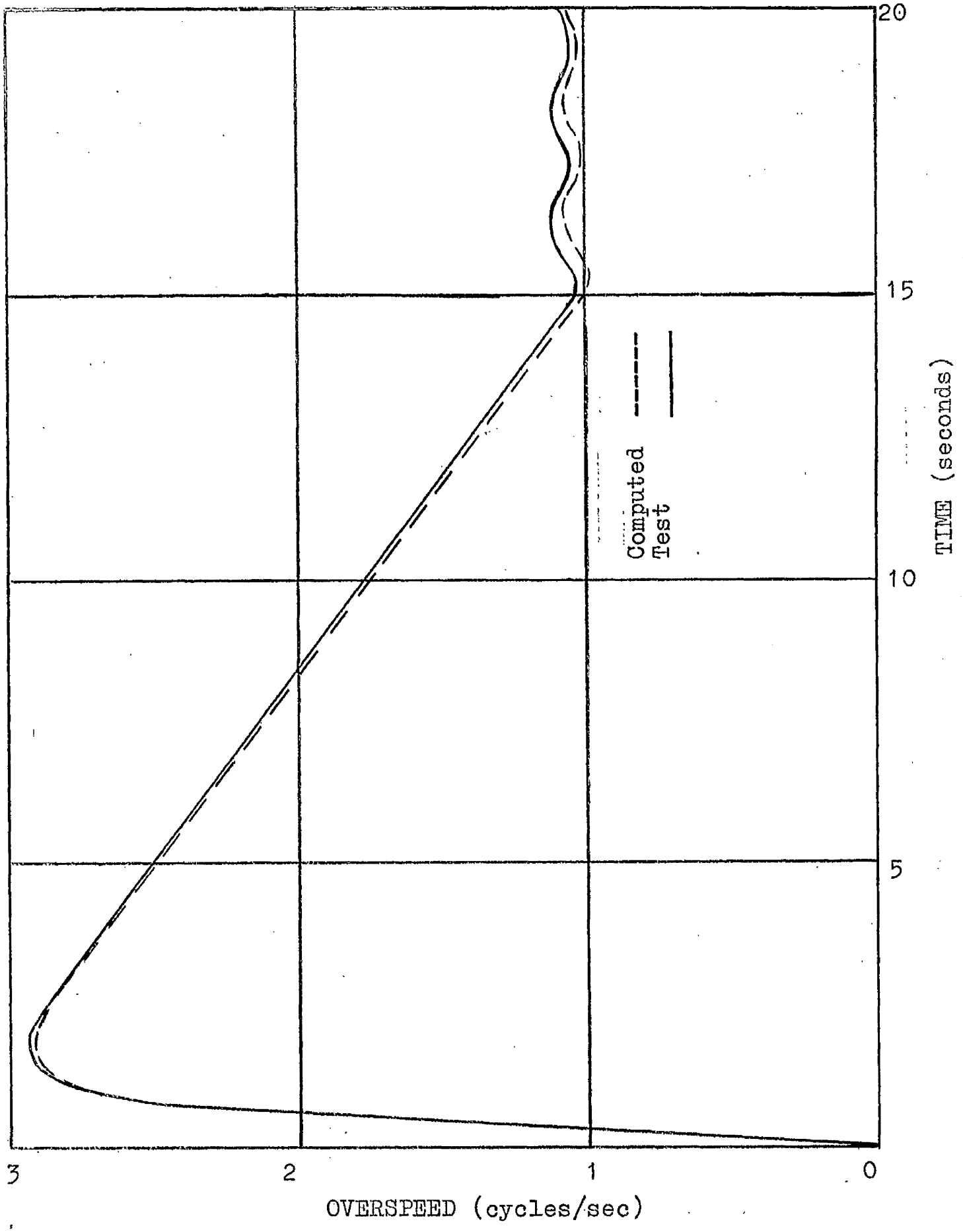

FIG. 23. GOVERNOR RESPONSE CHARACTERISTICS

illustrates the decay of the quadrature-axis flux at a rate controlled by the time constant associated with that axis.

The sudden rise from zero value in the test field voltage is probably caused by the changing characteristics of magnetic amplifiers during transition from a saturated to unsaturated state. The governor response characteristics in Fig. 23 notwithstanding that a very simple representation has been adopted, shows good agreement.

(4.4.2) SYMMETRICAL 3-PHASE FAULT

The symmetrical 3-phase fault at the transformer terminals described in Chapter III, Section (3.5.1) was repeated with the variable-parameter model. The steady state values of the machine variables are given in Table IV and they show good agreement with the site-test results.

Considering all the traces that are shown in Figs.10, 11 and 12 by curves marked (b), it can be generally concluded that the variation of the machine parameters on the basis of magnetic circuit saturation has appreciably improved the mathematical model as the results obtained from this model show closer agreement with site-test results. The reasons for the discrepancies that still exist are the same as mentioned in Chapter III.

The analysis of the 3-phase fault reveals several interesting aspects of machine operations. In the conventional machine study it is assumed that during a 3-phase

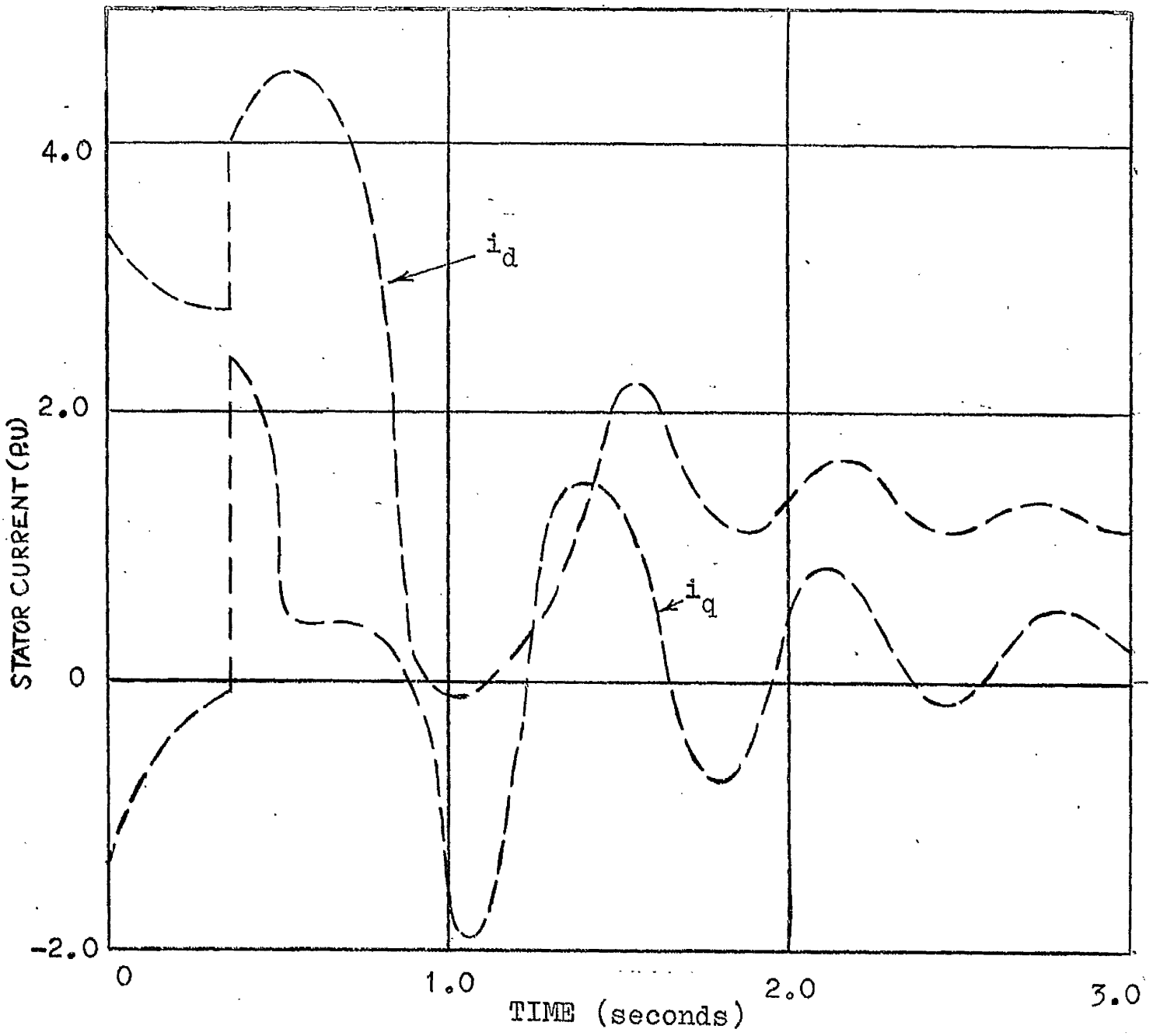

FIG. 24 AXIS - CURRENT TRANSIENTS

fault the direct axis voltage and quadrature-axis current is instantaneously reduced to zero. From the present analysis it is found from Fig.24 that as soon as the fault occurs the quadrature axis current jumps to a negative value and then decays exponentially based on the quadrature axis subtransient time constant until the fault is removed. The direct axis voltage, shown in Fig.25, follows the same trend. Though currents and voltages exist along both the axes, the phase difference between the voltage and current at the generator terminal is maintained at 90^{o} so that the power output during the fault period is zero, as shown in Fig.26. The dynamic impedance measured at the machine terminal looking towards the system is given in Fig.27. Immediately after the fault is cleared, it is found from Figs. 26 and 27 that the generator delivers power at a leading power factor. This follows logically from the fact that during the fault duration, the firect-axis flux-linkage is reduced to a small value due to the heavy fault current and consequently the terminal voltage is small compared with the system voltage. Though the field winding carries a large current, yet the operation of the generator is, for a short time, similar to that of an under excited one. The flux, however, builds up rapidly and the power factor swings back to the lagging region.

The variation of terminal power and slip is shown in Fig.(28) as a function of rotor angle. The nature of power

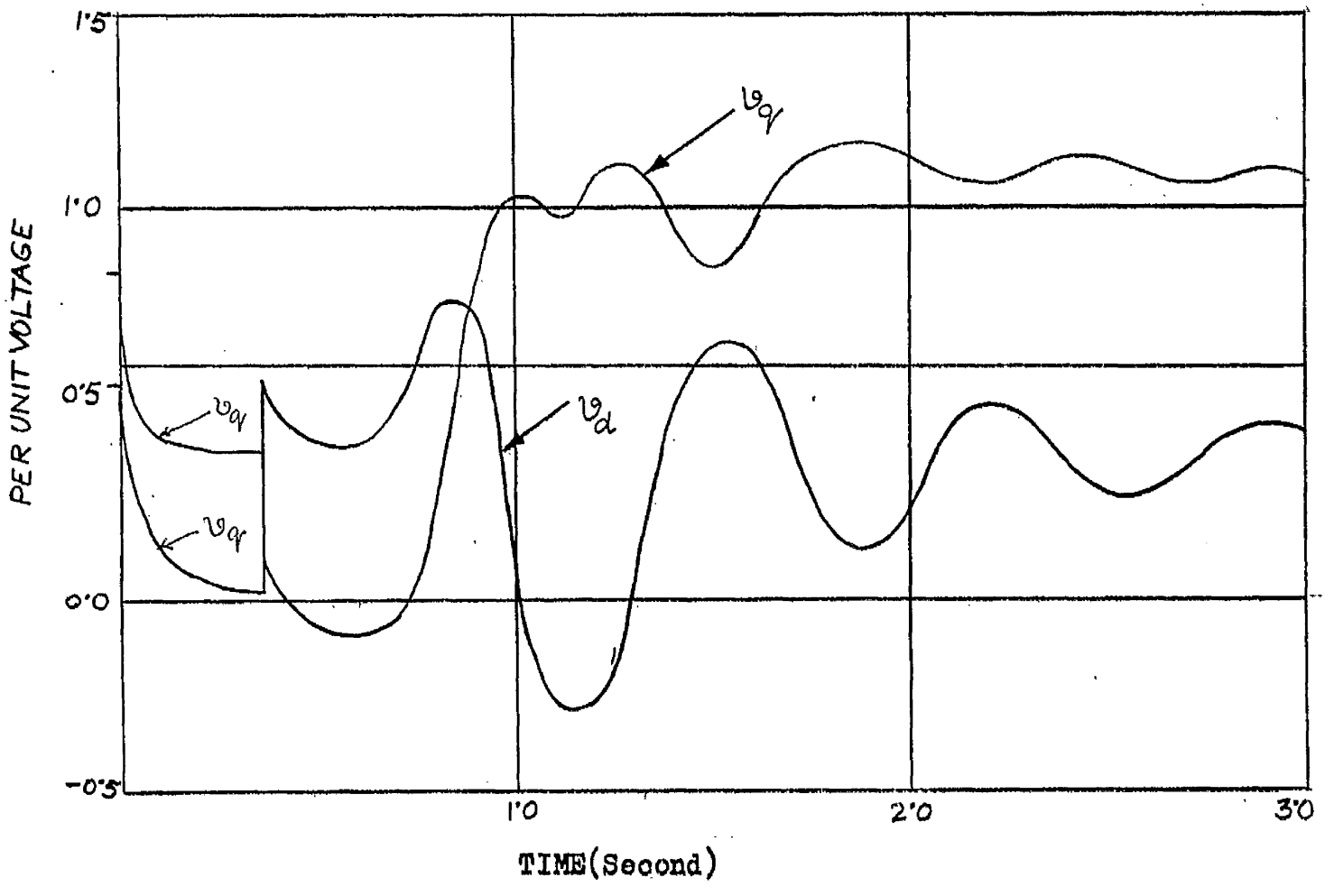

FIG. 25. VARIATION OF DIRECT AND QUADRATURE AXIS VOLTAGES DURING 3-PHASE FAULT.

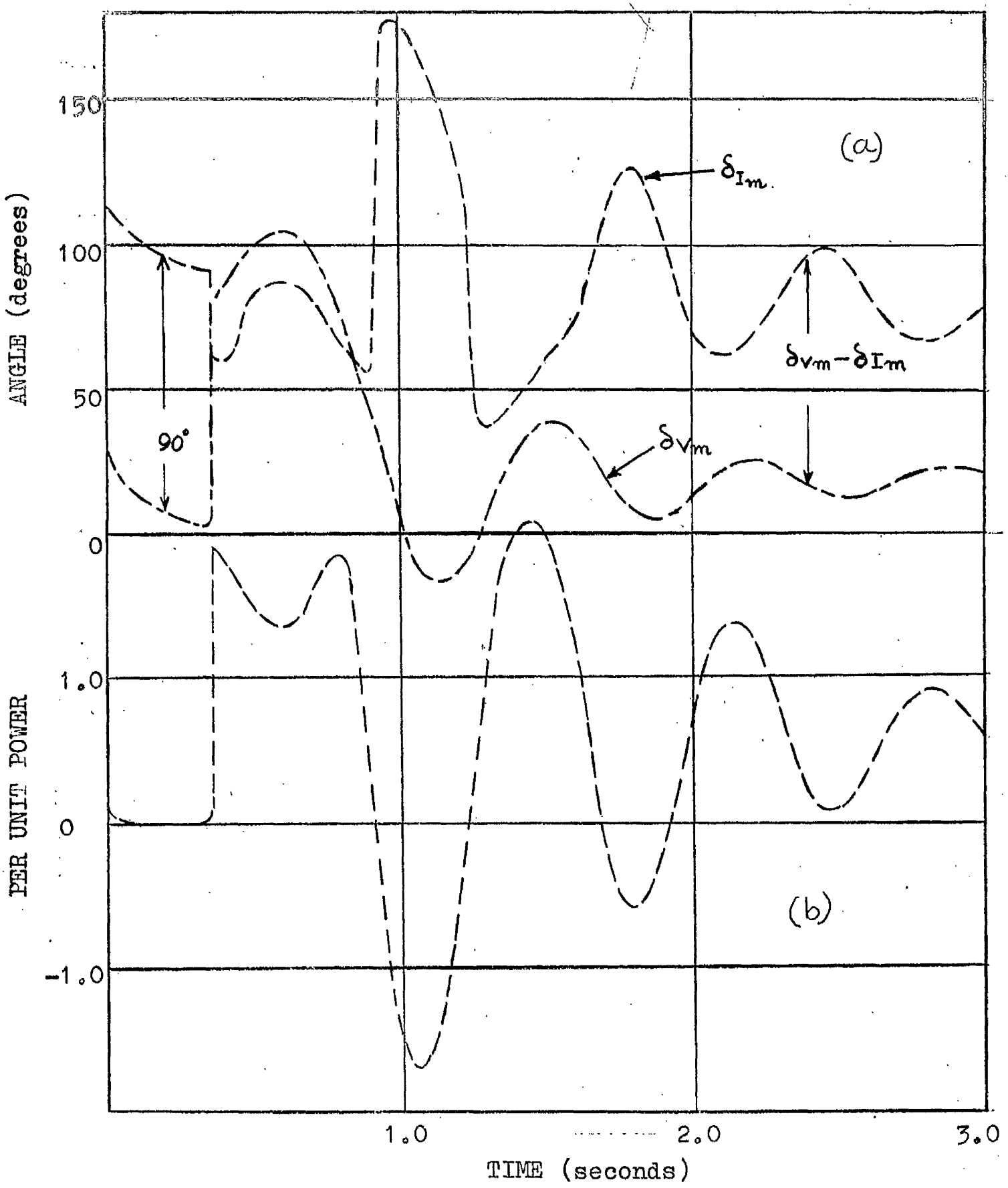

FIG. 26 (a) RESPONSE OF ROTOR ANGLE AND ANGLE BETWEEN d-AXIS AND I_m

(b) OUTPUT POWER TRANSIENTS

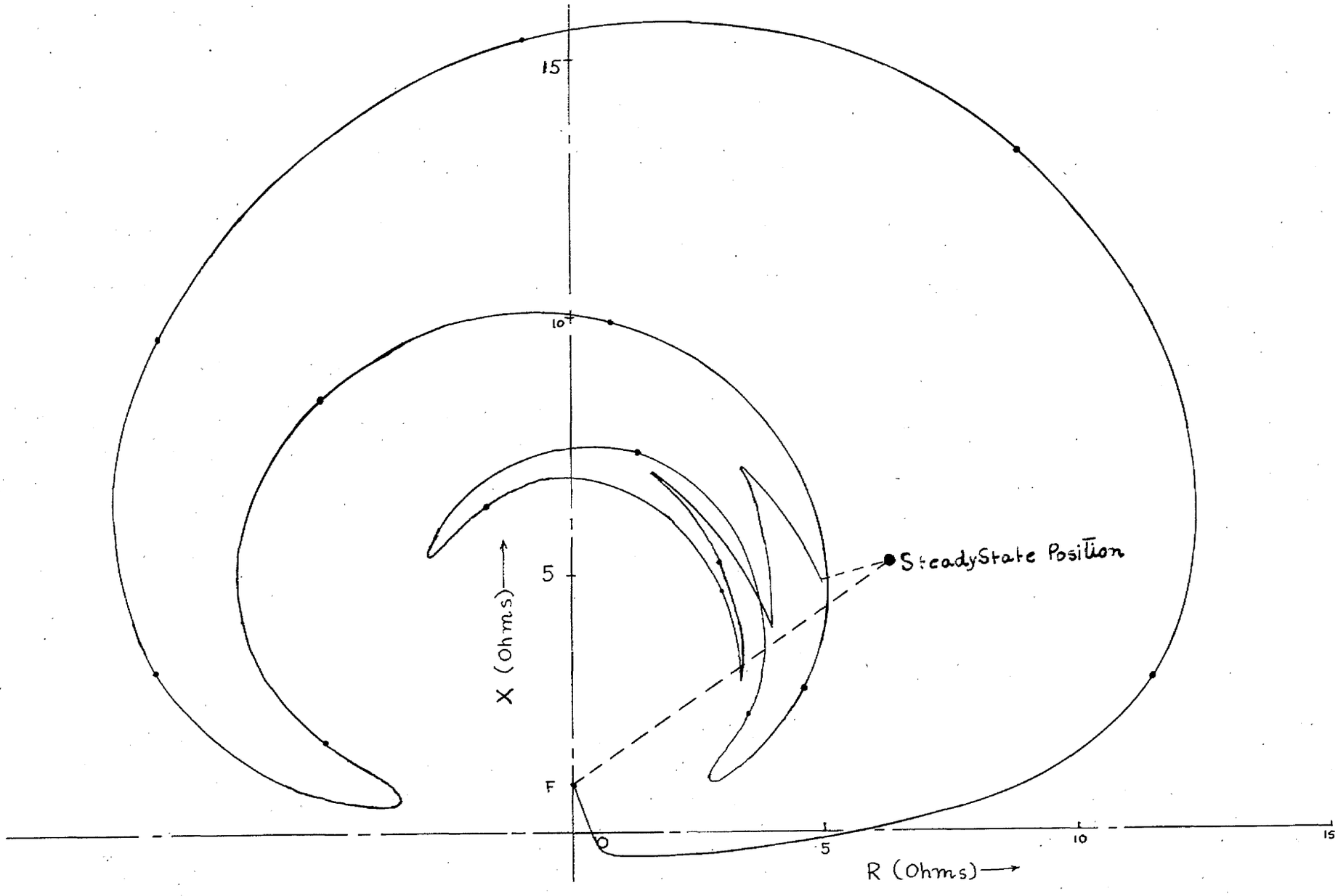

FIG. 27. DYNAMIC IMPEDANCE DURING 3-PHASE FAULT MEASURED AT MACHINE TERMINAL

transient illustrates the phenomena of flux variation. If the flux linkages would remain constant, the power would have followed a fixed power-angle characteristic. Similar curves have also been obtained from tests.[7] This also shows the effect of the voltage regulator in that the machine retains a higher amplitude for the first few seconds before settling down to the steady condition.

The wide range that the impedance locus covers in Fig. (27) may be of interest from the protection point of view. The usual practice of calculating a fixed impedance circle on the basis of a constant voltage behind the transient reactance is somewhat unrealistic when compared with the results that are likely to be observed in an actual system.

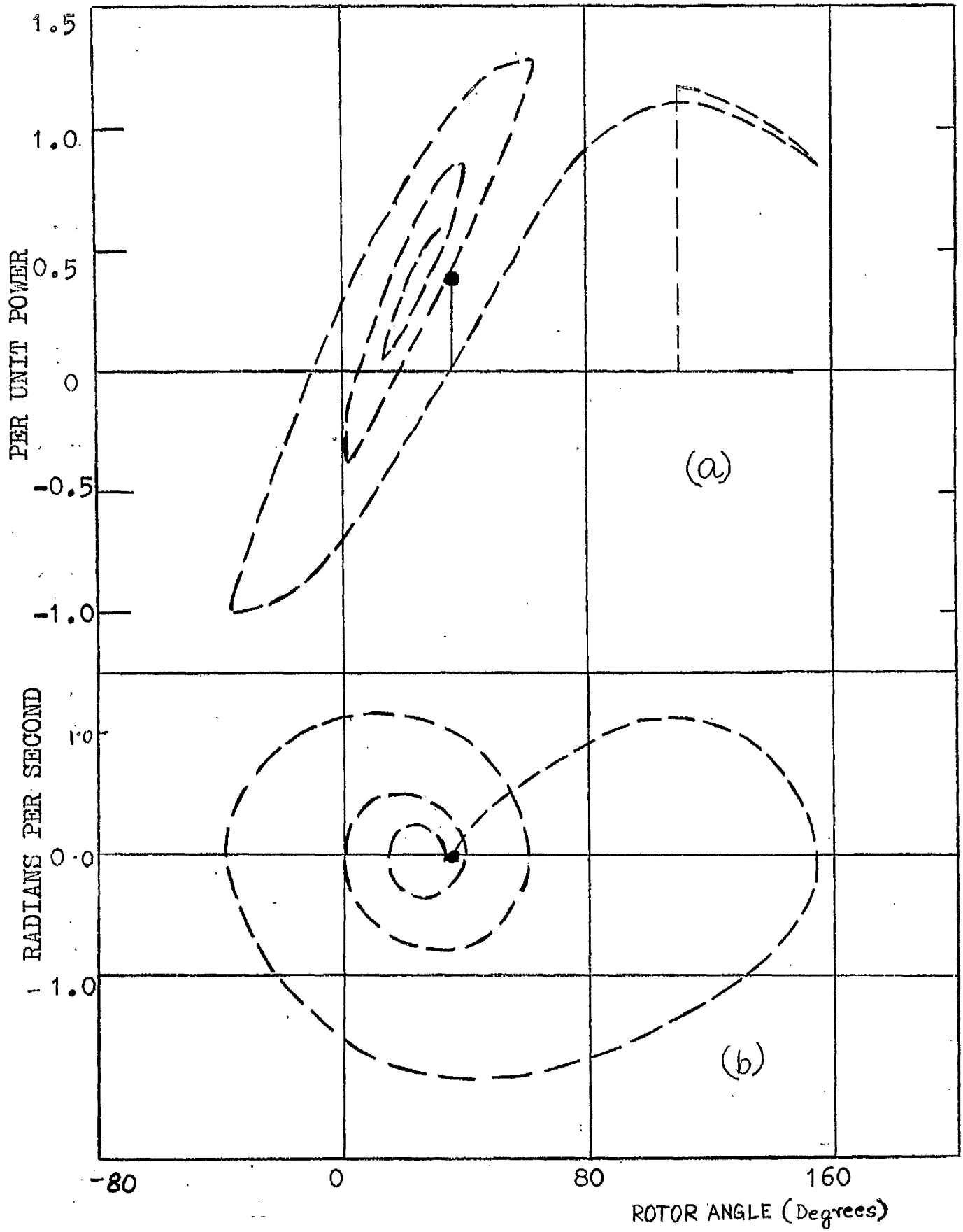

FIG. 28 (a) VARIATION OF POWER AS A FUNCTION OF ROTOR ANGLE

(b) DISPLACEMENT AS A FUNCTION OF ROTOR ANGLE

CHAPTER V

ROTOR OVER-VOLTAGES IN A.C. EXCITATION SYSTEM

(5.1) LIMITATION OF D.C. EXCITATION SYSTEM

For many years it has been the general practice to supply the excitation-power requirements of turbogenerators from d.c. generators driven from the main shaft or a combined induction motor d.c. generator unit running at a relatively low speed. This arrangement, particularly the direct-driven d.c. excitation has, in general, proved to be a reliable, economic and satisfactory source of power for synchronous generators of considerable size. With the present trend of increasing size of individual units, the excitation power requirements, however, tend to exceed the practicable limit of a d.c. generator. With higher output and the consequent reduction in speed, the d.c. generator size becomes uneconomically large. The higher voltage and larger current ratings of the d.c. exciter to cope with the demand of power requirements aggravate the commutation problem.

(5.2) A.C. EXCITATION SYSTEM

The recent development of semiconductor rectifiers of large current and high peak inverse voltage rating[31] has made the rectified output of an a.c. supply a practical source of excitation power of modern large turbo-alternator units. The

elimination of brushgear and consequent reduction of maintenance problem make this arrangement an attractive proposition and a.c. excitation systems are now finding widespread application.

(5.2.1) ARRANGEMENT OF THE RECTIFIER UNIT

The source of a.c. power may be obtained either from the normal station auxiliary supply or from an a.c. generator coupled directly to the main alternator-shaft.

In the case of a static excitation system where the supply is obtained from the station auxiliary transformer, the power, after rectification, is supplied to the main generator field winding through slip rings. This arrangement has the advantage of greater reliability with less maintenance problem in case of any fault in the rectifying elements. The main disadvantage, however, is that the excitation is influenced by the system-voltage disturbances and it is required to convert the constant voltage supply from the transformer to a variable-voltage input to the rectifier-unit to correspond to the response characteristics of the regulating devices.

In the alternative arrangement of a.c. excitation the rectifying unit is mounted directly on the main generator-shaft.[32] The source of supply is an a.c. generator of the usual rotating field type coupled also to the main alternator shaft. The armature which may sometimes be rotating type

instead of the field, can have three or poly-phase construction. The rotor is usually made up of laminated iron in order to eliminate the generation of eddy-current. The frequency of the exciter is increased to 100 c/s or 150 c/s in order to reduce the response-time of the exciter. Other special design features of an a.c. exciter have been discussed in reference (33). The main advantage of direct-coupled exciter is that it maintains independence of excitation supply. The rectifying elements are mounted on the shaft and provides a brushless machine with the added benefit of unit principle in plant layout. The main disadvantage, however, is found while replacing faulty diodes or any other maintenance work for which the complete turbo-generator unit has to be brought to rest.

(5.2.2) RATING OF THE RECTIFIER UNIT [34]

To obtain the proper current and voltage ratings, the rectifiers are used in series and parallel combinations as shown in Fig. 29 .

(5.2.2.1) CURRENT RATING

In selecting the current rating of the diodes a number of operating conditions must be considered. Firstly, the continuous rating, with one section of the diode-units isolated for maintenance or remaining faulty in case of rotating unit, must exceed the rotor current for continuous maximum output of the generator taking into account any

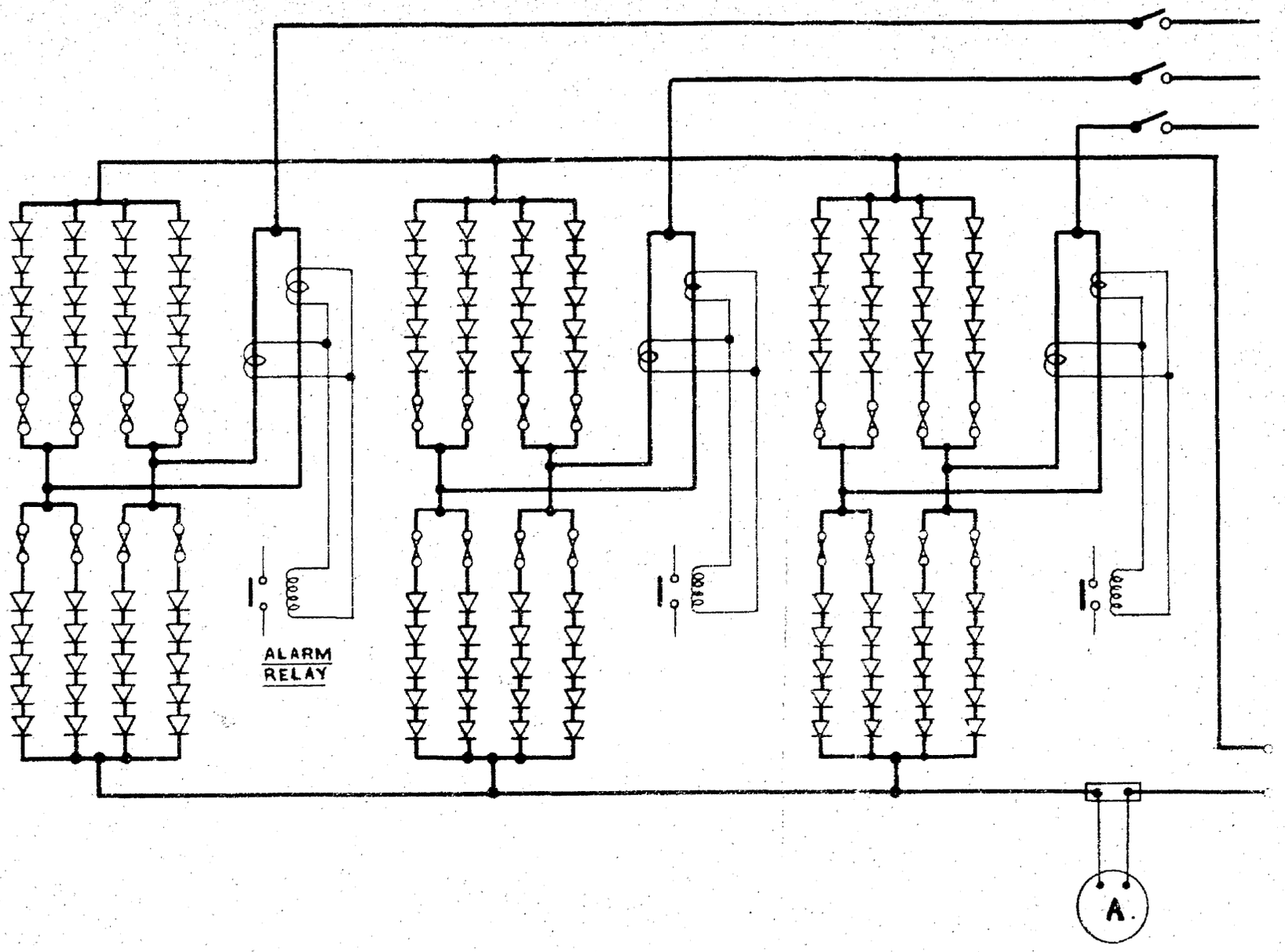

SIMPLIFIED DIAGRAM OF RECTIFIER CUBICLE CONNECTIONS

(SHOWING ONE BANK OF RECTIFIERS ONLY.)

FIG. 29.

derating of individual diodes. Secondly, the transient current to cope with any abnormal operating condition of the machine must be within the short-time capability of the diodes.

(5.2.2.2) VOLTAGE RATING

The two conditions governing the voltage rating of the diodes are the same as those for the current rating, namely, the m.c.r. excitation voltage and the exciter ceiling voltage. In addition, if the generator runs asynchronously with high initial loading or under pole-slipping with the main generator field circuit unexcited or open circuited high inverse voltage may be induced across the rectifier unit. The peak-inverse voltage rating of the complete rectifier unit should exceed the maximum voltage that can be induced under the worst operating condition.

(5.2.3) PROTECTION OF RECTIFIER UNIT

(5.2.3.1) EXCESSIVE FORWARD CURRENT AND OVER HEATING

High forward current can be caused by a fault at the main generator terminal or on the d.c. side of the rectifier stack. The excessive current raises the junction temperature to the damaging level. The present-day practice of protecting the diodes from faults due to large forward current is to fuse the individual strings of elements. This arrangement also prevents the possibility of feedback[35] from

other parallel circuits in the event of a short-circuit in the faulty diode string. Suitable alarm circuits are also incorporated for remote indication of the actual location of the fault.

(5.2.3.2) EXCESSIVE REVERSE VOLTAGE

High voltages may be produced across the rectifier unit for many reasons. In order to safeguard the diodes each one is shunted by a resistor and capacitor as shown in Fig.30 to grade the voltage distribution across the complete string. Sometimes thyrite variators are also used across the rectifier stack as shown in Fig.31 . The shunt capacitor and resistor arrangement also prevent the damage of the diodes during clean-up[36] intervals.

The prospect of manufacture of diodes with ultra-high peak inverse voltage and very large current rating in near future supports the possibility of using a.c. excitation in large turbo-alternator units that are manufactured nowadays and will be in future.

The overall advantage of using a.c. excitation system is that of availability of large amount of power as demanded by increasing synchronous-generator size, less space requirement and less maintenance problem. Reliability as to the long-time durability of such system will, however, be confirmed from experience.

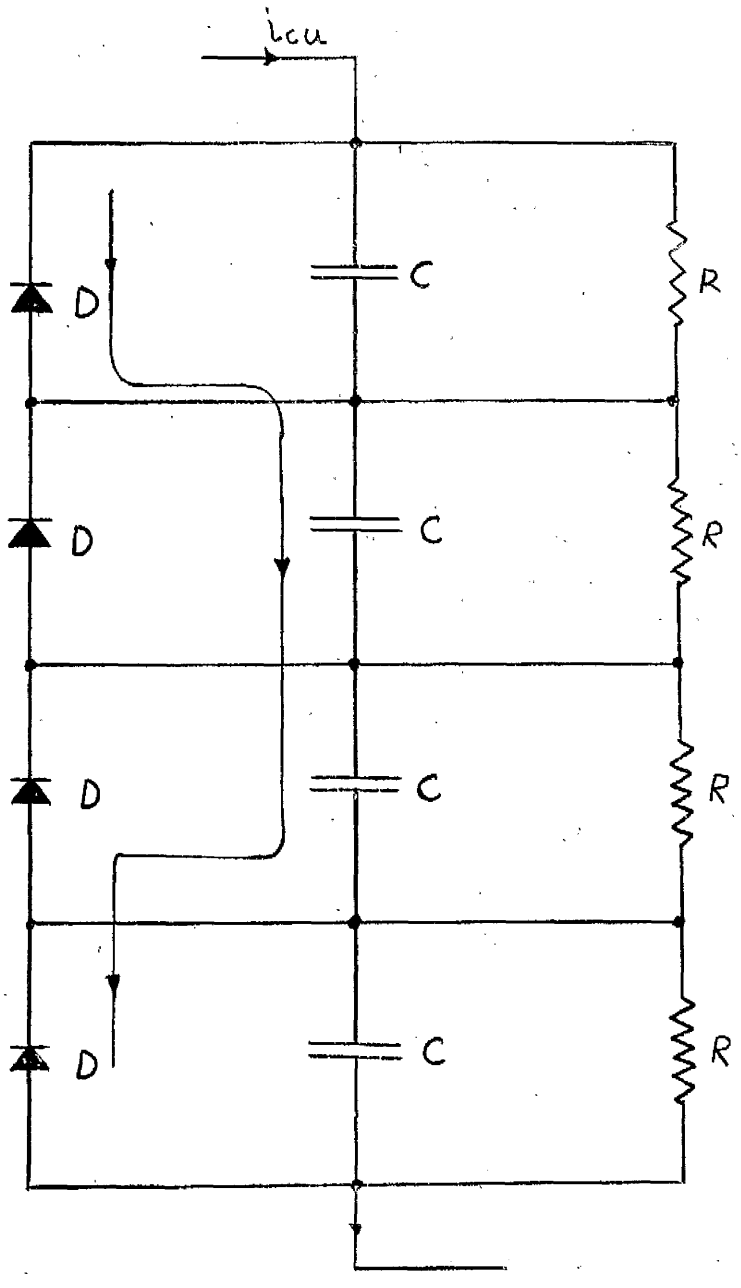

FIG. 30. USE OF CAPACITOR AND RESISTOR TO PREVENT CLEAN-UP CURRENT FAILURE

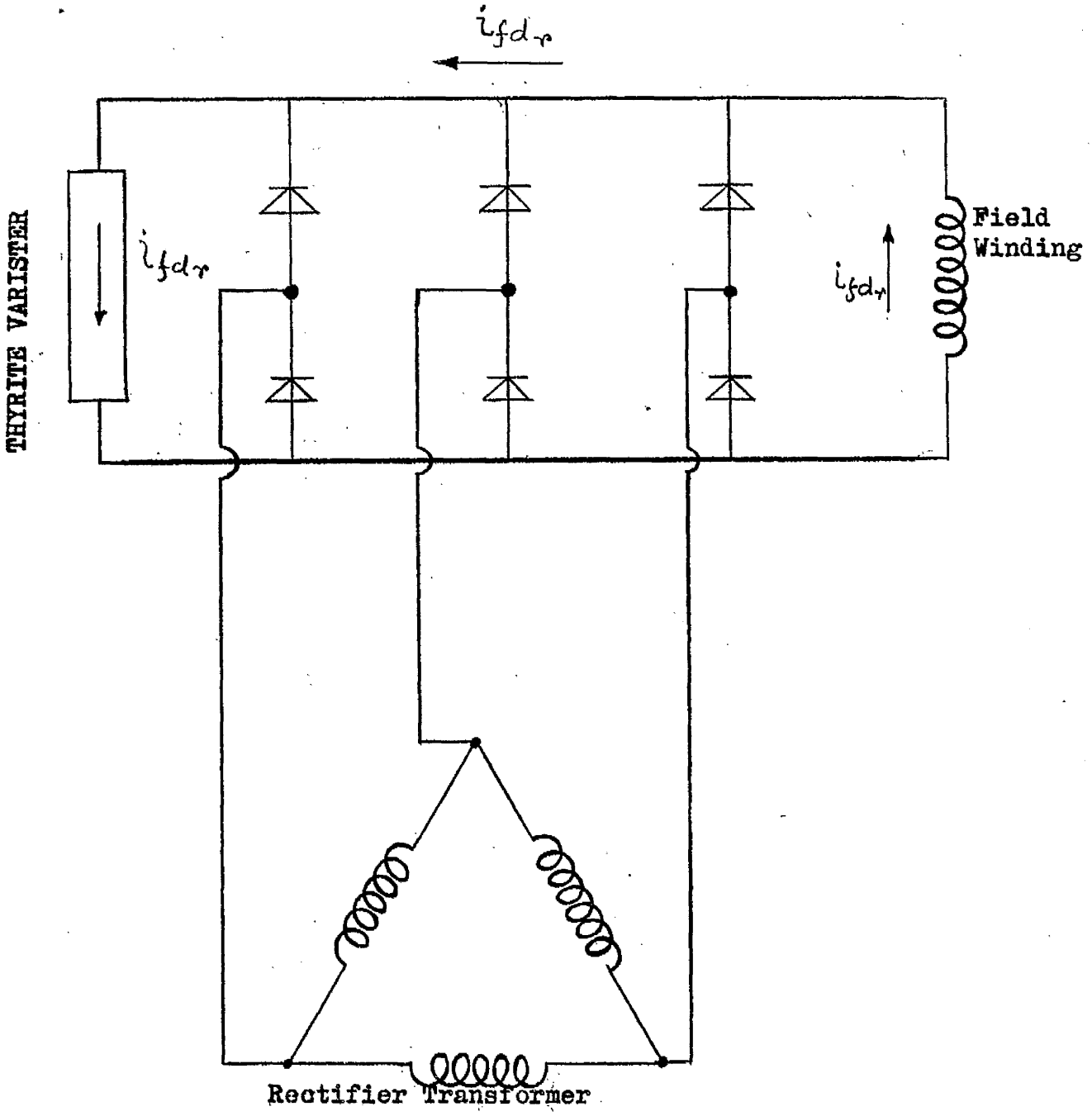

i_{fd_r} = Reversed Field Current

FIG. 31. USE OF THYRITE VARISTER FOR FIELD CURRENT FLOW DURING ASYNCHRONOUS RUNNING.

(5.3) OVER-VOLTAGE IN THE GENERATOR ROTOR CIRCUIT

The a.c. excitation system using semiconductor rectifiers differs from the conventional d.c. system in that it is not possible to have negative rotor currents or voltage. Whenever the main generator field current attempts to reverse its direction of flow, the high resistance presented by the rectifiers prevents it from doing so. In practice, this does not result in any appreciable loss of control. On the other hand, limitation of current flow is advantageous under such circumstances as resynchronisation. The major issue that stems out of this, however, is that under the conditions of pole-slipping and asynchronous running, when the rotor current attempts to reverse its direction but is prevented from doing so, a high rotor voltage is induced across the slip-rings.

(5.3.1) THE PHENOMENA OF POLE-SLIPPING

The phenomena of pole-slipping can be conveniently explained by referring to Figs. 32 to 35 . In these figures, the machine variables have been converted to dqo frame of references from the 3-phase quantities obtained from the site-tests described in Section (5.4). The machine variables are plotted as functions of rotor angle and time respectively to bring out a close insight into what exactly happens during pole-slipping.

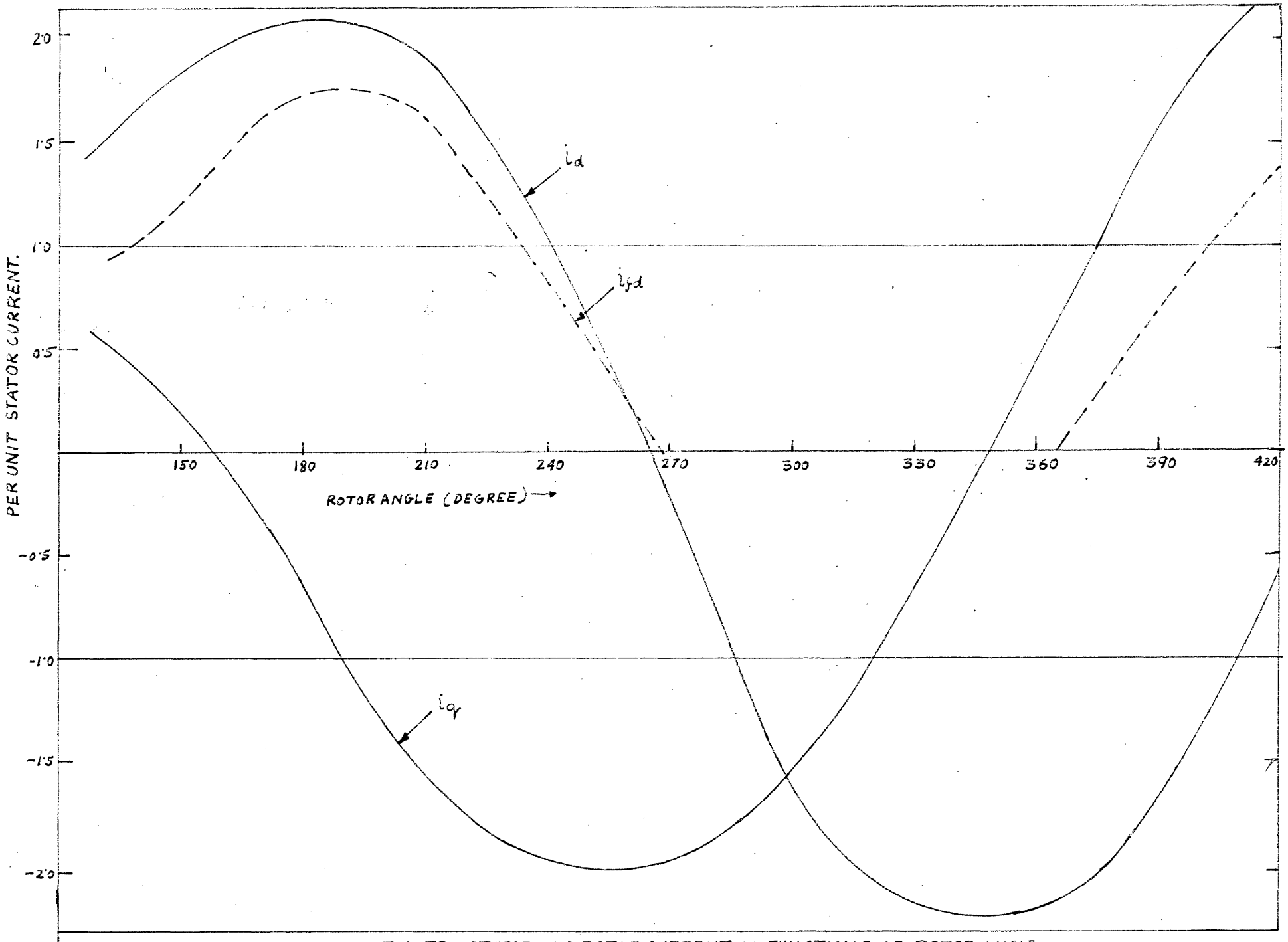

FIG. 32. STATOR AND ROTOR CURRENT AS FUNCTIONS OF ROTOR ANGLE DURING POLE SLIPPING.

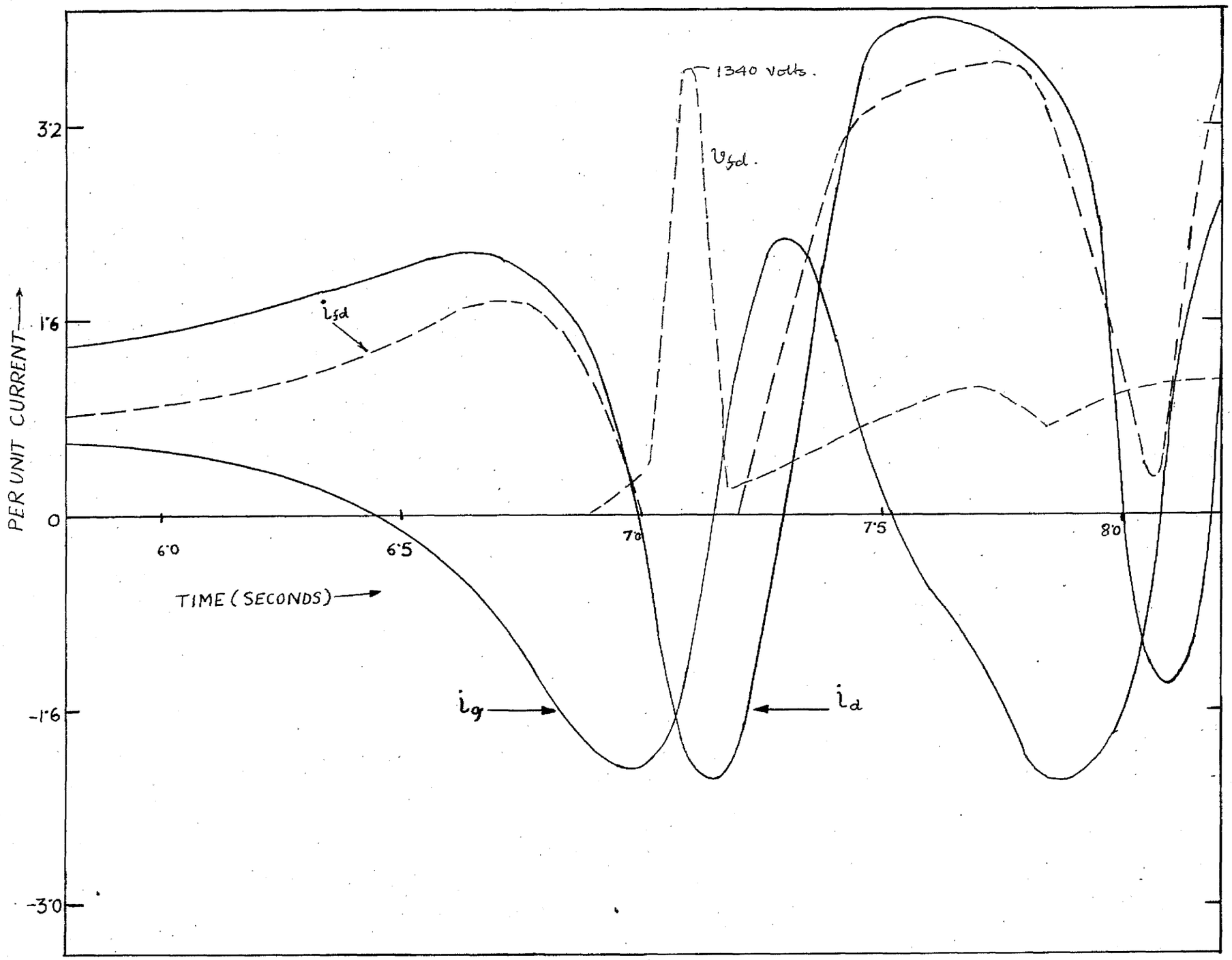

FIG. 33. VARIATION OF STATOR AND ROTOR CURRENTS DURING POLE SLIPPING.

Referring to Fig. 32 , it can be seen that the direct-axis stator current increases as the rotor angle moves from about 120 degrees to 180 degrees. Then between 180° and 360° of rotor angle the direct-axis current changes very rapidly from about 2.2 p.u. to -2.3 p.u. The high negative rate of change is shown in Fig. 33 . From equation (3.3) the expression for field current is given by

$$i_{fd} = \frac{(1 + \tau_{kdo}'p)v_{fd} + L_{ad}(1 + \tau_{kd}p)pi_d}{r_{fd}\{1 + (\tau_{kdo}' + \tau_{do}')p + \tau_{do}'\tau_{do}''p^2\}} \quad \text{and}$$

indicates that the rate of build-up of direct-axis stator current has a marked influence in the flow of the rotor current, particularly during the interval when the field-voltage remains more or less constant. When the direct-axis stator current has a high negative rate of change, the field current is also progressively reduced until it becomes zero. The change of both stator and rotor current tends to reduce the field- and stator-flux-linkages both of which have a maximum negative value when the rotor angle is about 180°. During this period, however, field forcing is slowly applied as the terminal voltage, which at this stage is largely dependent upon quadrature axis flux linkages, starts going below the reference level as shown in Fig. 35 .

(5.3.2) FACTORS THAT EFFECT THE MAGNITUDE OF INDUCED VOLTAGE

When the rotor current has been forced to zero and then,

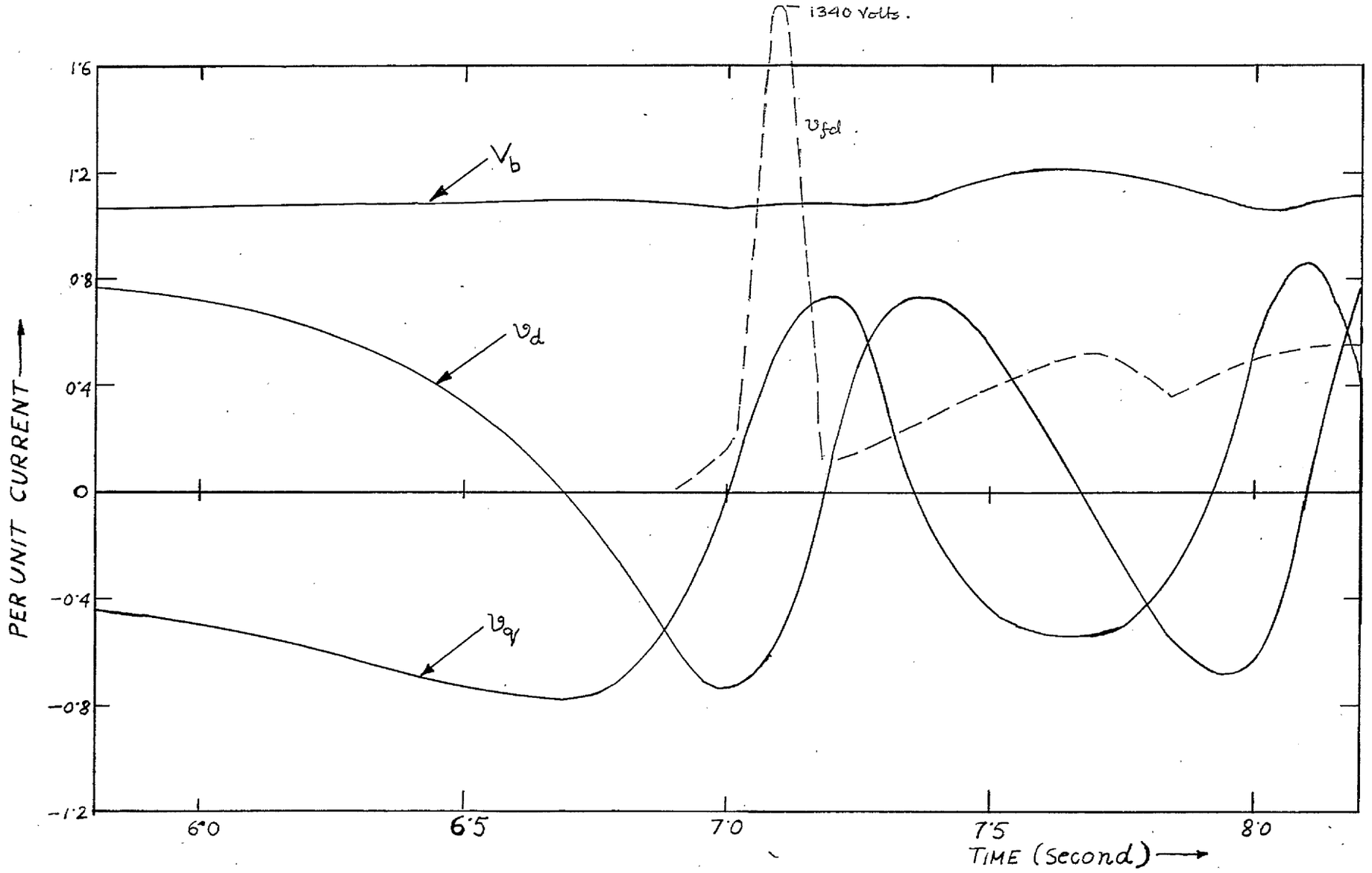

FIG. 34. STATOR AND BUSBAR VOLTAGE VARIATIONS DURING POLE SLIPPING

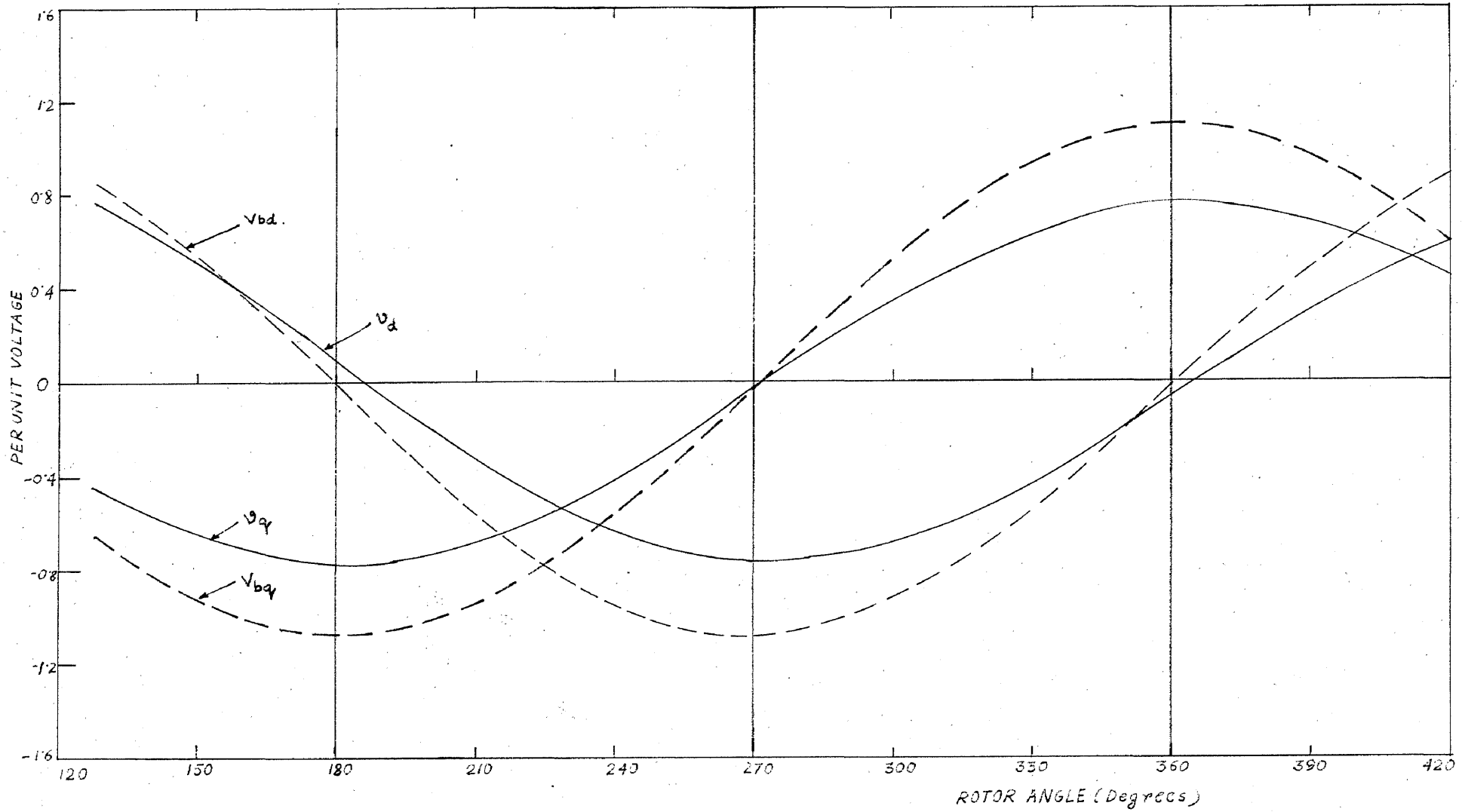

FIG.35. STATOR AND BUSBAR VOLTAGES AS FUNCTIONS OF ROTOR ANGLE DURING POLE SLIPPING.

because of the characteristics of the semiconductor rectifiers, is prevented from flowing in the opposite direction, a situation which is different from that of a conventional d.c. excitation system, arises. At the instant of field current being zero, if the rotor circuit is not short circuited through discharge or any other external resistor, the rotor winding behaves like an open circuited coil having electro-magnetic coupling with the other direct-axis circuits. This, in effect, reduces the open-circuit time-constant of the field winding to zero and the flux build-up becomes much more rapid, as this is now arrested only by the transient and subtransient time constants which are much smaller than the field circuit time constant. Because of the absence of any de-magnetising ampere-turns from the field circuit a high induced voltage proportional to the rate of change of the field flux-linkage appears across the field winding as shown in Fig.33 and also in Fig.34 .

Beyond rotor-angle values of 360°, the direct-axis stator current continues to increase with even higher positive rate-of-change thus boosting up the field current to a very high level as can be seen in Fig. 32. The magnitude of the induced voltage depends on a number of factors, of which the following are important.

(5.3.2.1) INERTIA CONSTANT

As can be seen in Fig.32, the phenomena occurs during

the period when rotor angle moves from about 120^{o} to about 360^{o}. The rate-of-change of rotor angle greatly influences the rapidity of current and flux changes along the direct axis. For a particular input power, a larger inertia constant will slow-up the movement of the rotor-angle and vice-versa with a smaller inertia constant.

(5.3.2.2) INITIAL MACHINE OPERATING CONDITION

When a generator is operating at a large load angle due to its being under-excited it can be seen from the vector diagram in Fig. 36 that the current in the field winding is small. It is, therefore, more likely that the rotor current will be forced to zero and the duration of current-zero can also be prolonged. On the other hand, with an initial large current in the field circuit the negative rate of change of the direct-axis stator current may not be able to force the field current to zero and thus the possibility of generation of induced voltage may be avoided during a cycle of pole-slipping.

(5.3.2.3) OPEN CIRCUIT TIME CONSTANT OF THE FIELD WINDING

As the load angle between the direct-axis of the machine and the busbar to which it is connected, moves away during the pole-slipping, both the direct- and quadrature-axis components of the terminal voltage move along with those of the busbar. The magnitude of the direct- and quadrature-axis currents depends on the difference of the corresponding

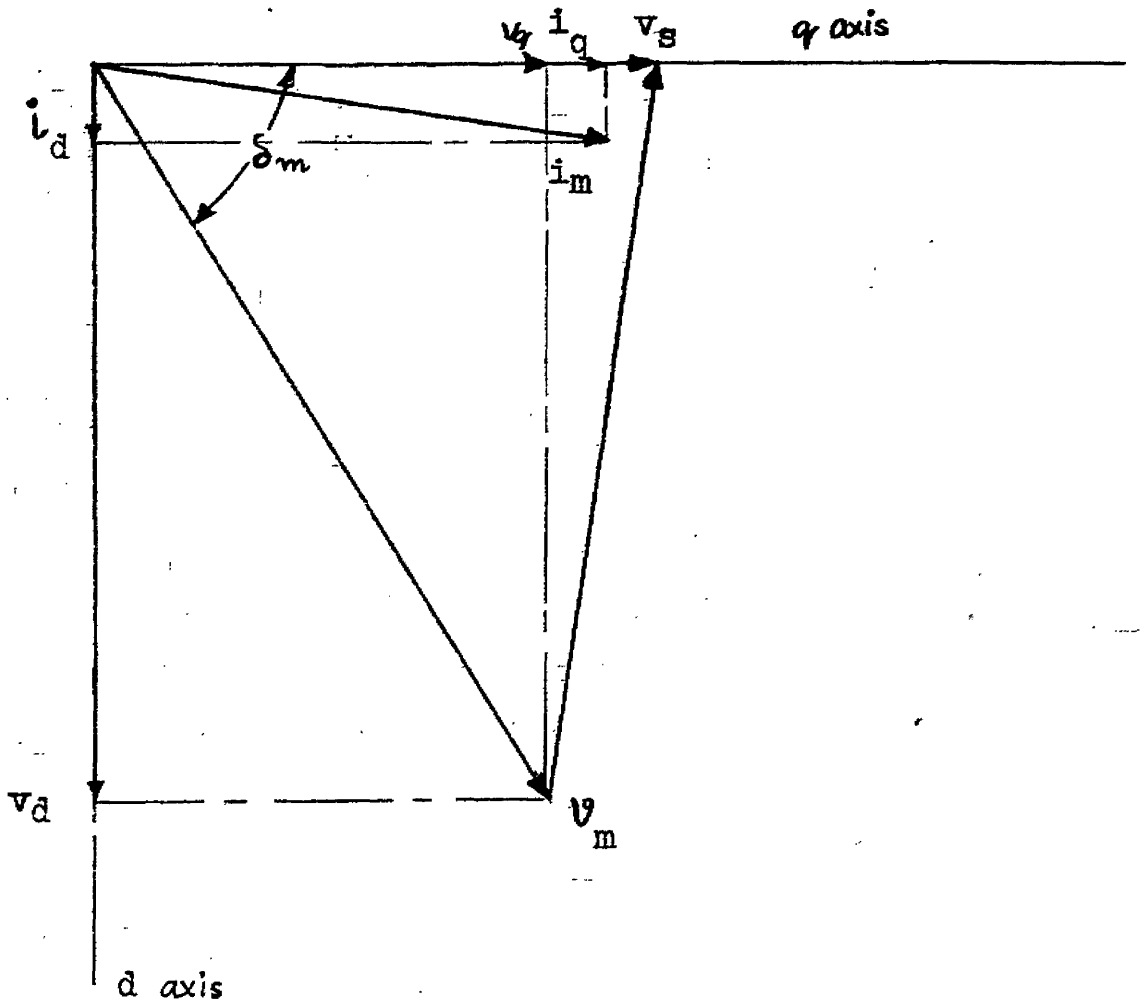

FIG.(36) SIMPLIFIED VECTOR DIAGRAM OF AN UNDER EXCITED GENERATOR

voltage components for a constant external impedance. That is, neglecting resistance

$$i_d = (V_q - V_b \cos \delta)/X_t$$
$$i_q = (V_b \sin \delta - V_d)/X_t$$

Now, how closely the machine terminal voltage will follow the busbar voltage depends on the rapidity of flux-linkage response on the two axes. A smaller equivalent time constant in any axis indicates that the flux linkage will follow more rapidly the component of the busbar voltage in that axis. With a larger time constant in the direct axis, it is more likely that the direct-axis stator current will be larger both in the negative and positive direction with a possibility of more rapid current variation.

(5.3.2.4) SUBTRANSIENT TIME CONSTANTS

During the period when the field current remains zero, the rapidity of flux variation is determined mainly by the time constants of the damper windings in the direct axis. A large damper-winding time constant will reduce the rate of change of the flux linkages in the field circuit and consequently the reverse voltage appearing across the slip ring will be small. Apart from controlling the magnitude of the over-voltages, damper winding parameters play an important part in the response of the machine variables during the period when the field current starts flowing in the positive direction. During this period the flux-balance

for normal operation between the stator and the rotor circuits is established after it was lost during the period when field current remained zero. The response of stator current, particularly in the direct axis, corresponds to the difference of two flux linkages, one that builds up during the occurrence of the over voltage and the other that would exist if the field current was not kept at zero for a certain period. This difference is mainly a function of the sub-transient parameters.

(5.4) COMPARISON OF COMPUTED AND SITE TEST RESULTS

Tests were carried out in July 1962 on one of the generators in Belvedere Power Station[37] to ascertain the amplitude of the rotor voltage surges in order to confirm the adequacy of the peak inverse voltage rating of the excitation rectifiers. The test generator was connected to the system busbar and was delivering power to the system. The condition of pole-slipping was simulated by reducing the reference input to the voltage-regulator comparator to 60% of the normal value. During the test considered here for the purpose of comparison the reference input was reset to the original value after two pairs of pole slipping and the machine subsequently regained synchronism. The excitation control system of the generator is shown in Fig.37 and the equations pertaining to the various elements of the voltage regulating

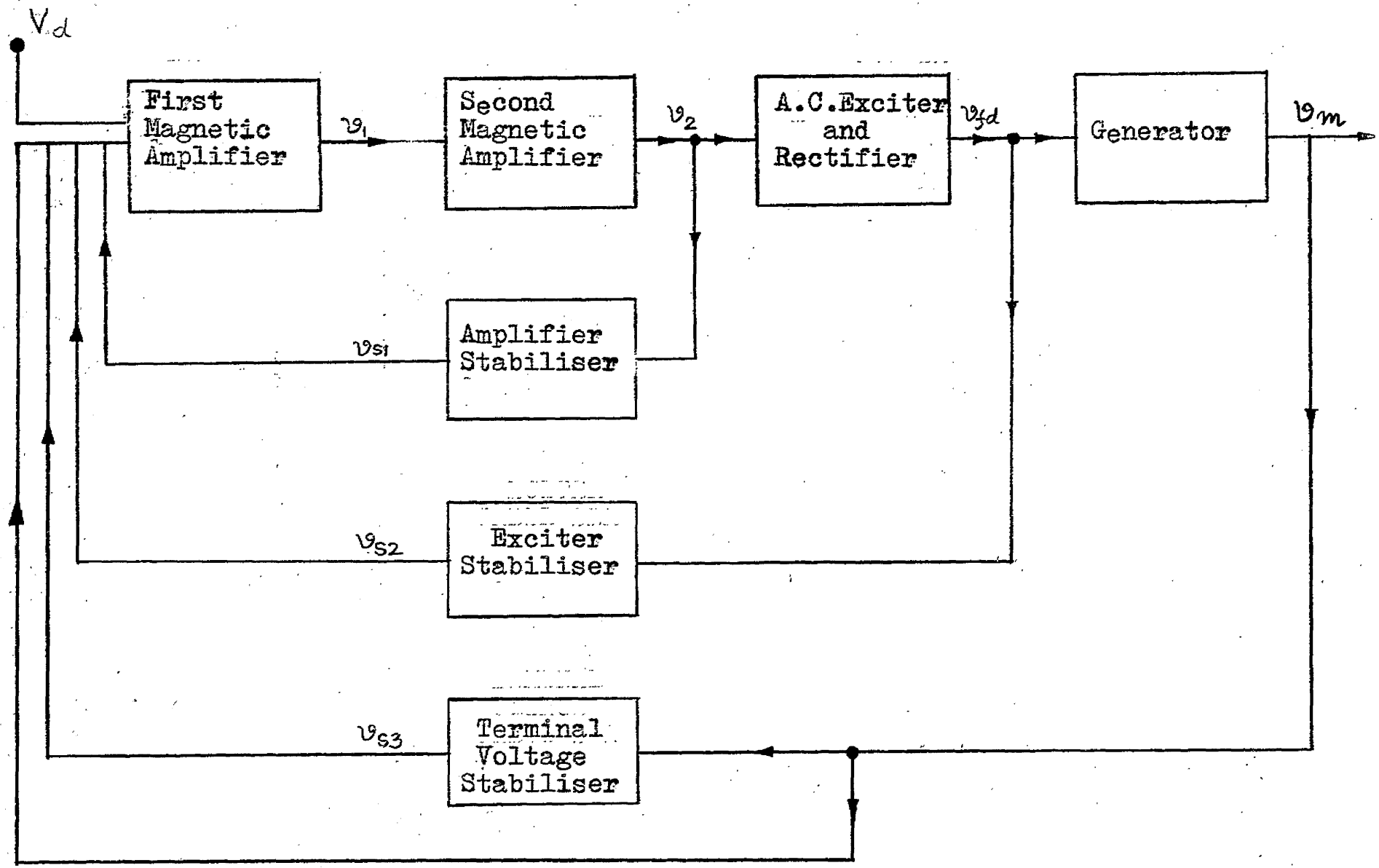

FIG. 37. BLOCK DIAGRAM OF VOLTAGE REGULATOR (BELVEDERE MACHINE)

system are given in Appendix D. The system interconnection, for the purpose of the study, can be represented in the same way as shown in Fig. 6 . For studying the phenomena of pole-slipping by digital computer analysis additional instructions were incorporated in the program to represent the constraints imposed by the field current having only one polarity and consequent changes of some of the differential equations. The difficulty that was encountered in formulating the constraint without losing the generality of the program, was overcome in the way as described in Appendix D. The data for the test generator supplied by the manufacturers and obtained from the calculations are given in Tables VI and VII.

The initial values of some of the machine variables obtained from site tests and computation are given in Table VIII. The transient response of these variables during pole-slipping are shown in Figs. 38 to 44 by curve(b). The computed results show close agreement with those from site tests until the pole-slipping occurs with the consequent generation of the high rotor voltage. The maximum over-voltage and the subsequent overshoot of field current obtained from computation as shown in Figs 38,39 are satisfactory. After the first pair of pole-slipping, the computed results deviate appreciably from those obtained from site-tests.

TABLE VI

Parameters	Supplied Values	Calculated Values at 1.0 p.u. terminal voltage
Generator Ratings	120 MW, 13.8 kV, 0.9 P.F.(lag), 3 phase, 2 pole, 50 c/s, Hydrogen cooled	
X_d	1.36 (unsaturated)	1.255
X_q	-	1.255
X_{ad}	1.24 (unsaturated)	1.135
X_{aq}	-	1.135
x_{ffd}	-	1.227
x_a	0.12	0.12
x_{lfd}	-	0.092
X_{lkd}	-	0.032
X_{lkq}	-	0.032
X'_d	0.2035 (unsaturated)	0.233
X''_d	0.1415 (unsaturated)	0.143
X''_q	-	0.151
R_{fd}	-	0.000862
R_a	-	0.002
R_{kd}	-	0.01128 (0.00564)
R_{kq}	-	0.01128 (0.00564)
τ'_{do}	-	3.708
τ''_{do}	-	0.02
τ'_d	-	0.606
τ''_d	-	0.014
τ'_{kdo}	-	0.201
τ''_q	-	0.065
	-	0.025

TABLE VI (continued)

Parameters	Supplied Values	Computed Values at 1.0 p.u. terminal voltage
T_{kd}	-	0.025
H	3.87 kW sec/KVA	
K_d	-	0.00319
ω_o	314 radians/sec.	-
M	-	0.0246
	Generator Transformer	
Rating	128 MVA	-
O.C. Turn Ratio	13.8/140.5 kV	-
Reactance	15%	-

TABLE VII

Parameters for the Excitation System

Parameters	Supplied Values
τ_1	0.30 second
τ_2	0.244 second
τ_3	0.035 second
$v_1$max	60 volts
$v_1$min	-60 volts
k_1	63
τ_4	0.007 second
k_2	4.76
τ_5	2.19 second
k_3	0.00198
τ_6	0.122 second
τ_7	0.3 second
k_4	0.00225
τ_8	0.3 second
k_5	0.346
τ_9	0.3 second
$v_2$min	0.0 volts
$v_2$max	126.0 volts
v_{fd}min	0.0 volts
v_{fd}max	540.0 volts

TABLE VIII

Steady State Readings at Start of Test

Test 1/3	Pole Slipping	
	Test Results	Computed Results
Stator voltage (kV)	14.8	14.75
Stator Current (kA)	4.56	4.68
Active Power (MW)	115.5	116.5
Reactive Power (MVAR)	28.0	26.7
Rotor Voltage (volts)	210	214
Rotor Current (amps)	1314	1280
Rotor Angle (degrees)	35	36
Measurement During Test		
Peak Induced Rotor Voltage (volts)	1340	1295
Stator Voltage (kV) at this time	10.5	10.5
Stator Current (kA) at this time	12	10.8
Instantaneous slip (%)	2.5	2.8

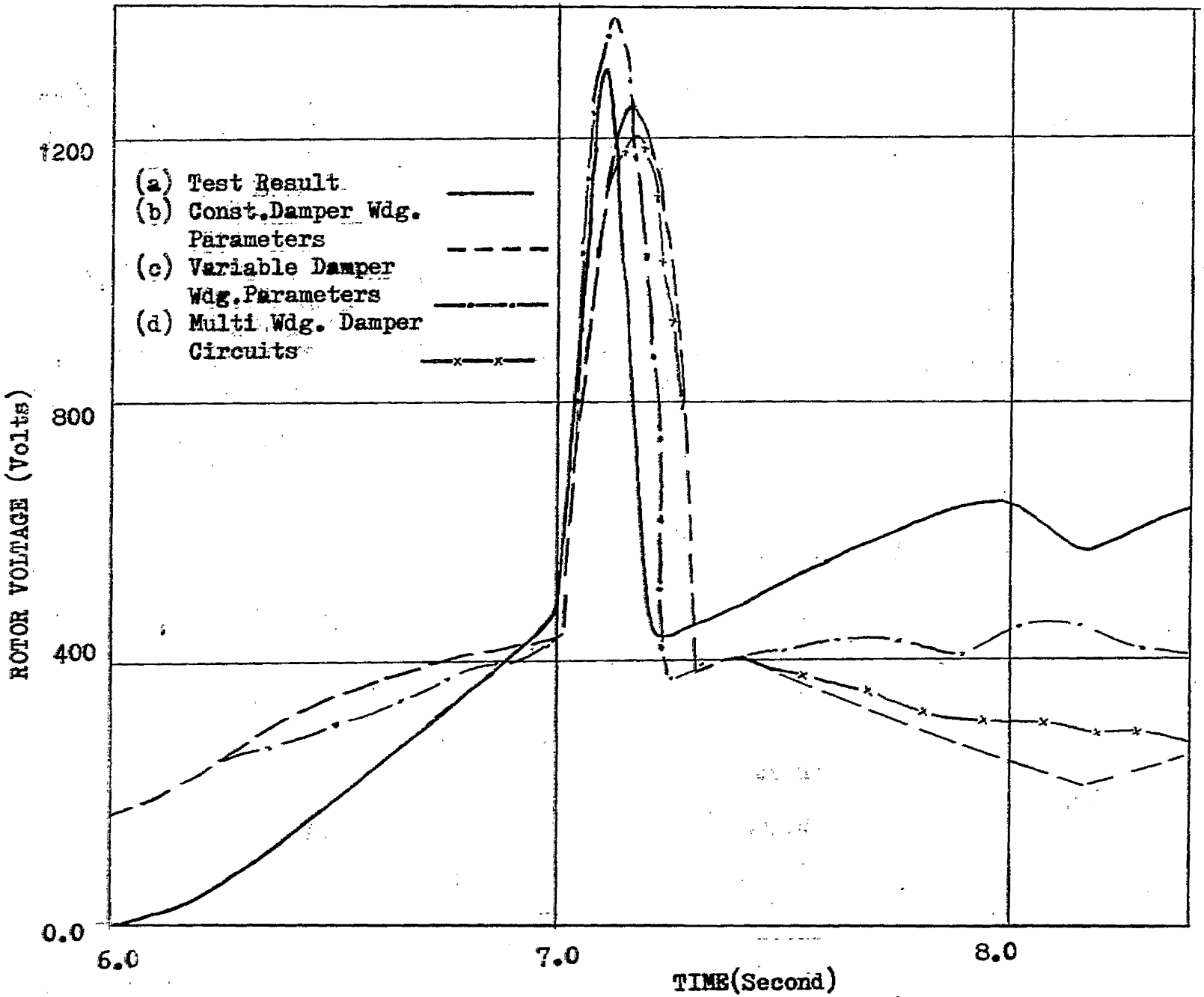

FIG. 38. ROTOR VOLTAGE VARIATION DURING POLE-SLIPPING.

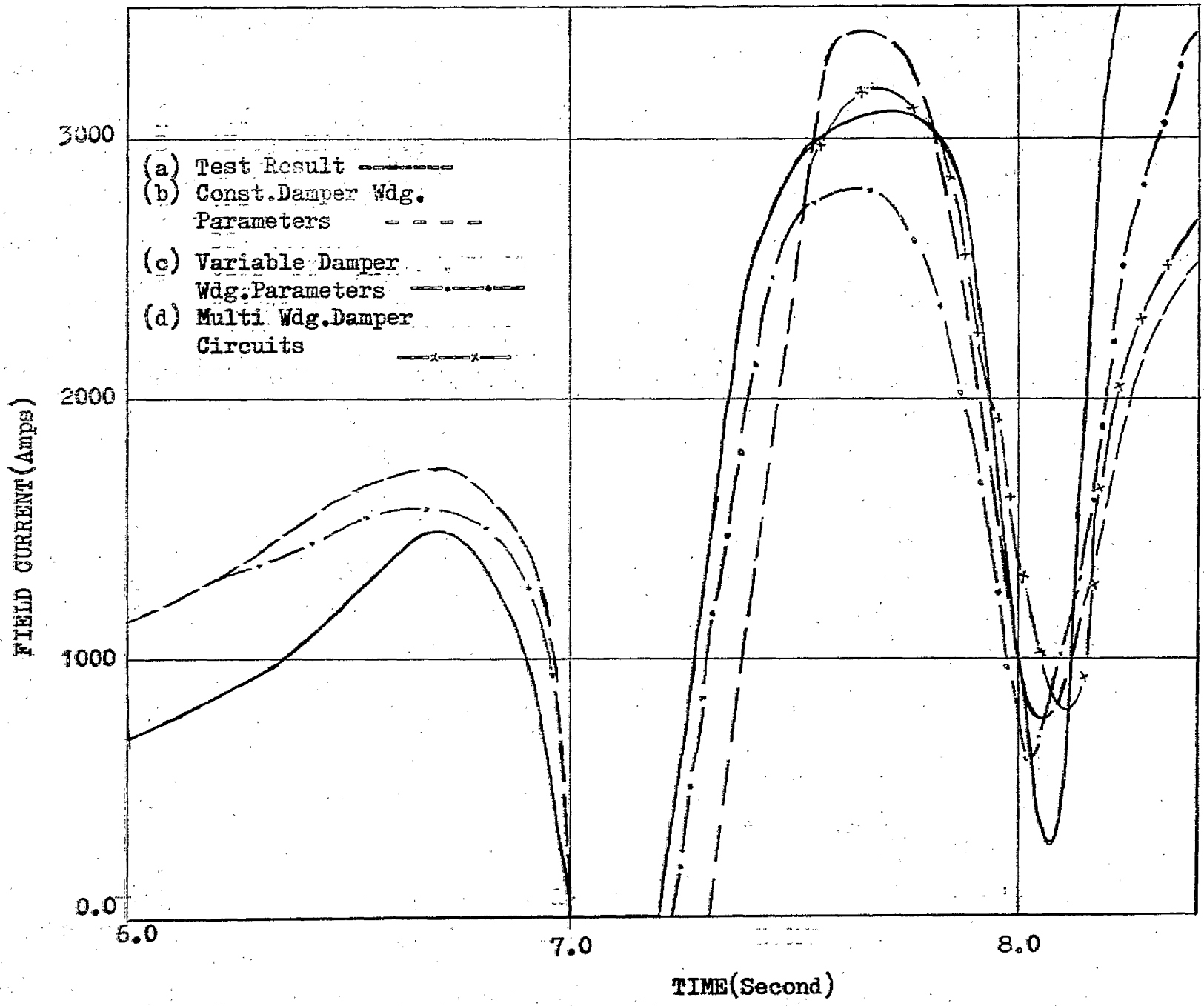

FIG. 39. ROTOR CURRENT VARIATION DURING POLE_SLIPPING$_3$

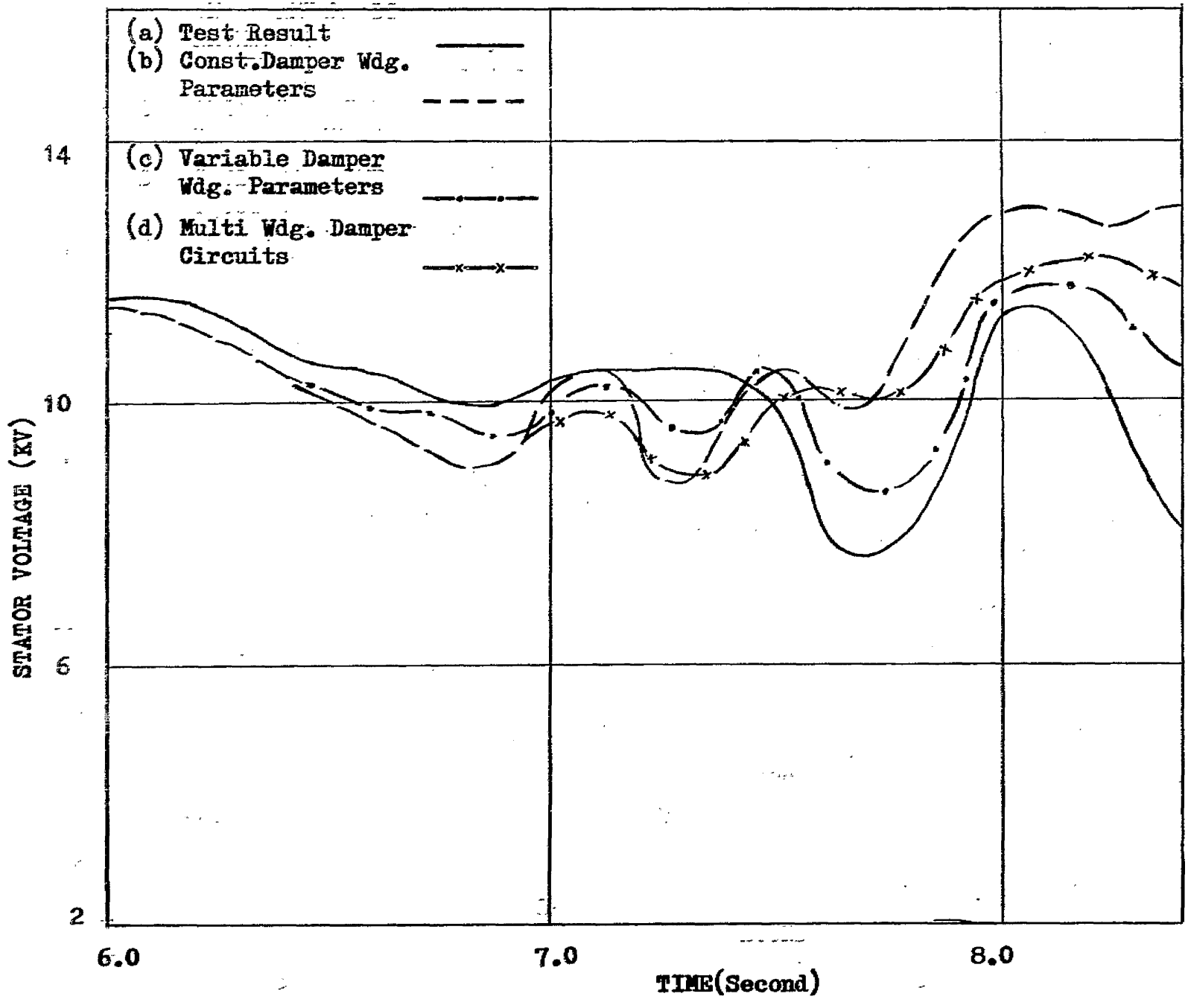

FIG. 40. STATOR VOLTAGE TRANSIENT DURING POLE-SLIPPING.

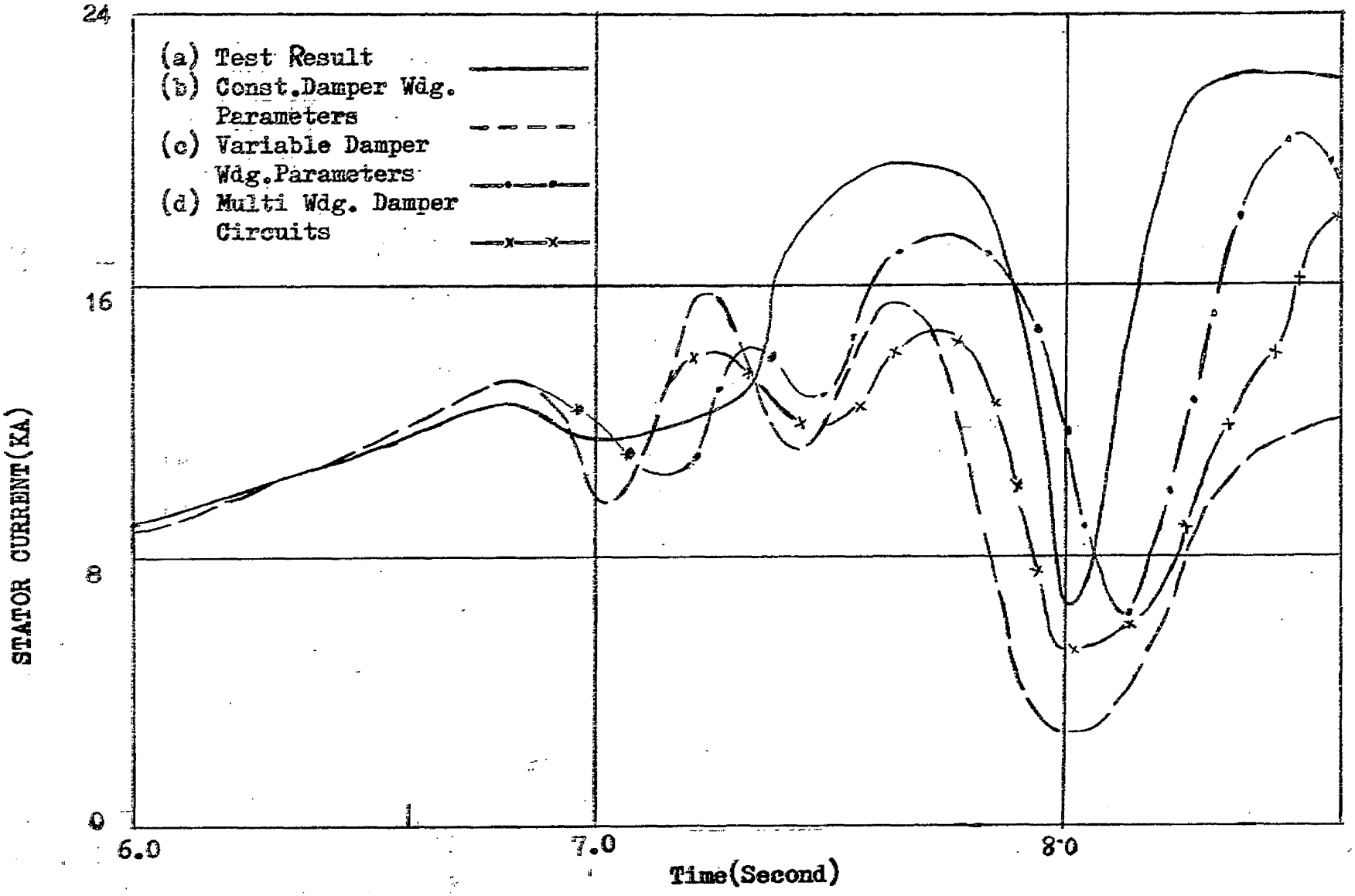

FIG. 41. STATOR CURRENT TRANSIENT DURING POLE SLIPPING

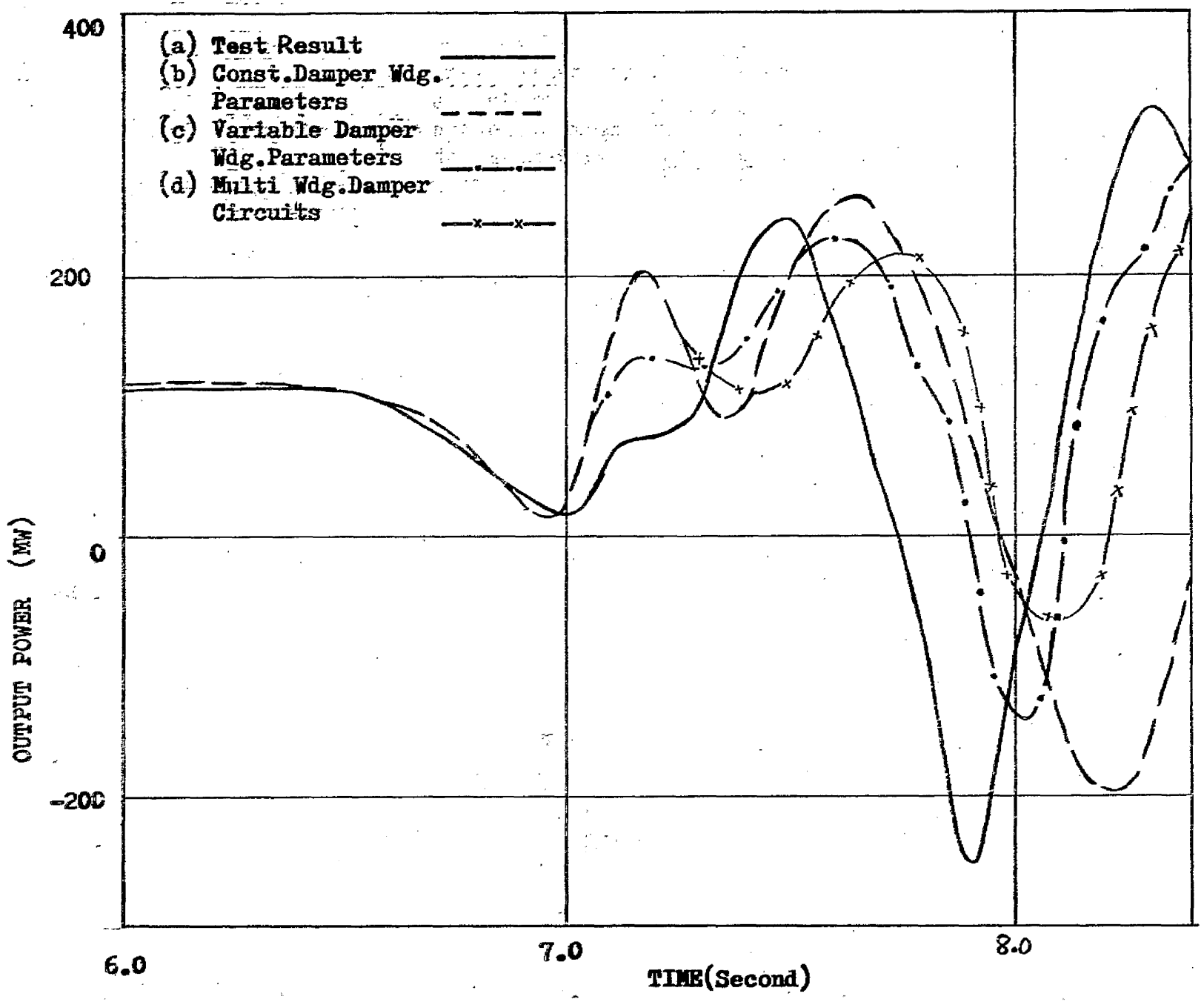

FIG. 42. OUTPUT POWER VARIATION DURING POLE-SLIPPING

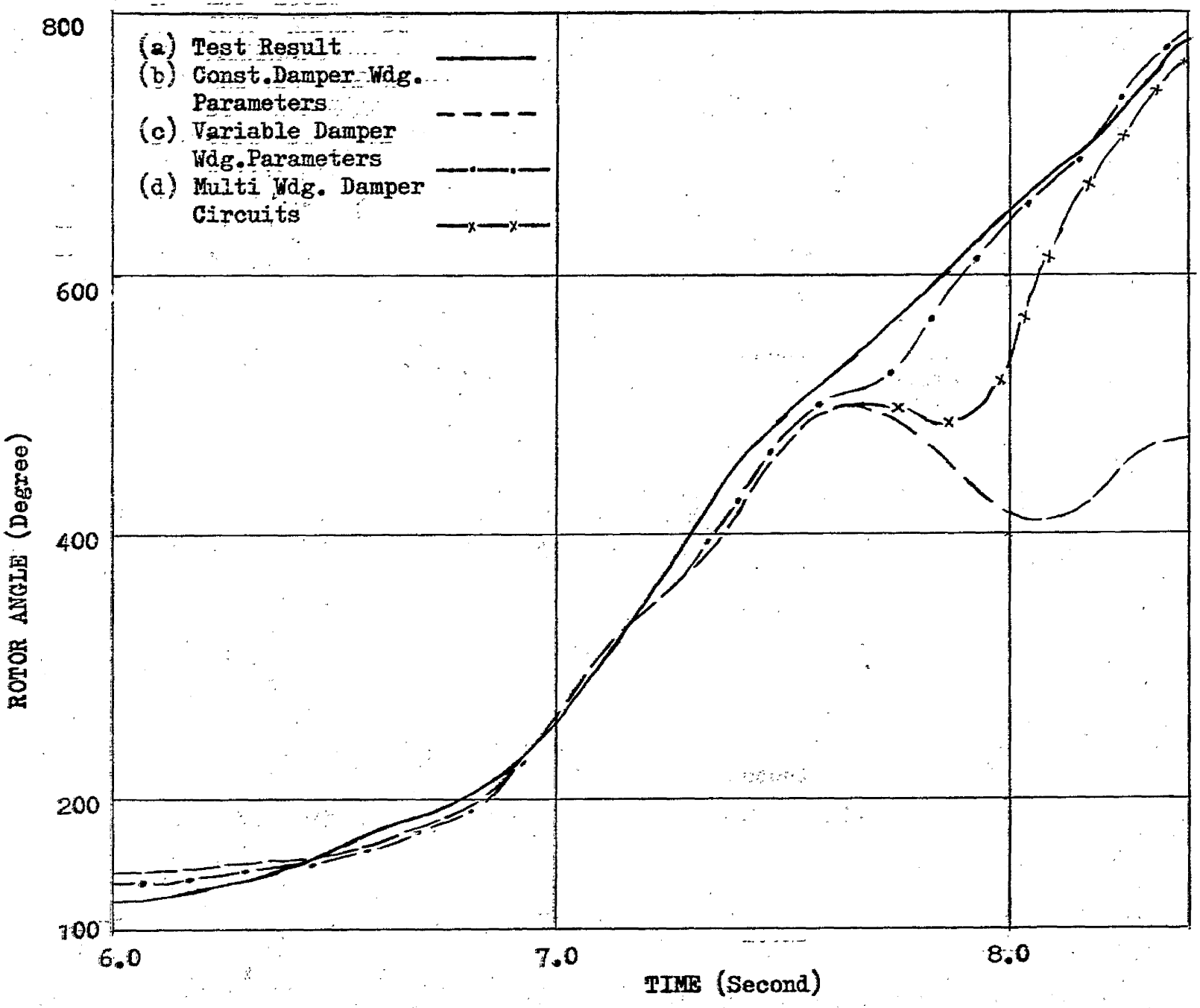

FIG. 43. ROTOR ANGLE VARIATION DURING POLE-SLIPPING.

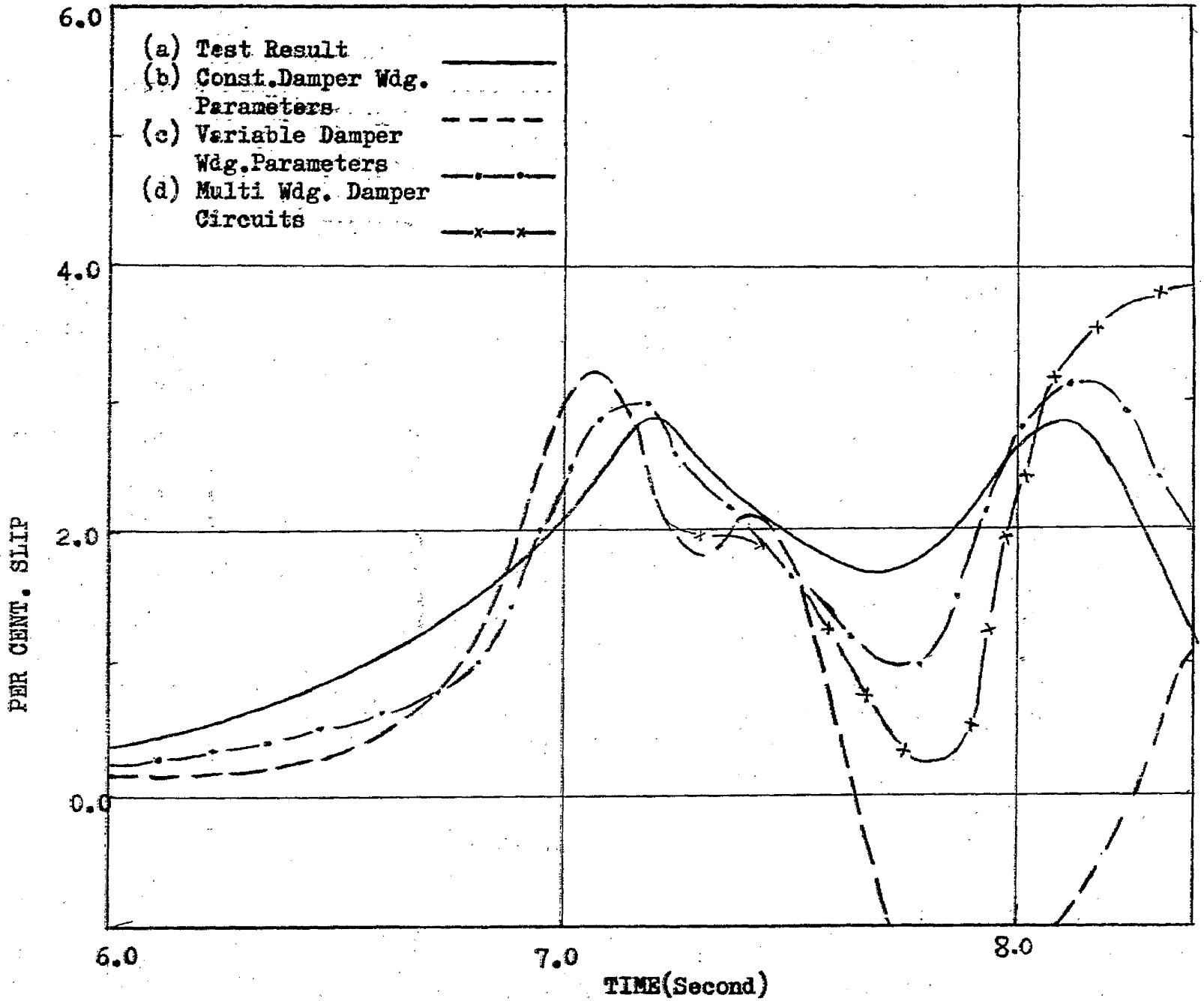

FIG. 44. VARIATION OF SLIP DURING POLE-SLIPPING.

(5.5) GENERAL COMMENTS ON THE RESULTS

During the transient periods when machine operations do not correspond to the steady state conditions the solution of the machine variables from the differential and other equations is influenced by the parameters used. When the parameters are in error, the deviation is progressive with the duration of transients. In case of analytical studies of prolonged disturbances, the accuracy of the available data is very important in making any worthwhile assessment of machine operations. While trying to program the correlation study for the pole-slipping condition widely varying results were obtained by making small changes in subtransient parameters and it was necessary to adjust the value of the damper winding parameters as given in Table VI. In the direct axis the subtransient parameters are not so important until the field current is reduced to zero, whereas in the quadrature axis these are very critical, specially the time-constants since there is no other dominantly large time constant as in the direct axis.

The sources of error in the analytical results can be attributed to the following main reasons:

(a) Governing System

No information was available about the governing system of the generator turbine. The governing system of the test generator in Goldington Power Station was at one stage used

for the present study, but the results were not very encouraging. The input to the turbine was, therefore, assumed to be constant during entire transient. Satisfactory results were still obtained for the first several seconds due to the slip remaining well within 1% of the rated frequency for about 6 seconds and the input power may not change appreciably for such speed change.

(b) Busbar Voltage

The busbar to which the machine was connected was assumed to be an infinite source not being affected by the machine operating conditions. It can be observed from Fig.34 that the busbar voltage was not constant during pole-slipping. Such variations of busbar voltage and phase displacement have been recorded during site-tests.[29]

(c) Subtransient Parameters

The inadequacy of the eddy current representation by short circuited coils with fixed parameters is well known. The resistances and inductances of the amortisseur circuits are calculated from the short circuit tests whereas these depend, instantaneously, on the rate of change of flux on the rotor body. The single-valued parameters are, therefore, likely to introduce error in mathematical analysis wherever their contribution is prominent.

CHAPTER VI

EDDY CURRENT PHENOMENA IN FERRO-MAGNETIC MATERIAL

(6.1) GENERAL

A large amount of work has hitherto been carried out on eddy current phenomena but a mathematically sound method of considering the effects of eddy current in the analysis of synchronous machines under transient conditions has not yet been developed. Though the representation of eddy current paths by constant parameters yields satisfactory results under certain conditions, its inaccuracy for analysing prolonged transients has been realised on several occasions[20].

(6.2) PREVIOUS WORK

Following the pioneering work of Thompson[40] and Rosenberg[41] analyses of eddy current phenomena have been considered for problems ranging from essentially academic studies to severely practical ones. In some cases, the treatment of the subject has been of a general nature, whereas on other occasions the investigations have been concerned with particular aspects of the applications of the effects produced by the flow of eddy currents.

The work of Pohl[42], McConnell[43], Thompson[40] and, more recently, by Agarwal[44], Keshavamurthy and Rajagopalan[45] and Subba Rao[46] have been concerned with analysing the effect of

the application of an electromagnetic field in a ferromagnetic material of comparatively simple configuration and the emphasis has been towards a qualitative assessment of the quantities such as flux variations and the current distribution within the material. The work of Concordia and Poritsky[47], Wood[48], Bharali and Adkins[49], and Hamilton[50] and others[51,52] on the otherhand, are more closely associated with eddy current phenomena related to rotating machines.

In most of the previous analyses except in references (45) and (42), the solution of the electromagnetic field equations are based on the existence of an harmonically varying forcing function. When it relates to rotating machines, particularly to alternators where the rotor is forged out of solid iron, the solution takes a difficult form because of the complicated nature of the flux path and the presence of slots round the periphery of the rotor. Due to a pronounced skin effect during flux variation, the degree of saturation of the material is not uniform all over the flux path and the treatment of the complete problem poses a formidable task. It therefore becomes necessary to calculate an equivalent flux path which corresponds reasonably to the total effect of saturation. Wood and Concordia[53] have shown that the curvature of the rotor body has relatively minor effects.

(6.3) ELECTROMAGNETIC FIELD EQUATIONS

The generalised Maxwell's field equations of particular interest for the present purpose are:

$$\nabla \times \underline{H} = \underline{J} + \frac{\partial \underline{D}}{\partial t} \tag{6.1}$$

$$\nabla \times \underline{E} = -\frac{\partial \underline{B}}{\partial t} \tag{6.2}$$

where $\underline{H}$ = magnetic field

$\underline{E}$ = electric field

$\underline{J}$ = conduction current density

$\underline{D}$ = displacement current density

$\underline{B}$ = magnetic flux density

The other relations that are of importance while dealing with ferromagnetic materials are

$$\underline{J} = \frac{\underline{E}}{\rho} \tag{6.3}$$

$$\underline{B} = \mu \underline{H} \tag{6.4}$$

Making use of these two relationships the following equation may be derived from equations (6.1) and (6.2)

$$\nabla^2 \times \underline{H} = \frac{\mu}{\rho} \frac{\partial \underline{H}}{\partial t} + \times \frac{\partial \underline{D}}{\partial t} \tag{6.5}$$

A general solution of equation (6.5) that can be applied to a medium of any boundary and excited by any arbitrary forcing function is not available in literature and assumptions are, therefore, made to reduce equation (6.5) to a form that is amenable to solution. With particular reference to the study of eddy-currents in rotating machines, the following

assumptions are usually made:

(a) Displacement current is neglected.

(b) The material is assumed to be electro-magnetically homogeneous.

(c) Curvature is neglected.

(d) End effects are neglected.

(e) By assuming a simple shape of the material as shown in Fig.45 where the material extends to infinity in the z direction the equation is usually reduced to a two-dimensional form.

Equation (6.5), on the basis of these assumptions, becomes

$$\frac{\partial^2 H_z(x,y,t)}{\partial x^2} + \frac{\partial H_z(x,y,t)}{\partial y^2} = \frac{\mu}{\rho} \frac{\partial H_z(x,y,t)}{\partial t} \qquad (6.6)$$

(6.4) SOLUTION OF THE FIELD EQUATIONS

(6.4.1) LINEAR SOLUTION

A solution of the field equations is based, as mentioned earlier, on the consideration of a sinusoidally varying magnetising force. The effect of hysteresis may be included by assuming a constant complex permeability[54] but within the range of flux variation that is encountered in synchronous machine analysis, hysteresis is not important[49]. To achieve, first of all, a simple solution, equation (6.6) is further simplified by assuming an infinite half space for

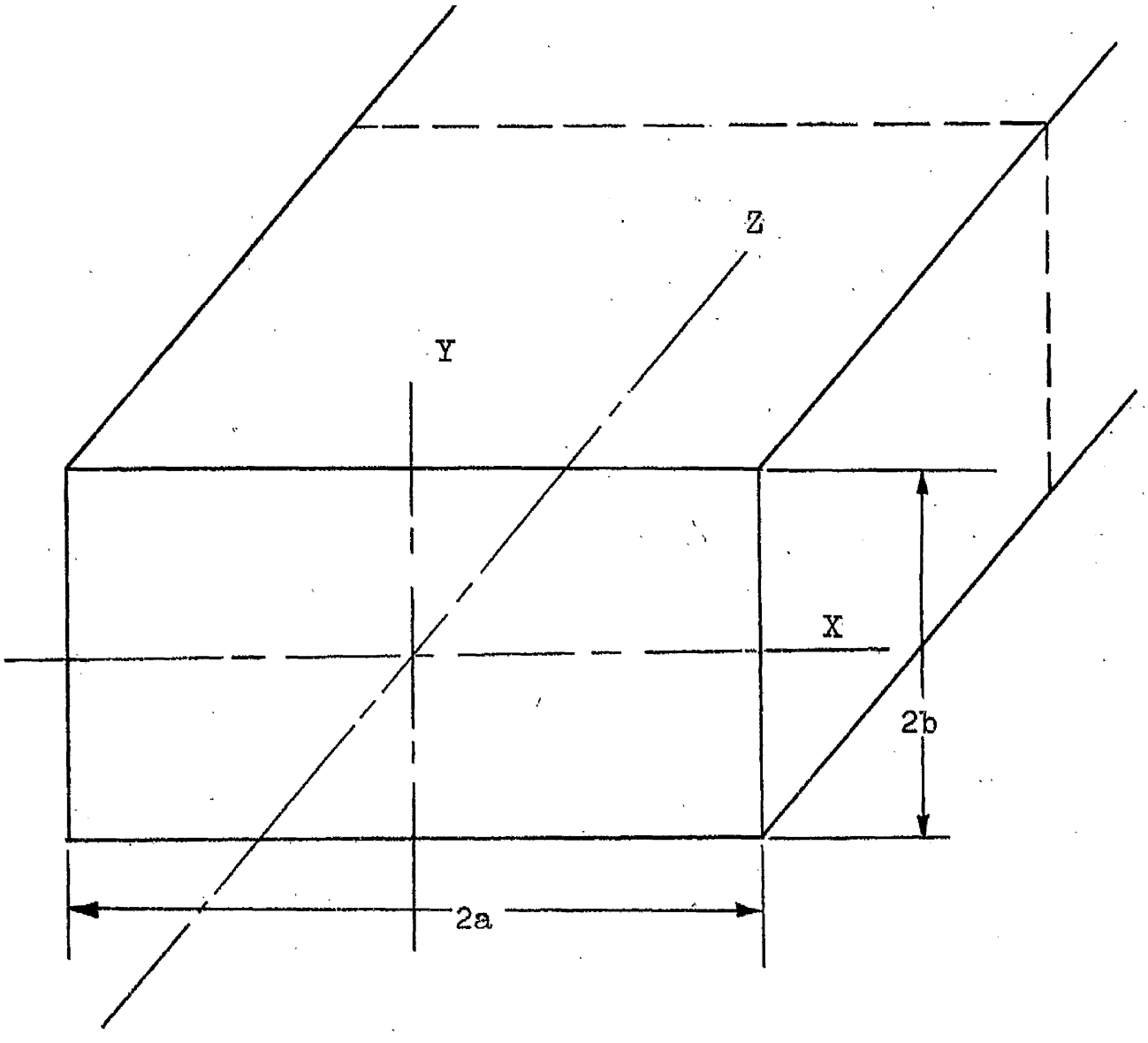

FIG.45 SECTION OF A SOLID IRON BLOCK SHOWING THE COORDINATE SYSTEM

(dotted line indicates unit length in the Z direction)

which case H_z, B_z, J_x are the only functions of y and t that exist. So the final equation is

$$\frac{\partial^2 H_z}{\partial y^2} = \frac{\mu}{\rho} \frac{\partial H_z}{\partial t} \tag{6.7}$$

For a magnetising force of the form

$$H_z = H_o e^{j\omega t} \tag{6.8}$$

the solution for (6.7) is

$$H_z(y_1 t) = H_o e^{-my} e^{j(\omega t - my)} \tag{6.9}$$

where $m = \sqrt{\frac{\omega\mu}{2\rho}}$

($\frac{1}{m}$ is usually known as the classical depth of penetration)

The expression for the impedance to the flow of the eddy current[51], that can be derived from the solution given above, is

$$z_{kd} = \sqrt{2}\ \rho m\ e^{j\pi/4} \tag{6.10}$$

The two points of importance that are indicated by equation (6.10) are:

(a) The impedance varies with $\sqrt{\omega}$

(b) The impedance has a constant phase angle of 45°.

Tests carried out on several occasions[55,49] have shown, however, that the impedance angle is much smaller than 45°. This discrepancy has led to a different approach to the solution.

(6.4.2) NON LINEAR SOLUTION

The nonlinear solution based on a rectangular magnetisation curve was first used by McConnell[43] and subsequently by Agarwal[44].

The flux density is assumed to have a constant saturated value $\pm B_s$ whenever the magnetising force H has a value other than zero, as is shown in Fig.46. This theory is based on the assumption that with a uniform magnetising force varying sinusoidally, flux waves of constant density B_s impinge on the outside of the material and propagate inwards towards the centre until waves from all directions meet at the centre. Thereafter, the flux remains unchanged until the magnetising force takes a reverse polarity.

This theory, on the basis of which Agarwal[44] has made a comprehensive analysis of eddy current phenomena, was recently adopted by Bharali and Adkins[49] for calculating the admittance functions of generators during asynchronous running condition for various slip frequencies. The effective admittance for the rotor body given in reference 49 is

$$Y_{kd} = \frac{1}{k_v k_i} \cdot \frac{9\pi^2}{640} \frac{\omega l}{w^2 \rho} \frac{\phi_m}{B_s} e^{-j26.6} \qquad (6.11)$$

where k_v and k_i are the factors depending on the effective number of turns in the stator winding.

ϕ_m = peak working flux in the rotor.

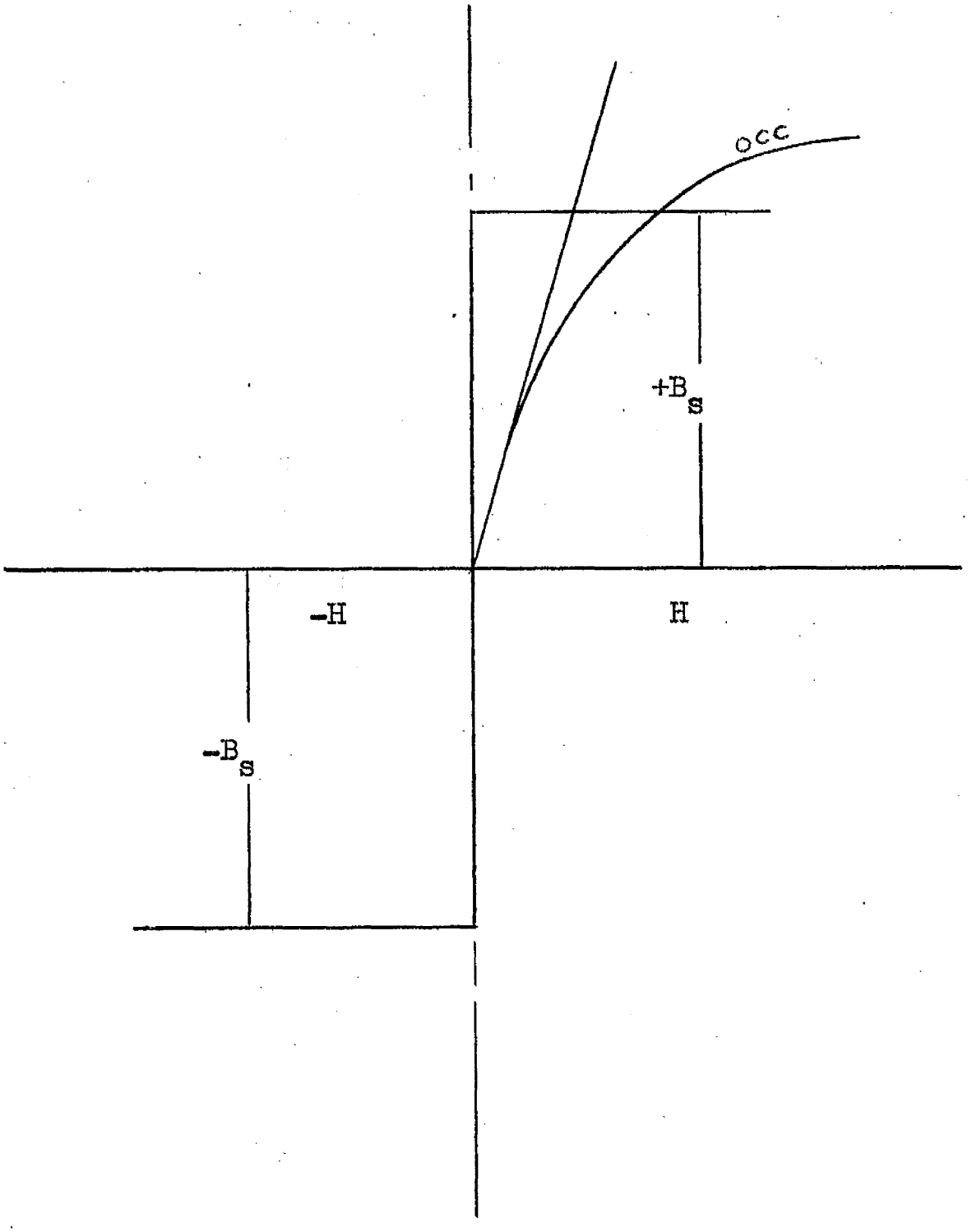

FIG. 46. RECTANGULAR MAGNETISATION CURVE

w = axial length of the rotor.

l = equivalent length of the flux path.

ω = frequency at which the flux is varying.

Equation (6.11) shows that the admittance, now calculated on the basis of nonlinear theory, has an angle smaller than 45^{o}.

From experimental verification, equation (6.11) has been found to provide more satisfactory results than equation (6.10), specially when flux follows a harmonic variation. The authors have concluded, however, that under the conditions where the flux in the core do not reverse the results obtained from linear solution are adequate. The success of applying the nonlinear method depends on the choice of an appropriate value of B_s for a particular condition of operation.

(6.5) DIFFICULTIES IN APPLYING THE SOLUTIONS UNDER TRANSIENT CONDITIONS

The expressions for the admittance of the rotor derived from the linear and nonlinear solutions have the following in common:

(a) The impedance angle is constant, irrespective of frequency or saturation.

(b) Both the resistance and inductance are frequency sensitive.

In both cases, solutions have been achieved by applying a sinusoidal magnetising force.

During transient operations of a synchronous generator, neither the magnetising force nor the flux, whose response is constrained by the operation of excitation system and terminal conditions of the machine, follows a harmonic variation and, as such, an instantaneous frequency of flux pulsation does not exist. The problem takes a more stringent form when the nonlinearity due to magnetic circuit saturation is included.

Bharali and Adkins[49] have used the expression given in equation (6.10) for analysing the 3-phase short-circuit currents of unloaded machines and showed that the subtransient components of the short-circuit currents do not decay exponentially, but follow a curve based on an error function[49]. While developing this method, the authors had to resort to a great deal of simplification by assuming a constant voltage behind the subtransient reactance for the entire duration of the fault. Magnetic circuit saturation was also assumed to remain unchanged.

CHAPTER VII

REPRESENTATION OF EDDY CURRENT WITH VARIABLE PARAMETERS.

(7.1) INTRODUCTION

The enormous complexity that is involved[45] in deriving a general solution of the field equations applicable for all conditions of flux and mmf variation has not yet been overcome. A compromise that has emerged from this situation, has encouraged the trend towards developing equivalent circuits to account for the flow of eddy currents. While in the case of a generator the parameters of these fictitious eddy current circuits are obtained from short circuit tests, theoretical analysis in deriving their expressions are also available[45,46].

One[46] of the analytical methods for developing an equivalent circuit for eddy current paths starts with sinusoidal solution of the field equations for an iron section having large width/depth ratio. The expressions that are obtained for the resistance and reactance of the eddy current paths, from this solution is again frequency-dependent. However, based on the assumption that the transient response of a function is largely characterised by the low frequency response of the system, Subba Rao[46] has finally produced an equivalent circuit with constant resistance and inductance for the eddy current path as

shown in Fig.47. The important assumption made in the analysis is that, at low frequencies, less than about 5 c/s, the depth of penetration is very large compared with the half thickness of an iron section. The reasonable agreement between the calculated and test results after including saturation by straight line approximation serves to justify the assumption made.

(7.2) DISCREPANCIES IN DAMPER WINDING PARAMETERS OBTAINED FROM CALCULATION AND TESTS

From Fig.47 and also from reference (46) it is found that the inductance of the eddy current path varies, depending on width/depth ratio, between 33.33% and 16.66% of the mutual inductance between the solid iron section and the magnetising winding. Pohl[42] has suggested a constant value of 22% of the mutual inductance. Though no precise relation between the inductance and the resistance appears to exist, it is invariably found that the numerical value of the former in henry is comparable with that of the resistance in ohms.

In the case of synchronous generator, however, where the resistances and reactances are calculated by well established methods[56] from short circuit tests, the corresponding values are usually much less. Taking the specific example of the test generator at Goldington Power Station the following data is available:

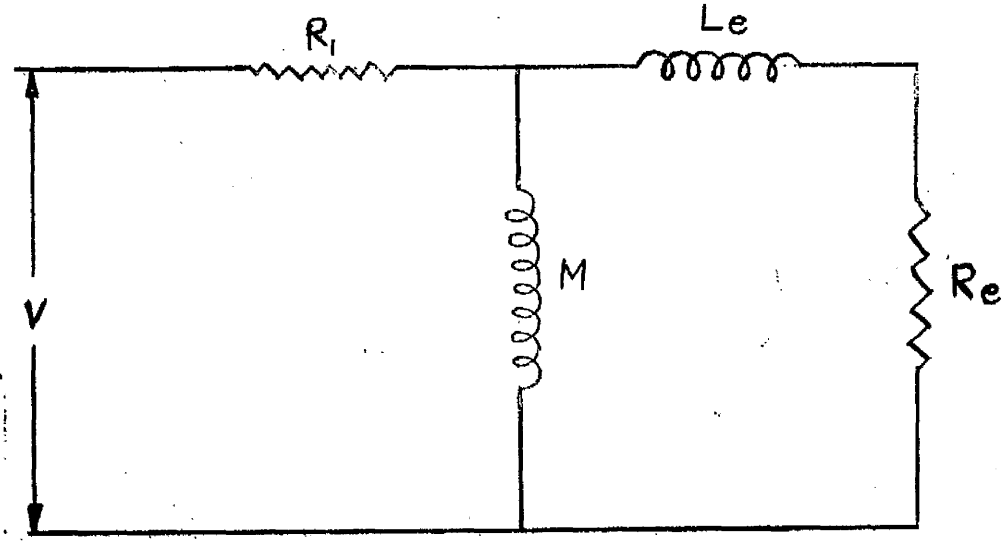

where $M = N_1^2 \frac{\mu}{l}(4ab)$

$L_e = \frac{1}{6}(\frac{1+r}{r})N_1^2 \frac{\mu}{l}(4ab)$

$R_e = N_1^2 \frac{\rho}{l} 8 \frac{(1+r)^2}{r}$

R_1 = Field Winding Resistance

$r = a/b$

μ = Permeability

ρ = Resistivity

FIG. 47. EQUIVALENT CIRCUIT OF A SOLID IRON CORE.

Mutual reactance, x_{ad} = 1.86 p.u. (unsaturated)

Amortisseur leakage reactance = 0.04 p.u.
= 2.15% of x_{ad}

Amortisseur resistance = 0.0125 p.u.
= 0.67% of x_{ad}

The resistance was further reduced by Shackshaft[20] by a factor of four to obtain a better agreement between computed and test results. The general trend of low numerical values have been observed by the author for machines of widely varying ratings.

Based on the nonlinear theory with rectangular magnetisation Agarwal[44] has developed an expression for the complex surface impedance by applying Fourier transform to the non-sinusoidal surface voltage expression. The impedance is

$$z_{kd} = \frac{16}{3\pi} \rho m \left\{ \left[1 - \left\{ 1 - (mb)^2 \right\}^{3/2} \right] + \frac{j}{2} \left[3mb - 2(mb)^3 \right] \right\} \qquad (7.1)$$

where $\frac{1}{m}$ is the depth of flux penetration

b = half thickness of the iron core.

Since m is proportional to $\sqrt{\omega}$ the equation (7.1) shows that the damper winding impedance varies between zero and infinity as the frequency of flux variation changes from zero to infinity. The power factor of the equivalent eddy current paths, based on the two theories outlined in Chapter VI has a constant value irrespective of the frequency. While the theoretical values of the power factor angle are 26.6° and 45°, those found from experimental results[55] appear

to be in the region of 35^{0}.

In a synchronous generator, from the functional point of view, the generation of eddy currents is important in that, on one hand, it creates losses in the rotor body, and it contributes to the air gap flux variation in the direct and quadrature axes on the other. It is the latter function that is of major consideration. Unless a generator is running asynchronously, the loss due to eddy currents is quite small compared with the rated output of the machine. On the other hand it has been found from the author's experience (mentioned in Chapter V) that the subtransient time-constant plays an extremely important part, specially in the quadrature axis flux variation. In conventional machine analysis where the subtransient quantities are included and also in the mathematical model developed so far, the subtransient time constants (equations 3·8 to 3·15) are calculated assuming a frequency of 50 c/s. From equation (7.1) it can be shown that for particular frequency ω,

$$R_{kd} = \frac{16}{3\pi} m\rho \left\{1 - \left[1 - (mb)^2\right]^{3/2}\right\}$$
$$X_{kd} = \frac{16}{3\pi} m\rho \frac{1}{2}\left\{3mb - 2(mb)^3\right\} \qquad (7.2)$$

And on the basis of sinusoidal quantities and assuming the depth of flux penetration to be less than the half thickness,[44] i.e. $(mb = 1)$

$$\tau_{kd} = \frac{X_{kd}}{\omega R_{kd}} = \frac{1}{2\omega} \qquad (7.3)$$

Similar equations can be derived from equation (6.10) but here time constant

$$\tau_{kd} = \frac{1}{\omega} \qquad (7.4)$$

These suggest that the time constants are, theoretically, inversely proportional to the frequency where as the reactance and resistance are proportional to $\sqrt{\omega}$.

(7.3) BASIS OF VARYING THE DAMPER WINDING PARAMETER.

Having determined the requirements of varying the parameters of the damper circuit a technique was developed to incorporate a method for changing the resistances and reactances at each step of solution. At the same time the basic idea of an equivalent circuit was still maintained.

To explain the technique, the following equation is considered:

$$i(R + Lp) = V \sin \omega t \qquad (7.5)$$

which corresponds to applying a sinusoidal voltage to an inductive circuit. A complete solution is simple if the boundary conditions are known. On the other hand, if the sine wave is divided into a large number of small sections as shown in Fig.48 and if the magnitude and slope of the curve at the beginning of each section is known then the sine wave can be replaced by an equation (Fig. 48).

$$f(t) = H_o + n\int\Delta t \qquad (7.6)$$

where H_o == H_o + $n\int\Delta t$ f the curve at a point

n = slope at that point.

Here, again, the solution of the current-equation (7.5) can

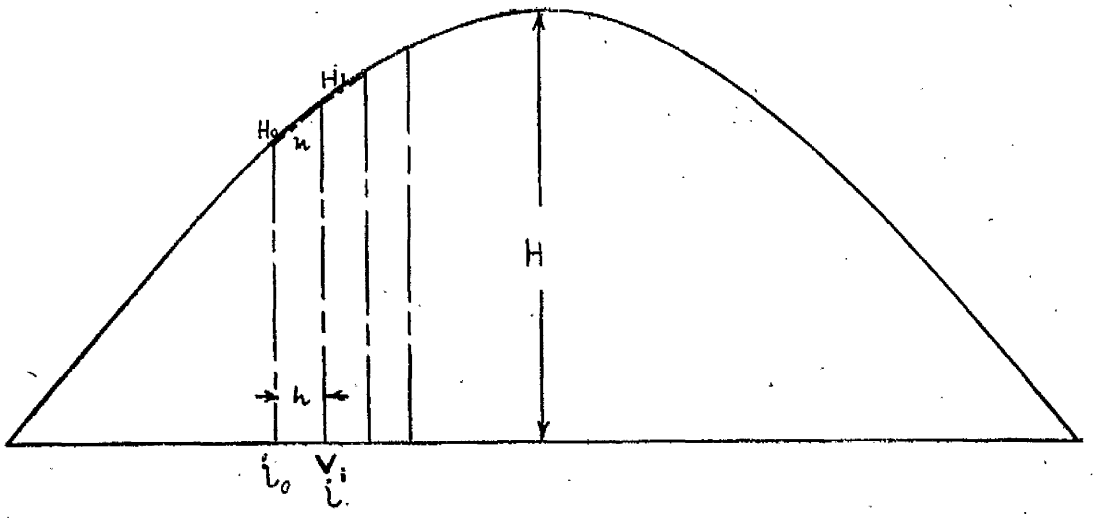

$$H_1 = H_0 + \int n \, dt$$

where $dt = \Delta t = h$

For an electric circuit $i = \frac{1}{\tau}(V_1 - i_0 R)$

where i_0 = current at the end of the first step (above)
τ^0 = L/R

FIG. 48. INTEGRATION OF A SINE CURVE BY STEP INTEGRATION METHOD.

be achieved by a step-by-step process of integration. This then suggests that if the magnitude and slope at every small interval of a time varying quantity is known then derivation of a transient response can be obtained without knowing a steady frequency response. In the step-by-step process of solution, this is fortunately available at each step. With the help of the finite difference method mentioned in Chapter III, the slope of the mmf functions producing flux in the rotor body along each axis can be calculated while the magnitude is obtained from the solution of the other equations. In per unit system the mmf's are equal to i_q along quadrature axis and $i_{fd}-i_d$ along the direct axis.

Again the following two equations are being considered:

$$H_1 = H_o \sin \omega t \tag{7.7}$$

$$H_2 = H_o + nt \tag{7.8}$$

Therefore $$\frac{\partial H_1}{\partial t} = \omega H_o \cos \omega t \tag{7.9}$$

and $$\frac{\partial H_2}{\partial t} = n \tag{7.10}$$

Now dividing (7.9) by H_o

$$\left\{\frac{\partial H_1}{\partial t}\right\} / H_o = \omega \cos \omega t \tag{7.11}$$

Dimensionally, the right hand side of equation (7.11) gives the instantaneous angular variation of magnetising force H_1. It is on this basis that the modulations of the parameters of the damper winding circuit are, in theory,

determined. At every step, the rate of change of the magnetising force was calculated and then dividing the slope by the mmf a quantity which can be considered as the instantaneous angular variation of mmf, was obtained.

(7.3.1) SELECTION OF INITIAL PARAMETERS

While applying this technique in the analysis of the Belvedere machine, the initial values of both the direct and quadrature axes inductances and resistances were calculated on the basis of the equivalent circuit shown in Fig.47. The following dimensions of the generator rotor were available.

Axial length of the rotor = 170 inches

Diameter of the rotor = 40 inches

Resistivity of the rotor iron = 29×10^{-8} ohm meter

Unsaturated permeability of iron = 60×10^{-4} (approximately)

Since the unsaturated value of the mutual inductance was known, information about the number of effective turns was not necessary for calculating the resistance of an equivalent circuit (Fig. 47).

The following dimensions were considered initially:

Width of the magnetic path = 170 inches

Depth of the magnetic path = 25 inches

Length of the magnetic path = 35 inches

The next step was to relate these parameters to a particular frequency of operation so that these could then be modulated

whenever the rate of angular variation changes from the one that is considered initially. No emperical relation is available for this and, as a result, it was a trial and error method. Initially an arbitrary frequency of 1 c/s was chosen to correspond to the parameters developed on the basis of the equivalent circuit. During transient analysis the parameters were then modulated in the following way

$$X_{(\omega)} = X_{(\omega_o)} \left\{ \frac{\omega}{\omega_o} \right\}^{\frac{1}{2}}$$

$$R_{(\omega)} = R_{(\omega_o)} \left\{ \frac{\omega}{\omega_o} \right\}^{\frac{1}{2}}$$

where ω_o = the chosen frequency, 1 c/s = 3.14 rad/sec.

ω = the angular variation calculated in the way described in Section (7.3).

(7.3.2) ADJUSTMENT OF THE INITIALLY SELECTED PARAMETERS

During initial programming with the variable parameters for the damper windings, the main mathematical instability that was found to occur was due to the damper winding time constants τ'_{kdo} and τ_{kd} becoming very large when the rate of change of the magnetising force along either of the two axes became very small. This difficulty was overcome by keeping the damper winding parameters fixed during the period when the rate of variation would become less than 0.025 c/s. There was no difficulty on the higher ranges of frequencies.

The other adjustment that was necessary was in selecting the original value of ω. From several trial runs of the

program better results were obtained by selecting the damper winding impedance of·46 p.u. at a frequency of 1 radians per second. The value of the resistance at this stage was adjusted to give a power factor angle of 32^{o}. The variation of the inductances due to saturation was included throughout on the basis of the theory developed in Chapter IV.

According to equation (7.11) it was necessary to divide the slope by the mmf at each step of calculation. While in that equation H_o is constant, the magnetising force in the pole slipping test varied between wide ranges. It was therefore necessary to adjust the value of the dividing factor at some stages of computation. Again from trial run, the selection of·24 p.u. for the dividing factor along both direct and quadrature axes immediately after the field current started building up in the positive direction was found to yield satisfactory results.

(7.4) COMPARISON OF COMPUTED AND TEST RESULTS

The pole-slipping test on the Belvedere generator was considered for comparing the experimental results and those obtained from computation including the variation of the damper winding parameters as developed in the last Section. The results are shown in Figs. (38) to (44) by the curves marked (C).

The improvement, specially during the period when the field current builds up in the positive direction after remaining zero for a short time, is remarkable when compared with the results obtained in Chapter V with the machine parameters calculated from short-circuit tests. The induced rotor-over voltage (Fig. 38) is about 5% higher than that found during live-tests. This is due to the damper winding time-constants becoming small when the rate of change of the magnetising force in the direct axis is very high during pole slipping. Though the rate of change of i_d immediately after first pair of pole slipping is very high, the field current does not overshoot (Fig. 39) because the field winding time constant, which is much larger than the damper winding time constant, comes into action. The stator voltage and current follow reasonably closely the tested curves.

The overall satisfactory agreement between the test and computed results therefore justifies the validity of the technique developed to modulate the parameters of amortisseur circuits during transient operations of a synchronous generator.

It may, however, be commented that there is scope to improve the theory developed here. Applying the same technique to machines of various ratings and to different types of operating conditions a general conclusion may be drawn about the nature of adjustment of the initial data

that may be required under different machine performances. In the present investigatory work the parameters were adjusted on the basis of the results obtained from computer analyses for only one type of test and no theoretical basis was possible to be developed.

(7.5) MULTIWINDING REPRESENTATION OF EDDY CURRENT PATHS

The alternative method by which eddy current paths were represented was based on the theory developed by Kesavamurthy and Rajagopalan[45]. To represent both the steady state and transient behaviour of a solid core the authors have developed two different equivalent circuits of which the one that seems to be of particular interest with regard to the analysis of turbogenerator is in the form of a ladder network as shown in Fig.(49). The inductances and resistances of the circuit developed by the authors, are given by (Fig.49):

$$L_o = ab\mu \tag{7.12}$$

$$R_n = \frac{1}{2} q_n \left[F'(q_n)\right] \rho \tag{7.13}$$

$$L_n = b^2 \frac{F'(q_n)}{8q_n} \mu \tag{7.14}$$

where R_n = resistance of the n th. circuit of the complete eddy current path.

L_n = inductance of the n th. circuit of the complete eddy current path.

L_o = mutual inductance between the magnetising winding and the iron core.

R' = magnetising winding resistance

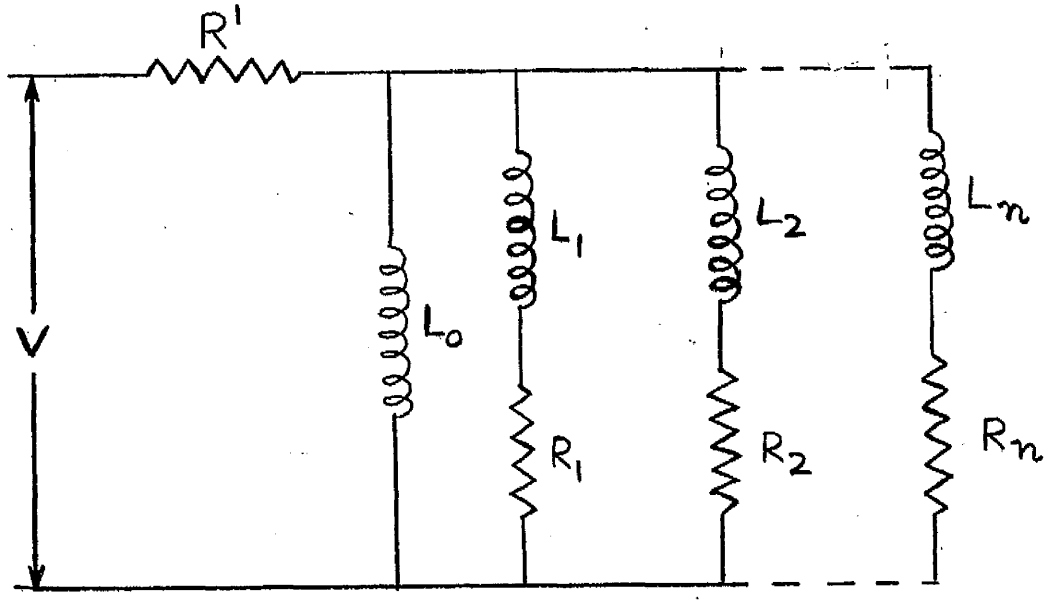

FIG. 49. LADDER NETWORK REPRESENTATION OF EDDY CURRENT PATHS

r = width/depth = a/b

q_n = n th. root of the equation
$-(4+r)q \tan q - 8 + 8 \sec q = 0$ and
$F'(q_n) = 4(r-1)\tan q_n - 4(r+1)q_n$

Dividing equation (7.14) by (7.13)

$$\frac{L_n}{R_n} = \frac{1}{16}\frac{b^2\mu}{q_n^2} \qquad (7.15)$$

which is an expression for the time constant of the n th. circuit. Equation (7.15) suggests that the time constant of the n th. circuit varies inversely as q_n^2. This is because of the higher rate of increase of resistance as the order of the circuit increases.

Since the first circuit of the ladder network has no resistance, the current through the entire circuit is limited by the series resistance which in case of a synchronous machine corresponds to the field winding. The other parallel circuits are therefore significant only during transient periods.

As the impedance of each parallel circuit increases rapidly with the increase of n, it can be assumed that only the first few parallel circuits are important to apply the theory for investigating the transient behaviour of a ferromagnetic material.

(7.5.1) APPLICATION OF THE ANALYSIS IN SYNCHRONOUS MACHINE PROBLEM

In an attempt to apply the technique in machine analyses, two parallel circuits were assumed along each axis. The

specific case of the Belvedere test-set was again considered. L_o was made equal to the mutual inductance of the generator. The parameters of other circuits were calculated from the dimensions of the generator given in Section (7.3.1). To take the effect of other circuits that are in parallel, the parameters of the second damper windings along each axis were reduced by a factor of two. Variation of permeability due to saturation was also taken into account.

(7.5.2) SOLUTION OF MACHINE EQUATIONS

Having the mutually coupled circuits increased to four in the direct axis and three in the quadrature axis, difficulties were encountered in arranging the necessary differential equations into operational form since the expression became quite complicated.

Matrix method[10] of solving the machine equations was therefore adopted. The voltage regulator and excitation system remained unchanged. The arrangement of the machine equations for matrix method of solution is shown in Appendix E.

(7.5.3) COMPARISON OF COMPUTED AND TEST RESULTS

To provide a check on the analytical method of multi winding representation of the eddy current paths, performance characteristics of the Belvedere test-unit was considered. Computed results of the important machine variables are compared with those from site-tests in Figs.(38) to (44).

From initial programming adjustment of the parameters obtained from theoretical basis was necessary. The inductances of the first circuit in both the axes had to be reduced to 70% of their original values.

Though the results show slightly better agreement with the test results than those with one damper winding, they are, however, much inferior to the results obtained with variable damper-circuits parameters. It was not possible to further optimise the parameters as was felt desirable. Considering the necessity of changing the method for solving the machine equations, it was felt by the author that the variable parameter-model for the damper circuits is preferable to the multi-winding representation.

CHAPTER VIII

SYNCHRONISATION OF TURBO-ALTERNATOR

(8.1) GENERAL

Synchronisation is the operation of putting a generator into service by connecting it to a system that is already in operation. It is always necessary to ensure that conditions are electrically favourable for synchronisation at the instant of connecting two alternating sources in parallel to guard against the disturbances that may otherwise arise and may be, at times, as severe as that due to any other fault in the system. In the method of synchronisation that has been most widely used, the incoming machine is brought close to the rated speed of the system with which it is to operate in parallel and the machine, at the same time, is excited so that its terminal voltage corresponds to that of the system. Much of the success of the method then depends on securing small and preferably diminishing deviations in the magnitude, phase and frequency of the two sources at the instance when the electrical connection is made between them.

No previous account appears to have been devoted to a study of synchronising conditions for ranges of different parameters, such as is encountered in the present trend towards larger individual generator-units. In one aspect the present study is related to the predetermination of the

permissible amplitude, phase and frequency deviations as is required in formulation of the limits to be incorporated in automatic synchronising sequences. Both the changing parameters of synchronous generators and the increasing interest in automatic control technique in the running up and synchronising of generators suggest, in the author's view, the desirability of applying an accurate and comprehensive mathematical model of a turbo-alternator unit to provide reliable and desirable appraisal of synchronisimg conditions in forming a basis for automation.

(8.2) IN-RUSH CURRENT AND SYNCHRONISING TORQUE

The two quantities that are of primary importance during the process of synchronisation are:

(a) In-rush current

(b) Synchronising torque

(8.2.1) IN-RUSH CURRENT

Due to the presence of phase and amplitude difference between the voltages of the incoming machine and the system there is flow of current, usually referred to as in-rush current, at the instant of circuit breaker closing. The direction of flow of this current either into or out of the machine is determined by its phase relationship with respect to the large system. The magnitude of the current is limited by the equivalent impedance of the two sources which

under subtransient conditions comprises of the subtransient impedance of the machine and the input impedance of the system. Fig. 50 shows the nature of typical in-rush current as a function of phase-difference for different values of the terminal voltage of the incoming generator.

The limitation imposed by the in-rush current is that of mechanical force produced by the flow of such current. For a phase difference of 180^{o} the maximum current can be as much as twice that of a 3-phase short circuit at the machine terminal, and the mechanical force to which the windings will be subjected to, may be four times that during 3-phase fault. From designers' point of view, definition of permissible limits allowable during synchronisation so that the surges are within safety margin, is an important task.

(8.2.2) SYNCHRONISING TORQUE

The success of connecting two alternating sources together depends to a large extent, on the generation, at the instant of connection, of a synchronising torque which tries to pull the two sources together. A formal expression for the synchronising torque in terms of frequency, phase and amplitude errors is difficult to derive since it is a function of all the variables of the turbo-alternator model. In the present study it is automatically computed from the expression

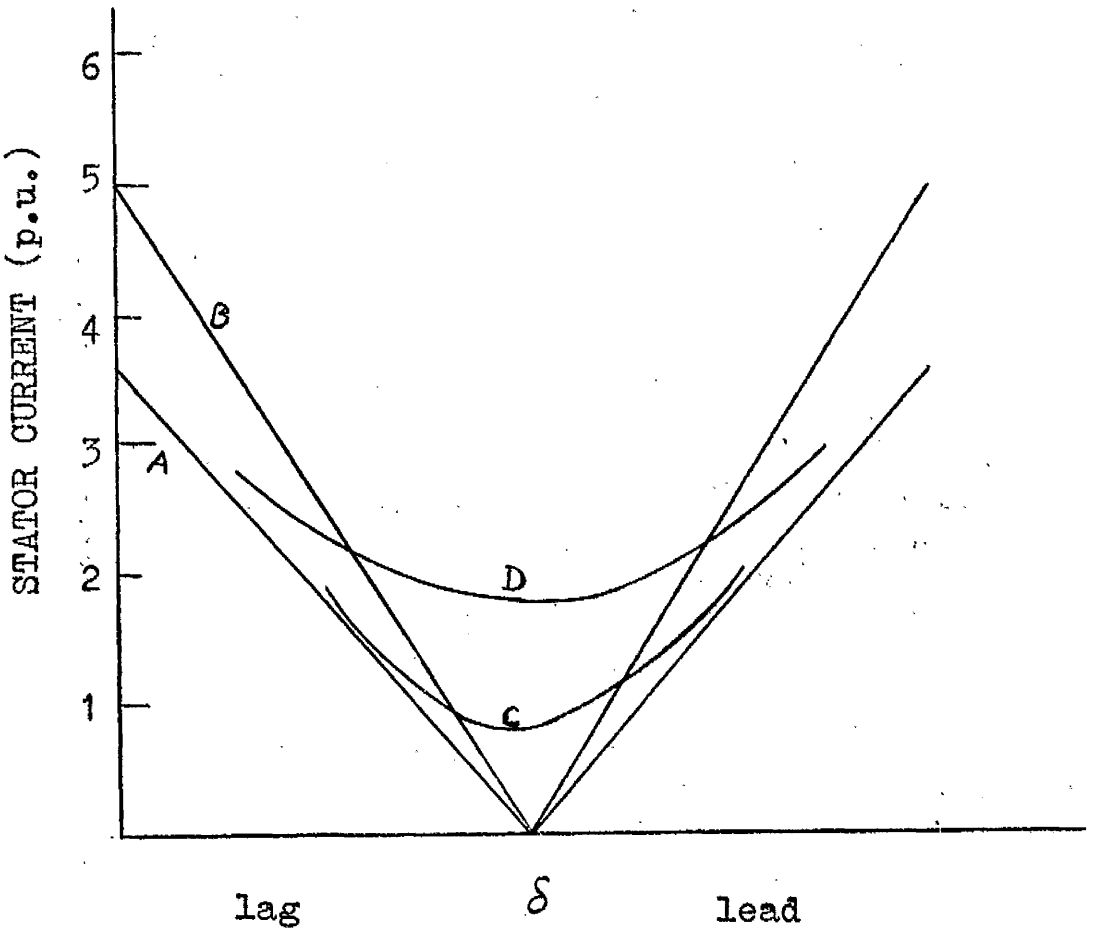

FIG.50 TYPICAL IN-RUSH CURRENT AS A FUNCTION OF ROTOR ANGLE AT THE TIME OF SYNCHRONISATION

A AND B FOR DIFFERENT VOLTAGE DIFFERENCES
C AND D FOR DIFFERENT FREQUENCE DIFFERENCES

$$T_s = \psi_d i_q - \psi_q i_d \qquad (8.1)$$

In general terms, the rotor of the incoming machine is subjected to the following torques at the instant of coupling.

(a) The electromagnetic torque produced by the interaction of the stator and rotor currents and flux-linkages.

(b) The inertia torque due to acceleration or retardation of the rotor with respect to the fixed frequency of the system.

(c) The electrical damping torque arising from the losses in the rotor of the generator.

The dynamic equation of motion for the rotor is then:

$$Mp^2\delta = T_i - T_e - T_l \qquad (8.2)$$

where T_i = torque input to the rotor

T_e = electromagnetic torque at the air gap

T_l = torque associated with rotor losses

(8.2.3) RANGE OF CONDITIONS ACCEPTED IN SYNCHRONISING

The maximum deviation in voltage, frequency and phase that appears to be recommended for synchronisation without producing any undue electrical surges or mechanical shocks are mentioned here. The limits are those that are used in connection with automatic synchronising gears.

(a) Frequency setting

0.25% - 0.5% - 0.75% of rated frequency

(b) Phase matching

Continuously variable between 20° to 45°

(c) Voltage setting

Steps of 2%, 4% and 6% of the rated voltage.

(8.3) PERFORMANCE CALCULATION FOR SYNCHRONISATION

In order to investigate the transient response of the various machine variables during synchronisation, particularly when the allowable limits are at their highest values, theoretical studies were carried out with the Goldington test generator. It was observed from the computed results that the changes in the terminal voltage and phase-difference within the permissible limits do not make a significant difference in the machine variables, for example shaft-speed and torque. Frequency settings, on the other hand, have marked influence on these quantities, particularly when the machine has a comparatively large inertia. Due to the stored energy the rotor, when the phase angle is diverging at the time of synchronisation, tries to deviate away from the nominal operating point and so a larger synchronising torque is required to obtain a successful synchronisation as shown in Fig.(51). Variations of rotor angle and slips for two different initial frequency settings are shown in Figs. (52) and (53). Considering the peak values of all the variables, it may be concluded that synchronisation within

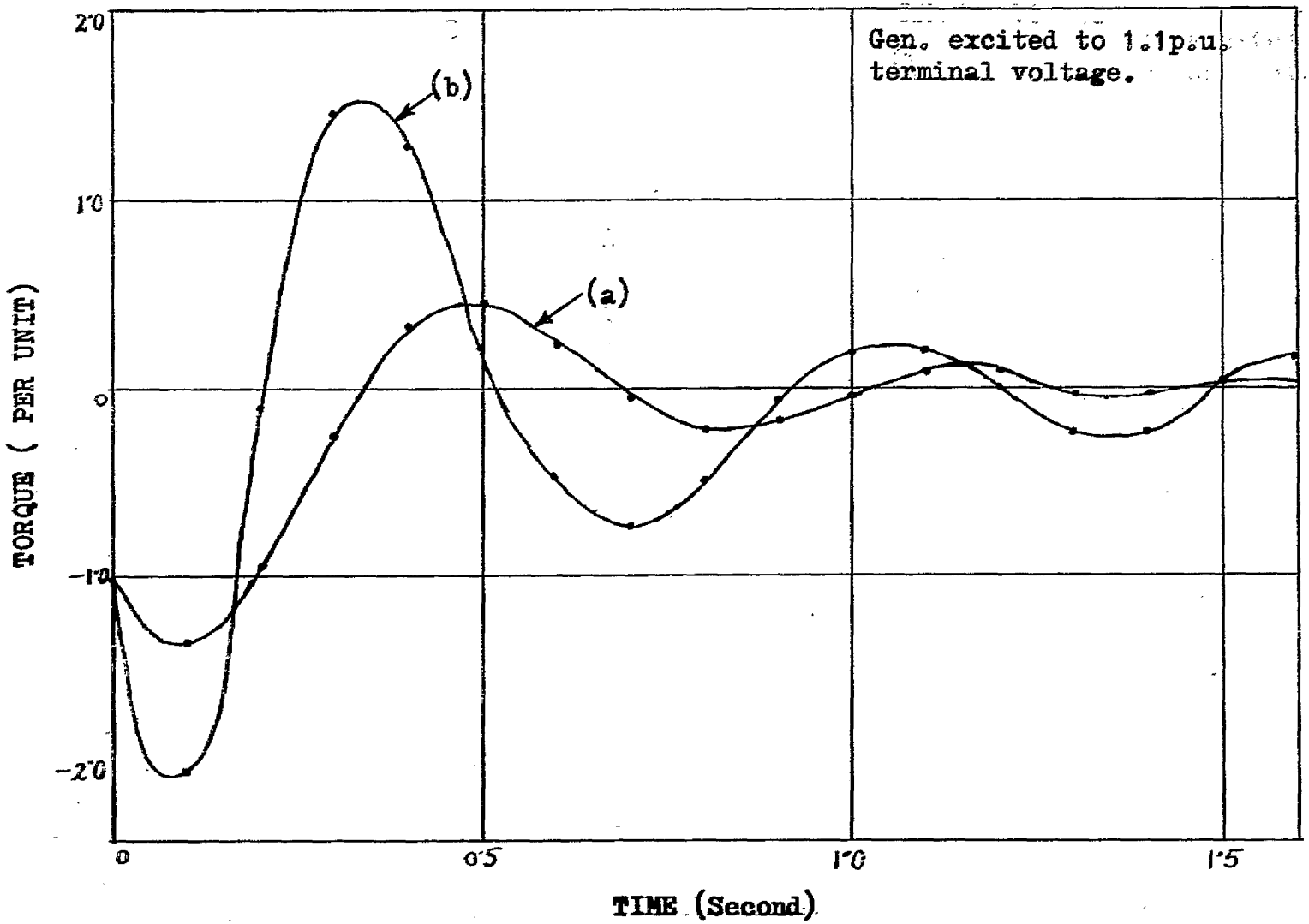

FIG. 51. VARIATION OF TORQUE DURING SYNCHRONISATION.
(a) With 0.26% Initial Slip.
(b) With 0.75% Initial Slip.

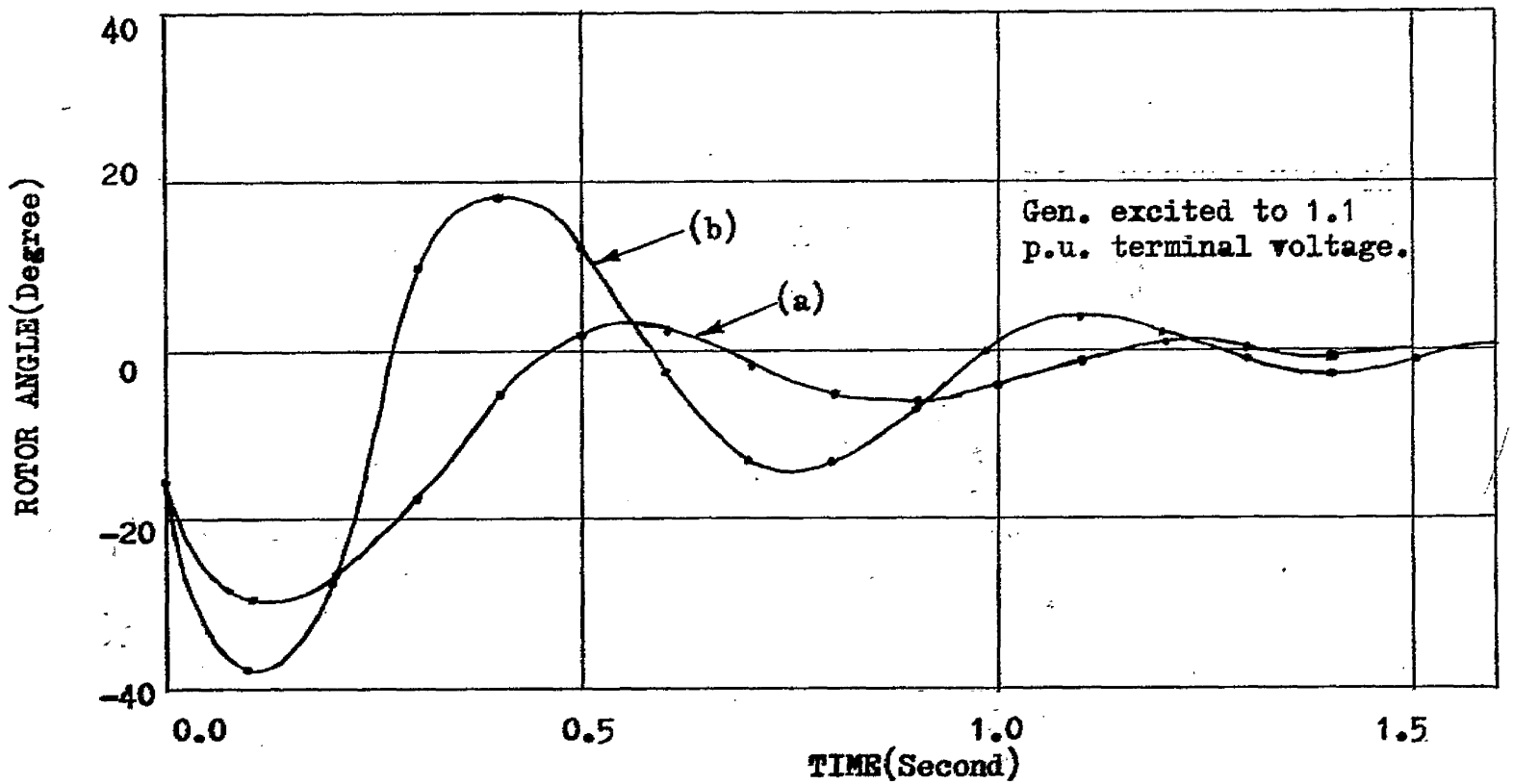

FIG. 52. VARIATION OF ROTOR ANGLE DURING SYNCHRONISATION.
(a) With 0.26% Initial Slip.
(b) With 0.75% Initial Slip.

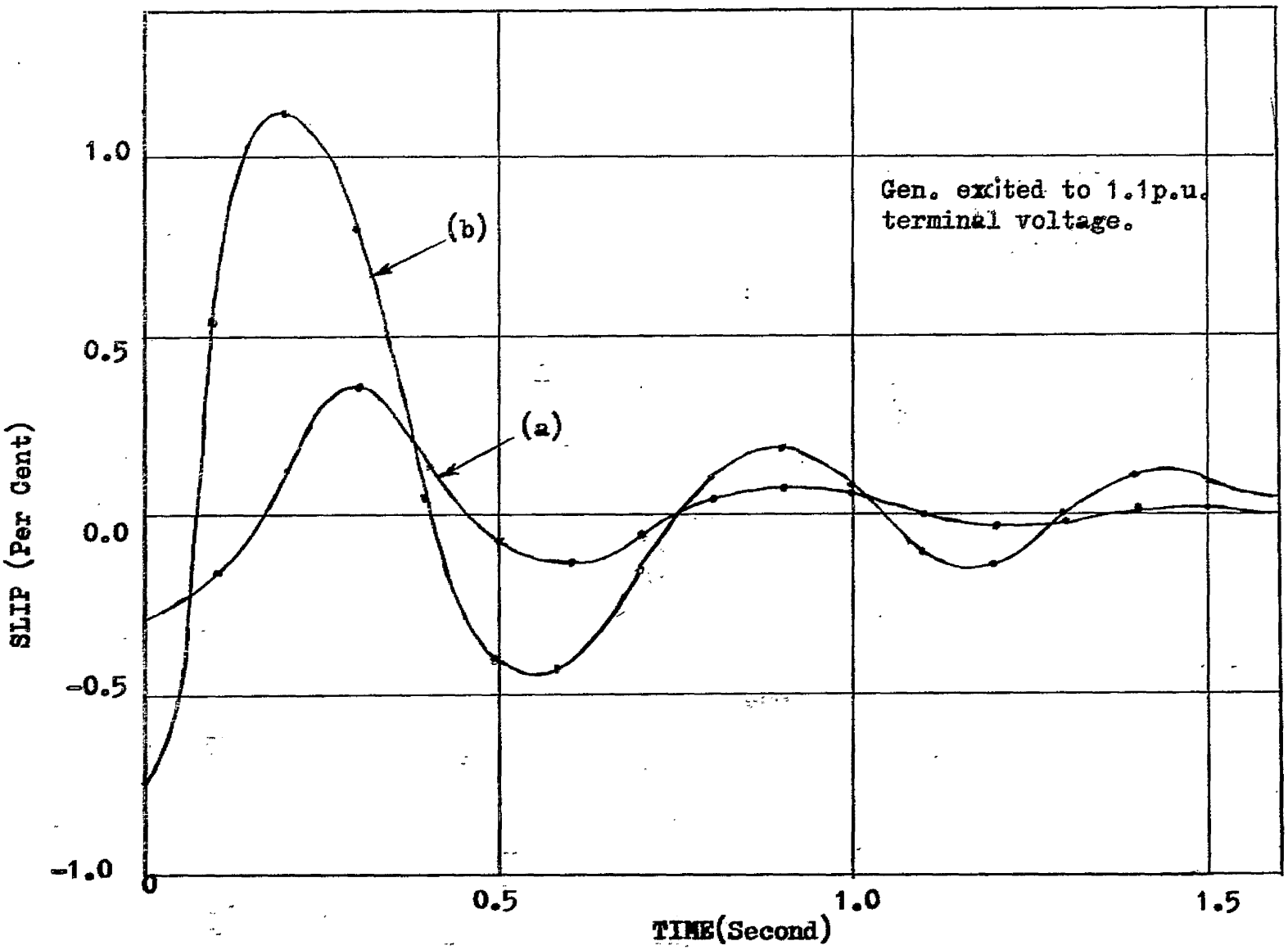

FIG. 53. VARIATION OF SLIP DURING SYNCHRONISATION
(a) With 0.26% Initial Slip
(b) With 0.75% Initial Slip

the limits usually recommended, is satisfactory since the maximum amplitudes are not unreasonably high.

(8.4) THE RUSSIAN METHOD

The method of self-synchronisation[58] or auto-synchronisation[59] is widely used in the Soviet Union. The method consists, first of all, of bringing the machine near to the synchronous speed (usually sub-synchronous) by controlling the prime mover speed-control. The rotor winding which remains unexcited until the coupling is done, is short circuited through discharge resistance. Coupling is done without controlling the phase difference between the two voltage sources. Immediately after the coupling, the field winding is excited; on account of the large time constant of the rotor circuit, the field current cannot reach the normal value for several seconds. The rotor oscillates for a few seconds before settling down to the mean value of the rotor angle, which corresponds to the loading condition of the generator.

(8.4.1) ADVANTAGES AND DISADVANTAGES OF SELF-SYNCHRONISATION

The merits of the self-synchronising method that are usually claimed[59] are the following:

(a) The method is simple and practically excludes the possibility of faulty connection to the system.

(b) The coupling is effectively quick having the particular importance in case the disturbances are to be removed.

(c) The process of connection can be easily automatised.

(d) The incoming generator can be connected to the system even if the magnitude of the line voltage and frequency are subjected to changes or swings.

(e) The connection of generator in parallel is simple even in cases when the speed of prime mover is not controlled automatically and when remote operating switches for connecting generators are absent.

(f) The coupling between the system and the power station through a transmission line, if disturbed, can be restored swiftly by automatic reclosing of the line, whereafter the generators of the station are brought to instep operation either all at a time or in sequence by the self synchronising method.

The disadvantages that are encountered, however, are the following:

(a) There is always some rush-current at the time of coupling the magnitude of such current depends on the condition under which the connection is done.

(b) In the system, momentarily, there is a brief voltage drop which again depends on the magnitude of the current drawn out of the system and dies away within several seconds.

In this country a considerable doubt is cast on the overall merit of this method of synchronisation, due to the possibility of high transient current creating, for a short time, a disturbance which may affect other parts of the system to which the incoming generator is connected. Particularly, when the rating of an individual unit is in the region of 500 MW or above, the possibility of a large dip in the system voltage is considerably increased. It was, therefore, thought desirable to subject this form of coarse synchronisation to a detailed analytical investigation.

(8.5) PERFORMANCE CALCULATION FOR SELF-SYNCHRONISATION

To make a comparative study of self-synchronisation it was felt desirable to make an assessment of the difference that is created by putting a generator in parallel operation with an existing system, with and without field circuit excited to correspond to the rated terminal voltage.

Figs. (54), (55) and (56) show the transients of shaft torque, stator current and slip of the Goldington Machine subsequent to an attempt to synchronise the generator at a phase difference of -120° when the machine was running at a sub-synchronous speed with a slip of -·055 radians/sec. It can be observed from the diagrams that while the stator current with excitation rises to about twice as much as that without excitation, the shaft torque swings upto more than

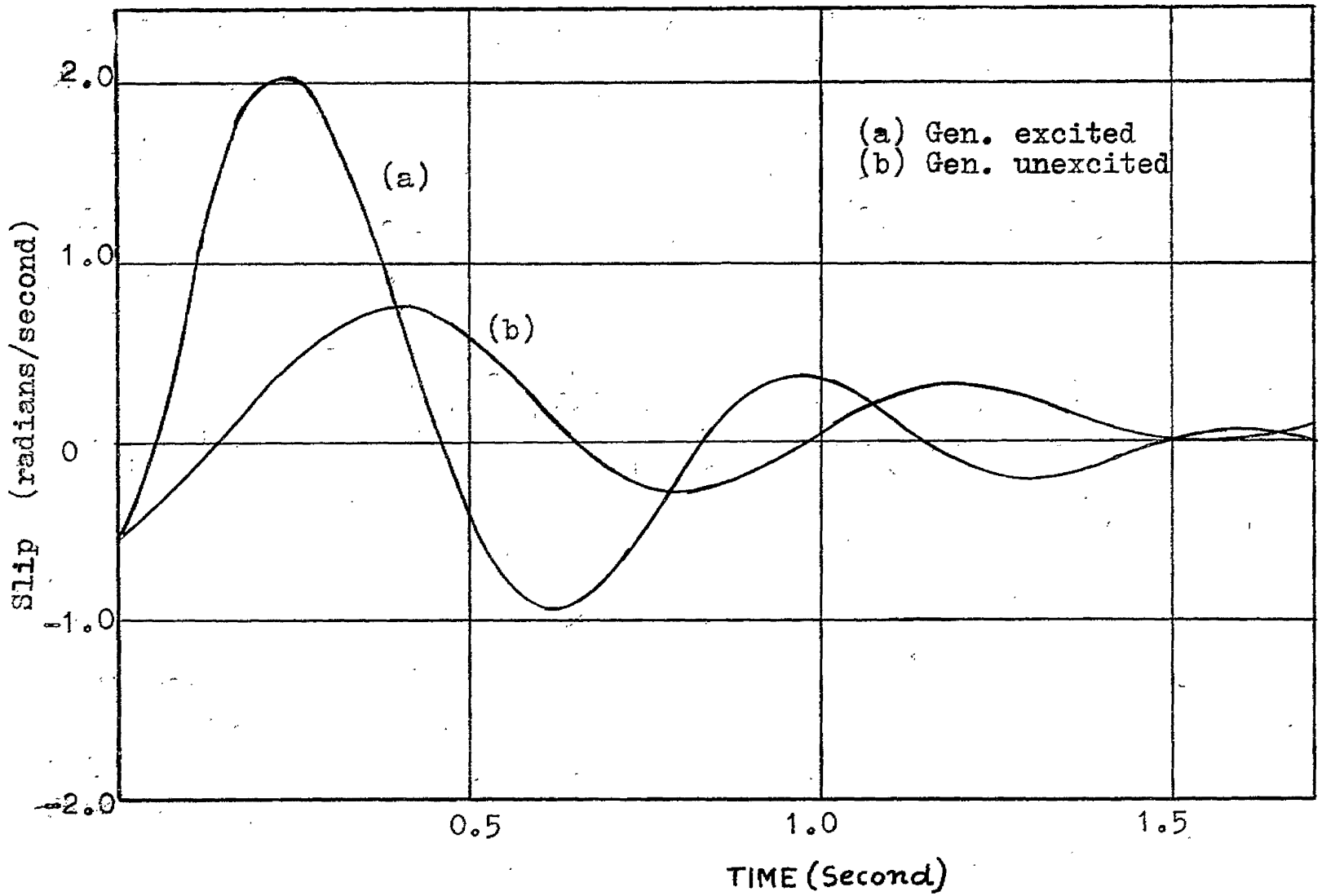

FIG. 54. TRANSIENT SLIP DURING AUTO-SYNCHRONISATION

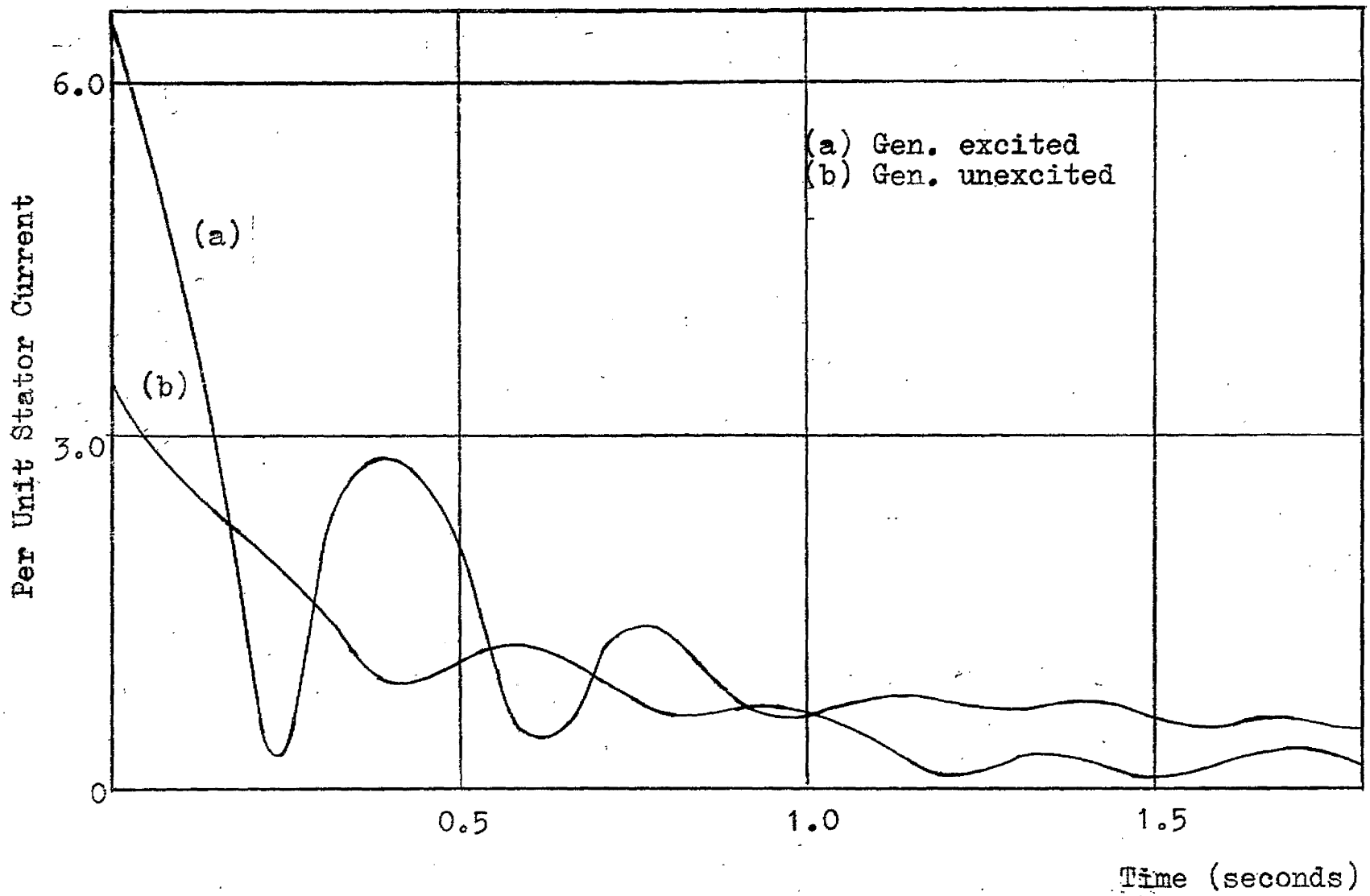

FIG.55. STATOR CURRENT TRANSIENT DURING AUTO-SYNCHRONISATION

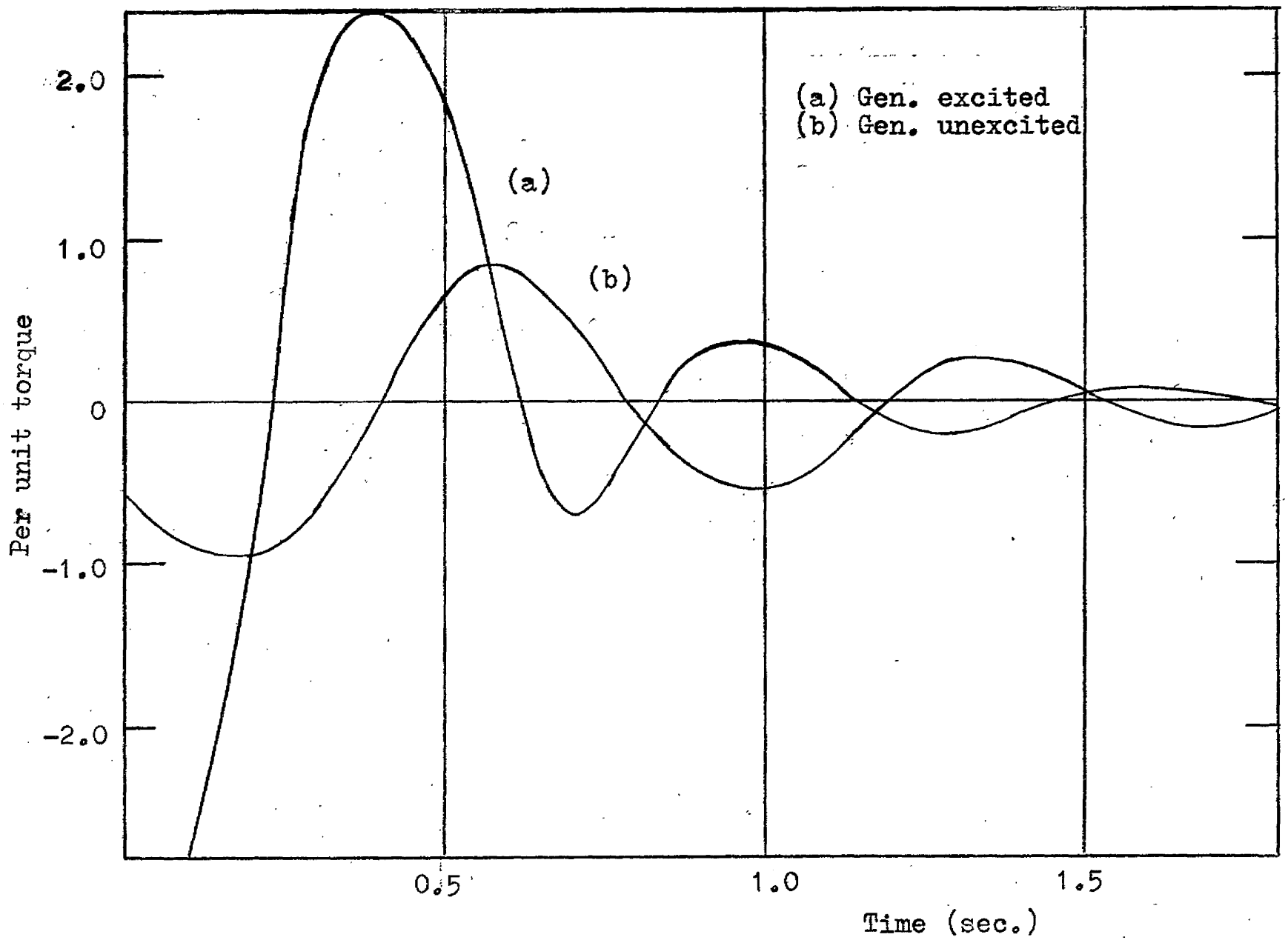

FIG. 56. TORQUE VARIATION DURING AUTO-SYNCHRONISATION

3 times. Subsequent to the circuit breaker closer, it seems that the transients decay faster in case of an excited generator than an unexcited one.

The results are, however, only comparative. It was not possible to study the effect of self-synchronisation on the system since, in that case, the system has to be represented as a source with a finite input or output impedance. Having no experimental information available for such representation, an analysis was not possible. Nevertheless, the results invariably demonstrates the relative severity to which an alternator may be subjected to, when synchronised with and without excitation.

CHAPTER IX

EXPERIMENTAL ANALYSIS OF LARGE POWER UNITS AND ASYNCHRONOUS MODE OF OPERATION

(9.1) GENERAL

An essential requirement of system design as the trend towards larger rating of synchronous generator continues coupled with a growing interest in the operation of generators under limited pole slipping conditions or short period of a-synchronous running is that of being able to reliably predict the effects that the changing machine parameters have on the performance of generators connected to a power system. Ideally a unique mathematical model should cater for all the different machine characteristics that are likely to be encountered in ordinary system operation. The model should, therefore, embrace the characteristics of a machine from both design and operational point of view so that while applying the model for analysing the different modes of operation, the necessary changes are reduced to few salient parameters.

The validity of a completely general representation of this kind would require to be exhaustively tested against site-test results as they become available, for there is only one way in which any mathematical model can be confirmed as a technically adequate foundation for power system application, and that is by the careful correlation of the results the

representation gives with those obtained from fully instrumented system tests.

Having developed a mathematical representation of a turbo-alternator unit to a satisfactory extent, the present Chapter is devoted to analyses of generator of larger power rating for which it has not been possible to correlate. From this point of view the analyses are therefore that of an experimental nature, but it is nonetheless thought that these will provide a sound indication based on a model which has higher accuracy over any other theoretical representation known to the author, to the performance trend of generators of increasing power output coming into operation as high merit order base load supplying units. To this end, the main electrical transients are examined here for generators upto 660 MW rating, including their mode of operation when synchronism is initially lost but where short period of asynchronous running is permitted with a view to subsequent and spontaneous synchronisation with minimum manual intervention and circuit breaker operation.

(9.2) ASSESSMENT OF MACHINE OPERATION DURING 3-PHASE FAULT WITH POLE SLIPPING.

In order to make an observation of the nature of the response characteristics of a widely varying generating units, a close-up 3-phase fault at the transformer terminals was applied to different machines whose ratings are in the range

of 30 to 660 MW. The fault duration was so chosen that pole-slipping occurs in every case before the generators return to steady state conditions. The machines were conditioned to deliver rated power before the fault was initiated. Only a few of many results obtained from computation are discussed here. The parameters for the damper circuits were kept unchanged for these studies.

(9.2.1) ROTOR ANGLE TRANSIENTS

Variations of the rotor angles of the generators are shown in Fig.57. Though limited pole slipping occurs in all cases, the positive damping present returns the generators to steady running conditions within about 3 seconds following fault incidence. In the upper range of power rating the damping appears to be fractionally less than at lower power rating but the trend is not emphasised. It is possible by the correct adjustment of the automatic voltage regulator parameters appropriate to a particular machine to promote the greatest positive damping torque. An optimisation of this form was not attempted in the present series of analyses; the regulator parameters in per-unit have been maintained constant for all the machines. In all cases a positive synchronisation appears to result after one pair of pole slipping, except that in the case of the 500 MW machine owing to somewhat unusual combination of parameters in the particular case, it slips two pairs of poles.

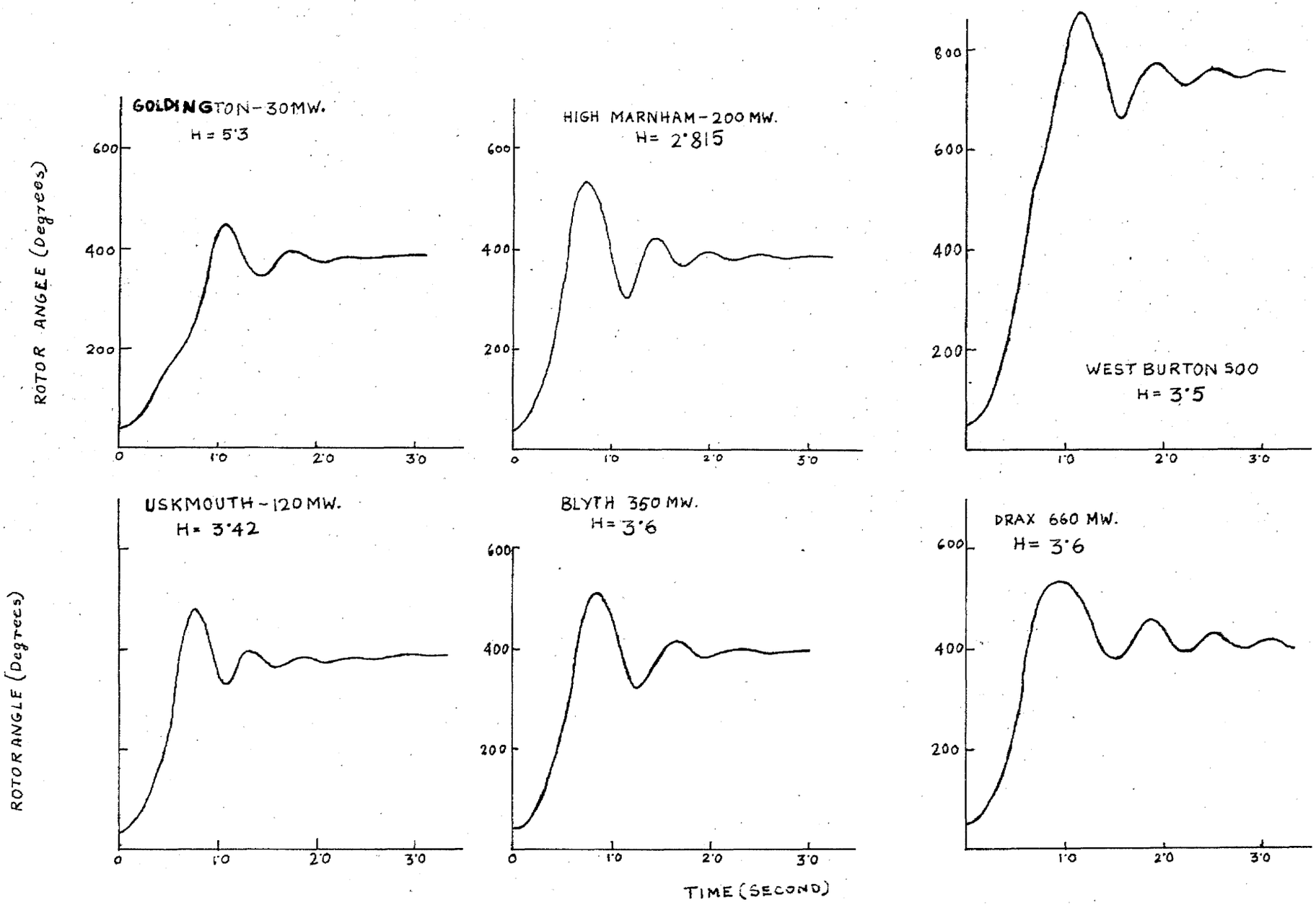

FIG. 57. ROTOR ANGLE VARIATION DURING 3-PHASE FAULT.

(9.2.2) TERMINAL VOLTAGE TRANSIENTS

For the same range of machine ratings and operating under the same disturbing conditions the terminal voltage variations are shown in Fig.58. In this the transients appear to follow a consistent pattern without excessive over voltage. If anything, the over voltages tend to reduce as the machine rating increases. Whilst a related study would be that of induction motor auxiliaries during busbar voltage transient, it is apparent from the voltage dip caused by a 3-phase fault with limited pole slipping that a precipitation of instability is unlikely due to the short duration of the voltage dip.

(9.3) EFFECT OF INERTIA CONSTANT IN MACHINE OPERATION

For assessing the effect of inertia constant in generator performances an experimental analysis was carried out by considering a particular machine subjected to a fixed disturbance while the inertia constant was varied within a wide range. The operation corresponds to that of a 3-phase fault at the unit transformer terminals for a duration of 0.38 seconds.

The variation of rotor angle and terminal voltage are shown in Figs. 59 and 60. The stabilising effect due to higher inertia constant is emphasised from the nature of the response characteristics of the machine variables subsequent to the fault clearance. Whilst with an inertia constant of upto 4 kw sec/kVA the machine slips two pairs of poles, an

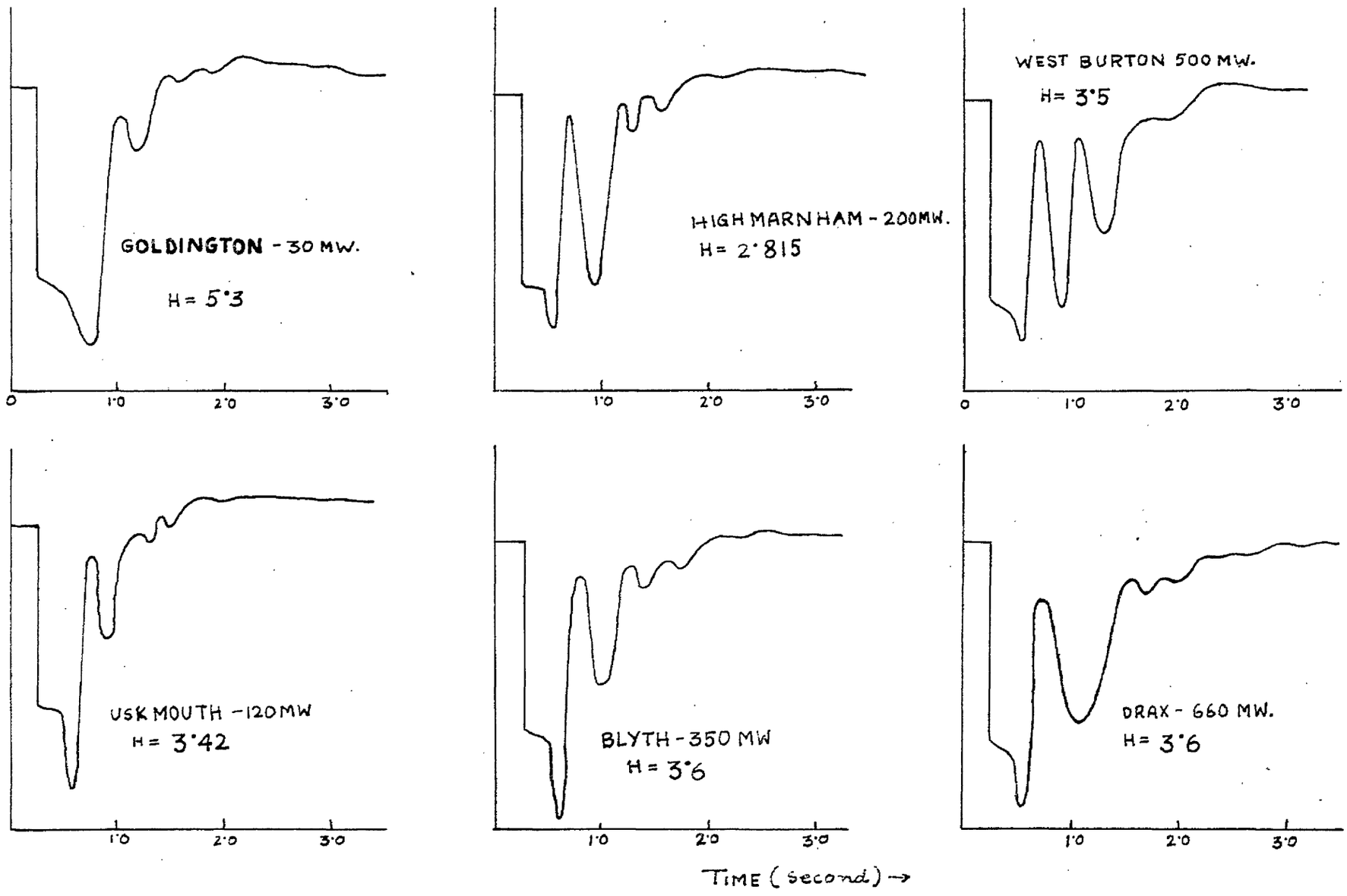

FIG. 58. TERMINAL VOLTAGE TRANSIENT DURING 3-PHASE FAULT.

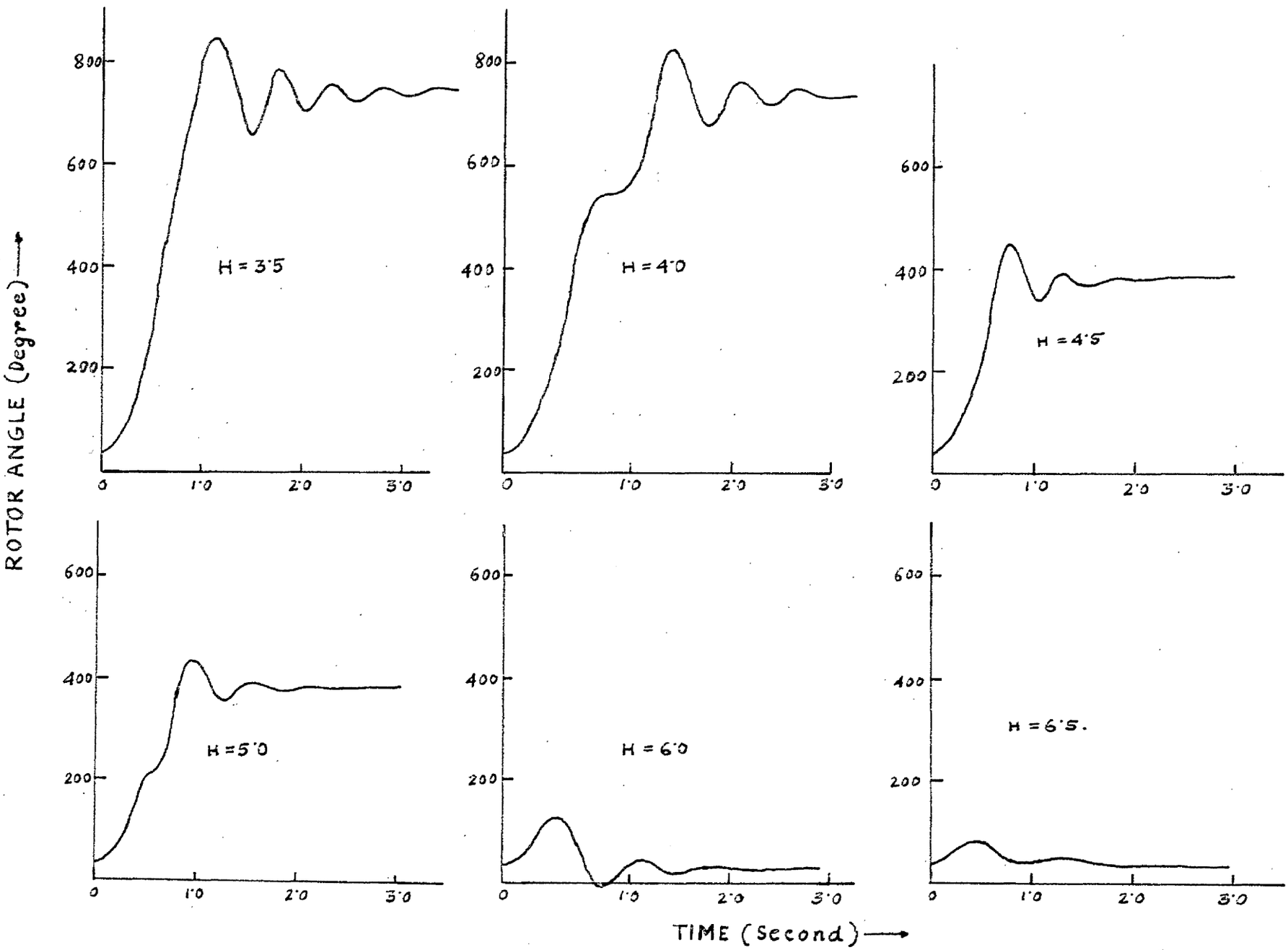

FIG. 59. ROTOR ANGLE TRANSIENTS DURING 3-PHASE FAULT FOR DIFFERENT INERTIA CONSTANTS.

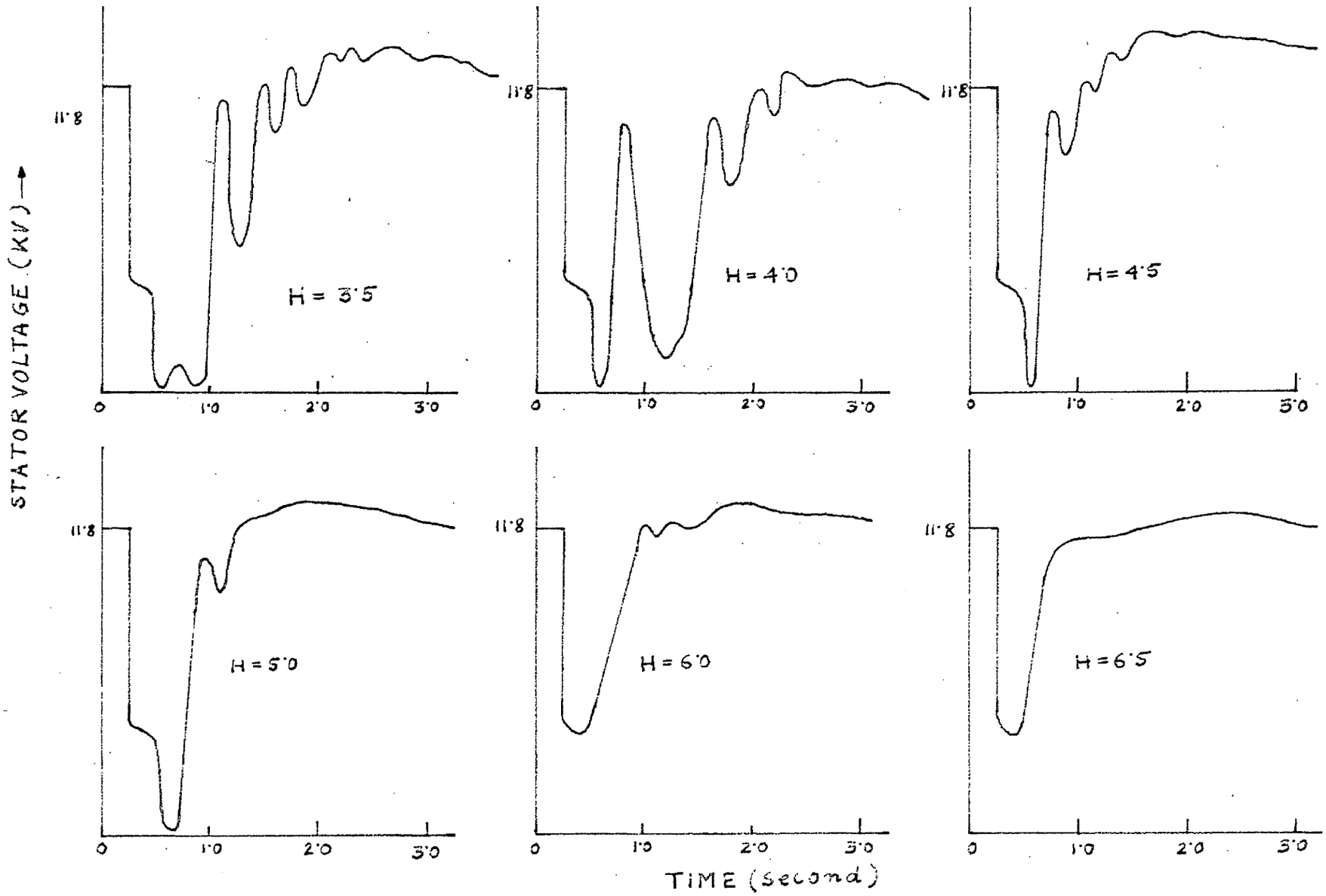

FIG. 60. TERMINAL VOLTAGE TRANSIENTS DURING 3-PHASE FAULT FOR DIFFERENT INERTIA CONSTANTS.

increase of the inertia to 4.5 stabilises the generator after the machine has slipped one pole-pair only. A still higher inertia of 6.0 kw sec/kVA develops enough positive damping for the machine not to slip any pole.

Similar effects are also noticeable in the stator voltage transients. After the initial drop in the terminal voltage, the rapidity with which the transients settle down, increases with higher inertia.

(9.4) ASYNCHRONOUS OPERATION

(9.4.1) VARIATION OF SLIP

Where as it has hitherto been the usual practice in analysing the operating performance of synchronous generators under asynchronous running conditions to assume a constant slip[60], the computed results in the case of the Goldington machine as shown in Fig.61 indicates that the slip is far from constant. The slip, corresponding to the rated output with the field circuit short circuited with discharge resistance varies between almost zero and 1.45% of the rated speed. The previous analytical methods based on constant slip throughout a cycle of operation seems to be in error on this account.

(9.4.2) STATOR CURRENT VARIATION

The fluctuation of stator current between about 1.25 p.u. and 0.7 p.u. is shown in Fig.62. The increased values of the stator current of course result in increased stator copper

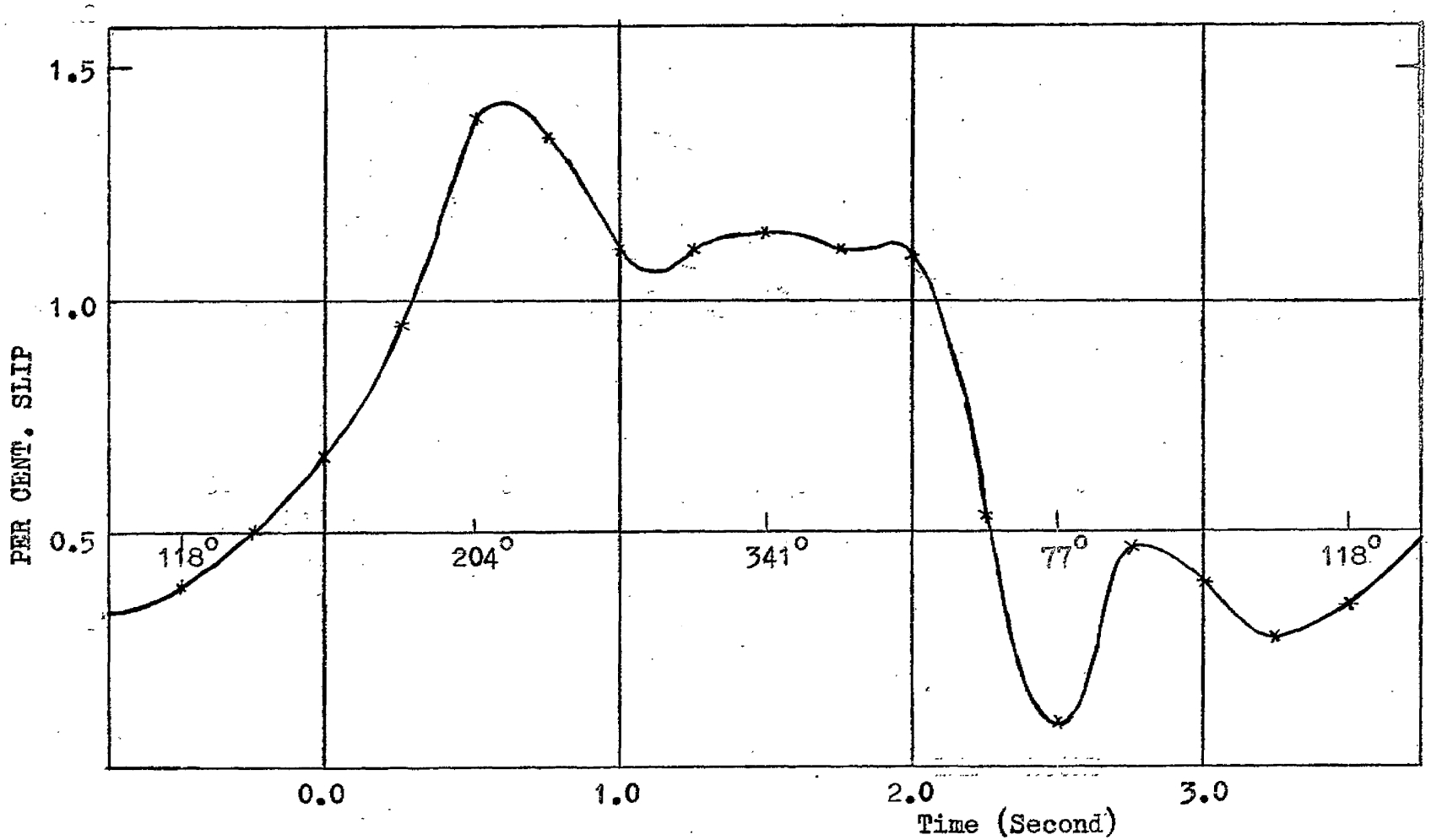

FIG. 61. VARIATION OF SLIP DURING ASYNCHRONOUS RUNNING$_3$

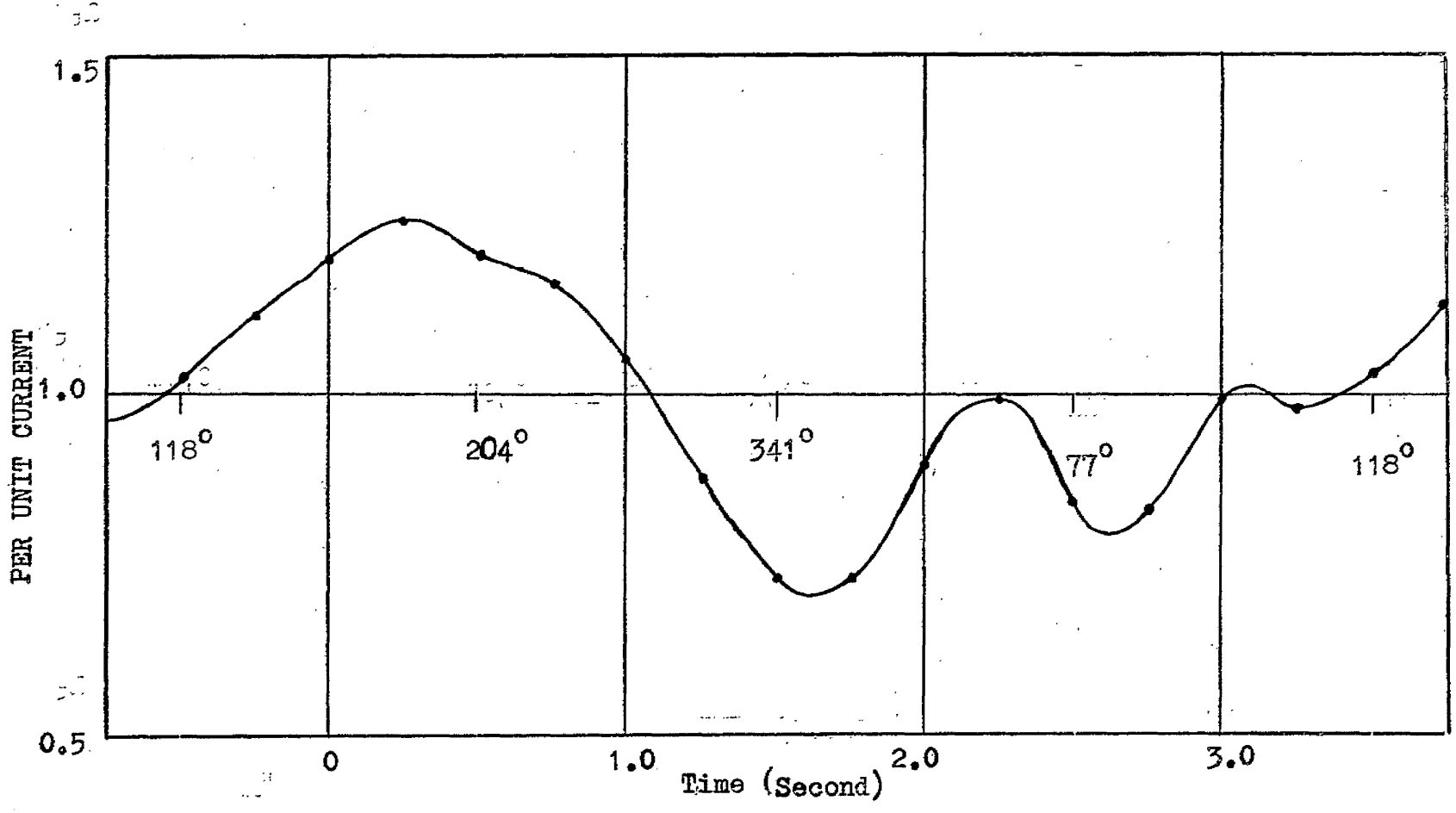

FIG. 62. STATOR CURRENT VARIATION DURING ASYNCHRONOUS RUNNING.

loss. At the same time, the limiting conditions so far as heating is concerned are more likely to be encountered in the rotor than in the stator.

It has not been possible to correlate the computed results with any site test results as the tests of Goldington did not include a test of this form but a comparison with those obtained from measurements at Marchwood[55] indicates a similar pattern of variation.

(9.4.3) TERMINAL POWER VARIATION

The operating conditions, as mentioned earlier, correspond to a mean rated output power. During a cycle of operation, however, the variation as shown in Fig.63 is substantial, fluctuating between 0.65 and 0.95 per unit.

(9.4.4) TERMINAL VOLTAGE

When a synchronous machine is run as an induction generator an important consideration is that of voltage variation that inevitably arise. In Fig.64 is shown the voltage response which varies between a wide limit.

(9.5) GENERAL DISCUSSION

The present section serves to indicate the range of studies to which the program developed may be readily applied. Studies of this kind are likely to be of increasing importance as machines and system development take

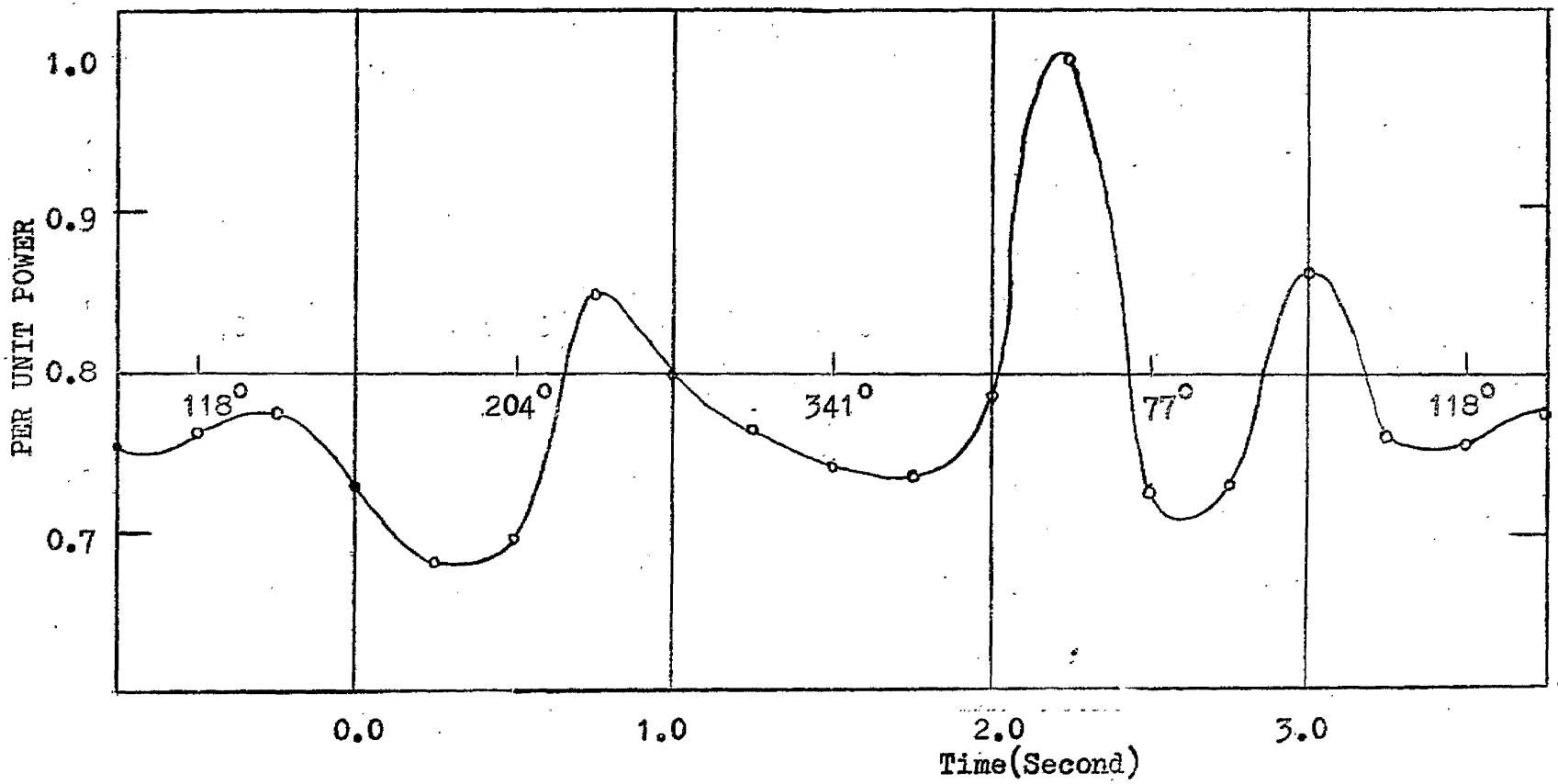

FIG. 63. OUTPUT POWER VARIATION DURING ASYNCHRONOUS RUNNING.

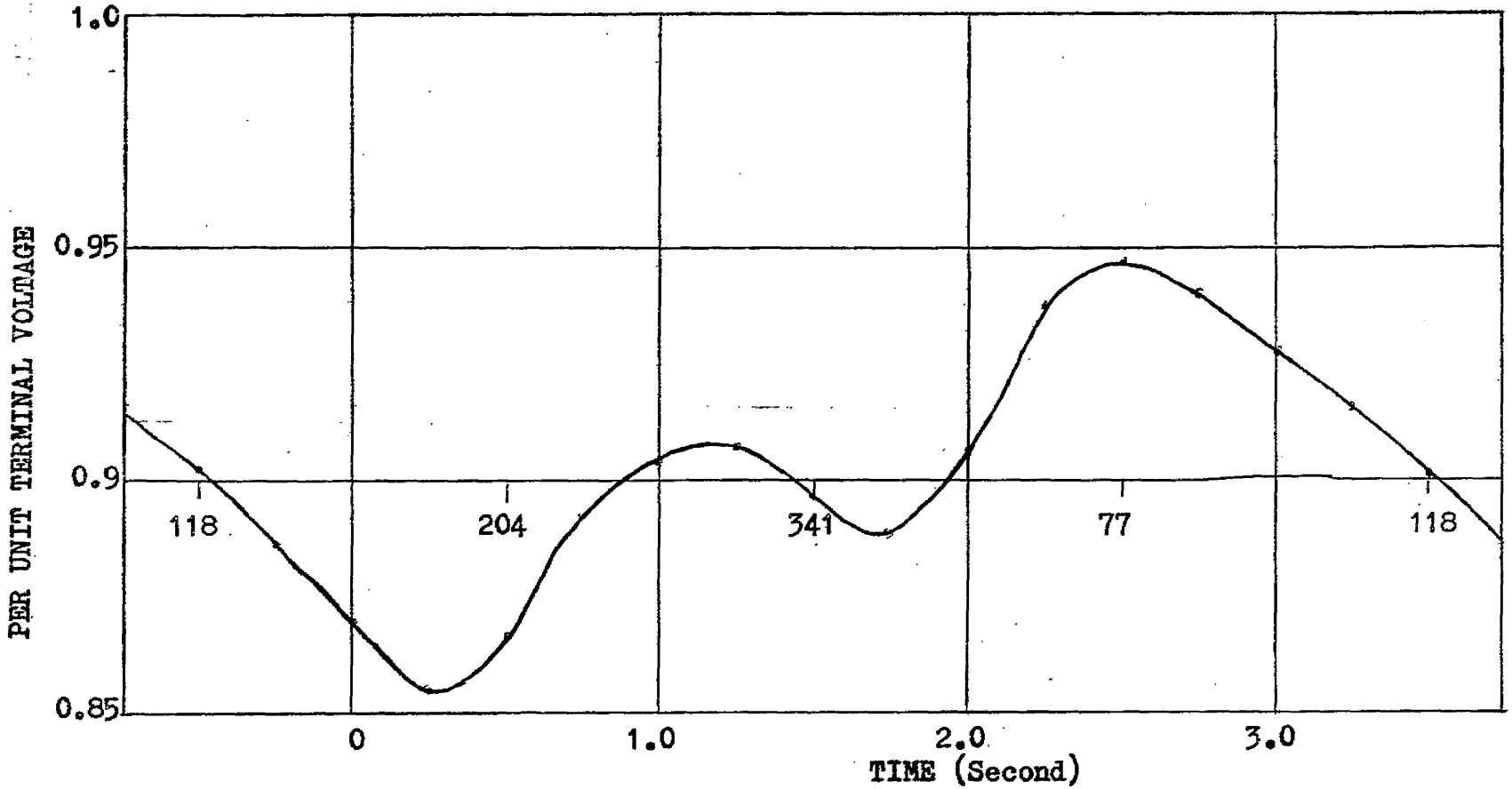

FIG. 64. TERMINAL VOLTAGE VARIATION DURING ASYNCHRONOUS RUNNING.

place, and where reliable information is required for disturbance conditions[61] other than those so far mentioned may be readily included in the program.

CHAPTER X

CONCLUSIONS

(10.1) PATTERN OF INVESTIGATION

The investigations documented in the present thesis have taken a pattern that may be summarised in the following way:

(a) A formulation of the fundamental equations of a synchronous generator in terms of dqo reference frame derived from the basic equations of a 3-phase machine.

(b) The inclusion of the equations of a complete excitation control system and, in approximate form, the equations of a prime-mover and its associated governing system to formulate a mathematical model of a complete turbo-alternator unit.

(c) The development of a range of digital computer methods with particular reference to the solution of the equations of the model with a view to the accurate pre-determination of the dynamic response of a turbo-alternator unit.

(d) In particular, account has been taken in the analysis of:

(i) Steady state, transient and subtransient saliency.

(ii) The voltage produced by the rate of change of armature flux ($p\Psi_d$, $p\Psi_q$ etc.).

(iii) Effects of the variation of the instantaneous speed of the rotor under transient condition ($p\theta$).

(iv) Representation of the subtransient conditions.

(v) Input power modulation due to governor-action.

(vi) Representation of saturation in the magnetic amplifiers and exciter characteristics in the automatic voltage regulating system.

(vii) Representation of constraints on the governor and main input valvesin the turbine.

(e) The correlation of the results obtained from the computer solution of the turbo-alternator model based on constant values of the machine parameters, with those obtained from site-tests at Goldington Power Station.

(f) The development of a variable-parameter mathematical model in which all the reactances and time constants associated with the generator are continuously varied on the basis of magnetic circuit saturation throughout the solution.

(g) An investigation of the phenomena of eddy current flow in the solid-rotor body and the development of methods by which the effects of eddy current distribution can be taken into account in digital solution with greater accuracy than if an equivalent short circuited winding in each axis is used. These methods include:

(i) The derivation of the equivalent-circuit parameters firstly from the solution of the field equations

of the rotor based on a sinusoidal forcing function.

(ii) Application of a technique by which the parameters obtained from frequency response can be used for transient response where the forcing function may take any arbitrary form.

(iii) Two equivalent short circuited windings in each axis.

(h) A correlation of these more advanced methods with the Belvedere site-test results, with particular reference to the calculation of rotor over voltages which represent a stringent test on the representation used for the flow and distribution of eddy current in the rotor for, where the mmf balance between the stator and the rotor is lost due to the rectifiers permitting only positive flow of field current in an a.c. excited unit, the machine variables are largely conditioned by the properties of the rotor.

(i) An evaluation of the electrical conditions subsequent to automatic and self synchronisation of turbo generators.

(j) The experimental analysis of asynchronous running and extension of the program for the analysis of generating units of up to 660 MW capacity.

(10.2) DISCUSSION OF DIGITAL METHODS OF ANALYSES

(10.2.1) GENERAL

The all-round analytical power of digital analytical methods appears to have substantial advantage in large scale

power system analyses and will, in many cases, be preferred to other alternative methods available. The ease with which a program once developed may, at short notice, be used is in many ways of significant advantage. The flexibility of programming to represent a machine model to such an extent as has hitherto been impossible, also emphasises the adoption of digital technique as an analytical aid.

(10.2.2) GENERATOR

The correlation studies that have been carried out in the present work give further support to the validity of the dq equations under balanced and symmetrical operating conditions and it appears that if an adequate rotor representation is included in it, then the approach will be satisfactory for a wide range of studies. The methods adopted in the present thesis to account for the effects of the eddy current flow in the solidly forged rotor, appear to be satisfactory for the range of studies to which they have been applied. The methods may be optimised on the basis of comparison with site-test results for different sizes of generating units operating under widely varying operating conditions. There is, therefore, further scope for work in improving the basic method outlined in the present work to render it applicable for a wide range of machines.

Some reservation on the accuracy of dqo formulation should be made with particular reference to the representation

of the saturation characteristics of the machine. The equations are based on the electrical and magnetic independence between the two axes. In the method of curve fitting developed in the investigation of magnetic circuit saturation is introduced in terms of total flux calculated from each axis component; the assumption is then made that the mutual inductance in the direct and quadrature axes are affected equally by saturation. In reality, of course, owing to the different reluctance paths caused by the presence of slots and windings in the rotor the effects will be different in the two axes. Means of taking the interaction between the two axes and effects of saliency into account represent an extension of the basis provided here.

Although the assumption of a constant leakage flux would appear to give small errors, the evaluation of means by which its variation can be taken into account would be a worthwhile improvement of the analytical method.

Hysteresis has been neglected altogether in the present work. The modulation of the machine parameters has been achieved from the flux and mmf relations of the mean magnetisation curve. If the hysteresis were taken into account it would appear from Fig.(68) that for the same mmf two different flux conditions may arise. Under steady operating conditions while the flux pulsates at 50 c/s in the stator, they remain unidirectional in the rotor. Investigation of the effects of

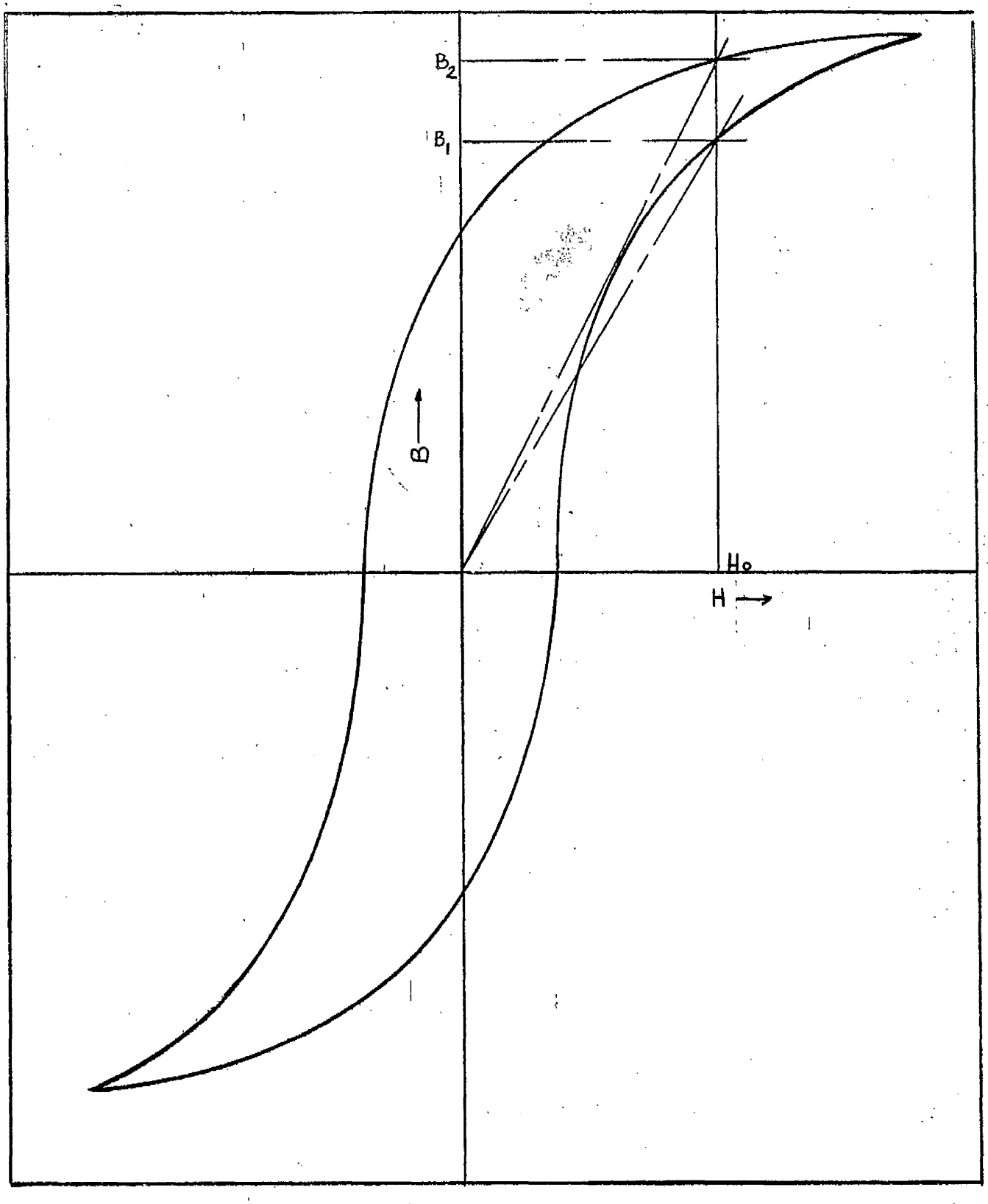

FIG. 68. EFFECT OF HYSTERESIS IN CHANGING PERMEABILITY FOR A PARTICULAR MMF.

hysteresis may also be worthwhile.

(10.2.3) AUTOMATIC VOLTAGE REGULATOR

Of the different parts of the complete mathematical representation, the automatic voltage regulating system presents, on the whole, the fewest difficulties in digital analys es. Its equations are formed on the basis of static characteristics of each element and the time constants associated with them appear to be readily available. The saturation limit of each element has been represented by straight line approximation and has been found to be satisfactory and the curve fitting for individual element does not appear to be justifiable when the additional complication that is involved, is considered. At the same time, where it is thought that the output impedances of the different units may reduce the effective forward gain of the loop as a whole under conditions of the units supplying substantial level of output current, then this may be accounted for in the equations when these impedances are available.

The constraints that are introduced in the analysis to correspond to the action of the rectifiers and based on their having zero forward resistance and infinite reverse resistance appear to be satisfactory for a wide range of analytical purposes.

(10.2.4) TURBINE AND GOVERNING SYSTEM

As used here, the representation of the prime-mover and

its governing system is of a simplified form, but it has been shown from correlation studies to give substantially close agreement with site-test results. However, there is scope for further development of this part of the model, particularly where limited pole-slipping and spontaneous resynchronisation is proposed. In general, the governor will have relatively small effect in preventing loss of synchronism, owing to the long time delay in the control loop, but it will assume a major importance in promoting conditions favourable to resynchronisation and subsequent build-up of load at a predetermined rate. Under those circumstances a greater degree of representation of the prime mover and the governing system would be necessary.

(10.3) MULTI-MACHINE SYSTEM ANALYSIS

The present thesis has been confined to the analysis of a single turbo-alternator unit, but the program and the methods underlying it, afford its direct application to those cases in which it is required to have regard for the interaction between machines. Since the machine equations are valid for steady state, transient and subtransient conditions, the extension can be achieved by calling, in the program, one machine after another and calculating the new values of the variables on the basis of the same equations at each step. When the values are obtained, in terms of subtransient quantities for all the machine, the inter-connecting network can be solved by one of the usual methods considering the

machine variables remain constant for the interval chosen. In this way the accuracy of a complete system representation can be greatly improved. What is required from the programming point of view is a large storage facility.

(10.4) SITE TESTING RELATED TO RELIABLE MACHINE ANALYSIS

A stage is reached in the theoretical formulation of machine representation in which its further development can only be profitably made by relating the computed results to those obtained from actual measurements on the system. Thus, in further improving the rotor representation detailed flux measurements at different locations within the rotor body becomes desirable to indicate, with greater accuracy than at present seems to be known, the flux distribution in the surface of the rotor. Local tooth saturation complicates any rotor representation and a knowledge of the likely flux distribution at different points around teeth at different locations on the rotor surface, may provide an analytical basis for taking the effect into account.

In a similar way, search coil measurement to indicate the leakage flux and its variation with saturation could assist considerably in including this into the mathematical representation. Of particular merit are search coil measurements in which the coils are arranged to be electrically at right angles to each other, so that one of them indicates the condition of the direct-axis flux path while the other

will do the same for the quadrature-axis flux path.

While carrying out site tests on a single machine connected to a relatively large system, it appears to be desirable to extract more information about the system. It has been mentioned earlier that the effects caused by a disturbance in the machine on the system could not be studied because the system was assumed to remain uneffected. If the system could, instead, be represented as a source with finite input-output impedance, such analysis would become feasible.

(10.5) OVERALL CONCLUSION

By providing a flexible, accurate and comprehensive method of representing a synchronous generator it is hoped that the present work will further contribute to the available knowledge of transient performance, and, through those aspects of the system design to which it relates, to the permanent requirement of increasing the security of synchronous power system.

ACKNOWLEDGMENTS

The author expresses his gratitude to Professor C. Adamson, Head of the Department of Electrical Engineering for providing the facilities to carry out the research work in the Power System Laboratory of the University of Manchester Institute of Science and Technology.

He gratefully acknowledges his indebtedness to Dr. W.D. Humpage, B.Sc., Ph.D.(Durham), for his constant encouragement, help and overall supervision of the entire project.

The financial support of the English Electric Company Limited is gratefully acknowledged. Thanks are due to the staff of the Manchester University Computing Service for running his very many digital programs.

The acknowledgments would not be complete without thanking his colleagues in the Laboratory for useful discussions with them and also Mrs. Wood for typing the thesis.

REFERENCES

1. Concordia, C.
   Synchronous Machines - Theory and Performance. John Wiley, 1951.

2. Kron, G.
   Classification of the Reference Frames of a Synchronous Machine. Trans.A.I.E.E., Vol.69 (1950), Part II, page 720.

3. Kron, G.
   A New Theory of Hunting. ibid, Vo..71(1952), Part III, page 859.

4. Blondel, A.
   The Two Reaction Method for Study of Oscillatory Phenomena in Coupled Alternators. General Electric Review, Vol.12(1923),page 235 and 515.

5. Doherty, R.E. and Nickle, C.A.
   Synchronous Machine - An Extension of Blondel's Two Reaction Theory. Trans.A.I.E.E., Vol.45(1926), page 912.

6. Park, R.H.
   Two Reaction Theory of Synchronous Machines - Generalised Method of Analysis, Part I, ibid, Vol. 48(1929), page 716.

7. Buseman, F. and Casson, W.
   Results of Full-Scale Stability Tests on the British 132 kV Grid System. Proc.I.E.E., Vol.105A (1958), page 347.

8. Rankin, A.W.
   Per Unit Impedances of Synchronous Machines, Part I and II. Trans.A.I.E.E., Vol.64(1945), page 569 and 839.

9. White, D.C. and Woodson, H.H.
   Electomechanical Energy Conversion. John Wiley, New York, 1959, page 522.

10. Laughton, M.A.
    Matrix Analysis of Dynamic Stability in Synchronous Multimachine System. Proc. I.E.E., Vol.113 (1966), page 325.

11. Concordia, C.
Steady State Stability of Synchronous Machines as Affected by Regulator Characteristics. Trans.A.I.E.E., Vol.63(1944), page 215.

12. Aldred, A.S.; Shackshaft, G.
The Effect of a Voltage Regulator on the Steady-State and Transient Stability of a Synchronous Generator. Proc. I.E.E., Vol.105A(1958), page 420.

13. Langer, P. and Johansson, K.E.
The Influence of a Load-Angle-Dependent Signal on the Voltage Regulation of Synchronous Machines. C.I.G.R.E., 1960, paper no.315.

14. Saha, T.N.
Digital Computer Study of Excitation System in Synchronous Machine, M.Sc.Tech. Thesis,October 1963.

15. Aldred, A.S.; Shackshaft, G.
A Frequency-Response Method for the Pre-determination of Synchronous Machine Stability. Proc.I.E.E., Vol. 107C (1960), page 2.

16. Doherty, R.E.
A Simplified Method of Analysing Short Circuit Problems. Trans.A.I.E.E.,Vol.42(1923), page 841.

17. Discussion of Reference 20, Proc.I.E.E.,Vol.110 (1963), page 1271.

18. Gupta, P.P., Humphrey Davies, M.W.
Digital Computers in Power System Analysis, Proc. I.E.E., Vol.108A(1961), page 383 and 398.

19. Humpage, W.D. and Stott, B.
Predictor-Corrector Methods of Numerical Integration in Digital Computer Analysis of Power System Transient Stability, ibid, vol.112(1965), page 1557.

20. Shackshaft, G.
A General Purpose Turbo-Alternator Model, ibid, vol.110(1963), page 703.

21. Shackshaft, G.
Study of Simulation of Synchronous Machine Report RD/A/R4 of Central Electricity Generating Board.

22. Kesavamurthy, N. and Rajagopalan, P.K.
Rise of Flux in Solid Iron Core due to Impact Excitation, Proc. I.E.E., Vol.106(1959), page 189.

23. Boffi, L.V.; Hass, V.B.
Analogue Computer Representation of Alternator for Parallel Operation, Trans.A.I.E.E., Vol.76(1957), Part III, page 153.

24. Steven, R.E.
An Experimental Effective Value of the Quadrature-Axis Synchronous Reactance of a Synchronous Machine, Proc.I.E.E., Vol.108(1961), page 559.

25. Singer, J.
Elements of Numerical Analysis, Academic Press, 1964, page 377.

26. Hamming, R.W.
Numerical Methods for Scientists and Engineers, McGraw-Hill Book Company, 1962, page 363.

27. Asynchronous Running Tests on Large Turbo-Alternator, The Engineer, 1962(Feb), page 362.

28. Mason, T.H., Aylett, P.D. and Birch, F.H.
Turbo-Generator Performance Under Exceptional Operating Conditions, Proc.IEE, vol.106A(1959), page 357.

29. Scott, E.C., Chorlton, A. and Banks, J.H.
Multi-Generator Transient-Stability Performance Under Fault Conditions, ibid, vol.110(1963), page 1051.

30. Saha, T.N.
Feedback Control of Effective Synchronous Machine Parameters, Int.J.Elec.Engng.Educ., vol.2(1965), page 554.

31. Howard, N.R. and Jones, A.K.
Silicon Rectifiers with Ultra-High Peak Inverse Voltage, A.E.I.Engineering, May/June 1965, page 140.

32. Dispaux, J.
Excitation of Large Output Turbo-Alternator by Means of Rotary Rectifiers, C.I.G.R.E., 1962, paper 117.

33. Easton, V.
Excitation of Large Turbo-Generators, Proc.I.E.E., vol.111(1964), page. 1040.

34. Easton, V.
Static Rectifier Excitation, G.E.C. Journ. of Sc. & Tech., Vol.30(1963), page 31.

35. Domeratzky, L.M., Rubenstein, A.S. and Temoshok, M.
A Static Excitation System for Industrial and Utility Steam Turbine-Generators, Trans.A.I.E.E.,Vol. 89(1961), Part III, page 1072.

36. Lane, L.J.; Rogers, D.F. and Vance, P.A.
Design and Tests of a Static Excitation System for Industrial and Utility Steam Turbine Generators. ibid, page 1077.

37. Holburn, W.W.
Site Test on Belvedere 5 Alternator and A.C. Excitation System, July 1962, Report No. S/CAs38, The English Electric Co.Ltd.

38. Adkins, B.
The General Theory of Electrical Machines. Chapman and Hall,1957.

39. Humpage, W.D. and Stott, B.
Effect of Auto Reclosing Circuit Breakers on Transient Stability in e.h.v. transmission Systems. Proc.I.E.E.,Vol.III(1964),page 1287.

40. Thomson, J.J.
On the Heat Produced by Eddy currents in an Iron Plate Exposed to an Alternating Electric Field, Journal I.E.E.,Vo..28(1892),page 599.

41. Rosenberg, E.
Solid Iron Conductors and Eddy Current Brakes, (German), Electrotechnische Zeitschrift,Austria, Vol.44(1923),page 1055.

42. Pohl, R.
Rise of Flux due to Impact Excitation: Retardation by Eddy-Currents in Solid Parts, Proc.I.E.E, Vol.96 (1949),Part II,page 57.

43. McConnell, H.M.
Eddy-Current Phemomena in Ferromagnetic Materials, Trans.A.I.E.E.,Vo..73(1954),Part I,page 226.

44. Agarwal, P.D.
Eddy-current Losses in Solid and Laminated Iron, ibid, vol.78,(1959),pt.II,page 169.

45. Kesavamurthy, N. and Rajagopalan, P.K.
Effects of Eddy Current on the Rise and Decay of Flux in Solid Magnetic Cores, Proc.I.E.E.,Vol.109C(1961), page 63.

46. Subba Rao, V.
Equivalent Circuit of Solid Iron Core for Impact Excitation Problems, ibid,vol.III(1964),page 349.

47. Concordia, C. and Poritsky, H.
Synchronous Machine with Solid Cylindrical Rotor, Trans.A.I.E.E, Vol.56(1937),page 49.

48. Wood, A.J.
An Analysis of Solid Rotor Machine - Part I, Operational Impedance and Equivalent Circuits. ibid,vol.79,(1960),Part III,page 1657

49. Bharali, P. and Adkins, B.
Operational Impedances of Turbogenerators with solid rotors. Proc.I.E.E,Vol.110 (1963), page 2185.

50. Hamilton, H.B.
Magnetic Saturation and Eddy Current Effect in D.C. Machine Voltage Build-up.Trans.A.I.E.E.,Vol.83(1964), Part III,page 606.

51. Brailsford, F.
Investigation of the Eddy Current Anomally in Electrical Sheet-steels. Proc.I.E.E., Vol. 95 (1948), Part-II page-38

52. Brockman, J.J. and Linkous, C.E.
D.C.Machine: Response to Impact Excitation. Trans.A.I.E.E.,Vol.74(1955),Part III,page 500.

53. Wood, A.J. and Concordia, C.
An Analysis of Solid Iron Rotor Machine - Part II Effect of Curvature, ibid, vol.79(1960), Part III, page 1666.

54. MacFadyen, K.A.
Vector Permeability. Journal I.E.E., Vol.94(1947), Part III,page 407.

55. Chalmers, B.J.
Asynchronous Performance Characteristics of Turbo-Generators,Proc.I.E.E.,Vol.109A(1962),page 301.

56. Wright, S.H.
Determination of Synchronous Machine Constants by Test, Trans.A.I.E.E.,Vol.50(1931),page 1331.

57. Shoults, D.R., Crary, S.B. and Lauder, A.H.
Pull-in Characteristics of Synchronous Motors, ibid, vol.54(1935),page 1385.

58. Koening, H.E. and Blackwell, W.A.
Electromechanical System Theory, McGraw-Hill, 1961, page 320.

59. Peniscu, C.
Considerations on the Parallel Coupling of Alternators by the Auto-Synchronisation Method, C.I.G.R.E.1954,vol.II,paper no.152.

60. Mamikoniants, L.G.
Connecting Synchronous Machines in Parallel by the Self-Synchronising Method, C.I.G.R.E.1954,vol.II, paper no.152.

61. Humpage, W.D. and Saha,T.N.
Development of a Digital Program for a Turbo-Alternator Unit and its Comparison with Site Test Results from Goldington Power Station, A Research Report submitted to English Electric Co.Limited, Turbo-Generator Division.

APPENDIX (A)

PARK'S TRANSFORMATION

(A.1) CLARKE'S COMPONENTS

A set of three vectors representing currents, voltages or fluxes of a 3-phase system can be replaced by any one of a number of different systems of component vectors. One of them, Clarke's αβo components, is related closely to Park's dqo transformation.

The coefficient matrix that transforms abc phase variables into Clarke's αβo components is given by

$$[C] = \frac{2}{3}\begin{array}{c|ccc} & \alpha & \beta & o \\ a & 1 & -\frac{1}{2} & -\frac{1}{2} \\ b & 0 & \frac{\sqrt{3}}{2} & -\frac{\sqrt{3}}{2} \\ c & \frac{1}{2} & \frac{1}{2} & \frac{1}{2} \end{array} \qquad (A.1)$$

giving the relation

$$[\alpha\beta o] = [C][abc] \qquad (A.2)$$

and for inverse transformation

$$[abc] = [C]^{-1}[\alpha\beta o] \qquad (A.3)$$

where

$$[C]^{-1} = \begin{array}{|ccc|} \hline 1 & 0 & 1 \\ -\frac{1}{2} & \frac{\sqrt{3}}{2} & 1 \\ -\frac{1}{2} & -\frac{\sqrt{3}}{2} & 1 \\ \hline \end{array} \qquad (A.4)$$

The coefficient matrix given in equations (A.1) and (A.4) can also be expressed in the following way

$$[C] = \frac{2}{3}\begin{vmatrix} \cos(0) & \cos(-120) & \cos(-240) \\ -\sin(0) & -\sin(-120) & -\sin(-240) \\ \frac{1}{2} & \frac{1}{2} & \frac{1}{2} \end{vmatrix} \qquad (A.5)$$

and

$$[C]^{-1} = \begin{vmatrix} \cos(0) & -\sin(0) & 1 \\ \cos(-120) & -\sin(-120) & 1 \\ \cos(-240) & -\sin(-240) & 1 \end{vmatrix} \qquad (A.6)$$

In a symmetrical system operating under balanced conditions, the α component is equal to phase 'a' of the 3-phase system in magnitude and direction. The magnitude of β component is equal to that of phase-a but lags phase 'a' by 90^{o}. The zero component is absent. In case of an unbalanced and asymmetrical system all the components are present and their magnitudes and phase relationship do not maintain any symmetry as in the former case. In machine analyses it is the usual convention to assume that under steady operating conditions the generated voltages and output currents are balanced and symmetrical so that

$$\left.\begin{aligned} \underline{K}_{\alpha} &= \underline{K}_{a} \\ \underline{K}_{\beta} &= -j\underline{K}_{a} \\ \underline{K}_{o} &= 0 \end{aligned}\right\} \qquad (A.7)$$

The physical significance of this transformation is that a

3-phase machine is now replaced by a 2-phase machine, the effective number of terms per phase being the same for both the machines.

(A.2) TRANSFORMATION FROM αβo TO dqo COMPONENTS

The αβo components can be transformed into dqo components in the following way. Assuming that the d axis leads the axis of the α components by an angle θ, the coefficient matrix that links the two components is

$$[D] = \begin{bmatrix} \cos\theta & -\sin\theta & \\ \sin\theta & \cos\theta & \\ & & 1 \end{bmatrix} \qquad (A.8)$$

so that

$$[dqo] = [D][\alpha\beta o] \qquad (A.9)$$

Substituting (A.2) into (A.9) a relation between the abc variables and the dqo components is now given by

$$[dqo] = [D][C][abc] \qquad (A.10)$$

and multiplying $[D]$ and $[C]$ together

$$[dqo] = [P][abc] \qquad (A.11)$$

where $[P]$ = Park's transformation matrix,

$$[P] = \frac{2}{3}\begin{bmatrix} \cos\theta & \cos(\theta-120^\circ) & \cos(\theta-240^\circ) \\ -\sin\theta & -\sin(\theta-120^\circ) & -\sin(\theta-240^\circ) \\ \frac{1}{2} & \frac{1}{2} & \frac{1}{2} \end{bmatrix} \qquad (A.12)$$

The different stages of transformation are shown in Figs 65 and 66

(A.3) PHYSICAL SIGNIFICANCE OF PARK'S TRANSFORMATION

The interpretation of Park's transformation as applied in synchronous machine analysis, may be described by considering an unloaded 3-phase machine generating symmetrical and balanced voltages. The voltage equations for the three phases of the machine can then be written as:

$$\begin{aligned} v_a &= v_s \cos \omega t \\ v_b &= v_s \cos(\omega t - 120^\circ) \\ v_c &= v_s \cos(\omega t - 240^\circ) \end{aligned} \qquad \text{(A.13)}$$

where $$v_s = x_{afd} i_{fd} \qquad \text{(A.14)}$$

In machine analysis, however, the usual practice of writing the phase-variables is

$$\begin{aligned} v_a &= v_s \\ v_b &= v_s \cos(-120^\circ) \\ v_b &= v_s \cos(-240^\circ) \end{aligned} \qquad \text{(A.15)}$$

The results obtained by applying Clarke's transformation to these two different sets of voltage-equations are entirely different.

When the phase-voltages of equation (A.13) are transformed to $\alpha\beta o$ components by applying equation (A.5), the following are obtained:

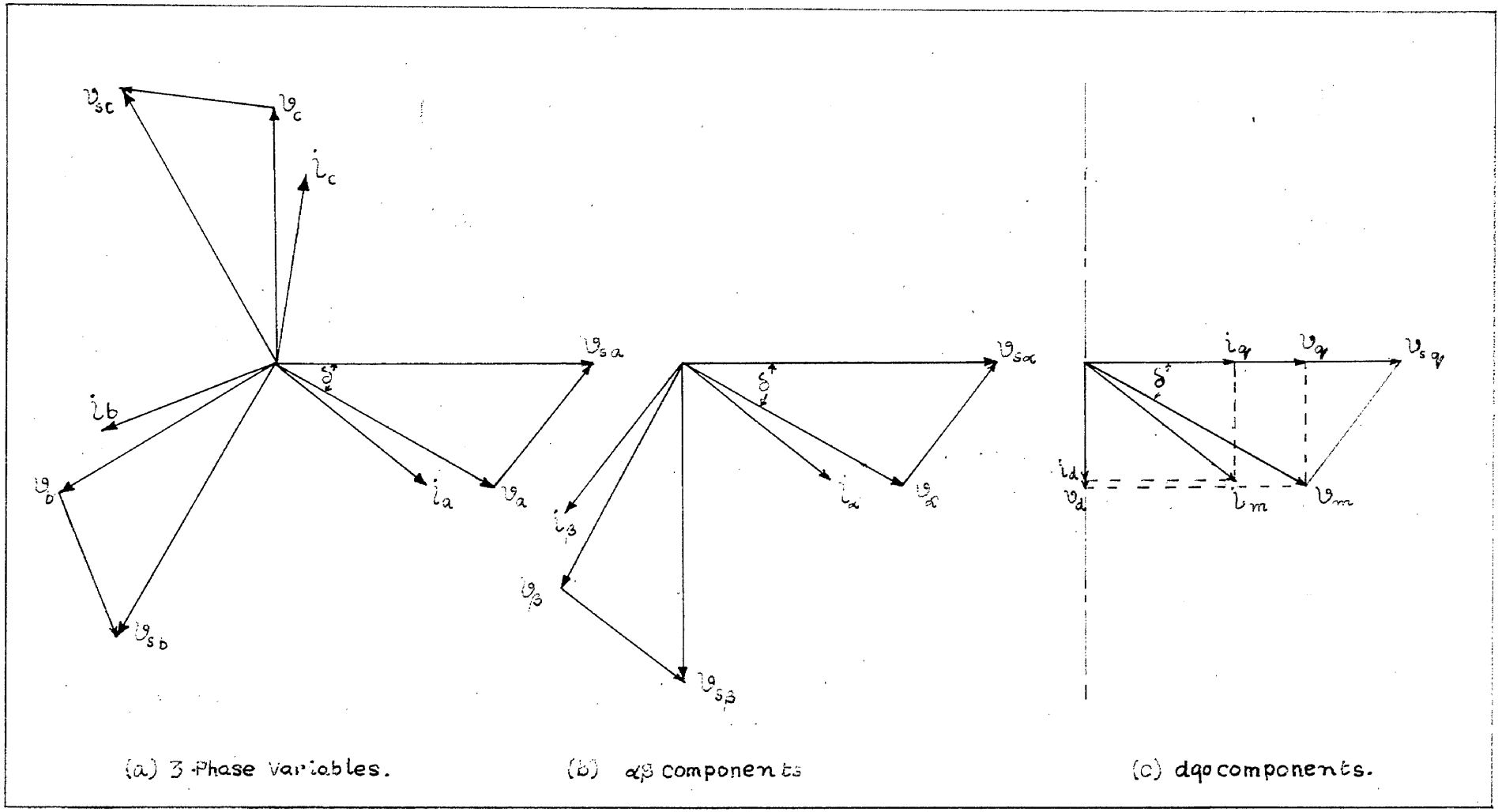

FIG. 65 TRANSFORMATION OF abc PHASE-VARIABLES TO dqo VARIABLES.

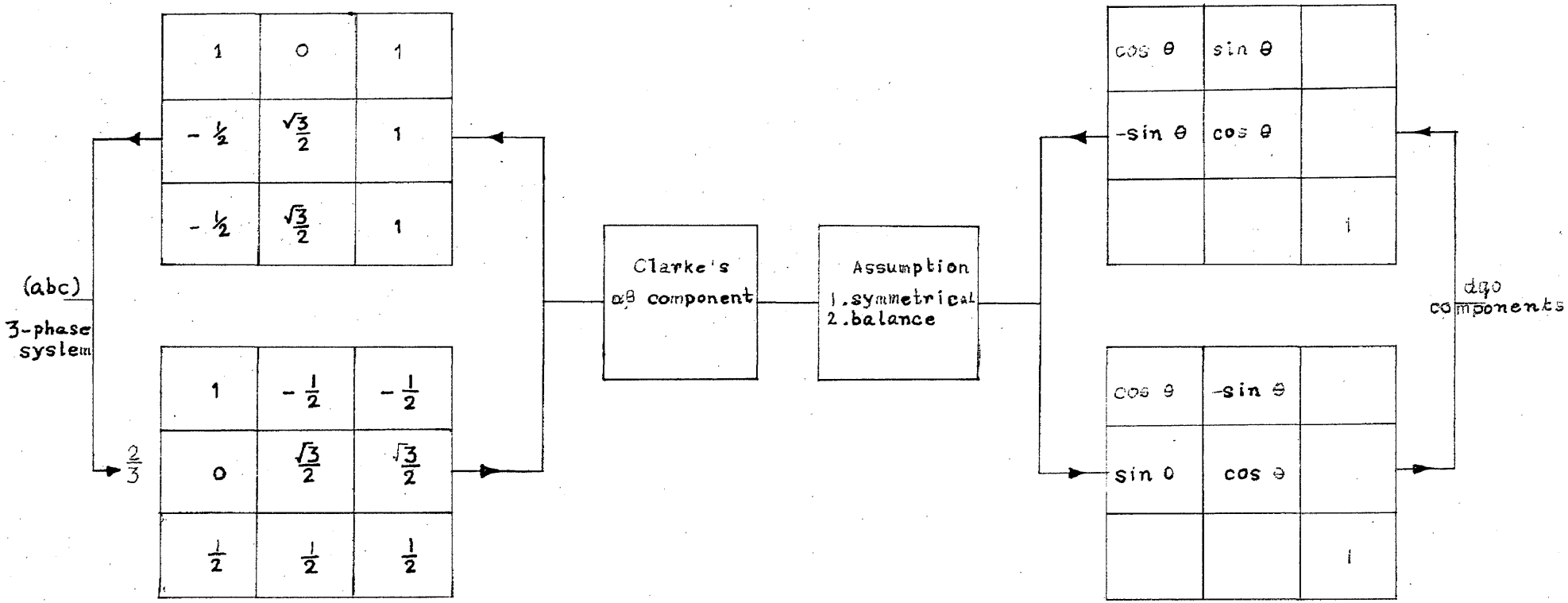

FIG. 66. PARK'S TRANSFORMATION AS APPLIED TO 3-PHASE SYSTEM TO OBTAIN dqo COMPONENTS.

$$v_\alpha = v_s \cos \omega t$$
$$v_\beta = v_s \cos(\omega t - \frac{\pi}{2}) \qquad (A.16)$$
$$v_o = 0$$

The results obtained by applying the same transformation to equation (A.15) are:

$$v_\alpha = v_s$$
$$v_\beta = 0 \qquad (A.17)$$
$$v_o = 0$$

In the particular case of an unloaded machine where the axis of phase 'a' coincides with the magnetic axis of the rotor, the dqo components are:

$$v_\alpha = v_q \qquad (A.18)$$
$$v_\beta = v_d$$

It is, therefore, true to say that in the conventional machine analyses, the application of Park's transformation eliminates the β components during the process. Machine analyses are carried out with the α component which under balanced and symmetrical conditions corresponds to phase 'a' of a 3-phase machine.

While the analytical work is concerned with symmetrical operation of a generator, the transformation outlined above is acceptable since the phase-quantities are identical except the 120^o phase-displacement. Under asymmetrical conditions analytical studies have been done[39] on the basis of Park's transformation assuming that the

generated voltages are balanced and symmetrical and are not affected by the external conditions. This is, however, unrealistic. Due to varying currents in the three phases during asymmetrical operation the rotating m.m.f. in the air-gap is not of constant magnitude and harmonic voltages are produced in the rotor and stator circuits.[29] The usual machine model in the dqo reference frame is, therefore, not adequate for analysing asymmetrical operations of a synchronous machine.

APPENDIX B

THE RECIPROCAL PER-UNIT SYSTEM

The first step in establishing a per-unit system is to define a set of base quantities. The widely accepted practice is to take the peak values of the rated armature current and voltage of the generator as the base quantities of the armature. This leads to the following definitions:

i_{ao} = rated phase current (peak)

v_{ao} = rated phase voltage (peak)

So $VA_o = \frac{3}{2} i_{ao} v_{ao}$ = (rated machine output)

$z_{ao} = \omega_o L_{ao} = r_{ao} = \frac{v_{ao}}{i_{ao}}$

= base impedance

$\Psi_{ao} = L_{ao} i_{ao}$ = base flux-linkage per phase

Similar quantities may be defined for the rotor circuits, but, at this stage, it is not possible to assign any physical value to these circuits. Nevertheless, what is important is to find a relation between the stator and the rotor circuit so that the mutual inductance is the same in per unit system. It could be easily done if the equivalent turns of the stator and the rotor circuits were known. In practice, the turns ratio is not usually known. In any case, the flux-linkage equations of Section (2.2.1) can now be expressed in per unit system, dividing each equation by the base flux linkage of the circuit to which the equation applied.

$$\frac{\Psi_d}{L_{ao}i_{ao}} = \frac{L_{afd}\cdot i_{fdo}}{L_{ao}i_{ao}} \cdot \frac{i_{fd}}{i_{fdo}} + \frac{L_{akd}i_{kdo}}{L_{ao}i_{ao}} \frac{i_{kd}}{i_{kdo}} - \frac{L_d \cdot i_d}{L_{ao}i_{ao}} \quad (B.2)$$

where i_{fdo} = per unit field current

i_{kdo} = per unit damper winding current.

Now indicating a per unit quantity by a bar under a symbol

$$\underline{\Psi}_d = \frac{L_{afd}i_{fdo}}{L_{ao}i_{ao}} \underline{i}_{fd} + \frac{L_{akd}i_{kdo}}{L_{ao}i_{ao}} \underline{i}_{kd} - \underline{L}_d\underline{i}_d \quad (B.3)$$

Similarly, dividing Ψ_{fd} by $L_{ffdo}i_{fdo}$

$$\underline{\Psi}_{fd} = \underline{L}_{ffd}\underline{i}_{fd} + \frac{L_{kfd}i_{kdo}}{L_{ffdo}i_{fdo}} \underline{i}_{kd} - \frac{3}{2} \frac{L_{ffd}i_{ao}}{L_{ffdo}i_{fdo}} \underline{i}_d \quad (B.4)$$

For a reciprocal per unit system the condition that is to be satisfied is, *from equations B3 and B4*

$$\frac{L_{afd}i_{fdo}}{L_{ao}i_{ao}} = \frac{3}{2} \frac{L_{fad}i_{ao}}{L_{ffdo}i_{fdo}} \quad (B.5)$$

The numerical values of L_{afd} and L_{fad} are the same and hence from equation (B.5)

$$L_{ffdo}i^2_{fdo} = \frac{3}{2} L_{ao}i^2_{ao}$$

or $$\omega_o L_{ffdo}i^2_{fdo} = \frac{3}{2} L_{ao}i^2_{ao} \quad (B.6)$$

This then proves that for reciprocal mutual inductances the volt-ampere ratings of the field winding should be the same as the generator volt-ampere rating. In a similar way it can be shown that the same condition holds for the damper circuits as well.

It is now required to find base quantities for the field winding. Of the several ways of defining the base field current, the one that is in wide use is to consider that

value of field current which produce in each stator phase, under open circuit conditions, a voltage v_a given by:

$$v_a = \omega_o L_{ad} i_{ao}$$

Therefore,

$$\omega_o L_{afd} i_{fdo} = \omega_o L_{ad} i_{ao}$$

or
$$L_{afd} i_{fdo} = L_{ad} i_{ao} \qquad (B.7)$$

Similarly
$$L_{akd} i_{kdo} = L_{ad} i_{ao}$$

$$L_{akq} i_{kqo} = L_{ad} i_{ao} \qquad (B.8)$$

Substituting these relationships in the flux linkage equations of Section (2.2.1) a new set of equations in the reciprocal per unit system are obtained as given in Section (2.2.2).

From equation (B.7) which is in MKS unit

$$i_{fdo} = \frac{L_{ad}}{L_{afd}} i_{ao} \qquad (B.9)$$

i_{fdo} can be obtained from the open circuit characteristics of the machine and thus the numerical value of L_{afd} can be found.

APPENDIX C

REARRANGEMENT OF DIFFERENTIAL EQUATIONS

(C.1) GENERATOR

(a) Direct-axis Flux Linkage

From equation (3.1)

$$\psi_d = \frac{L_{ad}(1 + \tau_{kdp})}{1 + (\tau_{do}' + \tau_{kdo}'')p + \tau_{do}'\tau_{do}''p^2} \cdot \frac{v_{fd}}{r_{fd}} - \frac{1 + (\tau_d' + \tau_{d1})p + \tau_d'\tau_d''p^2}{1 + (\tau_{do}' + \tau_{kdo})p + \tau_{do}'\tau_{do}''p^2} L_d i_d$$

Before any rearrangement, the quadratic expressions in p both in the denominator and numerator of the above equation is factorised from the following identities.

$$\begin{aligned} 1 + (\tau_{do}' + \tau_{kdo}')p + \tau_{do}'\tau_{do}''p^2 &= (1 + \tau_1 p)(1 + \tau_2 p) \\ \text{and} \quad 1 + (\tau_d' + \tau_{d1})p + \tau_d'\tau_d''p^2 &= (1 + \tau_3 p)(1 + \tau_4 p) \end{aligned} \qquad (C.1)$$

The direct axis flux linkage can then be written

$$\psi_d = L_{ad} \cdot \frac{(1 + \tau_{kdp})}{(1 + \tau_1 p)(1 + \tau_2 p)} \cdot \frac{v_{fd}}{r_{fd}} - \frac{(1 + \tau_3 p)(1 + \tau_4 p)}{(1 + \tau_1 p)(1 + \tau_2 p)} L_d i_d \qquad (C.2)$$

This can be conveniently arranged by rewriting

$$\psi_d = L_{ad} \cdot \frac{(1 + \tau_{kdp})}{(1 + \tau_1 p)(1 + \tau_2 p)} \cdot \frac{v_{fd}}{r_{fd}} - L_d'' i_d - \frac{\{k_{eq} + \tau_{eq} p\} L_d i_d}{(1 + \tau_1 p)(1 + \tau_2 p)} \qquad (C.3)$$

where L_d'' , usually called subtransient inductance

$$= \frac{\tau_3 \tau_4}{\tau_1 \tau_2} L_d \qquad (C.4)$$

$$k_{eq} = 1 - \frac{\tau_3\tau_4}{\tau_1\tau_2} \qquad (C.5)$$

and $$\tau_{eq} = \tau_3 + \tau_4 - \tau_3\tau_4\left\{\frac{1}{\tau_1} + \frac{1}{\tau_2}\right\} \qquad (C.6)$$

Now let

$$\psi''_d = \psi_d + L''_d i_d \qquad (C.7)$$

where ψ''_d represents direct axis flux behind the sub-transient inductance, then the first order equations can be formed from (C.7)

$$\psi''_d = \frac{\psi_1}{(1 + \tau_2 p)} \qquad (C.8)$$

where $$\psi_1 = \left\{L_{ad}(1 + \tau_{kd}p)\frac{v_{fd}}{r_{fd}} - (k_{eq} + \tau_{eq}p)L_d i_d\right\} \Big/ (1 + \tau_1 p) \qquad (C.9)$$

Equations (C.8) and (C.9) may now be put into the required first order differential form.

From equation (C.9)

$$p\psi_1 = \left\{L_{ad}(1 + \tau_{kd}p)\frac{v_{fd}}{r_{fd}} - (k_{eq} + \tau_{eq}p)L_d i_d - \psi_1\right\}\frac{1}{\tau_1} \qquad (C.10)$$

and $$p\psi''_d = \frac{1}{\tau_2}\{\psi_1 - \psi''_d\}$$

It is shown in Section (C.2) that $p(v_{fd})$ may be formed from excitation control system. The pi_d term is obtained by linear approximation as described in Appendix (C.4).

(b) Rotor Current

From equation (3.3)

$$i_{fd} = \frac{(1 + \tau'_{kdo}p)}{1 + (\tau'_{do} + \tau'_{kdo})p + \tau'_{do}\tau''_{do}p^2}\frac{v_{fd}}{r_{fd}} + \frac{(1 + \tau_{kd}p)L_{ad}}{1 + (\tau'_{do} + \tau'_{kdo})p + \tau'_{do}\tau''_{do}p^2}\frac{pi_d}{r_{fd}}$$

Applying equation (C.1) this can be written as:

$$i_{fd} = \frac{(1+\tau_{kdo}'p)}{(1+\tau_1 p)(1+\tau_2 p)} \frac{v_{fd}}{r_{fd}} + \frac{(1+\tau_{kd}p)L_{ad}}{(1+\tau_1 p)(1+\tau_2 p)} \cdot \frac{pi_d}{r_{fd}} \quad (C.11)$$

The first order equations are then found in the following way, the pattern being the same as used for direct-axis flux linkage.

$$i_{fd} = \frac{(1+\tau_{kdo}'p)}{(1+\tau_1 p)(1+\tau_2 p)} \frac{v_{fd}}{r_{fd}} + i_{fd}' - \frac{L_{ad}}{r_{fd}} \cdot \frac{(k_f - \tau_f p)i_d}{(1+\tau_1 p)(1+\tau_2 p)} \quad (C.12)$$

where
$$i_{fd}' = \frac{L_{ad}}{r_{fd}} \cdot \frac{\tau_{kd}}{\tau_1 \tau_2} \cdot i_d \quad (C.13)$$

$$k_f = \frac{\tau_{kd}}{\tau_1 \tau_2} \quad (C.14)$$

$$\tau_f = 1 - \tau_{kd}\left(\frac{1}{\tau_1} + \frac{1}{\tau_2}\right) \quad (C.15)$$

If, further, it is assumed that

$$i_{fd}'' = i_{fd} - i_{fd}' \quad (C.16)$$

then
$$i_{fd}'' = \frac{I_{fd}}{1+\tau_2 p} \quad (C.17)$$

where
$$I_{fd} = \frac{(1+\tau_{kdo}'p)}{(1+\tau_1 p)} \frac{v_{fd}}{r_{fd}} - \frac{L_{ad}}{r_{fd}} \frac{(k_f - \tau_f p)}{1+\tau_1 p} i_d \quad (C.18)$$

Then from (C.17)

$$pi_{fd}'' = \frac{1}{\tau_2}\left\{I_{fd} - i_{fd}''\right\} \quad (C.19)$$

and from (C.18)

$$pI_{fd} = \frac{1}{\tau_{do}'}\left\{(1+\tau_{kdo}'p)\frac{v_{fd}}{r_{fd}} - \frac{L_{ad}}{r_{fd}}(k_f - \tau_f p)i_d - I_{fd}\right\} \quad (C.20)$$

(c) Field Flux-linkage

From equation (3.2)

$$\psi_{fd} = L_{ffd} \cdot \frac{(1 + \tau_{do}''p)}{1 + (\tau_{do}' + \tau_{kdo}')p + \tau_{do}'\tau_{do}''p^2} \cdot \frac{v_{fd}}{r_{fd}} -$$

$$- \frac{(1 + \tau_{kd}p)}{1 + (\tau_{do}' + \tau_{kdo}')p + \tau_{do}'\tau_{do}''p^2} L_{ad} i_d$$

Proceeding the same way the above equation may be written as

$$\psi_{fd} = L_{ffd} \cdot \frac{(1 + \tau_{do}''p)}{(1 + \tau_1 p)(1 + \tau_2 p)} \frac{v_{fd}}{r_{fd}} - \frac{(1 + \tau_{kd}p)}{(1 + \tau_1 p)(1 + \tau_2 p)} L_{ad} i_d \qquad (C.21)$$

The first order differential equations will then be

$$\psi_{fd} = \frac{\psi_{fd}'}{(1 + \tau_2 p)} \qquad (C.22)$$

where

$$\psi_{fd}' = \frac{1}{(1 + \tau_1 p)} \left\{ L_{ffd}(1 + \tau_{do}''p)\frac{v_{fd}}{r_{fd}} - (1 + \tau_{kd}p) \cdot L_{ad} i_d \right\} \qquad (C.23)$$

or

$$p\psi_{fd}' = \frac{1}{\tau_1} \left\{ L_{ffd}(1 + \tau_{do}''p)\frac{v_{fd}}{r_{fd}} - L_{ad}(1 + \tau_{kd}p) i_d - \psi_{fd}' \right\} \qquad (C.24)$$

and from (C.22)

$$p\psi_{fd} = \frac{1}{\tau_2} \left\{ \psi_{fd}' - \psi_{fd} \right\} \qquad (C.25)$$

(d) Direct axis damper winding current.

From equation (3.4)

$$i_{kd} = \frac{L_{ad}}{r_{kd}} \cdot \frac{p(i_d - i_{fd})}{1 + \tau_{kdo}'p}$$

so

$$pi_{kd} = \frac{1}{\tau_{kdo}'} \left\{ \frac{L_{ad}}{r_{kd}} \cdot p(i_d - i_{fd}) - i_{kd} \right\} \qquad (C.26)$$

(e) Quadrature-axis Flux-linkage

From equation (3.5)

$$\psi_q = -\frac{(1 + \tau''_q p)}{(1 + \tau'_{kqo} p)} L_q i_q$$

Defining the sub-transient quadrature flux linkage as:

$$\psi''_q = \psi_q + L''_q i_q \tag{C.27}$$

where $$L''_q = \frac{\tau''_q}{\tau''_{kqo}} L_q \tag{C.28}$$

then $$p\psi''_q = \frac{1}{\tau''_{kqo}} \left\{ -L_q i_q - \psi_q \right\} \tag{C.29}$$

(f) Quadrature-axis Damper Winding Current

From equation (3.6)

$$i_{kq} = \frac{L_{aq}}{r_{kq}} \cdot \frac{p i_q}{1 + \tau''_{kqo}}$$

then $$p i_{kq} = \frac{1}{\tau''_{kqo}} \left\{ \frac{L_{aq}}{r_{kq}} \cdot p i_q - i_{kq} \right\} \tag{C.30}$$

(g) Equation of Motion

From equation (2.25)

$$P_i = Mp^2\delta + P_e + k_d p\theta + P_L$$

Introducing an auxiliary variable giving

$$p\delta = U \tag{C.31}$$

the equation of motion can then be written as

$$pU = \frac{1}{M} \left\{ P_i - k_d p\theta - P_e - P_L \right\} \tag{C.32}$$

(C.2) SINGLE STEP FINITE DIFFERENCE METHOD

Whilst, in solving the system equations, it is necessary to compute the rate of change with respect to time of several machine variables such as p_d or pi_d, explicit mathematical expressions for these are not available among the machine equations. They are, therefore, evaluated by a simple finite difference method in which the variables are assumed to vary linearly during a step length and their rates of change are then computed by dividing the increment over the step by the step length.

Referring to Fig.(8)

$$pY_n = \{Y_n - Y_{(n-1)}\} /h \qquad (C.33)$$

where pY_n = the rate of change of Y during the n th. interval.

Y_n = value of Y at the beginning of n th. interval.

$Y_{(n-1)}$ = value of Y at the beginning of (n-1)th. interval.

(C.3) EXCITATION CONTROL SYSTEM

(a) Magnetic Amplifier (1)

From equation (2.29)

$$v_1 = \frac{k_1}{1 + \tau_1 p}(v - v_{s1} - v_{s2}) + C$$

Since C is a constant the rearrangement can best be done by writing the above equation as

$$v_1 = v' + C \tag{C.34}$$

where $$v' = \frac{k_1}{1 + \tau_1 p}(v - v_{s1} - v_{s2}) \tag{C.35}$$

so that $$pv' = \frac{1}{\tau_1}\left\{k_1(v - vs_1 - v_{s2}) - v_1\right\} \tag{C.36}$$

within the range

$$v_1 min \leq v_1 \leq v_1 max$$

(b) Magnetic Amplifier (2)

Following the same step, equation (2.30) can be written as

$$v^2 = v_2 + C_2 \tag{C.37}$$

yielding $$pv^2 = \frac{1}{\tau_2}\left\{k_2 v_1 - v^2\right\} \tag{C.38}$$

for $$v_2 min \leq v_2 \leq v_2 max$$

(c) The Main Exciter

From equation (2.31)

$$v_{fd} = \frac{k_e v_2}{1 + \tau_e p}$$

therefore $$pv_{fd} = \frac{1}{\tau_e}\left\{k_e v_2 - v_{fd}\right\} \tag{C.39}$$

(d) Subsidiary feedback signals

From equation (2.32)

$$v_{s1} = \frac{k_3 \tau_3 p v_2}{1 + \tau_4 p}$$

Since C_2 is constant, from equation (C.37)

$$pv^2 = pv_2 \tag{C.40}$$

substituting this

$$pv_{s1} = \frac{1}{\tau_4}\left\{\frac{k_3 \tau_3}{\tau_2}(k_2 v_1 - v^2) - v_{s1}\right\} \tag{C.41}$$

Similarly from equations (2.33) and (C.39)

$$pv_{s2} = \frac{1}{\tau_6}\left\{\frac{k_4\tau_5}{\tau_e}(k_e v_2 - v_{fd}) - v_{s2}\right\} \qquad (C.42)$$

(C.4) PRIME-MOVER AND GOVERNOR

(a) Governor Valve Position

From equation (2.35)

$$u_1 = \frac{G_1 u}{(1 + \tau_7 p)(1 + \tau_8 p)} + u_k$$

Introducing two auxiliary variables, u' and v_3

$$u_1 = u' + u_k \qquad (C.43)$$

and $$u' = \frac{v_3}{1 + \tau_8 p} \qquad (C.44)$$

where $$v_3 = \frac{G_1 u}{1 + \tau_7 p} \qquad (C.45)$$

Then from (C.43) and (C.44)

$$pv_3 = \frac{1}{\tau_7}\left\{G_1 u - v_3\right\} \qquad (C.46)$$

and $$pu' = \frac{1}{\tau_8}(v_3 - u') \qquad (C.47)$$

for $$0 \leq u_1 \leq 1$$

(b) Turbine

From equation (2.37)

$$P_i = \frac{P_s}{1 + \tau_g p}$$

hence $$pP_i = \frac{1}{\tau_g}\left\{P_s - P_i\right\} \qquad (C.48)$$

APPENDIX D

(D.1) MATHEMATICAL REPRESENTATION OF THE BELVEDERE EXCITATION SYSTEM

The voltage regulator and the excitation system fitted to the test generator in the Belvedere Power Station is shown in block schematic form in Fig. 37. The equations of the different elements of the excitation system are:

Magnetic Amplifier (1):

$$v_1 = \frac{(1 + \tau_1 p)}{(1 + \tau_2 p)(1 + \tau_3 p)} v \qquad (D.1)$$

$$\text{for } v_1 \text{min} \leq v_1 \leq v_1 \text{max}$$

where $$v = (E_d - v_m - v_{s1} - v_{s2} - v_{s3}) \qquad (D.2)$$

Magnetic Amplifier (2):

$$v_2 = \frac{k_1 v_1}{(1 + \tau_4 p)} \qquad (D.3)$$

$$\text{for } v_2 \text{min} \leq v_2 \leq v_2 \text{max}$$

A.C. Exciter (including rectifier):

$$v_{fd} = \frac{k_2 v_2}{1 + \tau_5 p} \qquad (D.4)$$

$$\text{for } v_{fd} \text{min} \leq v_{fd} \leq v_{fd} \text{max}$$

Amplifier Stabilizer:

$$v_{s1} = \frac{k_3 (1 + \tau_6 p)}{1 + \tau_7 p} v_2 \qquad (D.5)$$

Exciter Stabiliser:

$$v_{s2} = \frac{k_4 p\, v_{fd}}{1 + \tau_8 p} \qquad (D.6)$$

Terminal Voltage Stabiliser:

$$v_{s3} = \frac{k_5 p\, v_m}{1 + \tau_9 p} \qquad (D.7)$$

The values of the time constants and the gains of the different elements are given in Table VII along with their saturating limits.

The solution of the equations are achieved in the same process of reduction as shown in Appendix C.

(D.2) PROGRAMMING OF FIELD CURRENT CONSTRAINTS

The technique of programming the constraint for field current having only one polarity, is illustrated in Fig.(67). The necessary changes that are required to be incorporated for such constraint are:

(1) Whenever the field current tries to be less than zero, it is to be kept at zero.

(2) When the field current is equal to zero, the field winding behaves like an open-circuited coil if it is not short circuited by an external resistance and coupled to the other windings on the direct axis. Hence

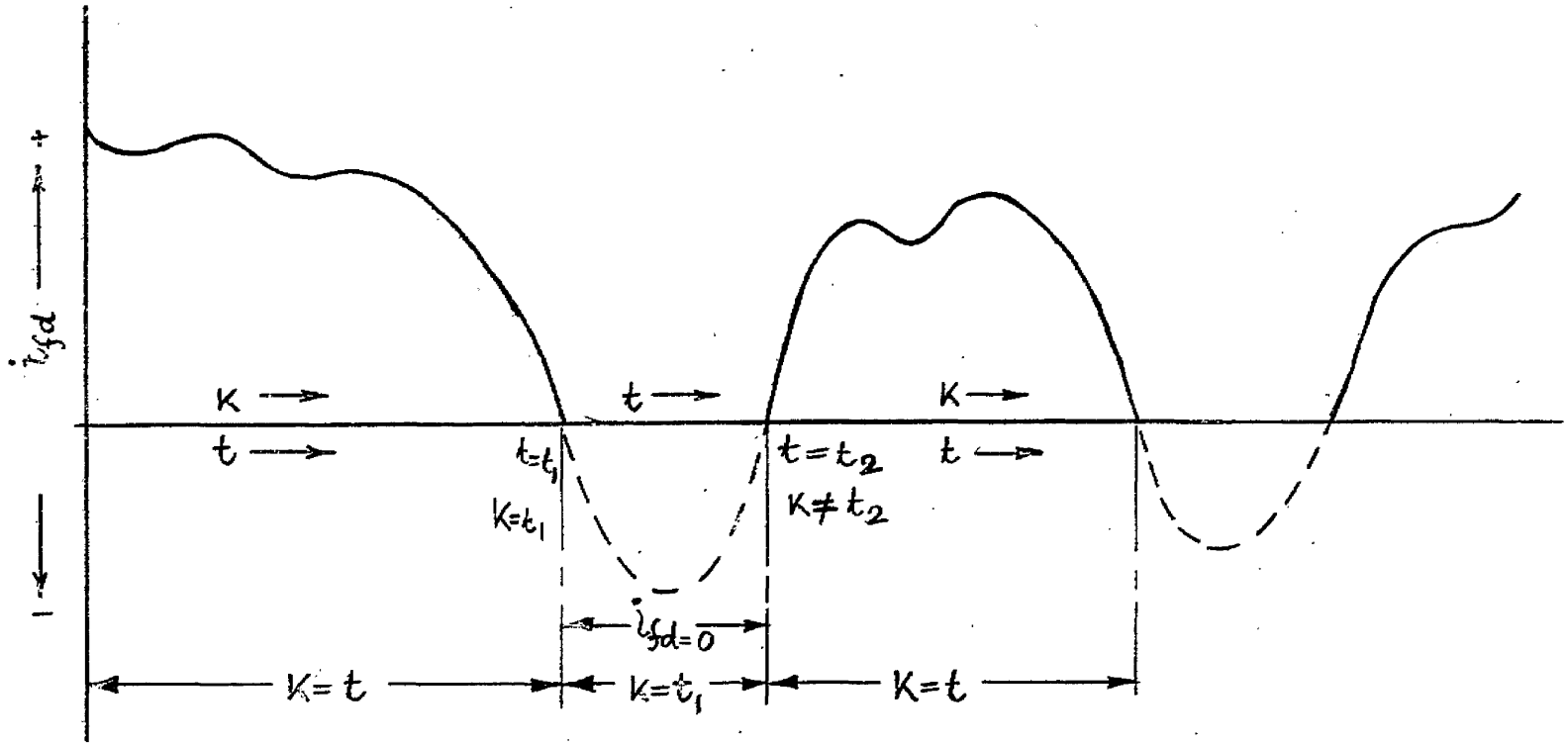

FIG.(67) REPRESENTATION OF FIELD CURRENT RESTRAINT IN COMPUTER PROGRAM

the operational equations for flux-linkages and voltages are different from those when the field-current is not zero.

(3) At the instant of the field current being zero, it is necessary to switch on to a different set of differential equations, the initial condition of which come from the last values of the previous equations. Computation then continues on the basis of new equations until the field current again tries to build up in the positive direction.

(4) At the time when the field current tries to become positive, it is again necessary to switch back to the former set of differential equations along with the proper transfer of initial conditions.

For each time that the field current goes to zero, it is evident from (3) and (4) above, that two sets of changes of differential equations and corresponding transfer of initial conditions, are necessary. For the computer to differentiate between the two different changes, a marker k, as shown in the figure, is used. So long as the field current is positive, the marker moves along with the independent variable, time. As soon as $i_{fd} = 0$, the marker stops. So the first set of changes as in (3) above, comes into action when

$$i_{fd} = 0$$

and $$k = t = t_1 \quad \text{(for example)},$$

and the second set of changes, as in (4) above, comes into

action when

i_{fd} is slightly greater than zero

but $k \neq t = t_2$

as shown in the diagram.

However, soon after incorporating the changes in the latter case, k is again set to move along with the time scale until the next stage of current constraint comes into action. The whole process is then repeated.

APPENDIX E

(E.1) SYNCHRONOUS MACHINE EQUATIONS WITH TWO DAMPER WINDINGS ALONG EACH AXIS

The machine equations with two damper windings in direct axis and two in the quadrature axis can be written in the reciprocal per unit system in the following way. Suffices 1 and 2 designate damper winding (1) and (2) respectively.

Flux equations:

direct axis:

$$\begin{aligned}
\psi_d &= L_{ad}i_{fd} + L_{ad}i_{kd1} + L_{ad}i_{kd2} - L_d i_d \\
\psi_{fd} &= L_{ffd}i_{fd} + L_{ad}i_{kd1} + L_{ad}i_{kd2} - L_{ad}i_d \\
\psi_{kd1} &= L_{ad}i_{fd} + L_{kkd1}i_{kd1} + L_{ad}i_{kd2} - L_{ad}i_d \\
\psi_{kd2} &= L_{ad}i_{fd} + L_{ad}i_{kd1} + L_{kkd2}i_{kd2} - L_{ad}i_d
\end{aligned} \qquad (E.1)$$

quadrature axis:

$$\begin{aligned}
\psi_q &= L_{aq}i_{kq1} + L_{aq}i_{kq2} - L_q i_q \\
\psi_{kq1} &= L_{kkq1}i_{kq1} + L_{aq}i_{kq2} - L_{aq}i_q \\
\psi_{kq2} &= L_{kq}i_{kq1} + L_{kkq2}i_{kq2} - L_{aq}i_q
\end{aligned} \qquad (E.2)$$

Voltage equations:

direct axis:

$$\begin{aligned}
V_{fd} &= p\psi_{fd} + r_{fd}i_{fd} \\
v_d &= p\psi_d - R_a i_d - \psi_q p\theta \\
0 &= p\psi_{kd1} + R_{kd1}i_{kd1} \\
0 &= p\psi_{kd2} + R_{kd2}i_{kd2}
\end{aligned} \qquad (E.3)$$

quadrature axis:

$$\begin{aligned}
v_q &= p\psi_q - R_a i_q + \psi_d p\theta \\
0 &= p\psi_{kq1} + R_{kq1}i_{kq1} \\
0 &= p\psi_{kq2} + R_{kq2}i_{kq2}
\end{aligned} \qquad (E.4)$$

Current equations:

(neglecting resistance for the sake of simplicity)

$$i_d = (V_q - V_b \cos \delta)/X_t \qquad (E.5)$$

$$i_q = (V_b \sin \delta - V_d)/X_t \qquad (E.6)$$

Substituting from equations (E.3) and (E.4) into equation (E.5)

$$X_t i_d = p\psi_q - R_a i_q + \psi_d p\theta - V_b \cos \delta$$

or
$$X_t i_d - \psi_d p\theta + V_b \cos \delta + R_a i_q = p\psi_q \qquad (E.7)$$

Similarly from equation (E.6) and (E.3)

$$X_t i_q - V_b \sin \delta + R_a i_d + \psi_q p\theta = p\psi_d \qquad (E.8)$$

For field winding

$$v_{fd} - r_{fd} i_{fd} = p\psi_d \quad (p\psi_{fd}) \qquad (E.9)$$

For direct axis damper windings

$$-R_{kd1} i_{kd1} = p\psi_{kd1} \qquad (E.10)$$

$$-R_{kd2} i_{kd2} = p\psi_{kd2} \qquad (E.11)$$

For quadrature axis damper windings

$$-R_{kq1} i_{kq1} = p\psi_{kq1} \qquad (E.12)$$

$$-R_{kq2} i_{kq2} = p\psi_{kq2} \qquad (E.13)$$

Replacing the left hand sides of equations (E.7) to (E.13) by y's, they can be rewritten as

$$y_1 = p\psi_{fd}$$

$$y_2 = p\psi_{kd1}$$

$$y_3 = pi_{kd2} \quad (p\psi_{kd2})$$

$$y_4 = p\psi_d$$

$$y_5 = p\psi_{kq1}$$

$$y_6 = p\psi'_{kq2}$$
$$y_7 = p\psi_q \qquad \text{(E.14)}$$

Now substituting from equation (E.2) into the first expression of (E.14), it can be written that

$$y_7 = L_{aq}(pi_{kq1}) + L_{aq}(pi_{kq2}) - L_q(pi_q) \qquad \text{(E.15)}$$

Proceeding in the same way, equation (E.14) can now be written in the matrix form in the following way:

$$\begin{bmatrix} y_1 \\ y_2 \\ y_3 \\ y_4 \\ y_5 \\ y_6 \\ y_7 \end{bmatrix} = \begin{bmatrix} L_{ffd} & L_{ad} & L_{ad} & -L_{ad} & & & \\ L_{ad} & L_{kkd1} & L_{ad} & -L_{ad} & & & \\ L_{ad} & L_{ad} & L_{kkd2} & -L_{ad} & & & \\ L_{ad} & L_{ad} & L_{ad} & -L_{ad} & & & \\ & & & & L_{kkq1} & L_{aq} & -L_{aq} \\ & & & & L_{aq} & L_{kkq2} & -L_{aq} \\ & & & & L_{aq} & L_{aq} & -L_q \end{bmatrix} \cdot \begin{bmatrix} pi_{fd} \\ pi_{kd1} \\ pi_{kd2} \\ pi_d \\ pi_{kq1} \\ pi_{kq2} \\ pi_q \end{bmatrix} \qquad \text{(E.16)}$$

(E.2) PROCEDURE FOR SOLVING THE EQUATIONS OF THE MACHINE MODEL

At the beginning of the step:

(a) the variable mutual inductances are calculated.

(b) inductance-matrix is reset with the new values.

(c) y's are calculated on the basis of the currents, rotor angle, field voltage and instantaneous frequency obtained at the end of the last interval.

(d) the coefficient matrix is inverted and the differential equations for the currents are solved by step integration

process. At the same time other differential equations relating to the excitation and governing systemsand the dynamic equation of motion can also be solved.

At the end of the step:

(a) Algebraic equations are solved to get the values of necessary quantities such as output power, terminal voltage, total loss, instantaneous speed and air-gap flux.

The process is repeated.

APPENDIX F: THE MAIN PROGRAM

The program, finally written in Atlas Autocode, consists mainly of several routines and blocks declared at the beginning of the program. Each of the routines or blocks are selected for execution at the appropriate time during the solution period. Spaces required for data storing and computation within a routine or a block are declared at the beginning of the routine whereas storage for variables common to several routines of same textual levels are declared at the beginning of the program. Care has also been taken to see that the stores are not kept occupied for a period longer than it is necessary. In this way the store-time has been substantially reduced. At the same time an attempt has not been made to reduce the computation time to the most efficient level.

The following blocks and routines have been used in the program:

(1) Curve fitting - This computes the coefficients of the polynomial expression for the machine-saturation characteristics.

(2) Machine Parameters - It calculates the machine parameters (unsaturated) based on open circuit and short circuit tests in the reciprocal per-unit system.

(3) Initial Conditions - This calculates the numerical values of all the machine variables including the voltage

regulating system and the turbine and its governing system corresponding to the operating conditions of the machine.

(4) Instep - This is a library routine for solving the differential equations by the Kutta-Merson Method.

(5) Field Current Constraint - The function of this routine is explained in Appendix D.

(6) Variable Parameter - This block calculates the new values of the machine parameters depending on the operating condition of the generator.

(7) Input and Output - By this block the test conditions are imposed on the machine according to pre-assigned constraints.

A flow diagram of the program is given in Fig.69 and a print out is attached at the back of the thesis.

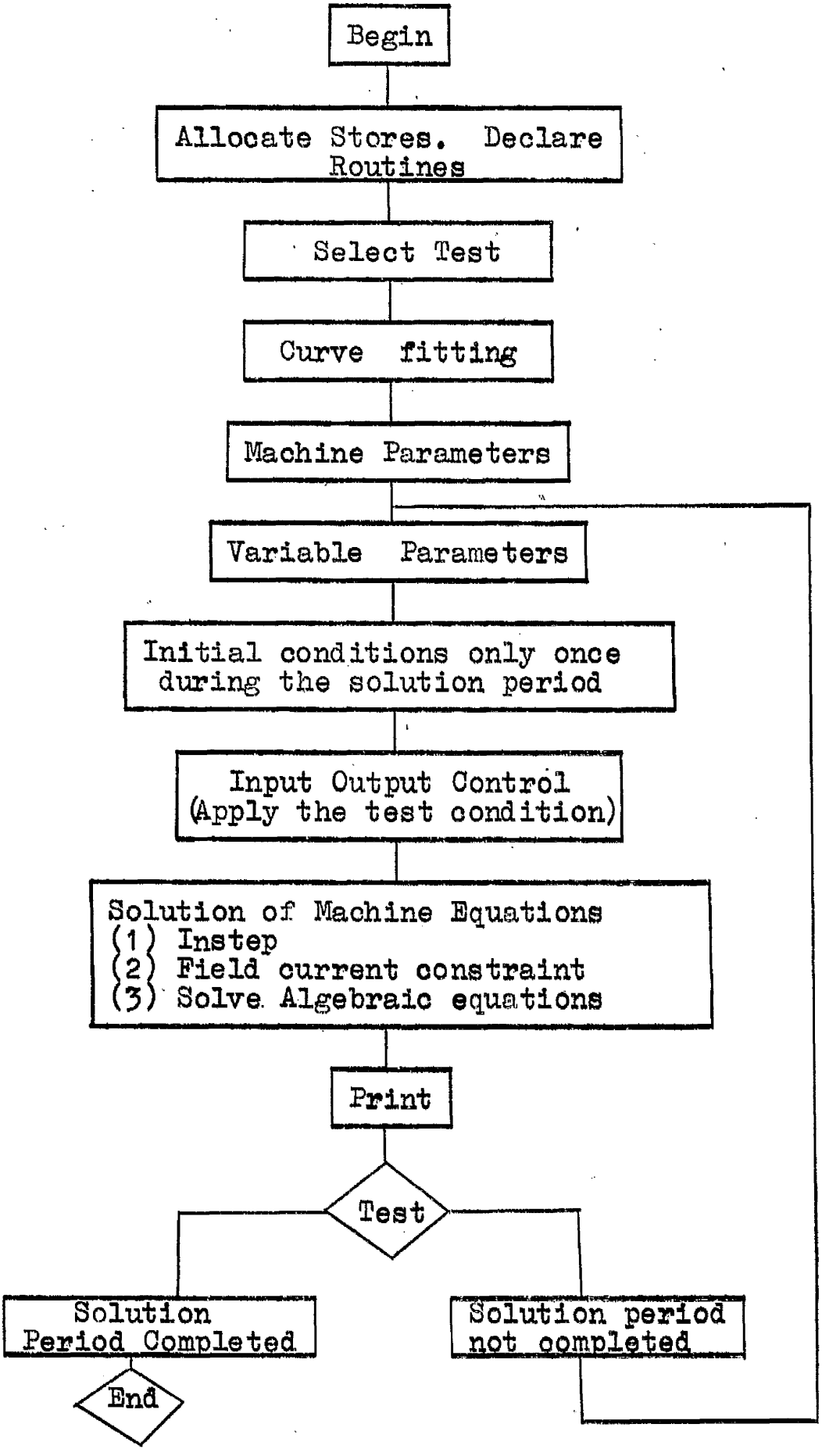

FIG.69 FLOW DIAGRAM OF THE MAIN PROGRAM

(1)

SECRETARY
for
EXAMINATIONS